Transactions of the Royal Society of Edinburgh: Earth Sciences, **96**, 197–307, 2006 (for 2005)

The structure of the sarcopterygian *Onychodus jandemarrai* n. sp. from Gogo, Western Australia: with a functional interpretation of the skeleton

Mahala Andrews†, John Long, Per Ahlberg, Richard Barwick and Ken Campbell

ABSTRACT: A description of the head, mandible, pectoral girdle, humerus, medial fins and their supports, and the dissociated vertebral column has been prepared for *Onychodus jandemarrai* n. sp. from the Gogo Formation (Frasnian) of Western Australia. This is the most completely known species of the genus. The feature influencing most of the head morphology is the retractable parasymphysial tusk whorls. Their presence has caused a reorganisation of the braincase, palate (including the loss of the vomers), and lateral displacement of the nasal capsules. The extensive mandibular articulation is in cartilage, and the mandibular symphysis is weak. This makes for a kinetic skull. There is a single submandibular on each side. The vertebral column is poorly ossified, consisting of intercentra which have no ventral contact, and pleurocentra. The neural arches have no longitudinal ligament, have unequal sides, and asymmetrical placing of the dorsal and ventral nerve root foramina. Each arch has an anterior surface that often attaches to the next anterior arch. The caudal fin is almost diphycercal; all the medial fins have strong support structures. An attempt is made to discuss the functional morphology of many features of the skeleton.

KEY WORDS: Anatomy, Devonian, Onychodontidae, sarcopterygians, skeletal functions.

Contents

https://doi.org/10.1017/S0263593300001309 Published online by Cambridge University Press

The genus *Onychodus* Newberry, 1857, is a Devonian sarcopterygian fish that has been described mainly from dissociated bones from North America, though its distribution is widespread on that continent. It is characterised by having two tooth whorls in the symphysial region of the mandible, and as a result of this remarkable feature, many structures of the head are modified. Also, the posterior part of the braincase is not extensively ossified and it is impossible to relate the posterior dermal bone structures to the braincase. As a result, most *Onychodus* material is profoundly disarticulated, and until articulated specimens were discovered in the Gogo Formation (Fig. 1), Western Australia, it was impossible to reconstruct the ossified part of the head and restore its postcranial skeleton.

The material from the Gogo Formation occurs in nodules which have been etched with dilute acetic acid, and large parts of single heads have been found within the one block. Although the heads are collapsed and sometimes partly disarticulated, the individual elements are fully three-dimensional, enabling the osteology of the head to be reconstructed. In addition, most of the postcranial material has been found in three specimens in calcarenites, and the caudal fins have been isolated in impressions in carbonates. It has been possible to make a rough reconstruction of the posterior part of the trunk, including the pelvic and median fins, and estimate the relative length of the body and tail.

Previous descriptive work on the Gogo *Onychodus* includes the description of the oticoccipital skull roof by Andrews (1973), and comment on tooth whorls by Andrews (1989). Long (1991) described the skull of *Onychodus* with the remains of a placoderm in the same nodule, suggesting that the *Onychodus* died while attempting to ingest the placoderm. In 1999, Long figured a reconstructed head of the Gogo *Onychodus*, and in 2001, he provided information on the ethmosphenoid of this species; he also suggested a close phylogenetic relationship between *Onychodus* and *Psarolepis* from China.

It is generally agreed that *Onychodus* belongs in a monophyletic group, Onychodontiformes (or 'Struniiformes'), together with the genera *Strunius* (Jessen 1966) and *Grossius* (Schultze 1973), but the affinities of this group within the Sarcopterygii are disputed (e.g. Panchen & Smithson 1987; Zhu & Schultze 2001; Long 2001). The main purpose of the present paper is to describe the Gogo specimens of *Onychodus*; there has been no attempt to address the phylogenetic position of the Onychodontida, and only limited comparisons have been made with other onychodont material. However, the wealth of anatomical information available from the Gogo material greatly advances understanding of the group and will provide a good basis for future phylogenetic analyses.

The nomenclature of the skull bones is problematic, not only because of the existence of two rival schemes for sarcopterygian bone identification (Westoll 1943; Jarvik 1967), but also because the bones in the skull table of *Onychodus* have a very different pattern from what is known in other sarcopterygians. The details of the posterior skull roof were discussed by Andrews (1973), and in her figure 2, she illustrated her nomenclature. She followed the pattern adopted by Westoll (1943) rather than the one used by Jarvik (1967). The present authors do not wish to become involved with arguments about homologies, a topic that has been discussed in detail by many authors and summarised by Borgen (1983), but they have decided to follow the nomenclature of Andrews (1973). This not only creates a desirable terminological unity for

https://doi.org/10.1017/S0263593300001309 Published online by Cambridge University Press

Onychodus, but aligns the present paper with current majority usage, as illustrated, for example, by Janvier (1996), Johanson & Ahlberg (1997, 1998, 2001) and Zhu & Schultze (2001).

The late Dr Mahala Andrews spent a great deal of time on the material collected by the British Museum of Natural History in 1967, and on specimens in the Bureau of Mineral Resources and Australian National University collections in Canberra. Dr Long made more than a dozen trips to Gogo between 1986 and 2001, and has put together a fine collection of new material, much of which comes from the limestone in the Gogo Formation, and some from the more clastic slope deposits of the Saddler Formation. Dr Andrews prepared many photographs and line drawings, some of which were in preliminary stages of development. Unfortunately, she left no written text. The authorities in the National Museum of Scotland have lent Andrews' drawings and photographs to Campbell and Barwick at the Department of Earth Sciences of the Australian National University, and free use of these has been made in preparing the present paper. The other authors have not always been in agreement with some of Andrews' interpretations, but it is difficult to be sure which of her drawings were the final ones in her collection. Because of her extensive work on this animal, Andrews is listed as the first author of this paper.

1. Systematic palaeontology

Order Onychodontiformes

Diagnosis. Sarcopterygian fishes having a highly kinetic skull with overlaps between most of the cranial bones; two parasymphysial tooth whorls which are longer than broad and fit into the palate in a pair of deep cavities; coronoids lack fang pairs; nasal capsules placed laterally; anterior and posterior nasal openings on dorsal and ventral sides of the lateral-rostral bone, which posteriorly contacts the orbital margin; intracranial joint present; cheek with equidimensional preoperculum and squamosal; maxilla with a wide postorbital blade and a lateral line canal system; quadratojugal absent; posterior infradentary not pierced by the lateral line canal; long single submandibular bone beneath the infradentaries; median gular absent; cosmine absent; scales highly ornamented; caudal fin symmetrical around the vertebral column.

Remarks. At present, numerous features of onychodont anatomy are known only from *Onychodus* itself. These features are not included in the above diagnosis even though they may be found to be characteristic of the group as a whole with further investigation. Other species of *Onychodus* from North America are known from fragments, but this material is in need of reworking. On the other hand, fragments of what are called *Onychodus jaekeli* from Germany, *Grossius* (Schultze 1973) from Spain, and *Strunius* from Germany (Jessen 1966) and from the Baltic States (Upeniece 1995), also help in interpreting the Order.

Genus *Onychodus* Newberry, 1857

Type species. *O. sigmoides* Newberry 1857, from the Middle Devonian of Ohio, USA.

Diagnosis. Onychodontiform fish with a pair of retractable, laterally compressed parasymphysial tusk whorls at the anterior end of the mandible; skull roof with median bone, the interparietal, situated between the parietals; supraorbital sensory canal runs along the lateral edge of the parietals; intertemporal absent; lateral rostral bone contributes to the orbital margin; extratemporal bone elongate, in contact with the supratemporal anteriorly; lateral extrascapulars flank lateral margins of the postparietals; maxilla with an expanded postorbital blade, and an extensive lateral line canal system; premaxilla high anteriorly and also with an extensive lateral line system; large circular fossa in the endopterygoid medial to the ectopterygoid; autopalatine and quadrate are only ossified parts of palatoquadrate complex; quadrate and articular lack defined joint surfaces; vomer absent but predermopalatine present; ethmosphenoid well ossified, showing a large posterior facet for the attachment of the notochord, and processes for the support of the skull roof and the autopalatine articulation; parasphenoid with a small denticulate surface anterior to the buccohypophysial opening, and with its anterior stalk clearly sutured into the median ethmosphenoid stalk; otic capsule with a large vestibular fontanelle; opercular overlapped anteriorly by the spiracular and the extratemporal, and overlaps the crest of the cleithrum posteriorly; subopercular broad and deep; single deep but very narrow branchiostegal at level of jaw hinge; dentary pierced by branch of mandibular sensory canal anteriorly; four infradentaries, the most posterior one not carrying the lateral line canal; a small symphysial bone in an infradentary position on the mandible; supracleithrum and post-temporal narrow and intimately sutured together; anocleithrum narrow with an arrowhead-shaped dorsal end, entirely concealed behind the cleithrum and supracleithrum; scapulocoracoid with a large imperforate attached base, and with a high median process supporting the humerus; second dorsal fin and anal fins large and supported by basal plates carrying parallel radials; first dorsal fin with a large basal support, but apparently no radials; caudal fin approximately diphycercal, and with the caudal peduncle carrying a lateral line canal that turns dorsally towards its tip.

Remarks. The new species *O. jandemarrai* is by far the best known of the species of this genus, and provides much of the detail given above in the diagnosis. Some details are still not available, including the shape of the posterior end of the tail, the details of the first dorsal fin, and the pectoral and pelvic fins, but sufficient information is available to draw a satisfactory diagnosis.

Onychodus jandemarrai n. sp.

Derivation of name. Jandemarra was the name of the Aboriginal warrior who fought for Aboriginal rights in the Kimberleys and lived in caves in the Devonian reefs.

Holotype. WAM 92.8.2, (Fig. 2) an almost complete skull, ethmoid braincase, elements of the gill arches, pectoral girdle and humerus, isolates scales, and some vertebral elements, Gogo Formation, Paddy's Valley, Upper Devonian.

1.1. Other material

WAM specimens: 86.9.693, coll. J. Long 1986, Paddy's Valley, almost an entire head (juvenile). 86.9.694 coll. J. Long 1986, south of Teichert Hills locality, 8 km east of Lloyd Hill; whole complete fish, with tail, parts of fins, head in resin mount (only head has been acid etched). 90.11.1, coll. J. Long 1991, described by Long (1991); braincase, articulars and quadrates well preserved. 01.10.01 small articulated snout, coll. J. Long 2001, Paddy's Valley. 01.10.04 complete juvenile head in resin transfer. 01.11.03 partial head in resin, coll. J. Long 1986, Paddy's Valley. 01.11.04 complete tail, coll. J. Long 2001, Paddy's Valley. 01.11.05 partial head, coll. J. Long 1986, Paddy's Valley. 01.11.06 partial anterior of fish, weathered specimen, Saddler Formation, Ross Hill. 01.11.15 isolated large tusk, Paddy's Valley, coll. J. Long 2001. All specimens except the one from the Saddler Formation are from the Gogo Formation.

https://doi.org/10.1017/S0263593300001309 Published online by Cambridge University Press

ANU specimens: 36844 a crushed head which has not been fully prepared so as to leave the elements in relative positions, coll. Brown & Campbell 1970, Paddy's Valley. 49504, a fragment of the body scales with part of the vertebral column present, coll. Campbell & Barwick 1990 from Paddy's Valley. 49211 dissociated body, coll. Campbell & Barwick 1990 from Paddy's Valley. 72975 etched specimen, coll. G. Young, Paddy's Valley. 72976 etched specimen, coll. G. Young, Paddy's Valley. 72977 etched specimen, coll. G. Young, Paddy's Valley. 72978 etched specimen, coll. G. Young, Paddy's Valley.

The Natural History Museum, London: All these specimens were collected by the WAM-NHM-HM expedition in 1967. They come from Paddy's Valley and the Gogo Formation. P63566, articulated head in ventral view (resin mount), at locality 67/30. P63570, partial skull and shoulder girdle, at locality 67/891. P63576, complete skull figured by Long (1995, p. 188) at locality 67/95. P63571, partial skull and isolated shoulder girdle, skull in resin mount, at locality 67/901. P63577, clavicles, at locality 6795cl. P64125, fairly complete head as isolated elements, at locality 67/92.

Diagnosis. A medium-sized species having a maxilla with a well-defined posterodorsal corner; about 30 maxillary teeth which decrease in size posteriorly; extensive maxillary sensory canal system; premaxilla with a straight ventral margin with from eight (8) to 14 teeth, the posterior ones being larger than those of the adjacent maxilla; parasymphysial tusks number from six (6) to juveniles to three (3) in adults; parasymphysial tusks are sigmoidal and lack barbs.

Remarks. *Onychodus jandemarrai* n. sp. differs from the type species *O. sigmoides*, most noticeably by its deeper, shorter dentary and maxilla, which do not tend to taper posteriorly. In addition, the dentary of *O. sigmoides* is weakly expanded anteriorly. *O. jaekeli* has barbed parasymphysial tusks, unlike the sharp-pointed tusks on *O. jandemarrai*. *O. obliquidentatus* is distinguished by the small number of large, oblique and posteroventrally directed teeth on the maxilla. Other species of *Onychodus* are poorly defined, based on isolated tusks, teeth and scales, and are not considered here as properly defined species (e.g. *O. articus* Woodward 1889, *O. anglicus* Woodward 1888, *O. hopkinsi* Newberry 1889 and *O. ortoni* Newberry 1889).

2. Description

2.1. The body form

WAM 86.9.694 represents a relatively complete individual found as a number of connected nodules from the southern Teichert Hills. It has the skull at one end, and the tip of the caudal fin at the other. The complete specimen is approximately 47 cm long, the head making up 10 cm of the reconstructed length. We have not attempted to prepare a whole body reconstruction because of the fragmentary nature of the material. The body would have been oval in cross section. Given that some of our skulls are 19 cm long, we conclude that the above complete specimen is only approximately half the size of our largest individuals.

A second approach to the size problem is derived from a single, 4-cm long tusk from the parasymphysial whorl of an isolated specimen. The tusks on WAM 86.9.694 are 1·2 cm long, and so the whorls of this large specimen are more than three times its size. Assuming a proportional increase in the size of the body, the animal with the large tusks would have been approximately 1·5 m long. Such a fish would have been a formidable predator, but it is only half the size of specimens of *O. sigmoides*, which were 3 m in length; this was the largest known osteichthyan fish of the Middle Devonian.

2.2. Oticoccipital skull table

The oticoccipital skull table is elongated and broadest in the centre of the oticooccipital shield. It contains the same set of bones as those of Rhizodontida and Osteolepiformes, but it has a very unusual and distinctive shape. The *postparietals* are elongate bones with their centre of ossification lying at about their mid-length (Figs 4 & 6a). These bones extend posteriorly between the lateral extrascapulars. The median extrascapular is subtriangular and small, and contains the backwardly directed arc of the lateral line occipital commissure. This arrangement differs radically from that in osteolepiforms and porolepiforms, where the three extrascapulars form a transverse row behind the postparietals, tabulars and extratemporals. The nearest analogy is with rhizodonts, where the postparietals project posteriorly between the lateral extrascapulars (Andrews 1985; Long 1989; Johanson & Ahlberg 1998, 2001), but even with these, the similarity is not very close. Because the oticoccipital braincase block is almost entirely unossified apart from fragments of the otic capsules and the parachordal elements, and has left no clear impressions on the underside of the skull table, we are unable to determine whether the unusual dermal bone morphology means that the postparietals extended posterior to the occiput of the braincase. As regards other onychodonts, the postparietals seem to extend between the lateral extrascapulars in *Grossius* (Schultze 1973), but do not do so in *Strunius* (Jessen 1966).

Anteriorly, the postparietals are bordered laterally by the tabulars and supratemporals, the normal situation for osteolepiforms (apart from the Canowindridae) and rhizodonts, but not for porolepiforms or coelacanths. This is the basis for the division between skulls of types X and Y by Andrews (1973). The posterior ends of the postparietals are wider than the anterior, and at about their mid-length there is a slight lateral extension (Fig. 6a, b) that shows up on the ventral surface because it is the basis for the attachment of the tabulars. Posteriorly, the bone narrows to accommodate an expansion of the lateral extrascapula which overlaps the postparietals. Anteriorly, the bone has a zigzag margin as though it was attached to another bone, but the posterior edge of the ethmosphenoid region will not match this zigzag edge. Hence, there must have been a gap in the bones between the ethmosphenoid and the otico-occipital region of the roofs.

Medially, the postparietals have a pair of pit-lines which diverge from immediately over the centre of ossification. The longitudinal pit-line is the longer of the two. The lateral pit-line is on the same lineation as the single pit-line on the tabular.

The *median extrascapular* is small, thin and usually poorly preserved. It slightly overlaps the postparietals. It has short straight lateral faces, and concave posterolateral faces, terminating at a posterior point. Posterolateral to the postparietal is an elongate bone, the *lateral extrascapular*, which carries the postotic lateral line from the tabular. A small pit-line lies above the centre of ossification. A median commissure turns posteromedially, making an arc around the posterior of the postparietals and through the anterior half of the median extrascapula. The lateral branch runs directly posteriorly on to the posttemporal. Unlike in osteolepiforms and porolepiforms, where there is a close overlap contact between the lateral and median extrascapulars (interestingly, the median overlaps the lateral in porolepiforms, but is overlapped by it in osteolepiforms), the bones are separated by an narrow gap in *Onychodus*.

Carrying the postotic lateral line anteriorly from the lateral extrascapular is an elongate narrow bone. It overlaps the postparietal, the amount of overlap being greatest in the

https://doi.org/10.1017/S0263593300001309 Published online by Cambridge University Press

middle of its length, and it has a pit-line aligned with the lateral pit-line on the postparietal. Andrews (1973) named this bone the *tabular*. This seems to be appropriate from the point of view of the position in relation to the lateral extrascapula, the lateral line and the small pit-line. Jessen (1966) named the corresponding bone in *Strunius* as the supratemporal, using the terminology of Jarvik (1967).

In outline, the tabular in ANU 36844 is parallel sided, but in WAM 98.8.2, it is wider at the front. In BMNH P63576, figured by Long (1995, p. 188), it has an anterior end which is expanded, and the extratemporal lies mainly behind this expansion. The lateral extrascapula fits into an embayment in the outline between the tabular and the extratemporal.

The dorsal lateral line passes through the tabular, and anteriorly, it enters the *supratemporal*. This bone is wide, and in ANU 36844, it is as wide as the tabular and the extratemporal together. In other specimens, it is different in shape, although it tapers slightly towards the front.

The *extratemporal* flanks the tabular, and usually contacts the supratemporal anteriorly, although the two are separated by a lateral process of the tabular in BMNH P63576. Long (2001) recorded that, in the holotype, and in some other specimens observed by us, this bone has a small anterior spiracular opening, but this structure is not present on all specimens. This is probably because the spiracular opening lay in the adjacent soft tissue rather than in a space within the bone. A supratemporal–extratemporal contact is otherwise only known in certain rhizodonts (Long 1989; Johanson & Ahlberg 1998, 2001).

In other sarcopterygians which possess an extratemporal, this bone is in direct contact with the squamosal. However, in *O. jandemarrai*, a second triangular bone lies between the extratemporal and the squamosal, immediately anterior to the opercular and on top of the anterior end of the hyomandibular. This bone varies greatly in length between specimens. We call this element the general name of *spiracular*, because of its position and because it is difficult to understand its homology with bones in this region of other osteichthyans. In shape and position, it closely resembles the dermohyal of primitive actinopterygians such as *Mimia* (Gardiner 1984), although, unlike a true dermohyal, it is not actually fused to the hyomandibular (Long 1985a).

2.3. Ethmosphenoid dermal bones

The *premaxillae* are large bones articulated by interlocking grooves at the median symphysis (Figs 7 & 8), but not firmly fused together. The premaxillae are highest about 5 mm lateral to the mid-line. The flanks of the bone are rather flat, but medially, it turns inwards to make a rounded surface. It contains eight to 14 teeth. The lateral teeth become smaller anteriorly and disappear against the gap left for the parasymphysial tusk whorls when the jaw is closed. Another large tooth, comparable in size to those on the lateral flanks, occurs adjacent to the symphysis. Along the ventral edge of the premaxilla is a line of very small teeth, each of which has a small pulp cavity. They are not present around the gap for the tusk whorls of the mandible, but they are present against the large tooth near the mid-line (Figs 7d & 8b). The maxilla lies against the expanded posterior end of the premaxilla, and the junction is very rugose, making a strong but flexible joint.

Approximately the dorsal half of the premaxilla, rising forwards, carries sensory line pores (ANU 36844; Fig. 7d). A sensory canal runs along the upper boundary of the premaxilla, joining it posteriorly at its junction with the lateral rostral. Branches from this lateral line extend ventrally into the premaxilla and terminate in the pores described above. The lateral line continues around the edge of the median rostral just dorsal to the junction between the two premaxillae and joins the dorsal edge of the premaxilla on the other side of the specimen.

Fitting into the groove between the dorsal edges of the two premaxillae is an elongate slightly irregular bone, the *median rostral*, posterior to which are slightly irregular bones flanked with smaller irregular bones, which are the *postrostrals* (Figs 2b & 4). Even further posteriorly are two bones which have an almost median position. Each has a pointed anterior, and of course, the more posterior one fits into the groove on the anterior one. The anterior bone we name the *median postrostral*, and the posterior one the *interparietal*. It is possible that the posterior element corresponds to the pineal plate(s) of osteolepiforms and porolepiforms.

The median postrostral and the interparietal separate two large bones which form the posterior end of the ethmosphenoid segment of the skull roof. These bones have a branch of the lateral line canal passing under the posterolateral corner, but each carries an oblique, curved pit line. They lie anterior to the bones we label as the postparietals, and on these grounds, we identify them as *parietals*. As in porolepiforms, there is no intertemporal ('dermosphenotic' of Jarvik) flanking the parietal. In porolepiforms, however, the parietal ('frontodermosphenotic' of Jarvik) carries the junction between the supraorbital and infraorbital lateral line canals, and that is not the case here. Rather, these canals seem to have met in or just above the posterodorsal corner of the posterior supraorbital (see below). On ANU 72978, branches of the supraorbital canal pass into the parietal and terminate, a pit line is present. Such a pit line is not seen on other specimens available to us.

Separation of the parietals by the *interparietal* is seen elsewhere only in *Diabolepis* (Chang 1995), but the skull roof of this taxon does not otherwise resemble *Onychodus*. The separation of the parietals in *Onychodus* may be explained by the fact that two 'cushion-like' dorsal processes of the braincase rise ventral to the these bones and have a gap between them. It is across this space that the median bone extends. The lateral line canals occur only in the corner of the parietals, and this is the result of the extensive joint which would require movement of the sensory canal when the movement took place during maximum gape of the mandible. By having the lateral line in a lateral position where it joins the infraorbital canal, a minimum of extension and compression would have taken place at that junction during feeding.

Lateral to the rostrals is a line of smaller polygonal bones of various sizes carrying small perforations which are part of the lateral line system. These make an arc, and are referred to as the *nasals* (Fig. 4). The lateral lines open to the surface, usually through one perforation per bone. The bones which carry the lateral lines also have branches which show up on X-rays (Fig. 5d).

On the lateral face of the snout, dorsal to the premaxilla, is a long bone which can be recognised on all the specimens. This bone has a long contact with the premaxilla and it has a notch in each of the anterodorsal and posteroventral margins. Its posterodorsal edge is marginal to the orbit. Although this bone is very large and reaches to the orbit, we consider that it is the *lateral rostral* because it makes the ventral edge of the anterior nostril (Fig. 9a, b). The dorsal edge of this nostril is formed by a smaller bone, the *anterior tectal*. This bone also has small branches of the lateral line canal. The posterior nostril, somewhat larger than the anterior one and forming a short gutter posteroventrally, lies on the suture between the lateral rostral and lachrymal. The orbital bone dorsal to the lateral rostral is the *posterior tectal*.

The terminology applied to these bones, following on from the terms applied to the osteolepiforms or the porolepiformes,

https://doi.org/10.1017/S0263593300001309 Published online by Cambridge University Press

is made somewhat more complicated by the fact that some of these fishes have two external nostrils on each side (e.g. porolepiforms and *Onychodus*), whereas others have only one (e.g. osteolepiforms and rhizodonts). However, it is fairly clear that the single nostril of osteolepiforms and rhizodonts (e.g. Jarvik 1980; Johanson & Ahlberg 2001) corresponds positionally to the anterior nostril of porolepiforms. In *Holoptychius*, the two nostrils are closely spaced and separated by a small bone that Jarvik (1972) termed the 'nariodal', but in the more primitive porolepiforms *Porolepis* (Ahlberg 1991) and *Glyptolepis*, the nostrils are widely spaced and are separated by a bone that clearly corresponds to the lateral rostral of osteolepiforms and *Onychodus*. The 'nariodal' of *Holoptychius* appears to be a reduced version of the same bone. Thus, we feel confident about the identification of the lateral rostral in *Onychodus*, even though the corresponding bone in osteolepiforms and porolepiforms never reaches the orbit. Long has observed a similar lateral rostral in *Psarolepis*.

An unusual feature of *Onychodus* is the position of the *lachrymal*, which straddles the contact between the maxilla and premaxilla (Fig. 9a, b), almost separating the two, and which could arguably be regarded as a bone of the snout rather than of the cheek as in other sarcopterygians. It makes a short contribution to the orbital margin between the lateral rostral and the jugal, and carries lateral line pores like those on the premaxilla. The anterodorsal margin of the orbit, between the postorbital and the lateral rostral, is formed by three bones. The most anterior of these, which sutures with the lateral rostral ventrally (Figs 4 & 9a, b), corresponds to the *posterior tectal*, as illustrated by Jarvik in *Holoptychius* (Jarvik 1972, fig. 7C, D; 45) and *Eusthenopteron* (Jarvik 1980, figs. 121, 122). The two more posterior bones we identify as *supraorbital 1* and *2*. Most unusually among sarcopterygians, both of these bones are pierced by lateral line canals. The infraorbital canal, rising through the postorbital, just enters an overlap under the posterodorsal corner of supraorbital 1, and anastomoses with the supraorbital canal either in the bone or just dorsal to it. The supraorbital canal continues forward along the dorsal margins of supraorbitals 1 and 2, eventually turning laterally to pierce the body of supraorbital 2 and crossing into the posteriormost nasal.

Before leaving the orbital region, it is worth noting that some sclerotic ossicles can be seen in ANU 36844, BMNH P63576 and WAM 01.10.01. They are small, square, unornamented elements similar to those of other sarcopterygian fishes, and indeed, to early tetrapods such as *Acanthostega*. The exact number cannot be determined.

2.4. Internal structure of the ethmosphenoid dermal bones

The premaxilla has a sharp ridge running around its internal surface, rising gradually towards the front (Figs 7c & 8). Anteriorly, it fades away, and disappears at the edge of the space occupied by the parasymphysial tusk whorls. The ridge has a slightly concave ventral surface and a flat top. The latter surface provides the base for the nasal capsules, which were laterally compressed, as shown by the ethmosphenoid braincase BMNH P64125. Inserted ventrally on this ridge are the teeth, the anterior three to five being small, but with a gradual increase in size posteriorly. The more posterior teeth in this row have a thick wall, as is shown by broken sections. Ventrally in the midline, and quite independent of the lateral ridge, is a thickening which forms a boss serving two functions. First, it provides a surface in which a large tooth is situated, and secondly, it supports the thick median septum of the braincase, the median ethmoid, which separates the two spaces into which the tooth whorls of the mandible fit on jaw closure. This is best shown on the holotype WAM 92.8.2, BMNH P64125 and ANU 72978 (Figs 53a, b, 55a & 56a). The anterolateral process of the braincase is directed towards the premaxilla, and at the junction of this process and the nasal capsule ossification (see 'Braincase' below), there is a laterally facing vertical strip of unfinished bone that represents the base of the cartilaginous postnasal wall. It seems likely that the postnasal wall attached to the posterior part of the lateral rostral ventrally, and to the posterior tectal dorsally, but no distinct attachment areas can be discerned on the inner faces of these bones.

The anterior tectal has a ridge around the dorsal edge of the anterior nostril, and there is a depression in the lateral rostral on the ventral side of the nostril. This pattern confirms that the inflow of water passed dorsally to ventrally through the anterior nostril. The lateral rostral plane, which contains the dorsal edge of the posterior nostril, has a shelving edge into the nostril, and the lachrymal on the ventral side also has a shelving surface (Fig. 9b). This pattern shows that the water flow passes out of the posterior foramen in a posteroventral direction.

2.5. The cheek

The homologies of the cheek bones in onychodonts have been subject to several different interpretations. This is partly because the pattern has been poorly understood (neither *Strunius* nor *Grossius* being perfectly preserved), and partly because the cheek structure varies considerably between different sarcopterygian groups, making it difficult to establish an overall homology scheme for the Sarcopterygii. However, the excellent preservation of the Gogo material, which shows the whole cheek pattern and allows us to trace the course of the lateral lines, has allowed us to establish a robust homology scheme for the cheek plate of *Onychodus*. It agrees in essence with that proposed by Ahlberg (1991).

The maxilla is a very large bone that extends back to the articulation with the mandible. This is a feature in common with *Grossius aragonensis* Schultze and *Strunius walteri* Jessen. The posterior extent of this bone is greater than in any other sarcopterygian. The ventral edge of the maxilla is not straight, having a distinct curve ventrally near the posterior end of the tooth row. Posteriorly, the edge curves dorsally to a slightly pointed posterior corner, and ventrally, it is rounded (Fig. 3a, c). The dorsal side of the bone has a long, slightly curved edge where it overlaps the preopercular, a shorter downturned edge overlapping the squamosal, and two excavated edges against the jugal and the lachrymal, the former being partly underlapping and the latter completely underlapping the margins. The junction with the premaxilla is acute but not pointed. Internally, there is a double crested ridge into which the teeth are inserted. Posteriorly, the ridge begins above the most posterior teeth, continues forwards in an arc, increases its strength anteriorly, but then thickens and presents a sharp inner edge about 1 cm behind the junction with the premaxilla. This expanded end has a concavity into which the premaxilla fits, and the ridge connects with the ridge inside the premaxilla.

The teeth form a continuous row, but they are not uniform size (Fig. 6j). The last 10 teeth are gradually reduced in size posteriorly. The largest teeth are at the area where the maxilla has a slight ventral bow. Anteriorly, they decrease gradually in size by a small percentage. In general, the teeth on the maxilla are smaller than those on the premaxilla, and much smaller than those on the dentary (Fig. 28c). The teeth are not straight, but curve slightly backwards and inwards. The ventral edge of the maxilla, lateral to the teeth, carries small very fine denticles.

A row of four smaller bones contacts the dorsal margin of the maxilla. These are, from anterior to posterior, the lachrymal, jugal, squamosal and preopercular. There is no quadratojugal.

The lachrymal straddles the boundary between the cheek and snout, and has already been described together with the dermal snout bones. The *jugal*, readily identified by its position, its relationship to the orbit, and by the fact that it contains the junction of the infraorbital and postorbital lateral lines (Figs 9a, b, 13 & 14), is a rather small bone somewhat less than twice the size of the lachrymal. The surface of the bone carries lateral line pores as on the lachrymal, and these extend down onto the maxilla, and dorsally to the postorbital which forms the posterodorsal edge of the orbit. X-rays show that the lateral line in the jugal has many branches extending ventrally and posteriorly from the centre of the bone. The ventral ones continue into the maxilla where numerous pores occur (Fig. 14). These are of the same kind as occur on the premaxilla. These canals can also be seen on ANU 72976 where the contact with the two bones is well exposed. The other interesting feature of the jugal is the presence of a deep depression up to 2 mm deep in its surface against the orbit and extending backwards for 7 mm across the bone. The function of this depression is discussed below.

The *squamosal*, which lies immediately behind the jugal, is a large bone, with its greatest length along its dorsal edge, and its shortest edge ventrally. Anteriorly, its edge has a concavity that underlaps the postorbital, and a lesser ventral concavity that underlaps the jugal. On its ventral edge it underlaps the maxilla, and posteriorly, it overlaps the preopercular. Along its central region, the bone has a slight rounded swelling. X-rays show the position of the lateral line that runs through the lower half of the bone into the jugal. The canal outline is unarched and this is to be contrasted with members of the porolepiformes. As usual among sarcopterygians, the squamosal carries a curved pit line that runs posteroventrally from the growth centre of the bone.

Dorsal to the posterior end of the maxilla, and contacting it for nearly half its entire length, is a large bone, the *preopercular*, which carries the lateral line to the posterior margin of the cheek. The edges of this bone are completely feathered posteriorly and dorsally, its is overlapped by the squamosal anterior to it, and along its ventral edge, it is overlapped by the maxilla. The posterior edge of the bone has a slight kink, and on the inner surface at this point, the bone has a ridge which fades towards the middle of the bone. Within this ridge is the lateral line canal. Just below the centre of the lateral surface lies a short, curved pit-line. Posteriorly, the preopercular lies against the subopercular bone.

Jessen (1966) named this bone the posterior squamosal in *Strunius*, and Schultze (1973) also used the same name in *Grossius aragonensis*. Long (1985c) used the terms preopercular and squamosal for these bones in *Strunius*. In addition, Schultze did not recognise a preopercular in *Grossius*, and the small unit named preopercular? in *Strunius walteri* by Jessen is not in the preopercular position at all. Indeed, it is poorly defined and restricted to an area well below the operculars.

The main problem in interpreting the cheek of *Onychodus* is the apparent absence of a *quadratojugal*, a bone that is well developed in porolepiforms and tetrapodomorphs (rhizodonts, osteolepiforms and tetrapods), and is also present in primitive actinopterygians. This bone is usually easy to recognise, being characterised by its position at the posteroventral corner of the cheek, behind the maxilla, and by the fact that it carries a short curved pit line but is not pierced by the cheek lateral line canal. No such element can be found in *Onychodus*, despite the fact that a number of well-preserved cheek plates have been recovered, and none of the specimens shows a space where such a bone could have fitted. Furthermore, the pit-line that normally lies on the quadratojugal is found on the preopercular in *Onychodus*. Could the quadratojugal be genuinely absent? Interestingly, the cheek of *Onychodus* is in this respect comparable to those of coelacanths (Forey 1998), which also lacks a quadratojugal and carry the posterior cheek pit-line on the preopercular. An alternative interpretation is that the fusion of the quadratojugal and the preopercular is a derived state of the coelacanthiforms and the onychodontiforms.

The condition in other onychodonts is less clear. In *Grossius*, the posterior end of the cheek is unknown (Schultze 1973). In *Strunius*, Jessen (1966) reconstructed a small element in the position appropriate for a quadratojugal, but this element was shown with dotted outlines and it is not clear from the figured specimens whether it really exists as a separate bone. Thus, it is uncertain whether any onychodont possessed a quadratojugal.

There is no evidence in *Onychodus* for a *preoperculosubmandibular*, the bone in porolepiforms that carries the lateral line from the cheek to the lower jaw (Jarvik 1972, 1980). On ANU 36844, a narrow, concave bone does lie immediately posterior to the jaw hinge, in approximately the position expected for such an element (Fig. 5a). A similar small bone was extracted from ANU 72975. It lacks a lateral line canal and does not make a firm contact with the cheek bones. It has a strong ridge on the internal side and its external concave surface has a very delicate ornament, presumably indicating that it was in contact with the external skin. We consider it best interpreted as a strongly modified branchiostegal, and thus, part of the opercular series. The lateral line canal must have been carried from the cheek to the lower jaw in soft tissue, as in osteolepiforms.

Returning to the anterior part of the cheek, the *postorbital* is a large bone with a small ventral groove that connects with the groove on the jugal (Figs 12 & 13). It has a dorsal projection that runs along the edge of the supratemporal and is overlapped by that bone dorsally. The thick bone of this projection contains the lateral line canal that on ANU 72977 passes up posterior to the next orbital marginal bone, supraorbital 1, but in some individuals, appears to enter only the posterior corner of this bone. As mentioned above, the supraorbital and infraorbital canals appear to anastomose in soft tissue just dorsal to this point.

2.6. Lateral lines

These have been described above, mainly as deeply buried structures seen on X-rays. Anomalies in the distribution of some of these canals are discussed under the description of the bones themselves, but some distinctive features are pointed out here. The X-rays show a branch of the canal from the jugal into the maxilla, which is a unique feature among the sarcopterygians. The position of the canal dorsal to the postorbital is related to the intracranial gap. The position of the canal along the dorsal edge of the premaxilla is comparable to that in *Youngolepis* (Chang 1982) and *Powichthys* (Jessen 1980), but the extension of this canal into the median rostral is not clear, although the canal is present in that bone. In the mandible, the absence of the canal in the most posterior infradentary, and the splitting of the canal into the anterior end of the mandible, is not known in any other sarcopterygian.

In addition to these, there are multiple lines seen near the surface of some bones (Fig. 14). They are not linear structures leading to the next bone, but rather, very fine ramifying lines close to the surface of the bone and they appear only after the bone has been exposed to slight wear (see section on surface

detail). Each of these lines opens to the surface in a pore. They are seen on the preopercular, squamosal, jugal, maxilla and premaxilla. Each of these bones has a main lateral canal, and although it is not possible to see how these subsidiary canals develop from the main canals, they must do so. The complex in the maxilla is derived partly from the lines on the jugal, and they can be seen crossing the bone boundaries when the specimens are disassembled. The fine canals do not pass in one direction only. For example, they pass in radial directions on all bones, and even on the maxilla, where they are derived from a short canal descending from the jugal, they turn around and have branches running dorsally. This produces a sensory array of pores, and this seems to imply that it was to detect static, rather than moving surfaces. The significance of these structures is discussed under 'Function' below.

On slightly worn specimens, the dentary has evidence of similar fine lateral lines, like those on the cheek, near its anterior end.

3. Opercular series

The opercular region of *Onychodus* contains a small *spiracular*, a large and well-developed *opercular* and somewhat smaller *subopercular* (Figs 4 & 6e–i), together with a much smaller bone of unusual morphology that we tentatively interpret as a modified *branchiostegal* (see above). It is worth noting a number of points with regard to these plates.

Even allowing for distortion caused by preservation, the anterior end of the *opercular* extends forwards well along the length of the postparietals. This is also a feature of porolepiforms, in which the anterior end of the opercular is pointed.

The opercular is a thin, rhombic-shaped bone. In the specimen figured by Long (2001), the opercular is depressed slightly into the skull, and therefore, it appears to be more lenticular than it really is. The other side of the holotype shows the bone in its normal position (Fig. 4). The ventral edge of the bone is free posteroventrally, but anteroventrally, it is overlapped by the preopercular. Anteriorly, the bone is overlapped by the spiracular and the extratemporal making a V-shaped outline. These overlaps are well seen on the holotype and ANU 72976. Posterodorsally, the bone has a free edge that lies against the lateral extrascapula anteriorly and the posttemporal posteriorly. At its posterior end, the opercular overlaps the dorsal edge of the cleithrum. The opercular has a slight swelling forming a rounded longitudinal surface approximately one-third of the way from the dorsal edge.

The overlaps described above indicate that the anterior end was not free to move outwards unless the expansion of the head during mastication enabled a disarticulation to take place. However, the posterior edge may have been able to swivel outwards. The looseness of the whole structure may have allowed more movement than the overlaps suggest.

Posteroventrally, the opercular has an even arc which abuts the preopercular along a neat line (but see the next paragraph) (Figs 4b & 5a), but a small space is left in the corner between the opercular, the subopercular and the preopercular.

The *subopercular* has a more or less squarish, ovate outline, its posterior edge is rounded and feathered, and its anterior end is tapered. Despite this ovate shape, some of its edges are short and straight. The preopercular lies anteriorly to it, but the suboperculum does not reach ventrally to the point where the lateral line canal enters the preopercular. The centre of ossification is well forward, being about two-thirds of the length from the posterior margin (Fig. 6e). The dorsal edge of the subopercular and the ventral edge of the opercular facing it have a very narrow groove indicating a skin attachment which must have joined the two bones together. In Figure 4b, a gap between these two bones is illustrated. Ahlberg thought that the gap was smaller, and considered that the edges are closer together and that Figure 5a indicated that the bones are not displaced to any extent. Campbell & Barwick, in the light of evidence available from all the specimens, thought that the subopercular had been displaced forwards, and the arrangement shown in Figure 4b is a more likely interpretation. There is no clear impression on the subopercular of any overlap of the preopercular.

This places the subopercular in a peculiar position in comparison with other sarcopterygians. Posteriorly, the subopercular lies against the *dorsal process* on the clavicle and the edge of the cleithrum ventral to where the opercular fits. Where this overlap occurs, the cleithrum and the clavicle carry reduced ornament. The ornament is also reduced beyond the overlap, and the surface of the bones is slightly depressed. We conclude that the subopercular was encased in a flap of soft tissue, and this accounts for the extended range of ornamental change. This is well shown on clavicle ANU 72978 (Fig. 48c, d).

Ventral to this area, however, restoration of the shoulder girdle into life position creates a triangular gap between the ventral margin of the subopercular, the anterodorsal margin of the clavicle, and the narrow element we interpret as a branchiostegal. Functional considerations suggest that this gap must have been covered by a soft tissue flap in life, and this must have carried the lateral line canal from the preopercular to the mandible.

These observations indicate that the subopercular was a mobile element and must have had a real capacity to modify the space in the branchial chamber. Ventral to the subopercular, the gill cover seems to have consisted of a fleshy flap, supported anteriorly by the modified branchiostegal. The opercular sits in a confined space anteriorly, and it is most strongly overlapped anteroventrally. This would have been the fulcrum around which is could have moved. Its movement to modify the shape of the branchial chamber is not well understood. Overall, it appears that the gill cover became progressively more mobile ventrally.

Only the anterior end of the opercular is known in *Grossius*, but this seems to agree well with *Onychodus*. By contrast, the arrangement of the opercular series in *Onychodus* is different from that described for *Strunius* by Jessen (1966). At least some of these differences may be a result of poor preservation of the latter genus. *Strunius* is figured as having a dorsal opercula and a distinct subopercular, and agrees with *Onychodus* in the strikingly anterodorsal position of the opercular. However, in *Strunius*, the subopercular is shown as very small, and the shoulder girdle is placed so close to the skull that the cheek overlaps directly on to the cleithrum.

4. Palatoquadrate and the endopterygoid

The palatoquadrate complex of *Onychodus* differs greatly from those of osteolepiforms and porolepiforms in that only the quadrate and autopalatine portions of the palatoquadrate are ossified. Thus, the middle part of the endopterygoid is not backed by endoskeletal ossification. This condition is generally similar to the coelacanthiforms.

The *endopterygoid*, the largest dermal bone in the oral cavity (Figs 15–17), has the same general shape as those of porolepiforms and osteolepiforms (Jarvik 1972, 1980; Lebedev 1995; Long *et al.* 1997). However, its detailed structure displays several unique features. From dorsal to ventral on the anterior of the bone, it can be divided into three parts: (1) a smooth

https://doi.org/10.1017/S0263593300001309 Published online by Cambridge University Press

dorsal strip that ends anteriorly in a distinct process; (2) a middle denticulated field (by far the largest part of the bone) that also ends anteriorly in a distinct denticulated process; and (3) a ventrolateral overlap area for the ectopterygoid and dermopalatine (Figs 15f, 16a, b & 17). Posteriorly, the bone has a high, smooth surface.

The smooth dorsal sector is a flat projection with a straight dorsal edge, and anteriorly, it is extended into a process carrying two distinct projections (Fig. 15a–c). This process seems to be a functional replacement for the endoskeletal processus ascendens and processus paratemporalis seen in porolepiforms and osteolepiforms. In these groups, there is a slight extension of smooth endopterygoid bone along the mesial face of the processus ascendens, but this is nowhere near as strongly developed as in *Onychodus*. The dermal process of *Onychodus* must, like the endoskeletal processus ascendens and paratemporalis of other sarcopterygians, be related to suspension of the endopterygoid to the braincase. However, it has no articular facets at its distal end, only a jagged edge that suggests a ligamentous attachment to the suprapterygoid process of the ethmosphenoid braincase. The ethmoid and basal articulations, which are formed between the autopalatine and the ethmosphenoid braincase, also seem to have been ligamentous (see below). This contrasts with the situation in the Osteolepiformes, Porolepiformes, *Youngolepis* (Chang 1982) and *Kenichthys* (Chang & Yu 1997), where the attachment to the ethmosphenoid occurs by apparently synovial articulations with a strong basipterygoid process and an excavated autopalatine connection.

The exposed, ornamented surface of the endopterygoid is in two major parts: a posterior section separated from the anterior section by an oblique rounded edge (Fig. 15a, c, d). The edge of this ridge has a deep pit incorporated as it reaches the ventral edge of the endopterygoid. We now consider these two sections separately.

Posteriorly, there is a large blade with a rounded crest, which varies in height from individual to individual. Its palatal surface has very small denticles or more likely granules, or it may be largely smooth. The granules on the surface increase in size anteriorly and grade into those on the more exposed part of the surface. The absence of true denticulation on this part of the dermal bone indicates that it was covered by skin in the posterior part of the mouth.

Anteroventrally, the blade turns laterally, and it is backed by a solid ridge of bone, which continues forward as a flange that separates the denticulated area from the overlap areas which support the ectopterygoid and dermopalatine. Posterior to this flange, the bone flattens out to make a rounded surface acting as a brace to the vertical blade. This extends posteriorly for only half the length of the vertical blade; the posterior half of the blade, which defines the posterior part of the mesial margin of the subtemporal fossa and which carries the quadrate on the posterior end of its lateral face, is straight.

The proximal end of the oblique ridge that divides the anterior and posterior parts of the endopterygoid splits into two ridges surrounding the deep pit at the ventral edge of the denticulated area (Figs 15a, d, 16b & 17). This pit cuts into the thickened ridge described above. Much of the inner face of the pit is made of coarsely pitted bone, and these surfaces have the appearance of passing into cartilage. The floor of the pit is made of shiny bone that lines the inner face of the endopterygoid. The axis of the pit is more or less vertically directed when the endopterygoid is placed in life position. So far as we are aware, no other sarcopterygian has a comparable structure, although the oblique ridge with which it is associated is widespread among both osteolepiforms and porolepiforms (Jarvik 1980; Lebedev 1995; Long *et al*. 1997). Its interpretation is given below under 'Function'.

Anterodorsal to the above pit, the half of the denticulated endopterygoid has a dorsal and a ventral section. The dorsal section is more steeply inclined, it has finer denticles than those on the ventral section, and the two parts are separated by a shallow ridge best seen in Figures 15c and 16b, c. The denticles are rounded on their tips, and when they are broken, they have an open central space representing the pulp cavity. On the dorsal edge, some specimens show fine lines, indicating arcuate growth patterns of the bone (Fig. 15g, h), and in places, these are followed by the groups of denticles. However, these are not shown by all specimens. The surface between the denticles consists of flat, shiny bone with occasional perforations (ANU 72976), but in places, this breaks down to expose the cellular bone. The shiny bone was deposited over the cancellar bone and the denticles protrude through it. In places, the shiny layer of bone breaks away from the underlying bone, leaving a sharp edge. No sharp edge of this shiny bone shows up against the underlying bone on the surface, but it has an irregular pattern extending ventrally across the ridge separating the dorsal and ventral surfaces. Along the dorsal and particularly the anterior surfaces, the number of denticles increases, and the smooth shiny bone occupies much of the surface. This indicates that the new denticles are not all added at the margins of the bone when it is first deposited, but grew upwards after they had moved away from the bone edge.

Anterior to the deep pit, the ventral part of the denticulated face of the endopterygoid has a longitudinal concavity that varies in depth from specimen to specimen. The surface of this concavity is covered with denticles which are several times larger than those on the adjacent dorsal area (Fig. 17c). Towards the ventral edge of the plate, the denticles become more prominent and are pointed. They are surrounded by radially arranged cancellar bone, and when broken, the base of the denticle stands up slightly as a ring. The tips of the denticles are not all uniformly directed, but most of them are pointed posteromedially (Fig. 15c). Between the denticles, the cancellar bone forming the base is readily observed, but on ANU 72976, the smooth surface described above for the dorsal part extends downwards onto the anterior edge of the ventral part of the plate.

The lateral (internal) surface of the endopterygoid is covered with a thin layer of bone that has no obvious cell structure. Near the anterior and posterior margins, it shows a radial bone pattern that radiates from a centre overlying the deep pit on the exposed face of the bone, and in the middle, it is mainly smooth.

The *quadrate* has been observed on the holotype WAM 92.8.2, WAM 90.11.1 and WAM 86.9.693. It is very lightly ossified, and it is found loosely attached to the endopterygoid on one side, but on the other, it is bordered by the unossified palatoquadrate which lies against the maxilla. Because of its loose relation to these bones, the quadrate falls free during preparation. It is a triangular bone, containing vesicular bone where cartilage was attached and with an anterior edge filled with vesicular bone for attachment to the unossified median part of the palatoquadrate (Fig. 19). This attachment area is shown on Figure 19d as a smooth surface anteriorly to the coarsely vesicular bone. The equivalent part is lost on Figure 19e. Posteriorly, the bone has a long dorsal and a shorter ventral surface also made of vesicular bone, and these form a convex posterior surface (Fig. 19c, d). The junction between the dorsal and the ventral cartilaginous surfaces is angular. The significance of these structures is discussed below after the structure of the articular is discussed. It is also

https://doi.org/10.1017/S0263593300001309 Published online by Cambridge University Press

discussed under 'Function', where the method of opening the jaws as well as the mandibular junction are outlined.

The morphology of the autopalatine is unique among known sarcopterygians. It falls free of the surrounding bones, but it is easily recognised (Fig. 18). It lies on the anterior end of the inflected flange of the endopterygoid, has a flattened face that lies against the vertical wall of that bone, and projects forward as a blunt prong which articulates with the posterior edge of the flange on the internal surface of the premaxilla, and perhaps with the edge of the maxilla as well (Fig. 3b). The posterior and lateral margins of the autopalatine are formed from an open meshwork that is joined to the unossified central part of the palatoquadrate. At the anterior end of the bone is an expanded, rounded, anteriorly facing attachment surface that forms the tip of the processus and autopalatinus. It articulates with the braincase, at the ventral margin of the unossified postnasal wall, but although both contact surfaces are unfinished (indicating the presence of a joint capsule rather than a ligamentous connection), the contact seems to have been rather loose. Posterior to the processus autopalatinus, the dorsal margin of the autopalatine makes a sharp dorsal turn before ending in a short dorsal process with an unfinished top; this would have been continued dorsally by a cartilaginous processus ascendens. At the point where the dorsal process joins the dorsal margin of the processus autopalatinus, the lateral face of the autopalatine carries a triangular area of unfinished bone surface. This is the basal articulation, which articulates with the basipterygoid process of the braincase. However, there is no real shape match between the two joint surfaces (this is well shown on BMNH P64125, where both elements are preserved) and the basipterygoid process does not have an unfinished surface. This strongly suggests that the connection here was ligamentous rather than synovial.

4.1. Comparison of the palatoquadrate with other osteichthyans

The palatoquadrate of *Onychodus* seems to have been broadly similar in shape to those of osteolepiforms and porolepiforms, but differs from them in being only partly ossified. In both osteolepiforms and porolepiforms, the quadrate and the autopalatine are co-ossified with the rest of the palatoquadrate, the middle part of which forms a thin layer on the inside of the endopterygoid. As has been indicated above, the end of the quadrate shows that the middle part of the palatoquadrate was probably cartilaginous in *Onychodus*, and that it lay flat against the endopterygoid. The autopalatine supports this interpretation.

Restricted ossification of the palatoquadrate complex is also seen in coelacanths (e.g. Millot & Anthony 1958) and in derived actinopterygians, but the overall shape of the palatoquadrate in these groups differs considerably from that of *Onychodus*. Unlike coelacanths and actinopterygians, *Onychodus* also lacks a metapterygoid ossification.

The palatoquadrate complex of *Onychodus* evidently articulated with the braincase at the postnasal wall, basipterygoid process and suprapterygoid process, much as occurs in osteolepiforms and porolepiforms. However, the connections seem to have been much looser: in particular, the basal and suprapterygoid articulations appear to have been ligamentous rather than synovial, and must have allowed exceptional flexibility between palatoquadrate and the braincase.

5. Ectopterygoid, dermopalatine and predermopalatine

The lateral part of the palatoquadrate complex carries three toothed bones on its ventral surface (Figs 10 & 11). Although these elements evidently constitute the dermopalatine series of *Onychodus*, they present a major homology problem. In osteolepiforms and porolepiforms, the palatoquadrate complex carries two marginal bones, the ectopterygoid and dermopalatine, while a third bone, the vomer, rests on the ventral surface of the ethmosphenoid more or less underneath the nasal capsule. In *Onychodus*, the ethmosphenoid does not carry a vomer, and indeed, the floor of the nasal capsule is unsuited to such a role, being both exceedingly narrow and unossified. Thus, it is tempting to assume that the anterior tooth-bearing bone on the palatoquadrate of *Onychodus* is a displaced vomer, and that the middle and posterior bones are the dermopalatine and ectopterygoid.

There are two main ways of approaching this question. In coelacanths, the palatoquadrate complex carries three bones – the ectopterygoid, dermopalatine and predermopalatine in the terminology of Millot & Anthony (1958) – while a vomer is also present on the ethmosphenoid. Hence, in one other osteichthyan, the palatoquadrate carries three marginal bones, and the vomer is still present.

Thus, the question is whether the anterior of the three bones in *Onychodus* is a displaced vomer or a predermopalatine (in which case, the vomer is absent). This is a difficult question to answer, but another clue is provided by the lower jaw of *Latimeria*, which has five coronoids (including the very strange and posteriorly positioned 'posterior coronoid', a unique feature of coelacanths) rather than three, as in osteolepiforms and porolepiforms. The coronoids and dermopalatine series are corresponding elements in the lower and upper jaws, so it seems likely that there is a causal, developmentally based, connection between the number of elements in the two series. Turning now to *Onychodus*, we find that its lower jaw carries four coronoids: this seems to suggest, albeit indirectly, that this animal has an elevated number of bones in its dermopalatine series as well, and that the three tooth-bearing bones of the palatoquadrate complex should be described as ectopterygoid, dermopalatine and predermopalatine. However, we acknowledge that the grounds for preferring this interpretation are extremely weak. They would be somewhat strengthened if the (as yet unknown) palatoquadrate complex of *Psarolepis*, a genus known to possess five coronoids (Yu 1998), were to prove to have a similarly elevated number of bones.

The *ectopterygoid* is elongate and tapers away to a posterior point (Figs 10 & 11). A small embayment occurs in its median side in front of this posterior extension, and this fits around the pit at about the mid-length of the endopterygoid. The structure that occupied this pit evidently extended ventrally. Anterior to that, the plate is wider and carries two large tusks. One of these is usually missing, but some specimens have the remains of the second tusk. The bases of these tusks are slightly infolded. A row of small teeth extend along the anterior and posterior crests of the bone, ca. 12–17 posteriorly and three to five anteriorly. The teeth have the usual structure with a large pulp cavity and pointed tips. They lie close to the outer rim of the ectopterygoid. The lateral rim is high-standing, and along its crest is a row of very small closely spaced pointed denticles with pulp cavities, which run continuously along the full length of the palatal side.

The face of the ectopterygoid lying towards the endopterygoid has elongate vertical ridges on its surface, and similar structures are present on the dermopalatine and the predermopalatine. These mark the surfaces into which the teeth on the dentary fit when the jaw is closed (Figs 10b, 11 & 75). On the outer side of the ectopterygoid, a face runs along the length of the bone, and this marks the edge of the bone that fits against the ridge on the inside of the maxilla. This holds the ectopterygoid in place. The anterior end of the ectopterygoid is slightly

concave against the dermopalatine, but it has short processes which also make a more secure contact between the bones.

On several specimens, the *dermopalatine* is well preserved. These include the holotype WAM 92.8.2, WAM 90.11.1 and WAM 92.8.2, and on three ANU specimens, 72975–72977. These specimens include those with the plate in position and others in which it is completely isolated. The dermopalatine is shorter than the ectopterygoid, mainly because it has no posterior extension (Figs 15d, 16a & 17). The body is also wider. The anterior end has an elongation that extends forwards beneath the predermopalatine. Facing the maxilla is a dorsal band for the attachment to the maxilla, and ventral to that is the groove into which the teeth on the dentary fitted on jaw closure. The edge facing the endopterygoid is sharp and it lies hard against that bone. Two large tusks are present on the plate and they lies to the endopterygoidal margin. ANU 72975 has lost both tusks, but the others have both present. These tusks are the largest of those on the three bones. As with those on the ectopterygoid, they have a fluted base. One of the tusks on ANU 72977 was in process of being shed, and has resorbed enamel around the base, and exposed dentine within it (Fig. 16b). In addition to the tusks, two other rows of teeth are present. Three to six small teeth are present along the ridge anterior and posterior to the tusks. They decrease in size away from the tusks. A lateral ridge is also present and the small denticles are present along its crest. This surface is slightly expanded to the tusks and it carries more than one row of denticles.

The *predermopalatine* is attached to the dermopalatine, lying partly on the flange on the inner face of the endopterygoid. It fits against the end of the dermopalatine on ANU 72976 (Figs 15a & 16a), but it lies anterior to the end of the flange on the endopterygoid. A similar plate is present on some of the BMNH specimens, and on the holotype.

ANU 72975 has all three bones present on one side of the skull, and the predermopalatine lies on the flange inside the maxilla and the premaxilla (Fig. 10a, b). Its anterior end has a nondenticulate projection, and this is sometimes lost from specimens isolated by erosion. In position, the autopalatine lies on the predermopalatine in part, but its posterior part is also attached to the dermopalatine. The predermopalatine is large, and it has some distinctive features. It has eight small teeth anterior to the first tusk, along the palatal side of the crest. The marginal ridge is much stronger than that on the smaller specimens, and it does have more than one row of small denticles along the crest. The ridge swells in some places and there are as many as four or five rows of small denticles on the maxillary side of the crest.

In ANU 72976–72977, a small flattened surface provides attachment to the maxilla and the premaxilla, but this is smaller than the attachment areas on the ectopterygoid and the dermopalatine. The groove adjacent to this surface also contains grooves for the dentary teeth (Fig. 16a). Two tusks are present and they vary in size relative to each other. On some specimens, including the holotype, the posterior tusk is at the posterior extremity of the bone, but in others, it is a little forward. Because of this difference, the number of teeth also varies. In the former group, there are no teeth behind the tusk, but in one other specimen, there are three. A lateral ridge carrying from two to five denticles in front of the anterior tusk is bounded laterally by a slight ridge on which much smaller denticles are present. These denticles are not continuous, but form small groups of three or four separated from the adjacent ones by an undenticulated ridge (Fig. 10).

As mentioned above, our identification of the anterior tooth-bearing bone of the palatoquadrate complex as a predermopalatine carries the implication that the vomer is absent in *Onychodus*. (For further discussion, see under 'Function'.)

6. The posterior part of the palate

On the posterior part of the palate, and in the pharynx, the surface was covered with a patchwork of bone on which was situated a mass of denticulated plates (Fig. 20), or by skin with patches of bone or denticles set within it. During preparation, the plates often fall free and appear as flat plates with denticles along one edge (Fig. 20). The shape and size of the plates show a wide range of variation, and the number of denticles varies from three to about 12. The individual plates vary from triangular to a flat irregular sheet. So far as we can determine, the orientation of the denticles is not regular, although there are patches in which they have a common orientation over small areas. One plate shows a regular arrangement of three teeth on bases in rows. Other isolated patches consist of bone with closely spaced rounded elevations; others have plates of porous bone with sharp denticles attached and these show a small pulp cavity when broken; still others are long spikes with rounded denticles attached.

Denticles of this kind are often seen on the gill arches, from which they fall free. In the pharynx, they may have had a protective function when large food items were being ingested. Alternatively, they may have had a transport function for food.

7. Hyoid arch

7.1. Hyomandibula

In an animal of this kind with a kinetic skull, and a non-ossified otoccipital part of the braincase, the hyomandibula is a most important suspensory structure. Several individuals have well-preserved complete hyomandibulae, and these are robustly ossified in complete contrast to the adjacent braincase.

The hyomandibula is elongate and has a strong open attachment at each end (Fig. 22g–o). The surface details are better preserved than in most other sarcopterygians, and the orientation of the element can be established with reference to specimen ANU 36844, a laterally collapsed skull in which the right hyomandibula can be seen in lateral view in approximate life position above the palatoquadrate complex. The holotype also has a beautifully preserved hyomandibula, as BMNH P63571 also has.

The proximal end of the hyomandibula is a flaring, conical structure with robustly ossified walls but very light internal ossification. In life, the 'cone' must have contained cartilage. It is very unusual for a sarcopterygian in that there is no suggestion of a double head; the proximal end has the shape of an oval with slightly flattened sides (Figs 22i, l & 23c), and evidently represents a single articular surface. A single-headed hyomandibula characterises non-sarcopterygian groups such as actinopterygians, chondrichthyans and acanthodians (Miles 1973; Jarvik 1980; Gardiner 1984), suggesting that this is the primitive state for the gnathostomes as a whole. The early and primitive sarcopterygian *Psarolepis* probably also had a single-headed hyomandibula, judging by the articulation facet for it on the braincase (Yu 1998). Long, after observation of the Chinese specimens, confirmed that the hyomandibula was single-headed in *Psarolepis*.

The overall morphology of the hyomandibula of *Onychodus* is best described as propeller-shaped. The long axis is virtually

https://doi.org/10.1017/S0263593300001309 Published online by Cambridge University Press

straight, and a narrow waist unites the flared, flattened ends, the axes of flattening of which lies at about 55° to each other. If the proximal end is oriented with its axis of flattening vertical, which we believe is anatomically correct, the axis of flattening of the distal end runs from ventrolateral to dorsomesial, at an angle of about 35° to the horizontal. Thus, the two broad faces of the distal part of the hyomandibula can be described as dorsolateral and ventromesial, whereas the broad faces of the proximal part are mesial and lateral. The following description is based on this orientation.

The general shape of the proximal part of the hyomandibula is, as mentioned above, a gently tapering cone with flattened sides (Fig. 22g, h). Along the dorsal surface of this cone runs a smooth ridge, originating about halfway along its length, somewhat asymmetrically towards the lateral face of the bone, but leaning mesially, that rises gradually and becomes sharper towards the middle of the bone. Past the middle, it decreases gradually in height (Figs 22k & 23b, c), but continues to be recognisable until it fades out on the dorsolateral surface of the flattened distal end of the bone. This crest seems to correspond to that labelled 'opercular process' in *Eusthenopteron* by Jarvik (1980), to an unlabelled dorsal crest in *Moythomasia durgaringa* (Gardiner 1984) and to a well-developed opercular process in *Howqualepis* (Long 1988). However, *Onychodus* differs substantially from these genera, and indeed, from most osteichthyans, in that there is no hyomandibular canal. It is very difficult to determine the course of the truncus hyomandibularis and efferent hyoid artery in *Onychodus* since the hyomandibula does not even show any distinct external grooves for these structures. We tentatively suggest that they ran across the dorsal surface of the bone, mesial to the aforementioned crest, because there seems to be no other sensible place to put them. However, this casts doubt on the identification of the dorsal crest with the opercular process of *Eusthenopteron* and *Moythomasia*.

Another lower but sharper crest runs along the ventral face of the proximal part of the hyomandibula. This also leans mesially and, once past the middle of the bone, extends onto the mesial part of the ventromesial face of the flaring distal end, where it joins the mesial margin of a large muscle attachment. The effect of these dorsal and ventral crests, both leaning towards the mesial face of the hyomandibula, is to make the middle part of the bone faintly concave in mesial view and distinctly convex in lateral view. The textures of the two faces are also different, the lateral face being quite coarsely striated anteriorly (the striae radiating approximately from the centre of the bone), while the mesial face is much smoother (Fig. 22g, h). A fairly large opening, presumably for a blood vessel, lies in the ventral midline at the proximal end of the ventral crest, and another, similar one lies on the lateral side of the crest just past the middle of the bone.

The distal part of the hyomandibula has distinctly different dorsolateral and ventromesial surfaces. The dorsolateral surface is essentially featureless, gently convex or flat depending on the individual specimen, whereas the ventromesial surface carries a large and deep muscle scar that occupies approximately the lateral three-quarters of the surface (Fig. 22g, j). The extent of this muscle scar seems to correspond to a subdivision of the distal end into a large lateral and a small mesial articular facet, although it should be noted that this subdivision is marked on the distal face purely by a slight change of orientation of the margin, not by any ossified boundary. It appears that the hyomandibula articulated distally with a large lateral element, connected to it by a powerful muscle, and a smaller mesial element that was not associated with such a powerful muscle, but may have had a ligament attachment. The significance of this pattern is discussed further below.

Along the mesial edge of the distal part of the hyomandibula runs a narrow depressed surface, bounded laterally by the distal end of the aforementioned ventral crest, and mesially by the mesial margin of the bone. Anteriorly, this depression extends onto the slightly concave mesial face of the middle part of the bone, but even its anterior end is faintly demarcated against this concave surface and seems to represent a separate structure. This depressed surface has the appearance of a muscle attachment, but unlike the aforementioned large muscle scar, it does not flare distally towards the articular facets, and does not seem to have served for a muscle running onto the more distal parts of the hyoid arch.

As can be seen, the hyomandibula of *Onychodus* provides a wealth of morphological detail, but it is very distinctive and consequently quite difficult to interpret. The identity of the dorsal crest has already been discussed. The narrow depressed surface between the distal part of the ventral crest and the mesial edge of the bone is, judging by its position and orientation, most probably the attachment for the adductor hyomandibulae muscle. Thus, the middle and anterior parts of the ventral crest should represent the boundary between the spiracular tract lying against the lateral face of the bone, and the solid soft tissue (including the adductor hyomandibulae, and more dorsally the truncus hyomandibularis and efferent hyoid artery) that invested the mesial face.

This leaves the question of the large muscle scar on the ventromesial face of the distal end. We have already noted that the hyomandibula seems to have articulated distally with two elements, a robust lateral bone and a slender mesial bone, and we believe that we have examples of the former and possibly the latter (see below). By comparison with *Amia* (Jarvik 1980; Grande & Bemis, 1998) and *Latimeria* (Millot & Anthony 1958), the lateral element should be the symplectic, and distally, it should articulate with the mandibular arch in the region of the jaw hinge, whereas the mesial element should be the stylohyal and should link the hyomandibula to the ceratohyal. Thus, it appears that a powerful ventromesial muscle ran from the hyomandibular onto the symplectic, and functioned as a flexor muscle for this part of the hyoid arch.

Such an arrangement makes functional sense since contraction of this muscle would depress the jaw hinge, and thus, contribute to the opening of the mouth and the rotation of the intracranial joint, but the fact remains that no comparable muscle is known in either *Amia* or *Latimeria*. These fishes have exclusively ligamentous connections between the hyomandibula and the more distal elements of the hyoid arch. Nevertheless, the ventromesial depression on the hyomandibula of *Onychodus* so clearly has the appearance of a muscle scar (and furthermore, is matched by a concavity on the ventromesial face of the symplectic) that were are forced to conclude that a muscle was present in this position. Thus, the hyoid arch of *Onychodus* was functionally as well as morphologically distinctive.

7.2. Symplectic

The right hyomandibula of ANU 72975 is associated with a smaller element that fits very well against the larger, lateral, of the two distal facets (Fig. 22a–d). A similar bone occurs in ANU 72976 and WAM 92.8.2. We interpret this element as a *symplectic*. It has a rather complex shape, narrowing rapidly from the proximal end to the mid-length, and then being almost parallel-sided. The proximal end is transverse, and the distal end is D-shaped. Both ends are open, containing little internal ossification, and were presumably finished (or perhaps continued) in cartilage (see below). The face joining the end of

the hyomandibula with the large muscle scar, is gently concave and it has an irregular surface on which a muscle scar is preserved (Fig. 22a, c). The other face is gently convex and it has no indication of muscle scars. The bone is not sufficiently long to reach the end of the ceratohyal, although the ceratohyal probably had a second unit made of cartilage. It was probable that the symplectic had a cartilage extension both proximally and distally, the latter extension probably being the longer.

7.3. ?Stylohyal

ANU 72975 also contains a fragment of a narrower pharyngeal arch element that fits quite well against the smaller facet on the hyomandibula, which may accordingly represent the stylohyal. However, this fragment is too small and featureless to allow for either positive identification or a meaningful description.

7.4. Basibranchial

A short, rounded bone seen in ANU 72978, and a similar but broken bone from the holotype WAM 92.8.2, are regarded as basibranchials (Figs 24 & 25). These specimens are medial bones, and have similar attachment surfaces on either side, giving the general form of a basibranchial. At first sight, it appears to have too few attachments to belong to a normal sarcopterygian, and it has a deep groove on the ventral surface not found in any other member of that group. This cavity is very different from the groove described by Jarvik (1972) in *Glyptolepis groenlandica*, which is at the posterior end of the unit. In *Onychodus*, the groove runs the length of the unit. It may have been for the attachment of the sternohyoideus muscle, as indicated by Lebedev (1995, fig. 18), or it may have been the attachment for the long sublingual rod.

The body of the element is in two parts. The anterior end has a concave surface with a raised edge laterally and posteriorly. This surface is covered with longitudinal striae on perichondral bone (Figs 24a, c & 25a). Posterior to this unit is the second unit separated off by a deep transverse furrow, within which it is possible to see a surface without perichondral bone, and showing nodes as seen on the cartilage bone. The anterior unit is basibranchial 1 and the posterior one is basibranchial 2, but the two units have been fused.

Once this fusion is accepted, it is possible to understand the other attachment surfaces. Anteriorly, there is an arcuate scar the dorsal part of which is separated from the ventral by a change in slope. The dorsal part was for the attachment of the hypohyal, and the ventral part, which is twice the size of the dorsal part, was for the attachment of the hypobranchial 1. The scars are illustrated in Figure 25.

This arcuate scar continues around the ventral surface onto a very large scar that occupies the posterolateral side of the whole unit. The anterior part of this scar was for the attachment of the hypobranchial 2, and the posterior part, which corresponds with the flanks of the basibranchial 2 element, was for the attachment of hypobranchial 3. There is no sharp division on the scar to separate these two attachment elements. As can be seen from this analysis, the attachments have been interpreted as though the basibranchial has the characteristics of a normal sarcopterygian.

At the posterior end of the basibranchial 2 is a scar that we interpret as the attachment of the urohyal, which is not found in our collection. From what we consider to be the anterior end of the basibranchial, we have identified an elongate bone with a distinctive posterior end, and we consider it to be the sublingual rod (Fig. 27o). It is approximately three times as long as the basibranchial. The basibranchial shows no sign of an attachment surface, and we conclude that the sublingual rod lay in the groove in its anterior margin. The length of this rod is no doubt related to the long space that existed between the symphysis of the lower jaws and the tip of the branchial apparatus posteriorly, and this indicates the position of the basibranchial with respect to the total buccal arrangement.

7.5. Ceratohyals

The holotype, WAM 86.9.693, ANU 72975, ANU 72976 and ANU 72978 have paired bones in the branchial series (Fig. 26). Other specimens from which isolated bones were retained are also available. These bones were obviously well ossified, and formed stable elements in the series. It is also larger than the other branchial elements. All these features suggest that they are ceratohyals, but it is necessary to demonstrate this by other means. Fortunately, the necessary evidence is provided by BMNH P63566, which preserves the ventral part of the branchial skeleton in life position on top of articulated gular plates. In this specimen, the aforementioned bones can be seen lying at the front of the series of ceratobranchials, some little way posterior to the basibranchial, and immediately below the hyomandibulae.

The surface of the ceratohyals is covered with moderately thick periosteal bone, and their ends are made up of open coarsely ossified tissue. The outer surface is convex and the inner surface is concave with a number of pits in the mid-length of the bone (Fig. 26d, e. g). These usually extend into radial grooves on the surface. Along the ventral edge is a shallow groove on many specimens (Fig. 26e, g), which we consider is the site of the efferent epibranchial artery of the first branchial unit (see Lebedev 1995, fig. 17a, for this position in *Medoevia*).

In outline, the narrowest part of the bone is mid-length, and both ends are expanded. The proximal end has a large open space for the junction with the hypohyal (Fig. 26i, j). This is a strongly arcuate opening, giving the appearance of an attachment to a second structure. Alternatively, the hypohyal could have had a broad curved attachment surface. In many sarcopterygians, this junction is small, but in others, it is large because the attachment surface lies against the length of the hypohyal (*Medoevia* described by Lebedev 1995, fig. 18). BMNH P63566 shows no connecting element between the ceratohyal and the basibranchial, indicating that the hypohyal was cartilaginous. The distal end looks similar to the proximal end, is filled with coarsely ossified bone and has a double termination (Fig. 26e, h, j. k. l). It is slightly smaller than the proximal end. We consider that this was for the attachment of the second ceratohyal, which was entirely cartilaginous.

8. Branchial arches

Many branchial arches have been isolated during etching. These have not been put back together in a confident manner. Specimen BMNH P63566 has the branchial arches all crushed together with the anocleithrum, but details are not preserved. The holotype has isolated fragments which can be photographed independently, as have WAM 86.9.693 and WAM 01.10.04. Specimen ANU 72976 has an opercular with parts of the arches attached to its inner face. All these specimens provide some clues for a reassembly.

8.1. Hypobranchials

Hypobranchials have been recognised by the shape of the terminations. The best specimen, WAM 92.8.2, is bent longitudinally, has an open distal end and a proximal end with a small scar, and on one lateral side is a projection that has the

https://doi.org/10.1017/S0263593300001309 Published online by Cambridge University Press

appearance of an attached surface (Fig. 27e, f). Furrows on the surfaces are weak. The open end would have been for the attachment of the ceratobranchials, the small scar would have been for the attachment to the basibranchial, and the lateral scar for the junction between it and the adjacent hypobranchials. Other units are not so clearly defined, but they have weak transverse furrows, and openings at each end; the proximal one for the attachment to the basibranchial and the distal one for the ceratobranchial. A small lateral scar is for an attachment to the neighbouring hypobranchial (Fig. 27i–j). These show a similarity to *Glyptolepis*, as figured by Jarvik (1972, fig. 29), which has the hypobranchials attached to the adjacent units. This similarity is not unexpected given the similarity between the basibranchials in the two groups.

8.2. Ceratobranchials

The ceratobranchials are straight to slightly curved, which is what would be expected from the various positions in which they lie in the series (Fig. 27k–n). Each has a deep furrow for the branchial nerve and efferent artery along its length. This usually fades towards one end, where the ceratobranchial becomes narrower. At the broad end, the opening of the bone has the cross-section of a deep arc around the branchial furrow, whereas the opening is less indented at the other end.

8.3. Epibranchials and pharyngobranchials

The epibranchials show a variety of forms, which is not surprising given the situation in *Eusthenopteron* where the infrapharyngobranchials and the suprapharyngobranchials, which are supported by the epibranchials, are so variable in shape. Two specimens show a distinctive morphology, divided at one end but with a single attachment at the other (Fig. 27a–d). The attachments are different in relative size in the two specimens. BMNH P63566 has a pair of these elements in an anterior and dorsal position within the gill region (one largely covered by the anocleithrum), indicating that they are probably first gill arch elements. The dividend end is posterior, with the diverging branch oriented dorsolaterally. We infer that this element corresponds to the suprapharyngo-infrapharyngobranchial of *Eusthenopteron* (Jarvik 1980, fig. 111). The main axis represents the infrapharyngobranchial, articulating with the braincase anteriorly and the epibranchial posteriorly, while the diverging branch represents the suprapharyngobranchial. Note that this element in *Eusthenopteron* has a small separate dorsal tip, presumably corresponding to the (inferred) cartilaginous element that articulated with the unfinished tip of the dorsolateral branch of *Onychodus*.

9. Mandible

The mandible of *Onychodus* is unusual in a number of respects: first, the Meckel's Cartilage is entirely unossified apart from a small articular ossification at the posterior end; secondly, the dermal bone pattern has a number of unique features; and thirdly, the anterior part of the jaw is modified to accommodate a very large parasymphysial tusk whorl.

9.1. Dentary

This element is well preserved in a number of individuals. Viewed dorsally, it is only slightly curved, indicating (as does the curvature of the premaxilla and maxilla) that, in dorsal view, the head of *Onychodus* tapered to a pointed snout. Both longitudinally and vertically, its external face is only slightly convex. Posteriorly, it tapers to a point and the posteriormost part of its dorsal edge is overlapped by the maxilla (Figs 5 & 28).

Internally, there is a strong flange that runs from the posterior end of the tooth row to the anterior end of the bone (Fig. 28c). Posteriorly, this flange is narrow and has a sharp ventral inner edge, and this joins the dorsal edge to make a sharp posterior end to the flange. The anterior part of the flange thickens and has a flat inner surface with a sharp ventral edge. As it approaches the anterior end, the flange becomes so thick that it occupies two-thirds of the height of the dentary (Fig. 28c). At its anterior end, it forms a robust shoulder, here named the symphysial plate.

Our interpretation of this structure depends partly on the shapes of the structures themselves, but also on the discovery of a mandible in the Middle Devonian Cravens Peak Beds of the Georgina Basin in Queensland, Australia, shown to us by Dr Gavin Young, and described by Young and Schultze (2005). In the Georgina Basin onychodont, the Meckel's Cartilage forms a distinct slightly concave trough for the tooth whorl. The dentary ridge in this specimen is much smaller than in *O. jandemarrai*, and the Meckel's Cartilage is an extensive body extending posteriorly under a thinner flange on the dentary. At its anterior end, Meckel's Cartilage expands dorsally and passes through a slight depression onto the inner face of the dentary. A similar pattern is observed in *O. jandemarrai*. We infer that the parasymphysial tusk whorl in *O. jandemarrai* sat in a trough of Meckel's Cartilage, within which was a layer of soft tissue that deposited the tusk whorls. This seems to be comparable with the situation in *Psarolepis* (Yu 1998). The inferred outline of the Meckel's Cartilage is shown as a broken line on Figure 38b.

The parasymphysial tusk whorl rested against soft tissue on the surface of the Meckel's Cartilage in life (Figs 33a, 38 & 42e). The centre of radiation of the symphysial plate lies in the middle part of this shoulder. As shown in the above-mentioned figures, the radial growth lines on this plate terminate posteriorly against the flange on the inner surface of the dentary. This morphology contrasts with that of the holoptychiids, where the parasymphysial tooth whorl rests on top of an expanded lamina of the dentary (Jarvik 1972, 1980; Ahlberg 1992). The shape of the anterior end of the dentary, and the lack of a defined contact area for its antimere, indicates that there was no strong dentary symphysis; the mandibular rami must have been held together by connective tissue and by a symphysis between the unossified Meckel's Cartilages. This suggests considerable flexibility of the gape.

The marginal teeth sit in a slight depression in the dorsal surface on the flange along the median face of the dentary (Fig. 28c), the inner margin of which is angled. At its anterior end, the tooth-bearing furrow narrows between the marginal lamina of the dentary and the top of the shoulder for the parasymphysial tusk whorl (Fig. 36b, c), which approaches the marginal lamina very closely without merging with it. This carries the interesting implication that the parasymphysial tusk plate attachment of *Onychodus* is somewhat more mesially located than that of porolepiforms. The latter extends laterally (i.e. externally) to the same level as the tooth row, and replaces the tooth row in the anteriormost part of the dentary (Jarvik 1972; Ahlberg 1992).

The smallest teeth of the dentary are anteriorly and posteriorly placed (Fig. 42f, e), three or four at each end of the row. The largest ones occupy most of the length of the dentary. These teeth are distinctly larger than those on the opposing parts of the maxilla. They are concave inwards and are sharply pointed. They are separated by replacement pits, which are ovate in shape in dorsal view, and project into the median ridge. Some specimens, especially ANU 72978 and

ANU 42975 (Fig. 42e, f), show a regular pattern of tooth absence, but we consider that this is accidental. Except at the anterior and posterior ends of the tooth row, every second tooth is missing. This gives the appearance that replacement of the teeth takes place alternately. Other specimens do not show this regularity of tooth omission (Fig. 28c). In a few places, the teeth which were to be shed, still have some of the basal tissue present, and this is much thinned. The process of tooth loss involves resorption of the inner walls around the pulp cavity, making shedding easier (Fig. 42e, f). This is well shown on ANU 72978.

The bases of the teeth have a crenulated surface, but the crenules do not extend upwards on the flanks of the teeth. Some of the spaces between the teeth have crenules around their edges and so confirm the view that they are spaces for missing teeth rather than gaps into which maxillary teeth occluded. In any case, as has been shown above, the dentary teeth do not occlude with the teeth on the upper jaw, but fit into the gap between the maxillary and the dermopalatine tooth rows (Figs 10 & 75). Where most of the small marginal teeth have been removed, the base of the tusk cavity is smooth, but occasionally, the bottom of the tooth is preserved. Although the upper parts of the teeth show no flexure, the base before it enters the bone is highly fluted. Individual crenules are often subdivided on the external surface, but internally, the subdivisions are clear. These show the fluted base to have a branching substance forming a meshwork of tissue lying in the underlying bone.

Along the lateral crest of the dentary, a number of small pointed denticles form a continuous line. On some specimens, it is a single line of denticles, but on others, there is a double line, and some of the denticles are stronger than those elsewhere. These are not granules such as those on the outer face of the dentary. They all have sharp tips, a conical shape and a definite pulp canal.

The likely relationship between the anterior end of the dentary and Meckel's Cartilage is discussed below, in connection with the parasymphysial tusk whorl.

9.2. Tusks and denticles on the parasymphysial whorls

These are well exposed on several specimens. Juveniles have more tusks than the adults, and specimens available to us, along with some individuals in the BMNH, have only three tusks (Fig. 28). New tusks are added at the posterior end of the whorl and the older tusks are lost anteriorly (Figs 29 & 37). Examination of a growth series shows that, during growth, new tusks were inserted at wider angles to the preceding tusks. Five tusks on ANU 72978 are separated from one another by angles of 20°, and occupy the same circumferential space as three tusks on ANU 72975, which are separated from one another by 40–45°.

Individual tusks are slightly ovate in cross-section towards their dorsal ends, but part of each tooth has a slight keel in the mid-lines along both their anterior and posterior faces. In lateral view, the tusks are curved posteriorly, except at their tips, where they have a slight forward tilt. The ventral part has a groove along the posterior face before it enters the whorl, and in this respect, they are similar to the tusks of *Onychodus jaekeli*, figured by Gross (1965, fig. 1d, e, g). The tusks fit almost orthogonally into the whorls (Figs 29a, d & 32), and not obliquely, as shown by Gross (1965, fig. 1f) for *Onychodus jaekeli*. He reconstructed the two whorls as being in contact medially, and certainly, *O. jandemarrai* is not of this kind, its two whorls being completely separate.

Small, pointed denticles are present along the flanks of the whorls. In adult specimens, several denticles lie between the tusks, and their tips project towards the mid-line (Figs 29d, h & 30); they are inclined against the tusks, and are more or less parallel with the whorls or are missing (Figs 29d & 30). In juvenile specimens, there are fewer small denticles between the tusks, and those against the tusks stand more nearly vertically (Figs 29a, e, 31 & 32). These denticles are all conical, and have a continuous or a discontinuous enamel covering. This is well shown by the scanning electron micrographs (SEMs) (Fig. 39) and the surface shows longitudinal ridges. In some individuals, these ridges are continuous and are of varying height along their length. On other denticles, the elevations form an irregular mass near the base, and merge into irregular ridges in places.

In each individual, tusks are well separated as new tusks are inserted, and so the denticles can be oriented in each position between the tusks. Once inserted, the denticles do not change their orientation during growth. This implies that the denticles in adults form an incomplete palisade across the spaces between the tusks. Because their surfaces must have been covered with ectodermal cells, the barrier would have been effective in keeping out loose food from the whorl tissue during feeding.

9.3. Structure of the parasymphysial whorls

The lateral faces of the whorls are not encompassed by any layers of thick tissue, and they are quite unlike *Strunius walteri* (Jessen 1966, fig. 10) in this respect. The outside layer of the whorls consists of a thin layer of tissue containing parallel layers indicating growth lines (Fig. 29c, e, j, k). In young specimens, these lines are parallel with the dorsal edge of the whorl, but are at an angle with the ventral edge (Fig 29b, f), indicating where the new layers of tissue are added during growth. In juveniles, the lateral walls of a single whorl do not meet, leaving a narrow ventral space between the walls over most of their length (Figs 29g & 31). There is also a wider open space left at the posterior end, indicating where the new tusks were added. This implies that the lateral walls of the whorls increased in length posteriorly and ventrally during growth.

Several specimens show the insertion of a new tusk, the best being an adult (ANU 72975) and a younger individual (ANU 72978). In each case, the tusk wall is separated from the outer wall of the whorl by a slight gap (Fig. 29f, g). In the adult specimen, there are small denticles inserted in the space between the new tusks and the walls of the whorl. These denticles are inclined to the top of the outer wall (Fig. 39) and do not reach the top level of that wall (Fig. 29h). The bases of the denticles are attached into the calcified cartilage (see below) immediately inside the external wall. The vesicular tissue (calcified cartilage as demonstrated in detail later) occupying the space between the walls of the whorl does not expand to cover the base of the tusk, and this must be added subsequently to enclose the tusk. This means that the dental lamina in which the tusk grew was sitting loosely in the walls, and subsequent growth saw the calcified cartilage tissue invest the base and the sides of the tusk. The uninserted tusks have open ends before insertion (Fig. 42g). The growth lines which appear on the outside wall must have been first deposited before the internal filling took place. In that case, they mark the advance of the calcification of the external walls as they grew ventrally and posteriorly during the insertion of new tusks into the calcified area.

At the early growth phases of the whorls, the two sides of the whorls do not meet at the base, but with further growth, junction takes place and only a small area at the posterior base is open for the insertion of new teeth. This also confirms the interpretation that the new tusks are added posteriorly. In adult specimens, the growth layers on the outer walls are almost parallel with the ventral edge, indicating that the

https://doi.org/10.1017/S0263593300001309 Published online by Cambridge University Press

addition of new tusks during the growth of the animal had been almost completed (Fig. 29i). The ventral growth lines are very closely spaced and are parallel to the ventral edge (Fig. 29j). Also in adults, the external surface contains a large number of perforations (Fig. 29k), but on the juveniles, these are proportionately smaller. This raises the question of what was attached to this surface. One possibility is that tendons at the end of muscles on the floor of the mandible were attached, and this would solve the problem of the retraction of the whorls during predation. This will be discussed below under 'Function'.

There is some wear at the anterior end of the whorls, but sufficient bone is preserved to show that resorption was taking place and teeth were being lost. The process of resorption involved the removal of the outer layer of the whorl at the anterior end, and the subsequent removal of the inner tissue of the whorl. This is well shown on one adult and some juvenile individuals (Fig. 29b, c, e).

9.3.1. Composition of the whorls. Beneath this external layer is a mass of fine-grained highly perforate hard tissue. Similar tissue occupies the entire whorl (Figs 34–36), as can be seen in eroded specimens or in thin sections. Well-preserved specimens show the material between the individual tusks to be made of the same substance.

The nature of this material is of major interest. We have examined the substance in optical thin sections, and by SEM examination of the broken surfaces and a transverse section. A cross-section of a whorl with the base of a tusk inserted shows the main features (Figs 34a, b & 35a–e). The base of the tusk shows sections of the infolded surfaces. Figure 34a shows that the marginal layers of the whorl are made of a series of rounded structures, some of which are almost circular and others oval. This outer layer of hard tissue shows no sign of banding parallel with the whorl surface. The central part of the whorl is made of more elongate layers of tissue which enclose open canals which housed nerves and vessels. There is no sharp boundary between these two types of tissue. Surprisingly, the marginal layers do not show evidence of finer banding such as would be expected from the external surfaces described above, although the coarser banding is obvious.

As shown in the vertical thin section illustrated in Figure 34a, b, each layer of hard tissue is composed of two units. The inner unit, which makes up the main part of the tissue, is dark coloured in the photograph, and in places has small perforations. The outer unit is light coloured and invests the other layer. No evidence of bone-like structure is present.

Two other ways of investigating the nature of this material have been used. The first method is the examination of the lateral whorl tissue in broken surfaces around the base of a tusk. In these illustrations, we are observing the surfaces cut through the tissue and not sections broken through it. The results of this are shown in Figure 36. Figure 36d–f, made from the place indicated by an arrow in Figure 36a, show increasing enlargements of the tissue. Figure 36d, e shows the apparently solid material composed of globular substance. In the space between them is a thin layer of smooth material. Figure 36e shows the hard layer made of globules of substance, and Figure 36f shows these globules to be made of loosely bound material. We consider that these globules are the same as those illustrated in the section of Figure 35c.

In the second method, a vertical edge of the base of a tusk lying in the whorl tissue shows details of a broken surface. The vertical section is illustrated on Figure 36. In Figure 36a, the folded tissue turned into the base of a tusk is clear, and to its left, further whorl tissue is present. Figure 36b is an enlargement of the wall of the cavity of the tusk that has broken away. Figure 36c is a further enlargement of the area outlined in Figure 36b. These illustrations show a mass of very fine tissue making up the hard layers and a layer of soft material lining the cavities in the walls. Figures 36d–e shows increasing enlargements of the lateral walls. The globules of hard tissue become more obvious as the enlargement increases.

In no sections can we find any evidence of bone present in the whorls that surround the teeth. On the contrary, the tissue of the whorls is composed of globular tissue, as shown in Figure 36f. As we have indicated elsewhere, the tooth walls lie in a cavity surrounded by the Meckel's Cartilage, and it is not in contact with the dermal bone of the mandible. We have concluded that the whorl is made of calcified cartilage.

9.3.2. Growth organisation of the whorls. The illustrated SEM vertical section of the whorl shown in Figure 34a, has the ventral edge broken off, but the optical section that was cut from an adjacent slice has this edge present. It shows no sign of a junction between the two sides of the whorl and shows continuous growth. As we have seen above, growth took place ventrally and posteriorly, and the old tissue was lost by resorption anteriorly. Once the two sides of the whorl have joined, the ventral edge is continuous and no new tissue is added to it.

The calcified whorl tissue contains a large number of perforations and canals which have the appearance of nerve and vascular channels. These are strongest along the ventral edge of the whorls, where they run parallel with the edge. Dorsal canals run off these in groups to supply nerves and blood vessels to the teeth. The arrangement of the canals in the vertical section is shown in Figure 34a, b.

9.4. Relationship with Meckel's Cartilage

The banding of the outer faces of the whorls, the layers of new tissue and the ventral separation of the two walls from each other in the early growth stages demonstrate that the surface of the tooth whorls were enclosed in some soft tissue. Alternatively, the wall was made by the hardening of tissue that previously formed the wall before it was calcified and this produced successive banding. It is interesting in this context to consider the relationship between the tusk whorl and Meckel's Cartilage, the inferred outline of which is shown as a broken line under an overhang of a dentary ridge, and as a complete line against the symphysial plate on Figure 38b.

9.5 Growth of the parasymphysial structures

ANU 36844 shows a number of small isolated parasymphysial tusks with thin proximal dentine, i.e. without attachments to the tooth whorls (Fig. 5a). BMNH P63566, which shows the lower jaws, gular plates and clavicles in undisturbed life positions, has a group of similar tusks forming a cluster anterior to the gulars and posterior to the junction between the two rami of the mandible (Fig. 46a). BMNH P63572 also has a cluster of three tusks with thin-walled proximal ends, and these decrease in size posteriorly. Also on the same specimen is a second group of four teeth in sequence decreasing in size posteriorly (Fig. 42g). Specimen BMNH P63571 also has isolated tusks which have not been integrated into whorls.

These tusks show early growth stages, and they lie in the area posterior to the parasymphysial whorls. Obviously they were not attached to any bone and they were being deposited in dental lamellae in the space anterodorsal to the gulars. When these teeth are undisturbed, their orientation is distinctively different from that of the attached teeth on the whorl: they are stacked closely one in front of another, the smallest at the posterior, and their tips are adjacent (Fig. 42g).

As we have indicated above, old tusks were being shed anteriorly, and new ones added posteriorly. Specimen

https://doi.org/10.1017/S0263593300001309 Published online by Cambridge University Press

ANU 72978, shows a newly inserted tooth without basal attachment, and not yet grasped by the lateral walls of the whorl (Fig. 29f, g). This, together with the shape of the lateral walls, suggests that the ossified lateral walls of the whorl were growing posteriorly and embracing newly formed teeth. Although the base of the tusk shows no evidence of detailed interfolding apart from the large folds, more complex folding occurs as the tusk is incorporated into the whorl. This is best illustrated by the examination of the base of a tusk in an adult in the middle part of a series of three tusks (Fig. 30). This tusk has been completely incorporated in the whorl, presumably as the cartilage was ossified more posteriorly. The interpretation of the insertion of the new tusks is shown in Figure 37.

What then was the matrix within which the new tusks were forming and reaching an appropriate size before being incorporated into the whorl? We consider that the walls of the whorl were extended posteriorly as an unhardened trough within which dental lamellae were incorporated. This agrees well with the structure of the loose tusks which consist of open-ended cones; they grow by the addition of cones of dentine on their inner surfaces (Fig. 35e). It also fits in well with the observations made on the nature of the walls themselves, which we have interpreted as calcified cartilage. This was probably surrounded by a thin layer of soft tissue lying on Meckel's Cartilage.

Such a method of growth explains a number of other phenomena. The embracing of a new tooth would require an outgrowth of enclosing hard tissue that would give strength to the bite. This is done by making a branching folded base (Fig. 30), but these folds are not of the same kind as occurs in osteolepiforms. Secondly, the spacing of the teeth changes during growth, larger and more widely spaced teeth being produced during the last phases of growth. Thirdly, it explains why the banding on the walls has the peculiar resorption at the anterior end and growth at the posterior end, and the junction between the walls ventrally.

It is worth nothing here that parasymphysial tusks are widespread among sarcopterygians, being present in porolepiforms, *Powichthys*, *Youngolepis*, *Psarolepis* and *Achoania* (Jarvik 1972; Jessen 1980; Chang 1991; Yu 1998; Zhu & Schultze 2001). This discussion presents the first direct evidence for the mode of growth and tusk replacement in osteichthyan parasymphysial whorls.

9.6. Histology of the tusks and teeth

Ørvig (1957) illustrated two parasymphysial whorls of *Onychodus* in a paper dealing with bone and tooth histology of 'crossopterygians', but he did not section these specimens. However, in 1968, Peyer (English Translation) illustrated two vertical sections of *Onychodus sigmoides*) from the Middle Devonian of Delaware. These show the thick enamel overlaying many banded layers of dentine. The tusks of *Strunius rolandi* were examined by Gross (1956). He cut thin sections of the parasymphysial tusks and the marginal teeth, and illustrated them by line drawings in figures 120 and 121.

Thin sections of the tusks of our specimens show thick dentine around the large pulp cavity and enamel over the surface of the whole tusk. New thin sections add little to the descriptions already given by Peyer (1968), Gross (1956) and Schultze (1969), and we have not illustrated them. The crystals making up the dentine are very narrow, making measurement difficult. The enamel varies in thickness, but is up to 12 μm in cross-sections. Sections of loose tusk which was not yet attached to the parasymphysial whorl show the walls of the tooth gradually thinning proximally, although details of the dentine can still be observed. This casts some interesting light on the growth of the parasymphysial dentition. The enamel of *Onychodus* has been studied by Smith (1979, 1989), but she apparently used marginal teeth rather than parasymphysial tusks.

We have examined the tusks by SEM. These show that the enamel is clearly differentiated from the underlying dentine. Some of the surfaces are relatively smooth or are slightly bumpy (Figs 40 & 41). On others, the surface is covered by raised ridges which are usually continuous over long distances, or alternatively, they split both distally and proximally (Fig. 40a). In other places, they merge into a surface which has no ridges, and this may take place along the length of the tusk, or it may be around the circumference as shown on Figure 40a–d. It may be thought that the smooth surface is the result of wear, but this is not so. Cross-sections of the broken edge show the linear structure well developed and passing laterally into a smooth surface with the enamel surface well preserved, and this surface grades into the ridged surface.

The arrangement of the crystals in the enamel is distinctive. Cross-sections of the ridges show radial arrangements of the crystals (Fig. 41d), although the clarity of the radial arrangement is not as strong as in Smith's figures (1989, fig. 4D, E). The ridges have thick enamel, and between them, the enamel thins out dramatically (Fig. 40b). The enamel against the smooth surface has vertical crystals against the surface.

The surfaces of the ridges sometimes carry chevrons of ribs with the sharp end of the chevrons pointed towards the tip of the tusk (Fig. 41e). As Smith (1979, fig. 1) pointed out, these chevrons are not always complete and they may leave a smooth surface along the crest. Other ribs lack such features and are either smooth or have small pits irregularly arranged on their surfaces (Fig. 41a).

The valleys between the ridges are sometimes smooth or have concentric lines related to growth (Fig. 41a; and Smith 1989, fig 4D). Other specimens have very fine lineations parallel with the main ridges. These are not continuous lineations, but range from short lines to almost globular patterns (Fig. 41b, c).

The tusks lie in the cavity in the dorsal surface of the whorls (Fig. 36a), and their bases are highly fluted. A broken tusk shows that the infolds of the tooth have a reticulated mass of tubes which join up with the mass of whorl tissue at their base (Fig. 30). SEM sections also show this fluting (Fig. 35a), and optical thin sections show a similar arrangement. The junction with the base is sufficiently strong to hold the tusks in position while an active bite was taking place.

9.7 Infradentary bones

Like so many other parts of the anatomy, it is difficult to fit the infradentary bones of onychodonts into a conventional sarcopterygian homology scheme. In the described onychodontids (*Onychodus*) and (*Strunius*), the infradentary bones vary considerably. *Onychodus rolandi* (Gross), subsequently transferred to *Strunius* by Jessen (1966), was described by Gross (1956) as having a small posterior plate ventral to the posterior part of the dentary. He interpreted this as infradentary 4. Anterior to this, he identified a thin single plate labelled as infradentary 2+3. In the interior tip of the mandible was infradentary 1, with a ventromedial extension. Posteriorly, the lateral line enters the mandible through infradentary 2+3 and not through infradentary 4 (Jessen 1966, figs 12 & 13), and continues into infradentary 1. Details of the infradentaries of the type species of *Onychodus* remain unknown.

In *O. jandemarrai*, five bones lie below the dentary and form the ventral margin of the jaw. The most posterior of these, which overlaps both the dentary and the infradentary in front of it, is the infradentary 4 of Gross, and like that bone, it does not contain the lateral line canal (Figs 28a, b, 36a, b, 42h &

https://doi.org/10.1017/S0263593300001309 Published online by Cambridge University Press

46a, b). Anteroventral to this element is an elongate bone with an elongate posterior extension and a sharp anterior termination about halfway along the mandible. We name this element infradentary 3. It contains the lateral line canal, which leaves the jaw at the posterior extremity of this bone, and about halfway along its length it carries an oblique pit-line in some individuals. Anteriorly, it passes into another elongate infradentary bone, infradentary 2, which terminates anteriorly partly against the downturned edge of the dentary and partly against another, much smaller infradentary. The lateral line runs along infradentary 2, but it divides near its anterior end, sending a branch into the dentary and another into infradentary 1. This latter bone is small and has an overlap for an even smaller element at its anterior end. The lateral line canal turns ventrally and exits the ventral edge of the bone just before reaching this overlap. We conclude from this that infradentary 1 is the most anterior of the true infradentaries, and that the lateral line canal passes from one jaw to the other at this point. The tiny bone anterior to infradentary 1, rarely preserved but visible on BMNH P65125 (Fig. 28a) and also on Figure 38, is most likely equivalent to the parasymphysial dermal bone sometimes encountered in porolepiforms (Jarvik 1972).

If we accept the nomenclature given above, assuming that the bones so named are homologues to those so named in the porolepiformes and osteolepiformes, we have a number of anomalies. First, infradentary 4 has no lateral line, whereas it carries the lateral line into the mandible in all other sarcopterygian genera with four infradentaries. (We exclude coelacanths from this discussion since they possess only two infradentaries and are clearly specialised in that regard.) Secondly, the pit-line that is located on this bone in other sarcopterygians is found on infradentary 3 in *O. jandemarrai*. And thirdly, the lateral line in the infradentary 2 branches anteriorly with a branch entering the dentary and the other passing on to infradentary 1. Most sarcopterygians lack the dorsal branch of the canal, but instead, have a vertical pit line on infradentary 2 that is missing in *O. jandemarrai*.

The last of these anomalies is the least problematic. Pit-lines and lateral line canals are related structures, and one can be converted to the other during evolution. Thus, in lungfishes (Campbell & Barwick 1987, fig. 14), the vertical pit-line on infradentary 2 is replaced by a vertical canal, although this differs from that of *Onychodus* in forming a bridge between the mandibular canal and the oral canal (which is absent in *Onychodus*). Thus, it seems reasonable to infer that the short vertical canal of *Onychodus* corresponds to the vertical pit-line normally seen on this bone. At any rate, there is no reason to conclude other than that infradentary 2 of *Onychodus* corresponds to that of other sarcopterygians.

The first and second anomalies are more troublesome. On the face of it, they suggest that the infradentary 4 of *Onychodus* is not homologous to that of other sarcopterygians, but is either something like an enlarged submandibular that has inserted itself onto the jaw, or else a neomorph bone comparable to the 'supra-angular' seen in *Moythomasia durgaringa* and more derived actinopterygians (Gardiner 1984). However, if this is true, it also implies that infradentary 3 of *Onychodus* corresponds to both 3 and 4 in other sarcopterygians because, as we have seen, 1 and 2 have their 'normal' identities. In other words, we are forced to accept that a new bone has been inserted posteriorly in the infradentary series, and one of the original set has been lost or fused with its neighbour.

An alternative interpretation is to conclude that infradentaries 1–4 of *Onychodus* correspond fully to those of other sarcopterygians, but that the lateral line canal has been rerouted so as to bypass infradentary 4, and that it has carried the pit-line with it to infradentary 3. We regard this explanation as the far more probable. In the first place, it obviates the need to explain the origin of infradentary 4 and the simultaneous loss of an infradentary between 3 and 2 of *Onychodus*, or the fusion of the original infradentaries 3 and 4. Secondly, it is well known that lateral line canals and pit-lines can change their position relative to dermal bones: examples discussed in the literature include the detour of the postotic canal into the postparietal in some rhizodonts (Andrews 1973, 1985; Long 1989), the lateral displacement of the same canal into the junction between skull roof and cheek in *Youngolepis* (Chang 1982), and the variable position of the anterior pit-line of the skull roof relative to the parietals/postparietals in actinopterygians, coelacanths and non-coelacanth sarcopterygians (Jarvik 1980; Ahlberg 1991). We have already seen that the supraorbital canal of *Onychodus* passes through supraorbital 2, a bone that it does not enter in most other sarcopterygians.

Thus, it seems reasonable to conclude that the infradentaries of *Onychodus* are comparable with those of other sarcopterygians and that it is the lateral line canal that has shifted. This also makes sense functionally: judging by the articulated specimens, the overlap of the cheek onto the lower jaw is much deeper than in other sarcopterygians, such that the posterior end of the maxilla almost completely covers infradentary 4 (Fig. 5). If the lateral line canal continued through infradentary 4 in the usual manner, this part of it would thus be buried underneath the maxilla, and the canal would have to make a rather strange trajectory in order to surface again posterior to the preopercular. By contrast, having the canal exiting the posterior end of infradentary 3 leaves it free to run through superficial soft tissue round the posterior end of the cheek until it reaches the preopercular.

9.8. Internal face of the mandible

As usual among sarcopterygians, the major dermal bones of the internal face of the jaw are the coronoids and the prearticular. However, the coronoids have a most unusual morphology. As shown on ANU 72975, WAM 90.11.1 and 92.8.2, and BMNH P63571 and 63572, the downturned face of the tooth-bearing flange of the dentary has four denticulated plates attached to it (Fig. 42a–e). Wear on the surface of the denticles shows that each has a pulp cavity in its core, indicating that it is tooth-like, and it is not similar to the pustules on the external surface of the dermal bones. These coronoid plates have interdigitating faces between adjacent plates, and the ventral parts of the mesial faces carry areas which are overlapped by the prearticular. Although these denticulated plates differ dramatically from the dermopalatine series in appearance, lacking both tusks and marginal teeth, it is clear from their position that they are the coronoids.

The anteriormost coronoid (coronoid 1) is a short element, missing in ANU 72975 (Fig. 42e), where it seems to have been lost during preparation, but known from several other specimens (Fig. 33). It has a deep overlap surface ventrally, and feathered ventral and anterior margins. The other elements (coronoids 2–4) are substantially longer and essentially parallel-sided, although coronoid 2 is deeper than the others and deepens further towards its anterior end (Fig. 42e). The size of the prearticular overlap increases on the more anterior plates because, beyond the supporting flange on its internal surface, the dorsal edge of the prearticular is free, allowing the overlap to be greater.

Coronoid 2 had denticles along much of its length, but the denticles are absent at three points. These mark the points where the tusks of the predermopalatine and dermopalatine lay alongside the inner faces of the coronoids. Ventrally, it has a narrow overlapped surface. Coronoid 3 has the denticles in contact with the first plate, and it also has one distinct surface

where the denticles are absent. This again marks where the tusk of the dermopalatines or the ectopterygoid engage the plate. The anteroventral surface of the plate has a large overlapped area which extends forwards beneath the first plate. Coronoid 4 is smaller than 2 and 3, and its overlapped edges are also small. Under the plate is a slight flange, and this must have lain along the flange on the prearticular in front of the adductor fossa, as described below. A similar but smaller flange occurs under the second plate, but the most anterior plate has no such flange.

This morphological disparity between the coronoids and the dermopalatine series is very strange. The tusks of the predermopalatine, dermopalatine and ectopterygoid do not engage any structure in the mandible, but they apparently made a grip on any prey by clasping it between the denticles and the tusks. A cross-section of the closure of the teeth and denticles in this region is shown in Figure 75.

Curiously, *Onychodus* bears a certain resemblance to early tetrapods in this respect. In Osteolepiforms and *Panderichthys*, both the coronoids and the vomer, dermopalatine and ectopterygoid bear tusks as well as marginal teeth. However, in early tetrapods, the coronoid dentition rapidly reduces first to a single tooth row and then to a denticle field, producing coronoids that look very much like those of *Onychodus*, while the palatal bones remain essentially unmodified and retain their tusks (Ahlberg & Clack 1998). The significance of this pattern is discussed further in 'Function'.

9.9. Prearticulars

Left and right denticulate prearticulars are known from ANU 72975, and well-preserved individuals WAM 90.11.1 and BMNH P64125; and several other BMNH specimens, also have prearticulars. Most of these are not complete, but a complete individual can be reconstructed.

The holotype also has a good prearticular (Fig. 44c, d), and some of the specimens in the BMNH collection also have them present. The plates are thin, but they bear a sharp internal flange beneath their dorsal edges (see below). The non-buccal surface is composed of shiny bone like that on the external bones.

9.9.1. Buccal surface of the prearticular. The buccal face of the prearticular is only gently convex. A furrow posterior to the internal flange mentioned above is directed posteroventrally. It sometimes joins a smaller furrow directed to the posteroventral end of the bone. The strength of these furrows varies between specimens. The main furrow cuts off a dorsal edge to the prearticular, and on this is a rounded surface of thickened bone forming the posterior corner of the bone. This provides a surface for the attachment of a slip of the adductor muscles as described below.

A pitted surface layer covers the posterodorsal corner of the bone ventral to the thickened surface, but small patches may have 'granules'. The remainder of the surface is largely covered with 'granules'. Ventrally, the 'granules' are more separated from one another, and in places, the bone structure on which they sit is visible. They are situated on thin cancellar bone, which is only 0·65 mm thick posteriorly and it thins to 0·2 mm anteriorly. The reason for this break in the bone is discussed below in section 12, 'Structure of the tubercles on the dermal bone'. During preparation, this bony layer tends to decompose and the surface layers of the bone fall free. Occasionally, the granules are broken through and a pulp cavity is present. We assume that the 'granules' are indeed small denticles.

At the posterior face of the bone, there is a large gap in the bone outline; the articular fitted into this, as shown by BMNH P64125 and WAM 90.11.1 (Fig. 44f, g). The articular projects only a short distance posterior to the prearticular, filling in the gap at the posterior end. At the top of this gap, the prearticular is developed into a thickened crest that extends a short way anteriorly, and that has a non-denticulate median surface exposing open bone spaces (Fig. 44c, f). Its surface is bent slightly medially. The posterior termination of this crest marks the posterior end of the inner face of the adductor fossa, and the inner face was for the attachment of a slip of the adductor muscles.

9.9.2. Lateral surface of the prearticular. On the internal (non-lingual) face of the prearticular, a strong posteriorly directed process springs from the area of thickened bone beneath the anterior end of the dorsal crest. This process is separated from the crest by a V-shaped notch that widens posteriorly, and the process is attached to the prearticular anteriorly. The notch is filled with the articular which makes a neat fit (Fig. 44g). The bony process provides a surface onto which the adductor muscles were probably attached.

Viewed dorsally, the bone thins out in front of this thickened crest and forms a sharp edge to the prearticular (Fig. 44b, c). Anteriorly to the adductor fossa, the margin of the prearticular has a long straight edge, and ventral to this edge is a laterally directed flange that has striations along its length (Fig. 44b, e, g). This flange is really an extension of the posterior process, and it provides support for the two most posterior coronoids.

Anteriorly, the prearticular stops well short of the anterior end of the mandible, and in our specimens exposes a large open space below the strong ridge which supports the dentary teeth. This space would have been occupied by Meckel's Cartilage.

9.10. Articular

The articular is best shown on WAM 90.11.1, and BMNH P64125 (Fig. 44c–g). In internal view, the articular has two extensions, one filling the notch between the dorsal crest and posteriorly directed process of the prearticular, the other lying around the ventral margin of the process; the articular also fills the concealed space between the posteriorly directed process and the main lamina of the prearticular. This complex interfingering, which is unique to *Onychodus* (in other sarcopterygians, the prearticular is a simple flat plate applied to the mesial face of the articular), means that the prearticular and articular are bound together to an exceptional degree in this species. The significance of this is considered further below. The body of the articular is thickest near its posterior margin, and thins out gradually towards the anterior.

The posterodorsal and posteroventral margins of the articular carry large unfinished areas where the vesicular interior of the bone is exposed; these must all have been continued in cartilage. As shown on Figures 44e and 45a, there is also an unfinished anteroventral area representing the contact between the articular and the unossified ventral strip of Meckel's Cartilage that joined the infradentaries to the prearticular.

In dorsal view, the unfinished cartilaginous attachment area leaves a small part of the articular covered with smooth periosteal bone exposed at the surface (Fig. 44c). It is slightly grooved, and lies in the position of the preglenoid process on Devonian dipnoans (Campbell & Barwick 1987, fig. 1d, e). Its function was probably to attach muscles or ligaments whose significance can be seen on Figure 74.

The posterior unfinished area on the ventral margin of the articular faces posteroventrolaterally, and is confluent with the posterodorsal unfinished area, although the two are demarcated by a bend in the outline of the bone. Of these two areas, the dorsal one clearly represents the glenoid, but the ventral one must be the base for the attachment of another cartilage, the significance of which has to be investigated under 'Function'.

https://doi.org/10.1017/S0263593300001309 Published online by Cambridge University Press

The posterodorsal surface of the articular shows only a faint longitudinal concavity and is, in fact, slightly convex transversely; in other words, it does not have the shape of a glenoid fossa. Nevertheless, it is incontestable that it supported the cartilaginous surface against which the quadrate cartilage articulated when the jaw was closed. The ventral surface of the articular has a much larger cartilage space than the dorsal surface and it is slightly convex. There is no possibility that this whole structure could serve as a ball and socket joint.

The nature of the junction has to be considered, and this requires a study of the quadrate. This also has a twofold cartilage surface, the dorsal surface being larger than the ventral surface. The dorsal and ventral surfaces meet at an angle of approximately 60°. This means that the two smaller surfaces on the quadrate and the articular face each other, although they are at an angle to each other (Fig. 74). One possibility is that the dorsal edge of the quadrate and the ventral surface of the articular were covered with thick cartilage that would, therefore, have been a stabilising feature when the jaw opened.

In this view, the articulation would have been a sliding one between the ventral cartilage on the quadrate and the dorsal cartilage on the articular. Such an arrangement would have been unstable, and large vertical and some lateral movements would have been possible. The angles between the two surfaces of the quadrate and the articular would allow the jaws to be opened by 70°, with the cartilage compressed during the widely opening phase. This matter will be discussed below under 'Function'.

9.11 Attachment of the adductor muscles

The shape of the prearticular–articular complex shows that, compared with other sarcopterygians, the adductor fossa of the lower jaw was both narrow and exceptionally short relative to the jaw length. Furthermore, the floor of the fossa, where the bulk of the adductor musculature would normally attach, was cartilaginous. Taken together with the unusual morphology of the prearticular, and its strongly interlocking relationship with the articular, this suggests a distinctive form of muscle attachment.

We propose that a substantial proportion of the adductor musculature attached not to the floor of the adductor fossa, but to the thickened inner face of the dorsal crest of the prearticular, labelled 'crest' on Figure 44c, e, g. This crest lacks denticles, is appropriately oriented for an adductor muscle attachment, and has a porous surface strongly suggestive of an attachment area. Furthermore, the presence of a muscle attachment on this bone explains the need for a strong bond such as has been described for the interlocking between the prearticular and articular.

10. Submandibular and gulars

10.1. Submandibular

As does *Strunius* (Jessen 1966), *O. jandemarrai* has only a single submandibular on each side, instead of the multiple submandibulars seen in porolepiforms, osteolepiforms and lungfishes. This is an elongate bone, completely preserved in the holotype. It is well preserved in many specimens (e.g. BMNH P64125), and is usually complete apart from its anterior tip (ANU 72975), where it can be seen in articulation with the lower jaw and gular (Figs 28a, b, 42 h & 46a–c). The submandibular has an elongated dorsal posterior extension, and the posterior half of the bone overlaps the infradentary 3 dorsally, and to a lesser extent, the gular ventrally. The anterior half is more rounded in outline and it has an extensive overlap of the gular ventrally and is less overlapped by the infradentary 3 dorsally. As is shown on the holotype, this bone terminates about one-third of the length of the mandible from its anterior end, where it is overlapped by the infradentary.

10.2. Gulars

Most of the gulars of BMNH P63566 are well exposed (Fig. 46a–c), and the right gular on ANU 36844 is complete (Fig. 5b). The holotype WAM 92.8.2 has a pair of plates which are largely complete (Fig. 46b, c). The information available allows us to make a complete description.

Unlike most other aspects of the anatomy, the gular plates of *Onychodus* compare closely with those of other sarcopterygians, and particularly resemble those of porolepiforms and coelacanths. The overall outline is triangular, with the lateral margin considerably longer than the medial.

Each plate has a strongly triangular posterior end, the posterior extremity being feathered without any sign of their surface being overlapped by the clavicle. However, articulated specimens, notably BMNH P63566 (Fig. 46a), show that the gular plates overlapped the anteromesial part of the clavicles, although the overlap produces only a change in the ornament on the clavicle and not an intimate overlap surface usually found between adjacent bones. Laterally, on the other hand, there is a significant gap between the gular plate and the clavicle.

A distinct gap is left between the anterior end of the gulars and the anterior of the mandible. We have no evidence that a small median gular plate was present, and this open space must have been covered by skin. This is quite unlike the anterior end of the gulars in *Strunius walteri* as figured by Jessen (1966, fig. 6).

Anteriorly, the right plate is overlapped by the submandibular, but it overlaps the infradentary 3 for a short distance posteriorly, and then it has a free edge. Medially, the right plate has a straight edge, but on ANU 36844, it has a smooth area anteriorly, slightly depressed below the ornamented central area. Such a depression is not present on all specimens.

The left plate has much the same shape, but it has an overlap area for the right plate on the anterior end of the midline. Laterally, it has a space for the submandibular and the infradentary 3 overlap. The exposed surfaces of both plates are covered with granules like those on the other external plates.

With the gulars and submandibulars reassembled, the gulars do not lie in a horizontal plane, but rather, they are inclined – perhaps by as much as 30° to the horizontal. This indicates that the ventral rotation of the gulars would open the pharynx, and so it is necessary to examine the overlapped edges of the gulars. The submandibular overlaps the gular extensively anteriorly, but posteriorly, the overlap is much weaker or is absent. Rather than indicating much lateral movement, this suggests that the movement between these two bones would be limited, unless the two overlaps are linear and provide an axis around which the gulars could rotate. Alternatively, the weakness of the overlap may have allowed a small rotation over soft tissue.

The inclination of the gulars also suggests that the anterior end of the clavicles were inclined to the horizontal, a point mentioned in the following section.

11. Pectoral girdle

11.1. The supracleithrum and the post-temporal

These bones are preserved on the holotype, and can be placed approximately in position (Fig. 48). Their ventral ends overlap

https://doi.org/10.1017/S0263593300001309 Published online by Cambridge University Press

the cleithrum. The supracleithrum is arcuate in shape and is of uniform width. It fits neatly into the posterior of the post-temporal, a bone which is narrowest near the cleithrum and expands dorsally. The internal surface is smooth dorsally and ridged ventrally, so that the appearance of these bones and the cleithrum are comparable in this view. The lateral line canal is visible on both bones and is shown in Figures 21a, b & 48g, f.

Dr Andrews reconstructed the post-temporal and supracleithrum as positioned dorsal to the cleithrum and slightly overlapped by it (Fig. 47c, d). This overlap relationship was based on the presence of an unornamented ventral margin on the supracleithrum and post-temporal, which she interpreted as an overlap area for the cleithrum. However, her reconstruction creates a set of anomalous contact relationships (post-temporal in contact with the cleithrum; supracleithrum overlapped by cleithrum rather than overlapping it; anocleithrum widely separated from supracleithrum; anocleithrum not overlapped by either supracleithrum or post-temporal) which are not seen in any other sarcopterygians. In holoptychiid porolepiforms (Jarvik 1972; Ahlberg 1989) and in the primitive rhizodont *Gooloogongia* (Johanson & Ahlberg 2001), which like *Onychodus* have subdermal anocleithra, the supracleithrum overlaps the anterior margin of the cleithrum. The comparison between *Gooloogongia* and *Onychodus* is particularly striking since the morphology of the supracleithrum and post-temporal is very similar in the two genera. Furthermore, *Gooloogongia* shows a well-defined area for the supracleithrum on the anterodorsal corner of the cleithrum, a feature than can be matched precisely in *Onychodus*. Moving the supracleithrum and the post-temporal to the matching positions in *Onychodus* (Fig. 48f, g) restores 'normal' sarcopterygian relationships between these bones while allowing the ventral unornamented area of the supracleithrum and the post-temporal to be reinterpreted as an overlap for the operculum. We are confident that this reconstruction is correct.

The lateral line in position indicates the position of the cleithrum in relation to the skull roof. Having established the overlap of the top of the cleithrum by the operculum, the dorsal end of the pectoral girdle is fixed in position. The ventral edge is to be described, and this is necessary because we do not have a specimen showing the lateral curvature of the cheek. The associated cleithrum and clavicle show what is the general lateral curvature, but the anterior position of the clavicle has to be determined by another means. Fortunately, the gulars of the some specimens are known and can be seen to overlap the clavicles. It is also clear that the gulars and the clavicles are inclined upwards away from the mid-line (Fig. 46a).

11.2. Anocleithrum

The anocleithrum is well preserved on the holotype as an isolated bone, but it is apparently almost in position on ANU 36844 (Fig. 5b). Other isolated bones are also known on ANU 72975–72976 (Fig. 21c–i). This bone is completely subdermal. In position, it projects beyond the dorsal end of the cleithrum. The proximal end of the anocleithrum consists of a flattened blade. In lateral view its anterior edge is rounded and its posterior edge is slightly concave. It fits down behind the cleithrum neatly. In large specimens (Fig. 21g–i), the dorsal edge is a knobbled arrow head, but the shapes vary even on the two sides of the one specimen. The inner face has a depression for the attachment of another surface, but this is not present on the other specimens. The outer face is rounded or it also has a few ridges.

11.3. Cleithrum

As in other sarcopterygians, the cleithrum can be described as comprising dorsal and ventral blades, joined at the level of the scapulocoracoid where the cleithrum is widest. The dorsal blade shortens gradually towards the dorsal edge where the exposed part narrows and an overlap area is present on its anterior face (Figs 47a, c, e & 48e). In this shape, it differs from the cleithra in osteolepiforms and porolepiforms, which are straighter and have broad dorsal ends (Jarvik 1980). The ventral blade is shorter and broader, and it is deflected mesially. This blade tapers to a sharp anteroventral point. The anterior margin is modified by overlap areas at its dorsal end where the clavicle overlaps it slightly (Fig. 47c), but ventrally the clavicle overlaps the cleithrum (Figs 47g & 48e). At the point where the posterior margin turns mesially, the inner face has a knob where the edge of the scapulocoracoid was attached.

In lateral view, the external surface of the cleithrum is gently convex except anteriorly where the surface turns mesially. Here, there is a broad general depression which continues forwards onto the dorsal process on the clavicle. This surface has reduced ornament or no ornament at all. Instead, the linear arrangement of the bone is exposed. Dorsal to this depressed area, the surface is covered with granules and has no depressions in its surface.

The dorsal tip of the cleithrum has marked overlap areas. One of the best specimens we have is the holotype, but other detail is known on several other BMNH specimens and ANU 36844 (Figs 5a, b, 47a, b & 48e). The dorsal tip is surrounded by an overlap indicating that the bone lay beneath a surrounding bone dorsally. The length of this overlap varies from specimen to specimen. The largest one observed is figured on Figure 47a. Much of the overlap would have been occupied by the supracleithrum, though the opercular would have contacted the ventral part of the overlap area. The area on the cleithrum posterior to the overlapped area, has a sharp anterior edge indicating that the overlapping plate fitted neatly into the surface and had a closure at that point.

The ventral tip of the cleithrum is long and pointed, and its anterior edge is almost straight and it underlies the edge of the clavicle (Figs 47g & 48e). In this respect, it is comparable with the cleithrum of *Strunius rolandi*, but the position of the posterior extremity is more dorsally placed in our species.

The surface of the cleithrum is covered by granules except in the dorsal part where the granules are more widely spaced and the linear basal bone is exposed. The outer layer of bone that carries the granules, readily peels off from the basal layer that makes up the bulk of the thickness of the bone.

Internally, the cleithrum has a wide thickening towards the anterodorsal end (Fig. 47f). At its ventral end, near the dorsal end of the clavicular process, it joins the wide thickening from a more posterior end, and it becomes narrower and sharp-crested dorsally. This thickening produces an irregular flange facing anteriorly dorsal to where the tip of the clavicle process lies against the cleithrum (Fig. 47c, g). At this point, the ridge has a small projection against which the tip of the process on the clavicle sits. The flange is the homologue of the branchial lamina in *Psarolepis* (Zhu *et al*. 1999; and also personal observation), even though it is greatly reduced in size.

Another thickening runs anteroventrally from the scapulocoracoid towards the anterior ventral tip of the cleithrum (Fig. 47d, e, f). This thickening lies inwards from the edge of the cleithrum and forms a rounded surface towards the cleithral edge. Unlike the dorsal thickening, it plays no part in the formation of the edge of the cleithrum, but merely forms a support from the whole cleithrum.

https://doi.org/10.1017/S0263593300001309 Published online by Cambridge University Press

At the anterior edge of the cleithrum, adjacent to where the process on the clavicle lies against the edge, the bone is serrated. This is presumably part of the system where the two bones could move together during feeding.

A small rounded knob lies at the most posterior corner of the interior of the cleithrum (Fig. 47b, g), and marks the position of the pectoral fin. In oblique light, the radii of the cleithrum run from this point, indicating that this was the centre of ossification of this bone. The knob lies over this centre, and shows radii imposed on the cleithral radii. Jessen (1966, p. 354) has figured the cleithrum of *Strunius rolandi* that shows an elongate ridge in the same position as the knob described above, and he refers it to the basal remains of the scapulocoracoid. In our material, the knob is much smaller.

11.4. Scapulocoracoid

The scapulocoracoid is preserved on both sides of the holotype. Its lateral parts cover a large flat surface as a thin bone, which is not readily preserved. Medially, it rises to a large process (Figs 47e & 68). The specimen does not have a three-pronged attachment to the cleithrum, like those in osteolepiforms (e.g. Andrews & Westoll 1970a; Jarvik 1980). The whole flat structure was attached to the cleithrum, and the nerves and vessels must have passed around the process. Thus, it resembles the scapulocoracoid of *Glyptolepis* (Ahlberg 1989). The anterior surface had a sharp edge, and this passed into a flattened surface facing medially. This may have been an area for muscle attachment. The surface for the attachment of the humerus is well defined, but it is not concave. Rather, it has a flattened surface composed of bone vesicles. The outline of this surface differs on the left and right sides of the specimen. The attachment of the humerus is also flattened. The surface of the cleithrum beneath the posterior edge of the scapulocoracoid carries a lump of bone which must have supported the scapulocoracoid. This lies at the junction of all the radial tissue making up the cleithrum, and shows that it was in position from the earliest growth stages.

11.5. Clavicle

Dorsally, the clavicle overlaps the cleithrum, and consequently, it is thinned out towards the overlapping edge (Figs 47g & 48e). Dorsal to this overlap is a process which lies up against the anterior edge of the cleithrum. The process fits approximately into a groove on the edge of the cleithrum making a smooth surface, but the inner edge lies away from the cleithrum, making an inwardly projecting flange terminating at a point (Fig. 48a, b). The posterior face of the process is distinctive, carrying one or two ridges and depressions between them. Its surface is smooth, or it contains longitudinal growth lines. In cross-section the process is rounded ventrally, but dorsally, it becomes sharper, and it contains the grooves mentioned above. The anterior face of the process is smooth, and it continues ventrally as a shallow groove (Fig. 48b, e). On the right girdle of ANU72976, this groove becomes more pronounced dorsally, and ventrally, it contains a number of pits which run ventrally off the process and onto the main blade of the clavicle. This inner process is the branchial lamina homologous with the much larger lamina found in dipnoans from the same locality. The remainder of the internal surface is made of smooth bone.

The ventral edge of the clavicle is almost straight. Externally, the bone carries a number of tubercles and granules. These vary in their distribution from specimen to specimen, but a general pattern is observed. The anterior edge of the bone has small granules on some individuals, but it is almost smooth on others. This area is where the clavicle lies against the gular (Fig. 46a). All specimens have the coarsest granules in the posteroventral corner of the clavicle. The dorsal surface, which is continuous with the smooth surface on the cleithrum, is sometimes large in size, and extends up onto the clavicular process. In others, it is restricted to the process, and in yet others, it is restricted to the main body of the clavicle and does not rise to the process. On ANU 72978, which has the surface well preserved (Fig. 48d), coarse ornament occupies the posteroventral corner. Fine ornament or a smooth surface occupies the anterodorsal corner and up onto the spine, which is broken off. This dorsal area was covered by a flap of soft tissue from the subopercular. This is the largest of the modified surfaces we have observed.

11.6. Cleithrum–clavicle interaction

This is a matter of contention, as is shown by the reconstruction given by Long (2001, fig. 1). For this reason, an extended summary is given here, rather than under section 17, 'Function', in the latter part of this article. Both the cleithrum and the clavicle are large, complete bones, heavily ossified, and assembled along grooves (Fig. 48a, b, e). With the two bones articulated, the clavicle overlaps the cleithrum ventrally. The dorsal end of the cleithrum has areas which show overlap, but preservation modifies this end of the cleithrum ANU 36844 and BMNH P63570 show this feature well. The dorsal and anterodorsal ends often do not have external ornament, and leave a thin layer of underlying bone exposed. This is in a position where the overlapping bone was the supracleithrum and the anocleithrum, but with the opercular overlapping the basal part. The subopercular fits beneath the posterior end of the opercular. The posttemporal and the supracleithrum can be placed in position because they contain the lateral line canals, and we know where they lie in relation to the cleithrum. Hence, the dorsal part of the cleithrum can be placed in position, and it must be possible to orient the pectoral girdle with respect to the remainder of the skull.

The anteroventral surface on the cleithrum and the dorsal part of the clavicle have surfaces which are depressed and have reduced ornament, or are unornamented. The extent of the smooth area varies from specimen to specimen, but on the clavicle, it is usually restricted to the dorsal process region and the area ventral to it. One specimen, ANU 72978, and three other individuals, have a surface that is separated off from the granulated surface by a sharp line. This surface has some fine granules along its anterior faces (described above), but these fade away posteriorly. The smooth area may have been overlapped by the subopercular, but the area is very variable in size, and in fact, the subopercular lies too dorsally to cover this space. In any case, such a ventral position would not permit the branchial chamber to be well enough enclosed for normal respiration. As we have shown above, the subopercular must have closed by lying against the overlapped area of the cleithrum, the process on the clavicle and the area ventral to that. The answer to the problem of the variation in the ornament on the clavicle is to be found in the extant *Latimeria*. Millot & Anthony (1958) recorded that the lateral covering of the head has a thick fibrous tissue attached to the supratemporal dorsally, and covers the pectoral girdle and extends onto the ventral side of the animal. This fibrous covering has a tuberculate surface. In *O. jandemarrai*, the depressed area on the cleithrum/clavicle overlap was covered with a fibrous layer of soft tissue, and this may also extend ventrally along some of the clavicle. The subopercular has granules like those on the other dermal elements and it is quite unlike the covered parts of the girdle in this respect. We assume that the fibrous tissue was wrapped around the subopercular and extended

posteriorly from it. There is no evidence that the fibrous layer was nearly as extensive as that on *Latimeria*.

With the cleithrum in the position stated, it is obvious that its dorsal end must have been bent inwards, and the clavicles must also have been inclined to the horizontal. The median edges of the clavicles are smooth and show no overlaps, and it is probable that these bones met edge to edge. No interclavicle has been found. Specimen BMNH P63566 has the clavicles exposed on the ventral surface of the animal (Fig. 46a). The overlap of the gular onto the clavicle is strong, and although there is some weak ornament on the adjoining surfaces, some motion between the bones must have been possible. The movement between the clavicle and the cleithrum has been established, and this, together with the gular overlap, indicates that the clavicular part of the pectoral girdle was very flexible. Given that the clavicle could move relative to the rest of the girdle, the gaps between the posterior end of the gular and the clavicle, and between the subopercular and the bones ventral to it, become interpretable. They would have made the lateral movement of the pharynx possible when the animal was swallowing large prey. The cleithrum, to which a large scapulocoracoid was attached, would have had less mobility.

12. Structure of the tubercles on the external bone

These have been examined by direct observation, by thin slides and SEM study of sections. The surface is covered by a layer of bone that decomposes when immersed in acetic acid for an extended period, and this makes examination difficult. Before the surface is coated with plastic, brushing causes the surface layer to disintegrate. Thin sections have to be prepared from bone that has not been placed in acid. Our thin sections were made from a cheek plate and another head plate.

12.1. Surface examination

Small projections of shiny material (tubercles) are scattered over the surface. These are harder than the surrounding bone, and stand out more clearly after abrasion. The density of the tubercles, and their size, varies on different parts of the skeleton.

On the isolated postparietal ANU 72975, the bone around the tubercles forms a circular rim. Occasionally, the shiny tip of the tubercles lies low within the rim of bone, and has the appearance of a reforming tubercle. Others show tubercles at all levels of formation, some almost filling the surface within the bony cavity. This is discussed in detail in the following section.

12.2. SEM examination

An oblique view of a surface (Fig. 49a) shows the fully formed tubercles in the background and partially reformed tubercles in the foreground. The partially formed individuals first appear as a slight hump in the middle of the space and ridges arranged semiradially to the margins. Later stages show how the space is gradually filled, and the intervening bone is finally left on the flanks of the tubercle dome. A single tubercle on the same figure shows partial removal of the laminar layer and the space for the lenticular opening in the centre.

A vertical fractured surface (Fig. 49b) and thin sections (Fig. 50a–c) show the tubercles with the spaces beneath them. The layers of bone forming the bone beneath the tubercular layer are well exposed.

Another specimen (Fig. 49d) shows a tubercle and an adjacent space from which the tubercle has been removed, and this shows the base of the open chamber with strong openings down into the bone beneath. Figure 49c shows a weathered-through section of a tubercle displaying coarse and fine concentric layers which made up the tubercle, along with a large central opening as is shown in Figure 49d.

12.3. Thin sections

The bone layer on which the tubercles sit is made of flat, elongate laminar layers of bone. This is the layer that breaks down on abrasion, and specimens which have been brushed during preparation have often lost the surface layer. Beneath it lies a more equidimensional bony tissue layer (Fig. 50a–c). The layer of bone forming the inner surface of the bone is also laminar, but it is not always present.

On the external surface of the bone is a single layer of tubercles, but in places, two or three tubercles are superimposed (Figs 49e & 50a, b). So far as we can determine, the tubercles do not have a separate identifiable surface layer of tissue, and we cannot identify a layer which could be enamel or enameloid.

The main body of the tubercle is made of lamellae arranged in an arcuate fashion in superimposed layers. The lamellae at the base of the lens are complete and cross the whole lens. Those distal to it are convergent laterally, and those close to the external surface are incomplete laterally and terminate against the exposed surface. This is shown on Figure 50d, the right side of which is complete, but the left side has been broken. A comparable section is shown in Figure 49e, but this is incomplete. This confirms the idea that the lamellae begin to form beneath the exposed surface, and the tubercle expanded laterally by the deposition of layers on its inner surface (cf. Fig. 49a). Under crossed polars, the extinction of the mineral is radial, indicating that the crystals are organised with their c-axes radially arranged normal to the outer surface.

The concentric lamellae are punctuated by fine tubules which have a diameter similar to those of the dentine tubercles in the tusks. In places, these tubules are filled with a dark mineral, and these show that the perforations branch repeatedly towards the external surface, producing a bush-like appearance. Although the pattern and distribution of these perforations suggest that the lenticular layer is made of dentine, this is not an acceptable view. The lamellae are laid down in layers around the open space at the base of the tubercle, the perforations arise independently from the same open space, and under crossed polars, the crystals making up the lamellae are seen to be arranged with their long axes normal to the surface of the tubercle.

The space between the laminated lens and the basal bone is occupied by another lenticular space that is now filled with matrix, usually calcium carbonate. In life, it must have been occupied by soft tissue, and the layers of the laminated lens were deposited from it. Usually, this open space has a clear-cut boundary, but occasionally, the margins of the space are filled with hard tissue (Fig. 50d). This means that the tubercle had been fully formed and the space was now losing the soft tissue that deposited the laminated lens.

What is clear is that the tubercles were generated by deposition on their inner face as a narrow structure, and as new lamellae were deposited on the inner face, the diameter of the tubercle and its height increased. Furthermore, the tubercles were shed at certain stages of the growth of the animal, and were then replaced.

12.4. Summary

These sections show:

a. that the tubercles were formed from soft tissue occupying a lenticle at the base of the tubercle;

https://doi.org/10.1017/S0263593300001309 Published online by Cambridge University Press

b. that the laminae were penetrated by perforations that divide distally, and presumably, these had some function in laying down of the hard tissue;
c. that the laminae were laid down as sequential layers and have no structure arranged around the perforations;
d. that the tubercles were replaced by resorbtion of the laminar layers forming the tubercle; and
e. that the replacement of the tubercle took place by upward growth through the space occupied by the previous tubercle.

No cosmine has been found on the surface of the animal. Tubercles occur on the head bones, gulars, pectoral girdle and scales. The tubercles were shed and replaced during growth, but the reason for this is not known. We know of no other surface system of this kind in the sarcopterygians.

13. The ossified braincase

13.1. Otoccipital braincase

The only preserved parts of the otoccipital braincase are the zygals and their surrounding hard parts, and the rarely preserved otic capsules.

13.1.1. Otic capsules. The braincase of *Onychodus* was only partly ossified, and the otoccipital block in particular seems to have been entirely cartilaginous in most individuals. Fortunately, however, the small disarticulated skull, BMNH P64125, which has also yielded the most completely ossified ethmosphenoid of *Onychodus*, preserves two partly ossified otic capsules which provide direct evidence for otic morphology in this genus (Fig. 51). Other fragments of the capsules of the holotype have also been found.

Each otic capsule comprises three main parts: anteriorly, a deep component incorporating the side wall of the cranial cavity and part of the otic shelf; in the middle, a dorsolaterally positioned curved portion containing the horizontal semicircular canal; and posteriorly, a deep but rather thin lamina carrying the tract for the posterior limb of the posterior semicircular canal on its internal face. The ventral parts of the anterior and posterior components are separated by a large vestibular fontanelle. The posterior extremity of the right otic capsule is incomplete, but the left capsule terminates posteriorly in a smoothly curved, natural-looking margin that appears to be the lateral otic fissure.

The semicircular canal tracts, which are lined with perichondral bone, are best seen on the inner face of the left otic capsule (Fig. 51c). Conditions on the right side agree, in so far as can be determined, with those on the left. The middle part of the horizontal semicircular canal tract forms a curving, open gutter on the upper surface of the ossified otic capsule. Posteriorly, this tract becomes enclosed in bone and disappears from view, reappearing again on the mesial face of the ossification immediately in front of the space for the posterior ampulla. A narrow canal, just less than 1 mm in diameter, connects the horizontal semicircular canal tract and the posterior ampulla at this point. Anteriorly, a gap in the perichondral ossification separates the anterior end of the horizontal semicircular canal tract from a set of curving perichondral surfaces which together define two linked, bulbous spaces, one above and slightly anterior to the other. Comparison with *Eusthenopteron* (Jarvik 1980) suggests that the dorsal space, which is on a level with the horizontal semicircular canal tract, housed the external ampulla of that canal, while the ventral space contained the utricular recess (Fig. 51b, c).

The anterior semicircular canal tract is not preserved in either otic capsule, and all that remains of the posterior canal tract is the posterior ampulla and associated vertical part of the canal, preserved only on the left side.

In external view, the most striking feature of the otic capsule is the large vestibular fontanelle. This occupies a slight recess below the projecting braincase rim that houses the horizontal semicircular canal. Interestingly, the dorsal margin of the fontanelle carries a substantial notch. Nothing similar is known in osteolepiforms or coelacanths, but in *Youngolepis*, a large canal of uncertain function (Chang 1982, fig. 15B, 19, 'f.lab.') pierces the side wall of the otic capsule in essentially the same position; this canal is also present in *Styloichthys* (Zhu & Yu 2002, fig. 1f, unlabelled). The canal in *Youngolepis* is not confluent with the vestibular fontanelle (*Styloichthys* lacks a vestibular fontanelle altogether), but this seems a relatively trivial difference. Accordingly, we interpret the dorsal notch in the vestibular fontanelle margin of *Onychodus* as having housed this canal (Fig. 51a).

Anterior to the dorsal part of the vestibular fontanelle, a well-defined groove runs horizontally along the side wall of the otic capsule, becoming more deeply incised towards the anterior. This must have housed the jugular vein. Approximately halfway between the vestibular fontanelle and the anterior end of the otic capsule, a substantial (1·5 mm) nerve foramen pierces the braincase wall just below the jugular groove. The position of this opening indicates that it transmitted the mandibular and palatine branches of nerve VII (Fig. 51a, b).

It is at first sight puzzling that the otic capsules preserve no trace of the lateral commissure or hyomandibular articulation. The explanation is provided by the limited extent of the ossification. Not only the dorsal surface of the capsule, but also the ventrolateral margin anterior to the vestibular fontanelle, consist of unfinished bone. Immediately above the jugular groove, there is a centimetre-long shallow notch in the dorsal margin of the ossification, indicating the presence of a laterally projecting cartilaginous structure; directly below the anterior part of this notch, just in front of the nerve VII foramen, the dorsal edge of the unfinished ventrolateral capsule margin flares outwards and upwards in a corresponding manner. These must be the dorsal and ventral attachments of a cartilaginous lateral commissure.

The ventral surface of the anterior otic capsule component includes a substantial posterior 'sole' of finished bone, covered with a network of fine grooves and pierced by a narrow canal that descends from the cranial cavity, splits into lateral and mesial branches, and opens onto the ventral face of the bone through a pair of foramina. The appearance of this sole, and its slight transverse concavity, strongly suggest that it rested on the dorsal surface of the notochord. This is an unusual arrangement; in other sarcopterygian fishes (Millot & Anthony 1958; Jarvik 1980), the anteroventral parts of the otic capsules clasp the sides of the notochord rather than resting on top of it. However, the condition here is consistent with the exceptionally large size of the notochord relative to the cranial cavity in *Onychodus*, evidenced by the proportions of the posterior face of the ethmosphenoid (see below).

The anterior end of the otic capsule narrows almost to a point, but terminates in a small notch of finished bone that connects the internal and external faces, thus separating the dorsal and ventral unfinished areas. The position of this notch, just dorsal to the jugular vein groove, suggests that it forms the posterior margin of the trigeminal nerve foramen. It is impossible to determine whether the foramina for the trigeminus and profundus were separate or confluent in *Onychodus*. The lack of a profundus foramen in the ethmosphenoid (see below) indicates that this nerve issued through the intracranial joint; it is possible that the anterior terminal notch of the preserved otic capsule represents the posterior boundary of the intracranial joint, in which case both trigeminus and profundus passed through the joint, but it is also possible that the otic capsule

continued forwards in cartilage and enclosed the trigeminal foramen.

By comparison with the elaborate anterior component, the posterior component of the otic capsule is relatively featureless. However, the ventral-most part of the posterior margin carries a small but deep notch that most probably transmitted nerve IX (Fig. 51b). The dorsal margin of this component shows no trace of the beginnings of a posttemporal fossa (fossa bridgei), suggesting that this fossa was absent as in *Youngolepis* and primitive actinopterygians (Chang 1982; Gardiner 1984).

13.1.2. Zygals. This part of the braincase is not ossified except for small elements around part of the notochord. Such structures occur in the extant *Latimeria*, and they have been observed in the Devonian *Eusthenopteron* and *Nesides*. Bjerring (1971) has described such structures in *Eusthenopteron*, and he has used the name zygals for them. The elements which lie above the notochord are termed anazygals, and they may be single or paired, one on each side of the notochord. Those below the notochord are catazygals, and these too are apparently single or paired structures.

According to Bjerring (1971), these structures consist of spongy bone partly covered by compact periosteal bone. Their detailed shape has not been described, largely because they have been studied by serial sections. The cranial parts of *Onychodus*, particularly ANU 72975 and WAM 90.11.1, have isolated bones which we refer to as zygals. They are of two types. The two ANU specimens are clearly medial bones, ovate in outline, their outside covered with strongly perforate periosteal bone (Fig. 52a), which also shows concentric lamellae. The inner face is made of spongy bone thinnest around the edges and with a deep median crest (Fig. 52b). The WAM specimens are also median plates which are almost hexagonal in outline. Both anterior and posterior ends have a slight indentation. In anterior profile, the plate is strongly arched, and the lateral profile shows a slight elevation at each end (Fig. 52f, g). The periosteal bone is perforate and also has fine depressions on its surface (Fig. 52e). The inner face is made of spongy bone, deepest at one end and tapering gradually to the other. Unlike the ANU specimens, this face is deeply concave instead of convex (Fig. 52g).

These two types of zygals must represent the anazygals and the catazygals, but the means for determining which one is which are not obvious. The following points suggest possible answers. The WAM specimens have an anterior surface that indicates mobility. This suggests that they come from a more posterior ventral position where they could move laterally during swimming. The ANU elements show no sign of fitting around the notochord, and their ends are not designed for mobility. They may have come from an anterior dorsal surface in a stable position. WAM 86.9.694 has a pair of poorly preserved zygals ventrally placed along the posterior part of the oticoccipital specimen that has the zygals in an approximate position, but it adds little to the above discussion.

13.2. Ethmosphenoidal braincase

Three examples of the ethmosphenoidal division in its articulated condition (the holotype WAM 92.8.2, WAM 90.11.1 and BMNH P64125) are available. The ethmosphenoid is preserved as individual ossifications, indicating that fusion between the units only takes place in the largest animals. In contrast to the oto-occipital, the ethmosphenoid of *Onychodus* is relatively well ossified and can be described in detail. It proves to have a very unusual morphology in comparison with most other osteichthyan fishes.

The best ethmosphenoid is provided by BMNH P64125, in which all of the ossifications are present. All other known specimens lack the lateral ethmoids. Valuable information about the composition of the ethmosphenoid is provided by certain individuals, such as the small BMNH P63570 and the very large BMNH P63571, in which the different ossifications are still wholly separate. Supplementary information from these specimens and from WAM 90.11.1 and WAM 92.8.2, have been used in the following descriptions.

The ethmosphenoid comprises four distinct endoskeletal ossifications, one unpaired and three paired; these may be termed the basisphenoid (paired), orbitotectal (paired), median ethmoid (unpaired) and lateral ethmoid (paired) (Fig. 56a). In addition, a dermal parasphenoid attaches to the ventral faces of the basisphenoids.

13.2.1. Notochordal facet. In terms of the general outline, the most striking features of the ethmosphenoid of *Onychodus* are the very large notochordal facet and the enormous internasal fossae. These combine to give the ethmosphenoid a very distinctive shape, quite different from the 'normal' pattern seen, for example, in coelacanths and osteolepiforms, but very similar to that of *Psarolepis* (Yu 1998; Long 2001), and confirmed by Long who has seen new Chinese specimens. The notochordal facet is approximately three times as deep as the cranial cavity dorsal to it (Figs 53c & 56c). This is in marked contrast to the condition in most other sarcopterygians: in *Eusthenopteron*, for example, the cranial cavity is slightly deeper than the notochordal facet (Jarvik 1980). Once again, *Psarolepis* provides the best match, with a notochordal facet approximately twice as deep as the cranial cavity (Yu 1998). The facet is flattened across the dorsal edge and pointed ventrally in posterior view, and is laterally continuous with a pair of small, semicircular, posterolaterally facing articular facets which must be the points of contact for the otic shelves. This contrasts with the 'normal' sarcopterygian pattern, where these articulations lie on the flanks of a distinct processus connectens that bounds the notochordal facet dorsally. The centre of the notochordal facet is pierced by an irregular hole that communicates with the top of the hypophysial fossa.

13.2.2. Orbitotectal. The boundary between the basisphenoid and orbitotectal ossifications can be recognised as a faint line running across the surface of the notochordal facet. Its lateral end lies just ventral to the articulation for the otic shelf, and it runs mesially in a gentle dorsal curve, rising and then falling again to end at the central hole in the facet.

Dorsal to the notochordal facet, the side walls of the braincase form a pair of robust pillars either side of the cranial cavity. In side view, the posterior margin of this part of the ethmosphenoid has a strong anterodorsal slope, and is markedly concave; the effect is of an exaggerated version of the coelacanth or porolepiform pattern, unlike the posterodorsal slope in *Psarolepis* or *Achoania* (Yu 1998; Zhu *et al*. 2001). In posterior view, the braincase walls can be seen to thin rapidly from ventral to dorsal before flaring out again to form a pair of cushion-like, dorsally unfinished structures which seem to have contacted the skull roof via a thin intervening layer of cartilage (Fig. 56a). At the posterior margin of each cushion-like structure, the braincase wall carries a distinct dorsally facing process tipped with an oval articular surface; between these processes lie, at a slightly lower level, a pair of oblong contact or attachment surfaces which meet in the midline and face somewhat posterodorsally (Figs 53e & 54). We interpret the dorsal processes as articulations for the dorsal part of the otic capsule, and the oblong areas as probable attachments for ligaments spanning the intracranial joint (Fig. 56a, c). Again, this arrangement is directly comparable with the conditions in coelacanths, porolepiforms and osteolepiforms (Millot & Anthony 1958; Jarvik 1980; Lebedev 1995).

The intracranial joint is known to occupy two distinct positions relative to the cranial nerves in sarcopterygians

https://doi.org/10.1017/S0263593300001309 Published online by Cambridge University Press

(Jarvik 1980; Ahlberg 1991). In osteolepiforms and porolepiforms, it is anterior, passing through the profundus foramen while the trigeminal nerve pierces the side wall of the otoccipital; in coelacanths and probably *Powichthys*, on the other hand, the profundus pierces the side wall of the ethmosphenoid and the trigeminus emerges at the level of the joint. The interpretation of *Onychodus* is hampered by the poor preservation of the otoccipital. However, no profundus foramen can be identified in the ethmosphenoid, which suggests that the joint occupied the anterior position.

In side view, the dominant feature of the ethmosphenoid is a large, approximately circular concavity at the centre of which lies the very large, teardrop-shaped or ovoid optic nerve foramen (Figs 53f & 56a). The dorsal half of this concavity is formed from the orbitotectal. Within the concave area, the braincase wall is mostly smooth or with small pits (see below); posterodorsally, it is demarcated by a low curving ridge from a rougher surface that continues to the intracranial joint margin, and which presumably served as an attachment area for connective tissue associated with the intracranial joint.

Dorsal to the posterior margin of the optic nerve foramen, immediately below the aforementioned curving ridge, sits a small but prominent suprapterygoid process (Fig. 56a). This is directed posterolaterally, and is tipped by a jagged surface which we interpret as the attachment for a ligament connecting to the ascending process of the palatoquadrate. The ligamentous rather than articular nature of the connection matches the condition of the basipterygoid process (see below).

In the area between the suprapterygoid process and the optic nerve foramen, the braincase wall is pierced by a number of small foramina. These vary significantly, even between the left and right sides of the same specimen, but it is possible to identify as constant features one small group of foramina (one main opening and several smaller holes) clustered on a slight protuberance near the dorsal margin of the optic nerve foramen, and a pair of foramina (similar in size to the largest in the aforementioned group) anterior to the suprapterygoid process. From their positions, we interpret these groups of foramina as representing the openings for cranial nerves III and IV (Fig. 56a).

The anterodorsal part of the smooth concave area is overhung by the projecting lateral part of the dorsal cushion-shaped structure. The ventral surface of this overhang carries a well-defined, quite deep, oval depression that houses a fairly large (about 1 mm in diameter) foramen anteriorly, and one or two slightly smaller openings posteriorly (Fig. 56a). The anterior foramen is the beginning of a canal that runs forwards to emerge on the anterior margin of the orbitotectal, while the canals from the posterior foramina run mesially and dorsally. We conclude that this is where the lateral ophthalmic nerve re-entered the braincase, apparently throwing off one or two mesially directed twigs as it did so.

Two further canals are represented on the orbitotectal by open grooves rather than foramina. On the external face, a short anteriorly directed groove below the projecting cushion-shaped structure probably led to a foramen in the (unossified) dorsal part of the postnasal wall; this may have transmitted a branch of the profundus nerve. On the internal face, a wide (approximately 2 mm in diameter) and deep groove runs anteroventrolaterally towards the nasal capsule. This is evidently the tract for the olfactory nerve. At a level just behind the posterior end of this canal, where the left and right cushion-shaped structures are united by a narrow bridge of bone, the roof of the cranial cavity rises in the midline into a distinct diverticulum that must have housed the pineal organ. This did not open through a foramen in the skull roof.

13.2.3. Basisphenoid. As mentioned above, the ventral half of the concave area is formed from the basisphenoid ossification. Its posteroventral margin is formed by a gently projecting, quite robust ledge that runs anteroventrally from the articular facet for the otic shelf to the ethmoid articulation and the attachment scar for the unossified postnasal wall. Somewhat posterior to the mid-point of this ledge, where it changes direction to run more anteriorly and less ventrally, lies the small basipterygoid process (Fig. 56a, b). This is a prominent button-shaped structure that, most unusually, does not carry an articular facet. Fortunately, the left autopalatine is preserved in articulation with the anterior part of the entopterygoid in BMNH P64125, and this complex can readily be restored to life position alongside the ethmosphenoid; thus, we can examine both sides of the basal articulation in this specimen. The articular surface on the autopalatine turns out to be nothing more than a triangular area of unfinished bone, lacking any specific match of shape or curvature to the basipterygoid process. Thus, it is clear that the basal articulation was ligamentous rather than synovial, as noted above for the epipterygoid process, an observation that further underscores the highly kinetic nature of the skull.

Anterior to the basipterygoid process, the ledge can be described as a subocular shelf. It is separated from the mesioventral part of the basisphenoid by the posterior part of the internasal fossa, which grows rapidly deeper towards the anterior. In this area, the ledge has a distinct, sharply demarcated ventrolateral face that begins at the base of the basipterygoid process and grows progressively wider anteriorly until it terminates at the ethmoidal articulation.

Two relatively large foramina lie on the orbitotectal-basisphenoid suture immediately behind the optic nerve foramen, where the concavity is at its deepest and most sharply delineated, while a third, slightly smaller foramen pierces the basisphenoid a few millimetres above the basipterygoid process. The two foramina on the suture are confluent in some individuals (such as WAM 92.8.2) and presumably represent two, somewhat variably developed, branches of a single tract. Long (2001) tentatively interpreted the single foramen in WAM 92.8.2 as transmitting cranial nerve III. However, the canal from this foramen runs posteromesially into the posterodorsal extremity of the hypophysial fossa, showing that it in fact housed a blood vessel associated with the hypophysis. The canal from the foramen above the basipterygoid process runs steeply down ventromesially to open into the ventral part of the fossa. We interpret this foramen as transmitting the artery of the orbital margin, and the foramina on the suture as the opening(s) for the pituitary vein (Fig. 56a).

Ventral to the ledge, the lateral face of the basipterygoid comprises two distinct surfaces, one anterior and one posterior, both of which slope ventromesially. The boundary between the two, which is quite sharp, lies just anterior to the level of the basipterygoid process. The anterior surface forms the posterodorsal boundary of the internasal fossa; it rapidly becomes more and more concave towards the anterior, and sutures anteriorly with the median ethmoid ossification. The posterior surface is almost flat, slopes posteroventromesially, and continues back to the margin of the notochordal facet. Ventrally, the basisphenoid sutures with the parasphenoid, which forms a small, wing-like dorsolateral process at the boundary between the two aforementioned surfaces. The large foramen for the internal carotid artery lies on the basisphenoid–parasphenoid suture, at the posterior margin of the wing-like process, and is directed posterolaterally.

In addition to the various foramina, the lateral face of the basisphenoid carries two small areas of distinctive surface texture which may represent muscle attachments. The more

posterior of these is a curving, narrow field of rugose texture that runs from the posterior pituitary vein foramen, down past the foramen for the artery of the orbital margin (the foramen lies on the ventral margin of the rugose field), and then continues in an attenuated and less obviously rugose form along the lateral margin of the subocular shelf, terminating half-way between the basipterygoid process and the postnasal wall scar (Fig. 56a). Comparison with *Latimeria* (Millot & Anthony 1958) indicates that this is a compound attachment area for (from posterior to anterior) the superior, external, inferior and internal rectus muscles of the eye. On the anterior part of the basisphenoid, anteroventral to the optic nerve foramen, lies a rounded, slightly sunken area with a matt surface texture indicating minute pitting. This is most probably the attachment for the inferior and superior obliquus muscles.

The anterior margin of the lateral portion of the basisphenoid consists entirely of unfinished bone. It sutures with the lateral ethmoid ossification (see below), but the sutural zone features a broad, laterally facing strip of unfinished bone that must be the attachment scar for the (cartilaginous) postnasal wall. The most ventral part of this unfinished area is expanded posteriorly and has a smoother internal surface than the rest; we interpret this as the ethmoid articulation for the palatoquadrate. A puzzling feature is a short but deep horizontal groove in the lateral face of the basisphenoid, anteroventral to the presumed obliquus attachment, that terminates anteriorly at the postnasal wall scar. It is clearly not a gutter leading into a canal, and indeed the right side of BMNH P64125 shows that the groove terminates abruptly with a rounded end. Nor did it receive any part of the autopalatine. As has already been mentioned, the autopalatine of BMNH P64125 is preserved and can be placed in life position alongside the ethmosphenoid; when this is done, the anterior ramus of the autopalatine comes to lie ventrolateral to the subocular shelf, well below the level of the groove. The significance of this groove remains uncertain.

Specimens BMNH P63570 and P63571, in which the various ethmosphenoid ossifications have not sutured together, reveal the cavity of the hypophysial fossa. It has an irregular ovoid shape, with a relatively straight anterior margin and more strongly curved posterior margin. The walls of the fossa are lined with perichondral bone, but have a very unusual honeycomb texture and are pierced by numerous small foramina. As mentioned above, the canal for the artery of the orbital margin pierces the side wall of the lower part of the fossa. On the other hand, the pituitary vein enters the posterodorsal margin of the fossa at a point just below the irregular midline hole that opens from the fossa to the centre of the notochordal facet.

13.2.4. Parasphenoid. The carotid foramen is not enclosed within the basisphenoid, but forms a large notch in the ventral margin of the bone, which is closed ventrally by the parasphenoid. The dorsal surface of the parasphenoid reflects this arrangement. It has two separate sutural areas, a large arrowhead-shaped anterior area, and a small triangular posterior area for receiving the parts of the basisphenoid which lie anterior and posterior to the carotid notch. The posterior sutural area is raised on a distinct stalk, but both sutural areas are deeply concave. Separating the two sutural areas is a non-sutural strip of bone, essentially corresponding to the anterior face of the aforementioned stalk, that forms the floor and rear wall of the confluent left and right carotid tracts. In the middle of this floor lies the large, transversely oblong dorsal opening of the buccohypophysial canal, which pierces the parasphenoid and opens through a similar large foramen on the posteroventral surface of the bone.

The ventral surface of the parasphenoid is, as is usual among sarcopterygian fishes, dominated by a sharply demarcated denticulated field. In *Onychodus*, this field projects so strongly below the main body of the bone that it can reasonably be described as forming a distinct process. In some specimens, notably BMNH P64125, it has the distinct appearance of a separate dental plate that is only imperfectly fused with the body of the parasphenoid, but in other specimens, this is less clear. On ANU 72975, the denticulated plate is firmly attached to the bone on one side of the specimen, but not on the other. In BMNH P64125, the denticulated plate forms a separate structure that lines the parasphenoid proper and extends some way anterior to it (Fig. 58). The ANU specimens do not show this feature, the denticulated plate (dental plate on Fig. 58) is restricted to the plate to which the denticles are attached, and it is firmly attached to the parasphenoid proper. This is another example of the variability of the whole parasphenoidal structure that will be dealt with below.

The parasphenoid dentition is extraordinarily variable. In BMNH P64125 and P63570, it takes the form of a fairly broad triangular area covered in denticles; in WAM 90.11.1, the anterior end of the triangle is shorter and carries a cluster of enlarged denticles (Long 2001, fig. 3H); in BMNH P63571, the dentition forms a trilobate structure comprising a single median denticle row and a pair of lateral lobes, each carrying a curving marginal denticle row and some additional denticles; in WAM 92.8.2, only the median denticle row is present; in ANU 72978, it consists of a median projection with denticles, and a distinct right process with a limited number of denticles, and a left swelling that is really not a process; and ANU 72975 is an irregular shape with the left projection the more dominant (Fig. 57). The shape of the dental area often shows significant asymmetry, particularly at the posterior end. The only wholly consistent feature is the position of the buccohypophysial foramen immediately behind and slightly dorsal to the dental field, bounded posteriorly by a very thin rim of bone that sometimes also carries minute denticles. *Youngolepis* is the only other sarcopterygian for which a comparable range of parasphenoid variation has been described (Chang 1982), but the actual parasphenoid morphology in this genus is quite different. In a personal communication to Long, Chang (2003) reported that more than one species of *Youngolepis* may be present.

Anteriorly the parasphenoid is attached to the well-ossified median ethmoid. The dorsal surface of this bone passes into what must have been a cartilaginous mass that bent laterally to form the dorsal surface of the cavities for the reception of the mandibular tusk whorls when the mouth was closed. As was shown above under the discussion of the orbitotectal, the olfactory canal runs in a groove around the posterior end of the space for the mandibular tusks, and the brain cavity must have been anteriorly compressed. The brain cavity would have extended only slightly into the cartilage dorsal to the internasal fossae, if at all.

13.2.5. Ethmoid ossifications. In Osteolepiformes, the division between the sphenoid and ethmoid divisions of the braincase are not obvious, but Long (1985b) noted a suture in *Gogonasus*. Compared to the sphenoid and parasphenoid ossifications, the ethmoid ossifications of the braincase are rather featureless in *Onychodus*. The median ethmoid is a blade-like bone, forming the ventral part of the septum between the internasal fossae, that sutures broadly with the basisphenoid and parasphenoid posteriorly. Anteriorly, it achieves a short ventral suture with the posterior median process of one of the premaxillae (the premaxillae are asymmetrical: in BMNH P64125 and WAM 92.8.2, it is the right premaxilla that produces a large posterior process), but the anterior face of the median ethmoid is separated from the

facial laminae of the premaxillae by a gap that must have been cartilage-filled in life.

The lateral ethmoids, known only from BMNH P64125 (Figs 55 & 56a), are flat elements which form the mesial walls of the nasal capsules. Each has a mesial and a lateral face covered with finished bone, but all the edges are unfinished. Posteriorly, the lateral ethmoid sutures with the basisphenoid and forms part of the scar for the postnasal wall. The mesial face, which forms part of the lateral wall of the internasal fossa, is smooth and continuous with the adjacent part of the basisphenoid. The lateral face, which is the surface lining the cavity of the nasal capsule, is rather more interesting. It is mostly smooth apart from a diffuse, posterodorsally located, circular patch with a rugose texture that may relate to a local differentiation in the overlying sensory epithelium. The posterodorsal corner of the lateral face is drawn out into a shallow gutter where the olfactory nerve entered the capsule. A narrow (less than 1 mm) horizontal canal that pierces the postnasal wall is developed as an open gutter on the left side of BMNH P64125 and as an enclosed canal on the right side. This most likely transmitted a branch of the profundus nerve. The overall shape of the nasal capsules was strongly laterally compressed to make room for the enormous internasal fossae.

The total shape of the spaces for the reception of the anterior tusks is shown in Figure 53a. This illustration also shows how the nasal capsules must have fitted dorsal to the ridge on the inner face of the premaxillae and the predermopalatine. Figure 53b also shows the strong dorsal process on the orbitotectal and the posterior part of the cushion-like process anterior to it. A reconstruction of the head with the mandible open and closed is given in Figure 59.

13.2.6. Ethmosphenoid mechanics. From a mechanical perspective, perhaps the most curious aspect of the ethmosphenoid is the lack of a sutural attachment to the skull roof. Apart from the short suture between the median ethmoid and the posterior process of the premaxillae, there is no direct contact at all between the braincase ossifications and skull roof. Even the cushion-like dorsal processes of the orbitotectal, which underlie the parietals, are not actually sutured to the dermal bones and must have been separated from them by cartilage in life. More anteriorly, in the middle part of the ethmosphenoid, the cartilaginous dorsal part of the braincase was at least as deep as the ossified ventral part. This is in complete contrast to the condition in other Devonian lobe-fins, where the ethmosphenoid is not only fully ossified but so firmly fused to the skull roof that the two cannot be separated. The unique construction of the ethmosphenoid of *Onychodus* must have imparted a certain flexibility to this otherwise rigid structure, a flexibility that probably functioned to dissipate the stresses created by the action of the parasymphysial tooth whorls during the bite.

14. Scales

Scales are known from a number of individuals, and they show the same overall pattern no matter where they come from on the body. The smallest scales available to us are only 5 mm across, others are 12 mm and the largest are 22 mm. One small ridge scale has been separated.

All the body scales have a large anterior overlap. The overlapped part carries fine radial ridges on a slightly depressed surface (Fig. 60). At the anterior end of the scale, each fine radial ridge extends as a short process, which is part of the growing edge. Towards the posterior end of the overlapped section, a number of isolated pustules are arranged in irregular rows more or less along the lines of the ridges. On some specimens, these have slight depressions in their surfaces.

The exposed surfaces are covered with pustules, many of which are rounded, but others have depressions in their surfaces like those on the radial overlapped parts. The pustules are not regularly arrayed, but in general, the largest pustules are close to the overlapped surface and they decrease in size towards the scale margin.

The internal face of the scale carries concentric growth lines. In places, the growth lines carry rough nodes along their length (Fig. 60a). The concentric centre of the growth lines is placed beneath the anterior end of the pustular surface. This position varies in different parts of the body.

Lateral lines enter the scale at the most anterior end of the pustules and exit it internally *ca*. 2 mm from the posterior margin. The position of the lateral line is shown on Figure 61c. Note that the canal proceeding anteriorly from under the exposed part of the scale runs along the surface between the scales and then passes upwards into the next scale. The lateral line scale has numerous pores, and pit lines are common. As shown in the X-ray on Figure 60e, there are numerous branches from the main canal, and it is to these that the surface pores are connected.

The caudal region shows the lateral line running slightly dorsally towards the posterior terminus (Fig. 63a, b). This is unexpected given the almost symmetrical shape of the caudal fins.

A scale from *Onychodus sigmoides* from the lower Middle Devonian from the Delaware Formation in Ohio, USA, was figured by Ørvig (1957, fig. 7F). It has what he calls dentine ridges covered with radial structures quite unlike those of *O. jandemarrai*. The overlapped portion shows closely spaced pustules with depressions in their surfaces. These are more closely spaced than those on our species.

15. Fin structure

15.1. Caudal fins

The specimens on which this description of the caudal fins structures are based are: WAM 01.11.04, an individual preserved in limestone from Paddy's Valley; WAM 86.9.694, which are impressions in calcarenite from south of the Teichert Hills; and an individual from Paddy's Valley numbered BMNH P6569. The specimens preserved in calcarenite have been studied by latex impressions, and those preserved in limestone have been examined by direct observation. None of the specimens is complete.

The caudal peduncle is deep and covered with scales (Figs 62 & 63). Casts of the caudal fin from WAM 98.9.694 show that the tail is almost diphycercal. As shown on Figures 62, 63a, b & 64a, c, the dorsal lepidotrichia gradually increase in length from the anterior end, and approximately 20 lines of lepidotrichia are present before the maximum height of the fin is reached.

As shown on Figure 63a, b, the scaled part of the axis has a drawn out structure and its margins diverge at about 20°+. The lateral line canal runs down the middle of the scales except near the caudal end, where it bends dorsally and terminates well before the terminus (Fig. 63a, b). Although the terminus of the caudal fin is not well preserved on any specimen, a thin row of scales can be seen extending beyond the end of the main scales on WAM 01.11.04. This does not extend beyond the lepidotrichia, as is usual on the epicaudal lobe in coelacanths.

The proximal lepidotrichia are very fine and numerous; measured laterally, they number between eight and 10 per centimetre near the scales. At a distance of *ca*. 20 cm from the anterior part of the fin, on a caudal fin *ca*. 14 cm high, the lepidotrichs split into two about 6 cm from the scales, making

https://doi.org/10.1017/S0263593300001309 Published online by Cambridge University Press

a very fine margin. The splitting takes place 1·5 cm from the scales on the posterior part of the fin. The proximal lepidotrichia number from nine to 12 per centimetre on the medial parts of the fin. The distal rays are also finely divided, *ca.* 15 per centimetre. The anterior proximal lepidotrichs on both dorsal and ventral surfaces are shorter than those making up the central part of the fin, and they split nearer their proximal ends.

The proximal structure of the caudal fin is partly preserved on WAM 86.9.694 (Fig. 64a, c) and on ANU 49504 (Fig. 65A). At the dorsal anterior part of the fin on Figure 64c, *ca.* 10 proximal lepidotrichia are supported by two radials. More posteriorly, the radials shorten and they are not distinguishable towards the posterior half of the tail where the fin rays come very close to the axis.

The situation is somewhat clarified by ANU 49504 and ANU 49505 (Figs 65A & 65Bc), which are caudal regions which have been etched. Orientation of these specimens is difficult because no head has been found in position with the bodies. Nevertheless, this orientation is important because it determines what we have to say about the median fins.

In ANU 49504, only the hypochordal proximal radials of the caudal fin have been preserved. They are strong structures and the complete ones are slightly swollen at their ends. In ANU 49505, most of the elements have been dissociated during preservation, but enough detail remains to clarify the main problems. Radials are scattered over the anterior part of the inner surface, indicating that they originally lay within the scale-covered part of the fin. Only a few small radials occur on the posterior part of the fin and they are only 5 mm long compared with the anterior ones, which are 13–14 mm long. The radials are dumbbell shaped and are slightly ossified. One end of a radial is larger than the other, and so far as we can see, the larger one is at the vertebral end. This end is sometimes not rounded, but is flattened and is cut off obliquely, indicating that it was attached to an internal structure. No ossification of their axes is present and they are easily broken. Those at the anterior end of the tail are more uniform in diameter than those further posteriorly.

As shown above, the radials must have supported several primary lepidotrichia, and from the numbers present, we conclude that each radial must have supported four primary lepidotrichia. The flared ends of the scattered radials, as shown in Figure 65Bc, allow this attachment to occur. The proximal lepidotrichia have long proximal ends, with a slight furrow on the medial surface, and they terminate at a point.

In WAM 01.11.04 (Fig. 63e), there is an unusual development of rows of expanded, posteroventrally orientated radials just below the distal region of the tail. These larger, broader structures are angled at about 60° to the tail and are positioned as two rows of subrectangular flat elements which ventrally articulate with a series of elongate horizontal lepidotrichia. To our knowledge, such an arrangement is not known in any other sarcopterygian fish.

The distal lepidotrichia are also well illustrated (Figs 63a, b, e, 64c & 65Bb, c). Their external surface is well rounded, and the internal surface is grooved as is normal.

15.2. Second dorsal fin

Part of the ray structure and the internal support features of the second dorsal fin, are preserved on ANU 49504. On WAM 86.9.694, the exterior of the base and much of the body of the second dorsal fin is preserved, but it lacks the distal posterior extremity of the lepidotrichs. The specimen BMNH P63569 (Fig. 62) is preserved as part and counterpart, but some material has been lost in the peduncle area. We have not been able to detect the lateral line in the caudal region, and so the orientation of the specimen is not clear. One long fin extends posteriorly along half the caudal fin and this could be the second dorsal fin.

In ANU 49504, the fin support is in two parts, the anteroventral part (labelled X on Fig. 65Ba) on which the attachment to the neural arch is present, and a much larger dorsal part (labelled Y on Fig 65Ba), to which the radials were attached. In the anteroventral part, the attachment has been broken, but its outline can be seen on the bottom side of the break. The ossified margin around the plate is not complete, and the attachment opening joins an elongate gap in the periossified bone on its dorsal side. The junction between the two plates is just a line, and we see no evidence of mobility along this edge. The attachment of the radials takes place along stepped edges, of which four are clear. The most ventral attachment is double, and it is also slightly bent. The most ventral radial is the largest one present, and the second radial is only about half the size of the ventral one. It is tucked into a small space. The third and fourth radials are similar in shape to the second, and the two attachments are each stepped forward one after the other. The edge of the support plate is broken beyond the fourth attachment, but the position of the radials and the lepidotrichs attached to the fourth radial demonstrate that no further radials were present. There are approximately 35 proximal lepidotrichs, which are up to 15 mm long, and are pointed at their proximal ends. They overlap the radials in places. The distal lepidotrichs have thick walls and number three or four per 5 mm. On WAM 86.9.694, the second dorsal fin is partially preserved (Fig. 64b). It is situated slightly posterior to the position of the anal fin. The size of the fin is not clear from our specimens, but it must have extended back to lie above the anterior caudal fin.

15.3. First dorsal fin

The first dorsal fin is incomplete on ANU 49504, consisting as it does of 16 or 17 proximal lepidotrichs only (Fig. 65A). There is room for several more lepidotrichs. No support structures are present, and etching has not produced any evidence of buried material.

BMNH P63571 preserves an isolated endoskeletal element that we interpret as a support for a first dorsal fin (Fig. 63c, d). It is evidently a median fin support of some kind since it is preserved in articulation with a number of lepidotrichia and it shows bilateral symmetry. We interpret it as a first dorsal fin support because it differs from the known second dorsal and anal fin supports of *Onychodus*, and because the lepidotrichia articulate directly with the basal plate – a phenomenon also seen in the first dorsal fins of *Glyptolepis* (Ahlberg 1991) and *Latimeria* (Millot & Anthony 1958). The dorsal margin is essentially straight, and it articulates with the lepidotrichia. Posteriorly, this margin carries an incised 'ledge' on each side, most probably for muscle attachment. A fairly large foramen (labelled foramen a in the figure), which may have transmitted a blood vessel or nerve, opens onto the floor of this ledge. On the posterior surface is a second foramen (labelled b in the figure) that has an unknown function. The ventral margin of the bone is jagged, and carries a large anteroventrally directed process with an open distal end that probably articulated with a neural arch. A smaller, ventrally directed process posterior to it may have contacted the next neural arch or supraneural, but the details are not clear.

If specimen WAM 86.9.694 is correctly oriented, the first dorsal fin is present, and part of it is overlapped by the scales. It is illustrated in Figure 64b, d. Only the secondary lepidotrichia, as they emerge from the scale covered area, are preserved. The fin has groups of short, stiff lepidotrichia emanating from a series of primary lepidotrichia. A small area of squamation

https://doi.org/10.1017/S0263593300001309 Published online by Cambridge University Press

showing small ovoid scales overlap across the base of the fin. Four or five secondary lepidotrichia attach to each primary lepidotrich, and these branch distally shortly after they pass out from under the scale covering.

BMNH P63569 has a fragment of a first dorsal fin, but requires further preparation of the surface before description.

15.4. Anal fin

The anal fin is a very large structure that extends back to lie beneath the anterior part of the caudal fin. On ANU 49504, the support structure is a single plate with a distinct outline (Figs 65A & 65Bb). It is not preserved in its normal position, being rotated slightly in a clockwise direction. The dorsal edge of the support is slightly sinuous, with the distal tip upturned. Approximately one-third of the length from the anterior end, the dorsal edge has a gap which may have been for the attachment of a ligament. This would have joined the vertebral column to give stability to the support. The distal end of the plate has places for the attachment of five radials. These are all stepped, the dorsal ones being placed progressively more posteriorly. The proximal attachment surface is marked with an arrow in Figure 65Bb, and the specimen from which it was taken is shown on Figure 65A. The two dorsal attachments are turned slightly with respect to the other attachments. The ventral edge of the support is only about half as long as the dorsal edge, and it is not formed of complete bone leaving an open ventral face. The specimen does not show how the attachment of this plate lies in relation to the attachment of the second dorsal fin. No radials are preserved, which is surprising. The attachment surfaces on the main structure indicate that the radials should have been like those on the second dorsal fin. They may have been cartilaginous, but they could have been bone lost during preparation. As the lepidotrichs are badly distorted, the fin may have been twisted during death and this may have broken the radials.

The lepidotrichia are so distorted that most details cannot be determined. The primary lepidotrichia are of the usual type with pointed tips, and they are 12 mm long. The distal lepidotrichs are robust. The shape of the fin cannot be determined from the etched specimen, but the greatest length of the lepidotrichia is *ca*. 60 mm. It is not possible to determine the number of rows of lepidotrichia, but it must have been approximately 30.

15.5. Pectoral fin

The pectoral fin is poorly known, but the right humerus of the holotype (WAM 92.2.8) is well preserved (Figs 66–68). It articulates with the well-preserved scapulocoracoid. It has two distal articulation surfaces, indicating that the pectoral fin had both a radius and an ulna. It is a stout, robust bone with a weakly concave *caput humeri* forming a broad bean-shaped articulation with the scapulocoracoid. The dorsal surface of the humerus (Figs 66b & 67b) is weakly convex with a slightly developed mesial projection of bone, and the ventral surface is strongly convex with a median ventrolateral process developed.

The pectoral fin apparently lacked mobility in the horizontal plane, and had only weak movement in a vertical plane unless a large cartilage pad was present at the articulation. In this respect, the *caput humeri* resembles that of *Glyptolepis* (Ahlberg 1989), but differs from the prominent convex *caput humeri* seen in osteolepiforms, or the almost hemispherical *caput humeri* seen in Rhizodontida (Andrews & Westoll 1970b; Long 1989).

A foramen exists mesial to the mid-line of the bone on the area we interpret as being possibly homologous with the supinator attachment area, as compared with *Strepsodus* (Andrews & Westoll 1970a, on *Eusthenopteron*; and *Mandageria* Johanson & Ahlberg 1997; Parker *et al*. 2005) and Rhizodontida. If this interpretation is correct, the foramen could be homologous to the entepicondylar foramen in Osteolepiformes and Rhizodontida. As there is no development of an entepicondyle, the exact identification of the foramen is uncertain, even more so that several foramina appear to be present in the region of the entepicondylar foramen in Rhizodontida (Parker *et al*. 2005, fig. 11A).

The mesiodorsal surface of the humerus, just anterior to the mesial process, has an area of smooth bone delineated by a short oblique ridge, here seen to be the equivalent region which in *Strepsodus* for the attachment of the deltoid muscles. There is no deltoid process present, as seen in the Rhizodontida and Osteolepiformes.

In ventral view, the humerus has a longitudinal median process (Figs 66d & 67d). On either side of this process are rounded areas of concave roughened bone for muscle attachments. The distal face of the bone is characterised by two articulation surfaces separated by a short oblique ridge. One faces posteriorly and the other posteromesially, indicating that the two mesomeres (ulna and radius) articulated with them. The two facets for these articulations are set at an angle of approximately 50°. There is some contention about which of these two attachments is for the radius and which for the ulna. *Sauripterus* and *Acanthostega* have the radius in an anterior position on the limb (Andrews & Westoll 1970b; Coates 1996), and this seems to have been the primitive condition for the fin.

The lateral face of the humerus (Fig. 67d) has a slightly irregular surface that, anteriorly, could have been for insertion of the latissimus dorsi muscles.

15.6. Pelvic fin

The pelvic fin is poorly preserved or absent on all the specimens. ANU 49504 has the best fragment (Fig. 65A). It has strong primibrachs, pointed at the proximal end and well rounded at the distal. The secondary lepidotrichia are up to 30 mm long, but details are not known. No supporting structures are known.

16. Vertebral column and neural and haemal arches

16.1. Intercentra

No vertebral elements are preserved in position, but isolated fragments have been found in the large individual (ANU 49504) from which the fin data have been extracted. These elements have been preserved in the anterior part of the individual in front of the dorsal fins. Isolated fragments are known from ANU 92572 and from ANU 72975. Interpretation is difficult, and our reconstructions have to some extent been guided by the work of Andrews & Westoll (1970a, b) for rhipidistians in which the vertebral elements have been preserved in articulation.

The intercentra are lunate arches, and should be compared with those of *Osteolepis* (Andrews & Westoll 1970b). Their inner faces are composed of coarse vesicular bone, and the outer face is shiny bone with an occasional perforation. One face of each unit is tapered (Fig. 69f–i), while the opposite face is abrupt and has a short flange (Fig. 69j–l). The flange is also shown on Figure 69a, c, e. From their position in specimens, we have not been able to interpret which of these faces is anterior or posterior, but we have oriented the face with the flange as anterior in Figure 69. The posterior face contacts the

https://doi.org/10.1017/S0263593300001309 Published online by Cambridge University Press

cartilaginous intervertebral tissue. Ventrally, there is no connection between the two intercentral arches, and unlike *Eusthenopteron foordi*, there is no support for the haemal arches attached to the intercentra.

16.2. Pleurocentra

Other structures with smooth external and rough internal faces are available from ANU 49504. The anterior and posterior faces of the units have bluff attachment surfaces. The terminal faces have flattened surfaces for attachment to other tissue. The inner face has coarse bony tissue like the intercentra, but the details are lost as a result of weathering. The interpretation of these structures depends on the five isolated individuals from the holotype in which the inner face is much better preserved (Fig. 70). The individuals are approximately the same size as the plates from the previous specimen. The periosteal face is either flat or slightly concave, indicating that the bone was not attached around the notochord. The inner face has a raised rim of hard bone outlining a depression that runs across the bone asymmetrically, and passes off the bone in a narrow furrow. In life, they were oriented so that the ventral nerve root passed across it from low on the neural arch (Fig. 72a, b).

16.3. Neural arches

16.3.1. General statement. Perhaps the most significant point to be made is that the arches are extremely variable, and description requires much detail. The neural arches were preserved as a sequence of five adjacent units on ANU 49211; the specimen is from the middle part of the body, and so it is not possible to interpret their structure in terms of the junction between the body and the head. The extent of the possible distortion during preservation is minimal. In addition, the large specimen, ANU 49504, has several arches preserved in various orientations, and these are considered below. One most important point is that the arches have clearly defined attachment surfaces to the vertebral column, and these have a long ventral edge for a direct attachment, and a dorsally turned edge that must have been for a junction with the next anterior unit. In addition, the posterior faces of some of the arches have attachment surfaces, indicating that they were joined to the next arch by ligaments. These two factors provide an explanation of why no dorsal longitudinal ligament is present on any unit.

A number of features concerning nerve roots can be recorded here. On the posterior face of the arch, dorsal to the attachment to the cartilage of the vertebral column, is a large furrow which is oriented ventrolaterally. It was for the ventral nerve root. It is usually a single opening, but it is occasionally divided, and it may contain one of the dorsal nerve roots as well as the ventral root. Usually the anterior side of the arch has two grooves in a more dorsal position, and these carry the dorsal nerve roots. On some specimens, these grooves are not present, and the dorsal roots pass out against the roof of the neural canal or they may pass out through a loop of bone on the anterior surface.

16.3.2. The neural arches. On ANU 49211, one neural arch is preserved intact, and the others were separated during preservation. This latter point is an advantage since it is possible to examine the internal structure of the unit. A main feature of these elements is that they are asymmetrical and their internal structures differ from one side to the other, and from arch to arch. On occasional arches, the two arches are joined together over most of its length, but adjacent units are loosely joined. Moreover, it is clear that the nerve foramina were different on the opposite sides of a single arch (Figs 71k, m & 73a, b). The notochordal canal must have been very large, even though no canal has been preserved.

First, we describe the complete individual ANU 49211 (Figs 71k–m & 73a). The arch is curved laterally, inclined posteriorly, and with the right side longer than the left. The junction between the arch and the tissue surrounding the notochord consists of coarse rough tissue. As one would expect from the posterior inclination of the arch, this attachment surface rises higher on the posterior side than the anterior. The ventral external surface is covered by deep incisions which have no definite arrangement. The anterior faces have loops of bone, but although the loop on the left side is broken, the points of its attachment are preserved. Two slight depressions occur in the walls, indicating that two nerves pass out through the loop, and these must be the dorsal nerve canals. The posterior faces of the arch show attachment surfaces probably for attachment to the next posterior arch. These surfaces are not symmetrically placed because the lengths of the arches are unequal. An opening for ventral nerve roots to pass out occurs just dorsal to the attachment area to the vertebral cartilage, leaving a deep furrow in the wall of the arch.

Internally, the arch is complete dorsally, and in the arch is a small perforation that passes into a dorsal tube that opens on the front wall of the arch. The significance of this arch is discussed below under section 17, 'Function'.

The space for the neural cord is large and open, and it is closed ventrally by ridges from each arch which join medially. Ventral to this is an open space that housed the top of the notochord. This is surrounded by the attachment surfaces for the lateral walls of the arch. This is an unusual pattern. No evidence of a foramen for the dorsal ligament is present on the arch, so that the adjacent arches were not joined in this position.

In this set of five neural arches, this is the only one that shows the junction between left and right sides ventral to the neural cord (Fig. 71 l, m). All other specimens show a thickening at the appropriate places on the arch, but a gap is left between them. The spinal cord must have been close to the notochord. Other features of these arches are: the weak junction between the two sides of the arches at their dorsal ends; the opening for the ventral nerve root just above the attachment areas for the arches at their bases; the foramen for the dorsal nerve roots on the anterior edges of the arches; and the ventral nerve root on the posterior face just dorsal to the attachment of the arches to the cartilage around the lateral walls of the notochord.

Secondly, we comment on ANU 49504, which as two neural arches from the medial part of the skeleton. They have been removed from the individual, during which one was broken. They have been reassembled to show the general form and most details. The specimen is highly asymmetrical, has a broken dorsal end, but the arches are well preserved (Figs 71s, t & 73c), and it was preserved in a position where it would have supported the second dorsal fin, and we assume that this was its function. The left arch has a projection on its anterior surface that is absent on the right arch, and the arch itself is shorter than the right one. This projection carries a surface for the attachment of a ligament that presumably attaches the arch to the one anterior to it. The left arch has a small attachment at its base just dorsal to the basal attachment. Dorsally, a groove runs off to the left side between the arches, but we have no evidence of where this terminates. It is most likely to be the carrier of the same tissue as runs through the crest of ANU 49211 and the other arch described below. The posterior side of the arch has a depressed attachment surface, and ventral to this is a furrow that carried the ventral nerve root. The left side is asymmetrical and has a surface close

https://doi.org/10.1017/S0263593300001309 Published online by Cambridge University Press

to the ventral attachment surface; it has no space for a nerve opening.

Thirdly, the second arch from the medial part of ANU 49504 is very informative. The two sides of the arch are joined dorsally and there is no evidence of a dividing wall between them (Figs 71c–f & 72b). The left side of the arch is longer than the right. On the posterior faces, both arches have elongated attachment surfaces (Fig. 72b). Between these attachments and the basal surface is a deep groove for the ventral nerve root. The anterior faces of the arches have no evidence of ligament attachment surfaces, but the surface on the dorsal spine has an ovate surface surrounded by a rim of hard bone. This has the appearance of a ligament attachment. Certainly, it contains no foramen for the passage of a vessel. On the other hand, before the specimen was broken, a small opening was present in the dorsal margin of the nerve cord and this opened into a branching canal that opened on the anterior face of the spine through paired openings, one on each side of the midline (Fig. 71c, f). This is the same structure as opens through a single opening in other specimens.

The posterior part of ANU 49504 has produced two arches which were adjacent. Both crests on the arches are more or less complete, i.e. they have a single dorsal spine that is almost complete and has a pit which connects with the inner surface dorsal to the spinal cord. One of these is figured (Figs 71a, b & 72a). The anterior face has no evidence of an attachment surface. The gaps for the dorsal nerve roots are not clear, but on the right side, a single furrow lies opposite the dorsal edge of the canal for the spinal cord. Presumably this was for the dorsal nerve roots. The two arches are of different sizes, the right one being the longer (this has a long ventral attachment surface). Dorsal to this attachment surface on the posterior face is a poorly defined gap for the passage of the ventral nerve roots. Dorsal to this and at the base of the dorsal spine, each side has a strong attachment area for the pleurocentrum. The ventral nerve roots are placed just below these attachments, and this places them in a very dorsal position, probably because of the inclination of the whole arch. The dorsal surface of the canal for the spinal cord canal is preserved, making an almost smooth surface, but the ventral edge is not preserved. There is no hard tissue separating the spinal cord from the notochordal cavity. The dorsal median canal opens directly into the spinal cord canal through a large opening. This is a larger opening than those observed on any other vertebra.

Other neural spines in which the dorsal spine is not a single unit are illustrated on Figure 71g–j, p–r. These show well the variation in the internal structure, the different shapes of the canals for the dorsal and ventral nerve roots, and the differences between the two sides of a single specimen.

16.4. Supraneural spines

On the anterior part of ANU 49504, several long spines are present. These clearly belong to the vertebral column. They have ovate or slightly expanded ends, indicating that they were attached to the ends of the neural arches. The spines are 1·5–2·0 cm long and are open at both ends. This suggests that there are distal supraneural spines present, but they have not been identified.

16.5. Haemal arches

Two haemal arches have been recovered from ANU 49211. The arches are two-sided, and individuals with the longest arches also have the two sides of the arches joined. The attachment surfaces to the vertebral column have a dorsal upturn on both the anterior and posterior faces, and this suggests that the arches of adjacent units were joined against the vertebral column. Dorsally, the arches were joined by an oblique transverse band which capped the haemal passage (broken in Fig. 71n, o), and the haemal arch is high and narrow. The posterior face of each arch has a deep furrow. From the shape of the basal attachment, we conclude that the arches were steeply inclined to the horizontal. Reconstructions of the neural are shown in Figures 73A and 73B.

17. Function

17.1. Features related to the development of parasymphysial whorls

A number of distinctive features of *Onychodus* can be related to the parasymphysial whorls and their function. These are: the large cartilaginous mandibular articulation; the large intracranial gap in the skull roof; the overlap of the premaxilla and the maxilla in the snout; the large internasal fossae which contained the whorls themselves when the mouth was closed; the position of the cavity in the endopterygoid; the position of the dentary teeth in relation to the teeth of the upper jaw; the large posterior swelling of the maxilla; the lateral position and reduction in size of the nasal capsules; the highly modified ethmosphenoid; the junction between the premaxillary and the maxillary; the loss of the vomer; and the flexibility of the shoulder girdle.

Long (1991) described a placoderm skeleton enclosed within the cranial bones of an *Onychodus*. The placoderm was estimated at 30 cm long and the *Onychodus* specimen was 60 cm long. He interpreted this as showing that *Onychodus* was a predator of large animals with massive skeletons. The capacity to attach such prey requires a number of morphological features, all of which are related. They have to be discussed along with the overall morphology of the skull to make sense of the total structure of *O. jandemarrai*. But of particular importance is the means by which the mandible is articulated.

17.1.1. Articulation of the mandible. The articulation is entirely in cartilage. Our interpretation of the total structure is given in Figure 74. There is no evidence that the articulation was in any way encased in bone. What we have to consider are the following points related to the jaw closure, all of which are related to the opening and closure of the tusk whorls: (a) the lack of a symphysis in the mandible would allow the opposing sides of the mandible to separate when the jaw strikes a prey item. They would have to be rotated inwards on closure in order to fit the tusk whorls into the spaces in the upper jaw, which are very restricted in width. (b) The position of the unconfined cartilage attachment of the mandible also causes difficulties with the closure of the tusk whorls. Because this articulation was capable of lateral movement, this would also cause the tusk walls to move out of alignment. (c) The closure of the mandible is a major problem. Consequently, the presence of the cartilage, or fibrous, pad in the pterygoid and the capacity of the teeth on the mandible to be enclosed by the tooth rows in the upper jaw, would keep the mandible and the tusk whorls in alignment.

Because the tusk whorls could rotate, the above points require us to offer a new method of mandibular articulation. Comparison with primitive actinopterygian and coelacanths does not offer a solution because they are suction feeders or they have a firm articulation of the mandible with the quadrate, or they have a retroarticular process.

Given the above information, we have suggested a hypothesis below that takes into account the structures which are preserved in our specimens of *Onychodus*. The posterior face of the quadrate is covered by bony surfaces to which cartilage

https://doi.org/10.1017/S0263593300001309 Published online by Cambridge University Press

was attached. The smaller ventral surface is set at an angle of 60° to the dorsal surface. Anterior to the cartilaginous attachment on the dorsal surface is a smoothed surface which was probably for the attachment of muscles or ligaments (arrowed on Fig. 19d, f). The articular also has two fold surfaces to which cartilages were attached (Fig. 44c–g), but these consist of a large dorsal surface that bends evenly around to a posterior surface on to the ventral edge of the mandible. The dorsal surface was opposed to the ventral surface of the quadrate and these two surfaces provided the mandibular articulation faces. The angle between these two surfaces is *ca*. 70°, and this provides a large angle through which the mandible could move. The spaces between the two surfaces may have been occupied by synovial fluid (Fig. 74), or there may have been a synovial layer attached to the opposing surfaces. Given this interpretation of the structure, we consider that the large surface anterior to the cartilaginous attachment on the quadrate was for the attachment of muscles, and the smooth area on the ventral surface of the articular was also for muscle attachment (see statement below). To maintain the lubricated joint, we suggest that an encompassing flexible layer of connective tissue surrounded the structure. Such an arrangement would allow the vertical and lateral movement of the mandible. The amount of lateral movement was restricted by the occurrence of the maxilla over the outside of the articulation.

The remaining problem is to understand the means by which the mandible was lowered. We see two options: (a) There may have been ventral longitudinal muscles attached to the anterior end of the mandible, and thence to the pectoral girdle and the hyoid arch. No evidence for this interpretation can be found in the skeleton, but this is not surprising because of the difficulty of observing muscle scars on the skeleton. On the other hand, muscles attached to the mobile symphysial region of the mandible would not have been effective. (b) The cartilage surfaces around the quadrate and the articular offer an explanation that has firm observational data to support it. The smooth space anterior to the cartilage attachment on the dorsal surface of the quadrate provides an attachment surface for muscles or ligaments, and one specimen of the articular has a ventral space which could also have been for the attachment of similar structures. Muscles attached to these surfaces would have had to be enclosed in the connective tissue encompassing the mandibular joint. Such a bend may have had an aponeurosis to allow the dorsal and the ventral components of the muscles to operate independently (Fig. 74). Although the muscles would have been short, even a contraction of 20% of muscles in the stated position would have caused a large mouth opening.

Ahlberg does not accept this interpretation, and he considers that the jaw was opened by the coracobranchial musculature, as this is the general condition for gnathostome fishes.

17.1.2. Did the parasymphysial whorls rotate? Two median parasymphysial whorls lie on the front part of the mandible. Andrews (1989) has commented on the specimen illustrated in Figure 3, that 'assembled jaws can be opened and shut, so that it is now possible to study the way in which the strange whorls of teeth worked. When the mouth opened they apparently rotated outwards and forwards to stab the prey.' We also note that the whorls lie in a position where the edge of the whorl overlaps the symphysial region of the mandible, thus placing it in a position to roll outwards. A similar position is also shown on the specimens on Fig. 28a, c).

As we have shown above, the whorls are composed of calcified cartilage, and they lie on a soft layer above Meckel's Cartilage. In a bite, the tusks must have transmitted pressure on the whorls, and thence to Meckel's Cartilage. The question then has to be posed concerning the relative immobility of the whorls, or if they were able to rotate anteriorly during feeding. A centre of ossification on the symphysial plate on the inner face of the dentary (Fig. 36b, c) indicates the early ontogeny of the parasymphysial whorl. A horizontal line through this point and the maximum curvature of the parasymphysial whorl provides a theoretical axis around which the whorl could rotate. However, this does not prove that the whorls could rotate during biting. Another line of argument must be used to support inferred rotational movement.

With the whorls placed in position, especially in the juvenile specimens, the array of tusks covers an arc of up to 100° (Fig. 28a, c). With the whorl in such a position so that with the jaws closed the anterior tusk would fit into the space allowed for it in the palate, the posterior tusk would be well down between the dentaries. This is the correct level for the insertion of new tusks into the whorl, but it leaves one further matter to be considered.

As illustrated on Figure 28 and elsewhere, the posterior tusks in a whorl are of approximately the same size as the anterior tusks. In other words, the tusks reached their maximum size when they were inserted in the whorl. Presumably this indicates that the whole parasymphysial whorl operates as a unit, and hence, could move independently of the tusk insertion tissue posterior to it. This is what one would expect if the whole whorl could move out to stab the prey. A second question concerns the function of the tusks. The premaxilla has a pair of slightly enlarged tusks, one on each side of the mid-line. These do not meet the parasymphysial tusks, but they lie anterior to and between the tusks when the jaw is closed. The parasymphysial tusks do not directly meet any teeth or tusks in the palate or in the upper jaw. Instead, the tusks on the whorl fit into cavities in the anterior of the palate. Their function must be for catching and holding the prey, and to do this they must have been able to extrude anteriorly beyond the anterior edge of the mandible. In addition, the posterior tusks would have no stabbing function if the tusks were always retracted in a position so that the tusks would fit into the cavities in the palate. A lurking habit with an ambush attack enabled the animal to surge forward, catching its prey on the tusks, and thence moving it into the mouth, rather like the Moray eel does at present. This animal has a maxillary process of the premaxilla that is posteriorly expanded and broadened transversely so that it can articulate against the internal process of the maxilla to maximise the gape during jaw opening.

Two points of view have been argued by the different authors of this paper. Ahlberg accepts that the whorls could be extended slightly outwards because of the method of tusk insertion, but he does not accept that they were retractible after catching prey. If the jaws were opened, only the anterior tusks would be in a position to stab the prey. Some other sarcopterygians, such as rhizodonts, derived tristichopterids and *Panderichthys*, have large fangs anteriorly in the mandible, and these function adequately in a fixed position without withdrawal. Comparison with the extant modern shark, *Chlamydoselache*, is useful in that its entire dentition is made of tooth whorls which are not retractible, but they rotate outwards only during growth.

Long *et al*. (1997), and also Andrews (1989), considered that an outrolling of the whorls was probable. Their interpretation is based on the following points:

a. The two whorls are not attached to any other bone medially or laterally. They were free to move. A comparison with the onychodont *Strunius rolandi* (Gross) is appropriate here. Jessen (1966) showed the tusks on a whorl incorporated in

https://doi.org/10.1017/S0263593300001309 Published online by Cambridge University Press

an ossified parasymphysial furrow that encloses the whorl laterally and medially. The tusks are much smaller than those of *Onychodus*, and the ability of the whorl to move them would have been limited because they are situated on a base that occupies the parasymphysial space. The freedom of the *Onychodus* whorls is significant, and they must have operated in a different way.

b. The tusks in *Onychodus* are larger than those of any other sarcopterygian apart from *Rhizodus*, and they were organised so that not all tusks would be in a position to take part in a bite unless the whorl were rotated outwards. As is shown in Figures 28, 29 and 31, the tusks are curved backwards, with a slightly forward turn at their tips. Even with the mandible fully opened, if the whorls did not rotate, the posterior tusks would be in too posterior a position to stab the prey.

c. As pointed out above, the structure of the whorls, with all the tusks of approximately the same size, shows that the whorl was an entity that could move as a unit independently of the growing tusks in a more posterior position. If the only mobility of the whorls was a slight forward movement to allow a new tusk to be inserted, one would expect the tusks to increase in size forward, and the open space at the posterior of the whorl where a new tusk was inserted would have the capacity to provide new growing surfaces. But this was not so. The dental laminae in which the tusks were developed must have been situated in the soft tissue posterior to the whorl because the tusks did not grow once they were inserted. This leaves a zone of transition between the whorl and the soft tissue containing the dental laminae that was restricted to the soft laminae posterior to the whorl.

d. It is worth noting that some onychodonts have tusks which are not pointed at their tips, but have notches which would hold the prey after it had been pierced (Gross 1965). But also note that the specimens of *O. jaekeli* figured by Gross have up to nine tusks, and these are approximately of the same size.

e. The tusks of *Rhizodus*, *Screbinodus* and *Strepsodus* are large, but recent work on these genera by Jeffery (2003) showed that the mandibles were in two functional units to accommodate the loading of the jaw during a bite. This was one way of dealing with the problem of large static tusks.

The arrangement of the muscles or ligaments which controlled whorl movement require special attention. The posterior and anterior ends of the whorls are involved with the insertion and loss of tusks, and hence, do not provide surfaces for the attachment of such muscles. However, the lateral sides of the whorl are modified and could have been for the attachment of muscles, or alternatively, cartilage attached to those surfaces could have been for muscle attachment. Those attached to the anterior end, anterior to the axis of rotation, would pull the whorl outwards, and those on the posterior end would retract it. One of the reviewers of this article has commented on the possibility of geniohyoideus/genioglossus muscles which may have acted passively or indirectly to cause rotation by opening of the mandible during the gape. These would have been attached to the external walls of the whorl. Further work is required on well-preserved material that has been prepared to examine muscle attachments in the anterior mandible. The absence of a clear mechanism to produce rotation in any extant species does not cause us to retract our views.

While dealing with this topic, we notice that the form described as *Onychodus jaekeli* Gross has nine teeth in the parasymphysial whorls which spread over *ca.* 135°, and that these are also of approximately equal length. These whorls are drawn as joined medially (Gross 1965, fig. 1f), and therefore, are not similar to *O. jandemarrai*. Despite this, the arguments suggested above would seem to apply to this species having outrolling whorls.

17.1.3. Small denticles in the symphysial whorls. In dorsal view, the space between the tusks is open. This is unlike the whorls of *Strunius* where the teeth are surrounded by bone referred to by Jessen (1966) as parasymphysial bone. The denticles in *Onychodus* are distributed along the walls of the whorls in an irregular pattern at different growth stages (Fig. 29a, d, e). In the largest specimen we have available, the denticles have a distinctive arrangement. Those lying between the tusks are inclined at a low angle towards the midline, protecting the space between them. The denticles beside the tusks have more vertical axes, and they lie against the tusks. These denticles are not part of the biting system, but protect the space between the tusks and the walls.

The smaller specimens have the tusks more closely spaced, and there is no large exposed space between the tusks. The longest denticles are upright against the tusks, and new smaller ones were being added between the teeth. Therefore, there was no overlap by the denticles of the tissue between the tusks.

We conclude that, as the space between the tusks increased during growth, new tusks were added further and further apart. Consequently, the need to protect the space between the tusks increased and the direction and size of the newly formed denticles changed. In adults, the space between the tusks was protected by the denticles and this was presumably to stop decay when food was left in the whorl after a bite.

We draw attention to the differences between the denticles in *Onychodus jandemarrai*, *O. sigmoides* and *Strunius rolandi*. According to Ørvig (1957, fig. 7F), *Onychodus* sp. from the Lower or Middle Devonian of Wijde Bay, Spitzbergen, has a single denticle standing vertically against the tusks. Jessen (1966, pl. 19, fig. 1) illustrates an incomplete specimen of *O. sigmoides* from the Middle Devonian of Ohio, USA, and this shows small denticles like those of our species, but the details are not clear. *Strunius rolandi*, as figured by Jessen (1966, fig. 10; pl. 17, fig. 4), shows a single large denticle on each side of the tusks. Presumably the denticles in *Strunius rolandi* acted as a means for disengaging the food from the tusks. Judging from Jessen's (1966) diagrams, the whorls had solid tissue between the tusks, and presumably they would not need protection such as we have proposed for *Onychodus jandemarrai*.

17.1.4. The significance of the adductor muscle attachment. At first sight, the small size of the adductor fossa seems puzzling in an animal that clearly had a highly kinetic bite, and would have needed powerful muscles to accelerate the jaw and drive the parasymphysial whorl tusks into the prey. Even the presence of additional muscle attachment area on the prearticular crest does not seem to provide adequate compensation. However, it may be that the ventral part of the adductor musculature was largely tendinous, and thus, not very bulky, while the larger active part of the musculature lay dorsally in the space between the palatoquadrate complex and the cheek, where there was ample space, and also into the cavity in the inner face of the quadrate. Such an arrangement would, in fact, be advantageous in an animal with a kinetic bite since it would reduce the amount of muscle mass that would actually move with the opening of the lower jaw, and hence, the inertia of the lower jaw as a whole. It is also worth noting that the anterodorsal orientation of the adductor muscles, which can be inferred with confidence as it is constrained by the shape of the palatoquadrate complex, means that the muscles would have pulled at 90° to the long axis of the mandible, and thus, have

had maximum effect, when the mouth was wide open. This is characteristic of animals with a kinetic bite.

17.1.5. Internasal fossae to receive the parasymphysial whorls on jaw closure. The retraction of the parasymphysial whorls was necessary if the mouth was to be closed. Since the tusks were large, gaps to enclose the whorls must have been deep, and they must also be placed quite precisely so that closure would not cause damage to the palate. Such structures are illustrated in Figures 53a and 59a, b with the median ethmoid bone in position. With lateral movement of the mandibular articulation, it is necessary to control the lateral movement of the mandible when the mouth is closed.

17.1.6. Pit in the endopterygoid. The pit in the endopterygoid, which has also been observed in *O. sigmoides* from Delaware, USA, may be a unique feature of the genus. We interpret this as having carried a mass of partly ossified cartilage or fibrous soft tissue that extended ventrally beyond the ends of the tusks in the ectopterygoid and lay on the inner face of the posterior coronoid during closure of the bite. It possibly acted as a guide to the movement of the mandible.

What evidence is there to support such an hypothesis? (a) The orientation of the axis of the pit is ventral, and the implication is that whatever occupied the pit was directed ventrally; (b) The thickening around the pit is such that it had the capacity to carry vertical stresses; (c) the ectopterygoid has a distinct bend in its outline opposite the position of the supposed cartilage, indicating that a vertical structure occupied that space; (d) The coronoids are remarkable in that they are lateral to the tusks of the ectopterygoids and the dermopalatines. This means that the tusks did not act as anything other than a grasping device; (e) The posterior coronoid is unlike the more anterior ones in that it is supported by a flange on the prearticular. This would have given it extra support if the cartilage stopper were slightly out of alignment.

Contrary to this view, one notes that the flange lies forwards within the bite, although the main part of the bite lies anterior to it. Hence, it could have been unusual to have a soft tissue in this region unless it was supported by some fibrous tissue. There is no evidence of any surface in the mandible to which any such soft tissue could attach, and so it must have been loose at its ventral end. It could be that this structure is related to the labial cartilage, as found in some teleostomes. An upper labial cartilage is present in *Polypterus*, and others are present in some sharks such as *Heterodontus*.

We still accept that a guide made of stiffened soft tissue, or partly ossified cartilage, is the best hypothesis available.

17.1.7. Position of the dentary teeth in relation to the teeth of the upper jaw. A support for the position taken above comes from the way in which the dentary teeth fit into the gap between the maxillary teeth and those of the ectopterygoid and the dermopalatine. As shown on Figures 10c, d, 11 and 75, the position of the dentary teeth allow little lateral movement of the mandible once the jaws continued to close. Note that the dentary teeth are larger than those on the maxilla (Fig. 28c), and that this gives them a powerful controlling position lying in the groove between the dermopalatine series and the maxilla. However, the engagement of the teeth becomes effective only after jaw closure permits these teeth to insert into the groove. Until this takes place, a guidance mechanism must be effective, and this is provided by the soft process attached to the endopterygoid. It is clear that the dentary teeth play the most important role in guiding the jaws through much of the closure.

17.1.8. Posterior expansion of the maxilla. The expanded post-orbital blade of the maxilla is similar to that in primitive actinopterygians. The maxilla overlaps the articulation with the lower jaw as in actinopterygians. Do these points imply a relationship of the onychodonts with actinopterygians, or are there other functional reasons for these structures? The teeth on the maxilla of onychodonts are restricted to the ridge along the internal surface of the bone (Figs 6j & 28c), whereas, in primitive actinopterygians, the teeth extend along the whole length of the maxilla, even the downturned edge (Pearson & Westoll 1979; Gardiner 1984). As shown by Schaeffer & Rosen (1961), Pearson & Westoll (1979, fig. 21d), and Lauder (1980), the gape of the mouth in primitive actinopterygians is very large, and maxillary teeth were functional along the whole length of the maxilla. Such is not the case in *Onychodus*.

In the second place, the posterior part of the endopterygoid in *Onychodus* is also turned ventrally inside the maxilla, which provides a shield for the adductor mandibulae. This system for the protection of the adductors relates directly to the degree of flexibility of the mandibular articulation with its cartilage junction.

We consider that the expanded posterior shape of the maxilla relates to the flexibility during feeding, the overlap with the lower jaw permits a wider gape, and it provides a cover for the capsule which embraces the mandibular articulation. In using the shape of the maxilla as evidence for a synapomorphy with actinopterygians, care must be taken to account also for the structure in *Onychodus* being the result of special adaptation related to the jaw articulation.

17.1.9. The position of the nasal capsules. The development of internasal fossae for the retracted parasymphysial whorls requires a major reconstruction of the anteromedial structures of the palate. In particular, the nasal capsules were displaced laterally, and they were decreased in size in comparison with other sarcopterygians. As can be seen from Figures 7c and 53a, the nasal capsules lie in a narrow space dorsal to the ridge that bears the premaxillary teeth. The inner face of the nasal capsules is formed by a thin lateral ethmoid. Obviously this position of the nasal capsules also controls the positions of the anterior and posterior nostrils.

17.1.10. Premaxillary and maxillary articulation. The posterior margin of the flange on the inner face of the premaxilla opens transversely for the articulation with the flange on the maxilla. This articulation is not fused, and movement at the joint was possible. Such would also be possible because the external dermal bones have overlapping surfaces. On extreme abduction of the mouth, flexure of this joint would have been similar to that of the premaxilla–maxilla joint observed in extant Moray eels such as *Lycodontis funebris* (personal observation).

17.1.11. The loss of the vomer. The retraction of the parasymphysial whorls also provides an explanation for the absence of a vomer. Either the vomer would have been displaced laterally as have the nasal capsules, or it could have been lost. If it had been laterally displaced, it would be the most anterior of the three bones in the dermopalatine series. But normally the vomers are defined as a median pair of palatal bones lying on the endocranium anterior to the parasphenoid. In *Onychodus*, the bone in question does not lie on the endocranium, but rather on the dermopalatine and the endopterygoid. Hence, not only is its position unusual, its relation to the surrounding bones is unusual. Therefore, we conclude that the vomer has been lost, and a predermopalatine is present.

17.1.12. Anomalies in the ethmosphenoid roof. A distinct intracranial gap lies between the two units of the skull roof. The posterior part of the ethmosphenoid unit is anomalous in that it has paired bones, the parietal bones, separated by a single median bone. The lateral line canal does not pass through the centres of ossification of the parietals, but rather, under an overlap in the posterolateral corners of the bone and

along its outer edges, and the infraorbital canal joins the longitudinal canal as it passes into the parietal suture. This organisation is not found in any other sarcopterygians, and is controlled by the support of the skull roof by cartilage loosely attached to the ethmosphenoid braincase, from which large processes rise beneath the parietals (Figs 53 & 54). The gap between the two parietals is occupied by the interparietal. The lateral line canals bypass the stress-bearing bones in the roof. The median part of the ethmosphenoid is occupied by a stout bony plate that separates the spaces through which the parasymphysial whorls are separated (Fig. 53a). This illustrates once again that the single fact of the modification of the anterior end of the skull by the parasymphysial whorls requires many changes, including extra bones in the skull roof pattern.

17.1.13. Braincase structure. The highly modified shape of the ethmosphenoid ossification, the extremely large cranial notochord and the fact that the otoccipital unit is largely cartilaginous is also a direct reflection of the feeding mechanism of *Onychodus* and the kinesis of the skull roof. The only ossified parts of the oticoccipital braincase are the partly ossified otic capsules and the zygals which support the ventral region. We do not know how posteriorly these units were situated, and they still leave a large ventral surface of the brain relatively unprotected. The small isolated teeth or those on thin bone in the pharynx found in some individuals (Fig. 20) provided some protection.

17.1.14. Attachment of the otico-occipital bones. The anterior ends of the postparietals overlie the posterior part of the ossified ethmosphenoid braincase block, anterior to the intracranial joint. The ethmosphenoid braincase has a surface that is visible when it is placed in correct position beneath the ethmosphenoid skull roof, and this underlies the anterior end of the postparietals (Fig. 53b). This surface would have provided a 'stabilising attachment' for the postparietals. The roofing bones were not firmly attached to the ethmosphenoid braincase, and we consider that it would not have impeded movement along the intracranial joint. Such a stabilising structure was necessary because the posterior part of the braincase was not ossified, and cartilage must have played some part in maintaining the posterior skull roof. The mobility of the intracranial joint depends on the flexibility of the parietal–postparietal junction. The wide gap between these bones in *Onychodus*, which must have been filled with soft tissue in life, is one of the features which point to unusual skull flexibility and kineticism in this genus.

17.1.15. The structure of the pectoral girdle. As we have discussed in the general description of the girdle, the position and orientation of the elements are difficult to determine because we have no assembled specimen. In his reconstruction of the holotype, Long (2001) left a gap between the cleithrum and the clavicle in his interpretation, and a gap between the operculum, the subopeculum and the pectoral girdle, and another gap at the top of the cleithrum largely because he has not included the posterior part of the skull roof. We have shown from overlaps that the bones are not separated as he suggested. The position of the lateral line entering the posttemporal places the cleithrum in its position, and this shows that the pectoral fin was high on the side of the fish. This is quite unlike the fin in *Strunius*, as shown by Jessen (1966, fig. 6B). It also shows that the ventral surface of the fish was convex. It lived above the sea floor, at least during feeding, although it may have lurked in cavities in the reef.

The operation of the gill system is also related to the arrangement of the pectoral girdle. The operculum overlaps part of the crest of the cleithrum, and its ventral edge lay against the edge of the preoperculum. The subopeculum fitted against the preopercular and against the process on the clavicle and the cleithrum posteriorly. Both the edge of the operculum and the crest of the subopeculum, where the two bones were adjacent, are feathered, indicating that the bones did not have a sharp contact, but had a mobile relationship. There is a problem of the loss of surface ornament in the cleithrum, the clavicular process and the surface ventral to it. On any reconstruction, the subopercular would have had to overlap these areas. This may cause other difficulties because it would put the postbranchial ridge on the clavicular process anterior to the posterior edge of the subopeculum.

The most striking feature of the gill cover of *Onychodus*, compared with those of other sarcopterygians, is the extremely short branchiostegal which creates a big gap in the gill cover skeleton between the subopercular and the gular plate. In osteolepiforms, porolepiforms and lungfishes, the branchiostegal(s) are the same length as the neighbouring bones, thus linking the subopercular and gular plates into a complete gular cover. The gap in *Onychodus* had a specific function. We have already noted that all the gill-cover bones seem to have been enclosed in a soft tissue flap, such as we see in *Latimeria* (Millot & Anthony 1958). Thus, the gap represents an area of soft gill cover. In the embryos of living jawed fishes, the posterior part of the hyoid arch (which forms the gill cover) contains an extensive constrictor hyoidei muscle sheet, and this tends to remain well-developed into adulthood in fishes which have small and widely spaced gill cover bones, such as modern lungfishes (Edgeworth 1935). Thus, we can infer that the soft gill cover flap contained the ventral part of the constrictor hyoidei muscle sheet and was strongly contractile. By analogy with modern lungfishes, the middle and dorsal parts of the constrictor ran, respectively, between subopercular and opercular, and between opercular and braincase. Given the dorsal-to-ventral sequence of an almost immobile opercular, a more mobile subopercular and a probably contractile soft flap, it seems most likely that the main water flow passed out of the gill chamber at the level of the soft flap.

Although the cleithrum and the clavicle do fit together in some specimens, they are not firmly joined and the possibility of movement between them was inevitable. In life, the movement of the jaws would have expanded the gill chambers, and the pectoral girdle would have expanded also. This would have been accomplished by the movement along the contact between the cleithrum and the clavicle. In addition, the overlap of the clavicle by the gulars must allow a gap to occur between the gulars and the mandible. This must also have been covered in skin, and it would have allowed considerable flexibility.

All this flexibility was probably related to the expansion of the pharynx during swallowing. Long (1991) has demonstrated that an *Onychodus* specimen has a placoderm skeleton preserved in the pharynx, and this is large enough to cause considerable extension of the pharynx. But it is possible that the *Onychodus* died while trying to swallow the placoderm, indicating that, although the prey was large, there was a limitation to the extent of opening the pharynx.

17.1.16. Flexibility of the mandible. The great flexibility of the mandible is emphasised by the relationship between the infradentaries and the dentary. As shown on Figures 28 and 46, the infradentary 4 laps onto the dentary and infradentaries 3–1 are strongly overlapped by the dentary. The coronoids are directly attached to the interior surface of the dentary. This pattern is very similar to, but not identical with, the pattern described by Jeffery (2003) for the rhizodonts, in which he comments that the mandible is in two functional units. He suggests that the rhizodont structure represents a longitudinal hinge, and the same can be said for the *Onychodus* structure.

17.2. Other functional features

17.2.1. Skeletal asymmetry. Asymmetry is a feature of many aspects of the skeleton, and this has been mentioned above in several places. Asymmetry in the skull roof patterns is common in early sarcopterygians, the dipnoans being a good example. It is worth noting that the elements in the ethmosphenoid braincase in *Onychodus* are asymmetrical. To support this statement, the parasphenoid is illustrated to show the high asymmetry in the pattern of denticles (Fig. 57), the dorsal process and the position of the buccohypophysial canal. This should be considered along with the asymmetry of many other features of the skeleton as indicating that bilateral symmetry in any part of the skeleton was not a feature for which selection was strong.

17.2.2. Depression in the jugal and postorbital. This depression occurs in all observed specimens. The external surface of the depression is covered with fine ornament, as occurs elsewhere on the surface, and we conclude that no external structure occupied this space. Some soft structure may have been attached internally to the depression. Some primitive actinopterygians have a gap in the jugal in the position of the posterior rectus muscle for the eye; for example, *Cheirolepis trailli* (Pearson & Westoll 1979). Observation of the internal surface of the jugal bone in *O. jandemarrai* shows that its anterior surface is rough, as though some soft structure were attached to it (Fig. 12a, b). The postorbital has a ridge towards its anterior margin. These could have been for the attachment of the posterior rectus muscles. The depression in the bones that carry these muscles would then have permitted the more posterior rotation of the eyeball.

17.2.3. Fin structure and movement. The body shape is not well known, but some of the details show that it was elongate and oval in cross-section. However, it was not eel-like, and it had no elongate median fins. The movement of the body was probably in the subcarangiform mode (Webb 1975).

The caudal fin was rounded and slightly elongate, and it would have been very flexible with a broad sweep producing forward motion. The shortness of the peduncle, and the long extension of the scaled axis between the dorsal and ventral caudal fin rays, indicate a strong lateral movement, but this would not have offered lift or depression.

The second dorsal fin was close to the caudal fin and was inclined posteriorly with a petaloid shape. The anal fin attachment was situated a little further forward than the attachment for the second dorsal fin, but it extends back beneath the anterior part of the caudal fin. On the other hand, the body was sufficiently long for subcarangiform motion to take place.

As we have discussed above, the fish was a predator, feeding on large items. Did it chase down its prey, or did it lurk in a cavity in the reef and descend on its prey as it swam past, behaving like extant Moray eels? The following point provides a possible answer.

17.2.4. Lateral line pores on the head. The preservation of the lateral line canals and the associated pores are well known in this species. The ramifying branches of the canals occur on both sides of the lateral line canals, and they terminate in fine pores which are sometimes difficult to see on exposed bone surfaces (Fig. 14). These canals lie immediately under the surface bone, and become visible after brushing the bone surface. The canals are restricted to the preopercular, squamosal, jugal, lachrymal and premaxilla on the lateral sides of the head, but similar small canals are also present on the dorso–rostral region. They are not present on the postparietals or the dorsal bones anterior to them.

Complex canal systems are also known in holoptychiids, rhizodonts and tristichopterids, but in many instances, it is difficult to trace the canal system that produces the pores. It is difficult to compare the patterns in the different genera. Nevertheless, it is probable that the lateral line pores provided a sensory system that enabled the animal to locate prey and to position itself in narrow spaces. Yu (1998) commented that, in *Psarolepis*, the large pores in the surface are openings for the pore canal system. The details of the lateral line canals themselves are not well known. Further examination of new specimens by Zhu Min and Ahlberg indicates that the large pores are genuine cosmine pores, and this is completely different from the situation in *Onychodus*.

17.2.5. Asymmetry of the neural arches. The two sides of each neural arch are sometimes joined by bone dorsally and sometimes not, they are asymmetrical in length, the thickened processes on the arches vary greatly, the positions of the dorsal and ventral nerve roots vary even within a single specimen, the ventral enclosure of the nerve cord is present in some specimens and not in others, and the positions of the articulation with the next arch vary from specimen to specimen. What is the significance of these asymmetries?

First, we can establish that they are not the result of distortion during preservation since they are in positions where the adjacent skeletons are entirely undistorted. Indeed, the Gogo material shows no crushing or compaction of elements in any specimens. Furthermore, some of the variation is not the result of the position along the vertebral column since some of the detail is from a group of arches in one position.

Secondly, the arches show no evidence of dorsal ligaments to bind them together. At least some of the arches were joined to the next arch in the series, and all the arches are attached to elements forming the vertebral column. The attachment surfaces against the vertebral column have an upturned surface on both anterior face, and these allowed the arches to contact the arch in front. This gives some stability to the system.

Thirdly, the inclination of the arches to the horizontal allows some variation in their length, especially if the arch is not exactly vertical. The attachment surfaces of the arch show variation in their length, and in the length of the anterior attachment surface relative to the posterior surface. The arches from the posterior part of the body show relatively larger posterior segments, indicating that they were inclined more acutely to the vertebral column.

Fourthly, the ventral nerve root must pass out just above the posterior attachment surface to the vertebral cartilage. This is observed on almost all specimens, but because of the asymmetry of the attachment surfaces, the positions of the ventral nerve roots are also asymmetrical.

Fifthly, the dorsal nerve roots leave the arch through paired openings which are more obvious on some arches than on others. On one of the arches from the most posterior part of the body, little space is available for the nerve roots to pass outwards from the arches. Only one gap is present for both the ventral and the dorsal roots. This variation would have been expected from our analysis given above. One individual from the anterior part of the body has a loop on each arch, and the two dorsal nerve roots pass out through it.

Bilateral symmetry requires a great deal of genetic control, as is shown by the wide variation in the skull roofing bones of this and other primitive fishes. Complete symmetry is not required to allow the vertebral column to operate, and the movement of the neural arches on the vertebral column is possible. It seems most likely that the difference in length results from the attachment of the base of the arch not only to the vertebral column, but also to the adjacent arch. With the absence of the dorsal ligament, there is obviously some freedom of movement of one arch with respect to the next.

17.2.6. Pit and tube in the crest of the neural arches. This pit occurs on the vertebra with complete neural arches, but not all complete neural arches have such a tube. There is no doubt that the pit opens directly into the top of the neural canal. Towards the posterior of the body, this foramen is large, and its entry into the roof of the neural arch grades down into a widening aperture. In addition, one specimen divides into a double tube opening separately on the dorsal spine. Some of the broken individuals have a clear gap, indicating that this foramen was present. The foramen leaves the front of the arch and runs as a shallow groove up the anterior face of the arch. In one specimen, the groove does not penetrate the arch, but runs across its anterior.

What is the function of this tube? We have never found an example of a nerve in this position in any other organism. With the arches in normal position, the tubes opening between the foramina stand vertically, and so they are not for dorsal ligaments. On the other hand, we notice that blood vessels encompass the spinal cord, and therefore, it is most likely that the tube is for a blood vessel. This view is encouraged by the fact that not all neural arches have such a tube, as would be expected if it were a neural tube.

18. Acknowledgements

We are indebted to the National Museums of Scotland for the photographs and drawings prepared by Dr Andrews. Dr Bobbie Paton arranged for this material to be sent to us in Canberra. Our colleague Dr Gavin Young gave us the opportunity to see a specimen from Cravens Peak Beds. Dr Roger Heady did the SEM work. Kristine Brimmell did photographic work in Perth. We are greatly indebted to four reviewers of this paper who made many comments on the expression and on the interpretation of the structures. There is no doubt that the reviewers did remarkable work on the manuscript. Dr Peter Bartsch has suggested ways in which the parasymphysial whorls could rotate. Although some of their suggestions encouraged our thinking, other suggestions were rejected. The final text is entirely our responsibility.

19. References

Ahlberg, P. E. 1989. Paired fin skeletons and relationships of the fossil group Porolepiformes (Osteichthyes: Sarcopterygii). *Zoological Journal of the Linnean Society* **96**, 119–166.

Ahlberg, P. E. 1991. A re-examination of the sarcopterygian interrelationships, with special reference to the Porolepiformes. *Zoological Journal of the Linnean Society* **103**, 241–287.

Ahlberg, P. E. 1992. The palaeoecology and evolutionary history of the porolepiform sarcopterygians. *In* Mark-Kurik, E. (ed.) *Fossil fishes as living animals*, 71–90. Tallinn: Academy of Sciences of Estonia, Institute of Geology.

Ahlberg, P. E. & Clack, J. A. 1998. Lower jaws, lower tetrapods – a review based on the Devonian genus *Acanthostega*. Transactions of the Royal Society of Edinburgh: Earth Sciences **89**, 11–46.

Andrews. S. M. 1973. Interrelationships of crossopterygians. *In* Greenwood, P. H., Miles, R. S. & Patterson, C. (eds) *Interrelationships of fishes*, 137–77. London: Academic Press, Linnean Society of London.

Andrews. S. M. 1985. Rhizodont crossopterygian fish from the Dinantian of Foulden, Berwickshire, Scotland, with a re-evaluation of this group. *Transactions of the Royal Society of Edinburgh: Earth Sciences* **76**, 68–95.

Andrews. S. M. 1989. Resurrecting dry bones. *Museum Reporter, National Museums of Scotland*. January–February '89.

Andrews. S. M. & Westoll, T. S. 1970a. The postcranial skeleton of *Eusthenopteron foordi* Whiteaves. *Transactions of the Royal Society of Edinburgh* **68**, 207–329.

Andrews. S. M. & Westoll, T. S. 1970b. The postcranial skeleton of rhipidistian fishes excluding *Eusthenopteron*. *Transactions of the Royal Society of Edinburgh* **68**, 391–489.

Bjerring, H. C. 1971. The nerve supply to the second metamere basicranial muscle in the osteolepiform vertebrates with some remarks on the basic composition of the endocranium. *Acta Zoologica* **52**, 189–225.

Borgen, U. J. 1983. Homologisations of skull roofing bones between tetrapods and osteolepiform fishes. *Palaeontology* **26**, 735–753.

Campbell, K. S. W. & Barwick, R. E. 1987. Paleozoic Lungfishes. *In* Bemis, W. E., Burggren, W. W. & Kemp, N. E. (eds) *The Biology and Evolution of Lungfishes*. *Journal of Morphology* (Supplement 1), 93–131.

Chang, M. M. 1982. *The braincase of* Youngolepis. *A Lower Devonian crossopterygian from Yunnan, south-western China*. Stockholm: Department of Geology, University of Stockholm, and Section of Palaeozoology, Swedish Museum of Natural History.

Chang, M. M. 1991. Head exoskeleton and shoulder girdle of *Youngolepis*. *In* Chang, M. M., Liu, Y.-H. & Chang, G.-R. (eds) *Early vertebrates and related problems of evolutionary biology*, 355–378. Beijing: Science Press.

Chang, M. M. 1995. *Diabolepis* and its bearing on the relationships between porolepiforms and dipnoans. *Bulletin du Muséum National d'Histoire Naturelle, 4 Séries* **17**, 235–268.

Chang, M. M. & Yu, X. 1997. Reexamination of the relationship of Middle Devonian osteolepids – fossil characters and their interpretation. *American Museum Novitates* **3189**, 1–20.

Coates, M. J. 1996. The Devonian tetrapod *Acanthostega gunnari* Jarvik: postcranial anatomy, basal tetrapod interrelationships and patterns of skeletal evolution. *Transactions of the Royal Society of Edinburgh: Earth Sciences* **87**, 363–421.

Edgeworth, F. H. 1935. *The cranial muscles of vertebrates*. Cambridge: Cambridge University Press.

Forey, P. L. 1998. *History of the coelacanth fishes*. London: Chapman & Hall.

Gardiner, B. G. 1984. The relationships of the palaeoniscid fishes, a review based on the new specimens of *Mimia* and *Moythomasia* from the Upper Devonian of Western Australia. *Bulletin of the British Museum* (*Natural History*) *Geology Series* **37**, 173–428.

Grande, L. & Bemis, W. E. 1998. A comprehensive phylogenetic study of amiid fishes (Amiidae) based on comparative skeletal anatomy. An empirical search for interconnected patterns of natural history. *Supplement to Journal of Vertebrate Paleontology* **18**, 1–689.

Gross, W. 1956. Über Crossopterygier und Dipnoer aus dem baltischen Oberdevon im Zusammenhang einer vergleichenenden Untersuchung des Porenkanalsystems paläozoischer Agnathen und Fische. *Kungliga Svenska Vetenskapsakademiens Handlingar* **5**, 1–140.

Gross, W. 1965. *Onychodus jaekeli* Gross (Crossopterygii, Oberdevon) Bau des Symphysenknochens und seiner Zähne. *Senckenbergiana Lethaea* **46a**, 123–131.

Janvier, P. 1996. *Early vertebrates*. Oxford: Clarendon Press, Oxford Monographs on Geology and Geophysics.

Jarvik, E. 1967. The homologies of the frontal and parietal bones in fishes and tetrapods. *Colloques Internationaux du Centre National de la Recherche Scientifique* **163**, 181–213.

Jarvik, E. 1972. Middle and Upper Devonian Porolepiformes from east Greenland with special reference to *Glyptolepis groenlandica* n. sp. *Meddelelser om Grønland* **187**, 1–307.

Jarvik, E. 1980. *Basic structure and evolution of vertebrates*, Vol. 1. London: Academic Press.

Jeffery, J. E. 2003. Mandibles of rhizodonts – anatomy, function and evolution within the tetrapod stem-group. *Transactions of the Royal Society of Edinburgh: Earth Sciences* **93**, 255–276.

Jessen, H. 1966. Die Crossopterygier des Oberen Plattenkalkes (Devon) der Bergisch-Gladbach-Paffrather Mulde (Rheinisches Schiefergebirge) unter Berücksichtigung von amerikanischem und europäischem *Onychodus*-Material. *Archiv för Zoologi, Series 2* **18**, 305–389.

Jessen, H. 1980. Lower Devonian Porolepiformes from the Canadian Arctic with special reference to *Powichthys thorsteinssoni* Jensen. *Palaeontographica A* **167**, 180–214.

Johanson, Z. & Ahlberg, P. E. 1997. A new tristichopterid (Osteolepiformes: Sarcopterygii) from the Mandagery Sandstone (Late Devonian Famennian) near Canowindra, NSW, Australia. *Transactions of the Royal Society of Edinburgh: Earth Sciences* **88**, 37–68.

Johanson, Z. & Ahlberg, P. E. 1998. A complete primitive rhizodont from Australia. *Nature* **394**, 569–573.

Johanson, Z. & Ahlberg, P. E. 2001. Devonian rhizodontids and tristichopterids (Sarcopterygii; Tetrapodomorpha) from East Gondwana. *Transactions of the Royal Society of Edinburgh: Earth Sciences* **92**, 43–74.

Lauder, G. V. 1980. Evolution and feeding mechanism in primitive actinopterygian fishes: a functional anatomical analysis of *Polypterus*, *Lepisosteus*, and *Amia*. *Journal of Morphology* **163**, 283–317.

Lebedev, O. A. 1995. Morphology of a new osteolepidid fish from Russia. *Bulletin du Muséum National d'Histoire Naturelle, 4 Séries* **17**, 287–341.

Long, J. A. 1985a. A new Osteolepid fish from the Gogo Formation of Western Australia. *Records of the Western Australian Museum* **12**, 361–377.

Long, J. A. 1985b. The structure and relationships of a new osteolepiform fish from the Late Devonian of Victoria, Australia. *Alcheringa* **9**, 1–22.

Long, J. A. 1988. New palaeoniscoid fishes from the Late Devonian–Early Carboniferous of Victoria. *Memoirs of the Association of Australasian Palaeontologists* **7**, 1–64.

Long, J. A. 1989. A new Rhizodontiform fish from the Early Carboniferous of Victoria, Australia, with remarks on the phylogenetic position of the group. *Journal of Vertebrate Paleontology* **9**, 1–17.

Long, J. A. 1991. Arthrodire predation by *Onychodus* (Pisces, Crossoptergii) from the Late Devonian Gogo Formation, Western Australia. *Records of the Western Australian Museum* **15**, 479–481.

Long, J. A. 1995. *The rise of fishes – 500 million years of evolution*. Sydney: University of New South Wales Press.

Long, J. A. 1999. A new genus of fossil coelacanth (Osteichthyes: Coelacanthiformes) from the Middle Devonian of southeastern Australia. *Records of the Western Australian Museum Supplement* **57**, 37–53.

Long, J. A. 2001. On the relationships of *Psarolepis* and the onychodontiform fishes. *Journal of Vertebrate Paleontology* **21**, 815–820.

Long, J. A., Barwick, R. E. & Campbell, K. S. W. 1997. Osteology and functional morphology of the osteolepiform fish *Gogonasus andrewsae* Long, 1985, from the Upper Devonian Gogo Formation, Western Australia. *Records of the Western Australian Museum Supplement* **53**, 1–89.

Miles, R. S. 1973. Relationships of Acanthodians. *In* Greenwood, P. H., Miles, R. S. & Paterson, C. (eds) *Interrelationships of fishes*, 63–103. London: Academic Press.

Millot, J. & Anthony, J. 1958. *Anatomie de Latimeria chalumnae*, Tome 1. *Squellette, muscles et formations de soutien*. Paris: Centre National de la Recherche Scientifique.

Newberry, J. S. 1857. New fossil fishes from the Devonian rocks of Ohio. *American Journal of Science, Series 2* **24**, 147–149.

Newberry, J. S. 1889. The Paleozoic Fishes of North America. *Monograph of the Geological Survey of North America* **16**, 1–3340.

Ørvig, T. 1957. Remarks on the vertebrate fauna of the Lower Upper Devonian of Escumenac Bay, P.Q., Canada, with special reference to the porolepiform crossopterygians. *Arkiv för Zoologi, Series 2* **10**, 367–426.

Panchen, A. L. & Smithson, T. R. 1987. Character diagnosis, fossils and the origin of tetrapods. *Biological Reviews of the Cambridge Philosophical Society* **62**, 341–438.

Parker, K., Warren, A. & Johanson, Z. 2005. *Strepsodus* (Rhizondontida, Sarcopterygii) pectoral elements from the Lower Carboniferous Ducabrook Formation Queensland, Australia. *Journal of Vertebrate Paleontology* **25**, 46–62.

Pearson, D. M. & Westoll, T. S. 1979. The Devonian Actinopterygian *Cheirolepis* Agassiz. *Transactions of the Royal Society of Edinburgh* **70**, 337–399.

Peyer, B. 1968. *Comparative odontology*. [Translated and edited by Rainer Zangerl.] Chicago, IL: University of Chicago Press.

Schaeffer, B. & Rosen, D. E. 1961. Major adaptive levels in the evolution of the actinopterygian feeding mechanism. *American Zoologist* **1**, 187–204.

Schultze, H.-P. 1969. Die Faltenzähne der rhipidistiiden Crossopterygier, der Tetrapoden und Actinopterygier-Gattung *Lepisosteus*. *Palaeontographica Italiana* **65**, 63–136.

Schultze, H.-P. 1973. Crossopterygier mit heterozerker schwanzflosse aus dem Oberdevon Kanadas; nebst einer Reschreibung von Onychodontida-Resten aus dem Mitteldevon Spaniens und aus dem Karbon der USA. *Palaeontographica Abt. A.* **143**, 188–208.

Smith, M. M. 1979. SEM of the enamel layer in oral teeth of fossil and extant crossopterygian and dipnoan fishes. *Scanning Electron Microscopy* **11**, 483–490.

Smith, M. M. 1989. Distribution and variation in enamel structure in the oral teeth of sarcopterygians: its significance for the evolution of a protoprismatic enamel. *Historical Biology* **3**, 97–126.

Uppeniece, I. 1995. A new species of *Strunius* (Sarcopterygii, Onychodontida) from Latvia, Lode Quarry (Upper Devonian). *Geobios* **19**, 281–284.

Webb, P. W. 1975. Hydrodynamics and energetics of fish propulsion. *Bulletin of the Fisheries Research Board of Canada* **190**, 1–158.

Westoll, T. S. 1943. The origin of tetrapods. *Biological Reviews of the Cambridge Philosophical Society* **18**, 78–98.

Woodward, A. S. 1888. Note on a species of *Onychodus* in the Lower Old Red Sandstone Passage Beds of Ledbury, Hertfordshire. *Geological Magazine* **5**, 500–501.

Woodward, A. S. 1889. On the occurrence of the Devonian *Onychodus* in Spitzbergen. *Report of the British Association for the Advancement of Science* **LIX**, 584.

Young, G. C. & Schultze, H.-P. 2005. New osteichthyans (bony fishes) from the Devonian of Central Australia. *Mitteilungen aus dem Museum für Naturkunde in Berlin–Geowissenschaftliche Reihe* **8**(1), 13–35.

Yu, X. 1998. A new porolepiform-like fish, *Psarolepis romeri*, gen. et sp. nov. (Sarcopterygii, Osteichthyes) from the Lower Devonian of Yunnan, China. *Journal of Vertebrate Paleontology* **18**, 261–274.

Zhu, M. & Schultze, H.-P. 2001. Interrelationships of basal osteichthyans. *In* Ahlberg, P. E. (ed.) *Major events in early vertebrate evolution. Palaeontology, phylogeny, genetics and development*, 298–314. Systematics Association Special Volume Series 61. London: Taylor & Francis.

Zhu, M. & Yu, X. 2002. A primitive fish close to the ancestor of tetrapods and lungfish. *Nature* **418**, 767–770.

Zhu, M., Yu, X. & Janvier, P. 1999. A primitive fossil fish sheds light on the origin of bony fishes. *Nature* **397**, 607–610.

MAHALA ANDREWS†, formerly at National Museum of Scotland, Edinburgh, UK.

JOHN LONG, Western Australian Museum, Francis Street, Perth, Western Australia, now at the National Museum of Victoria, Melbourne, Victoria, Australia.
e-mail: jlong@museum.vic.gov.au

PER AHLBERG, Natural History Museum, Cromwell Road, London, UK, now at Department of Evolutionary Organismal Biology, University of Uppsala, Sweden.
e-mail: Per.Ahlberg@ebc.uu.se

RICHARD E. BARWICK and KEN CAMPBELL, Department of Earth and Marine Sciences, Australian National University, Canberra, ACT, Australia.
e-mail: richard.barwick@anu.edu.au; ken.campbell@anu.edu.au

† Deceased

Explanation of Figures

We have been unable to locate some of the specimens photographed by Dr Andrews. The photographs have been used in our paper, and they have been used without specimen numbers. This is not the result of oversight on our part.

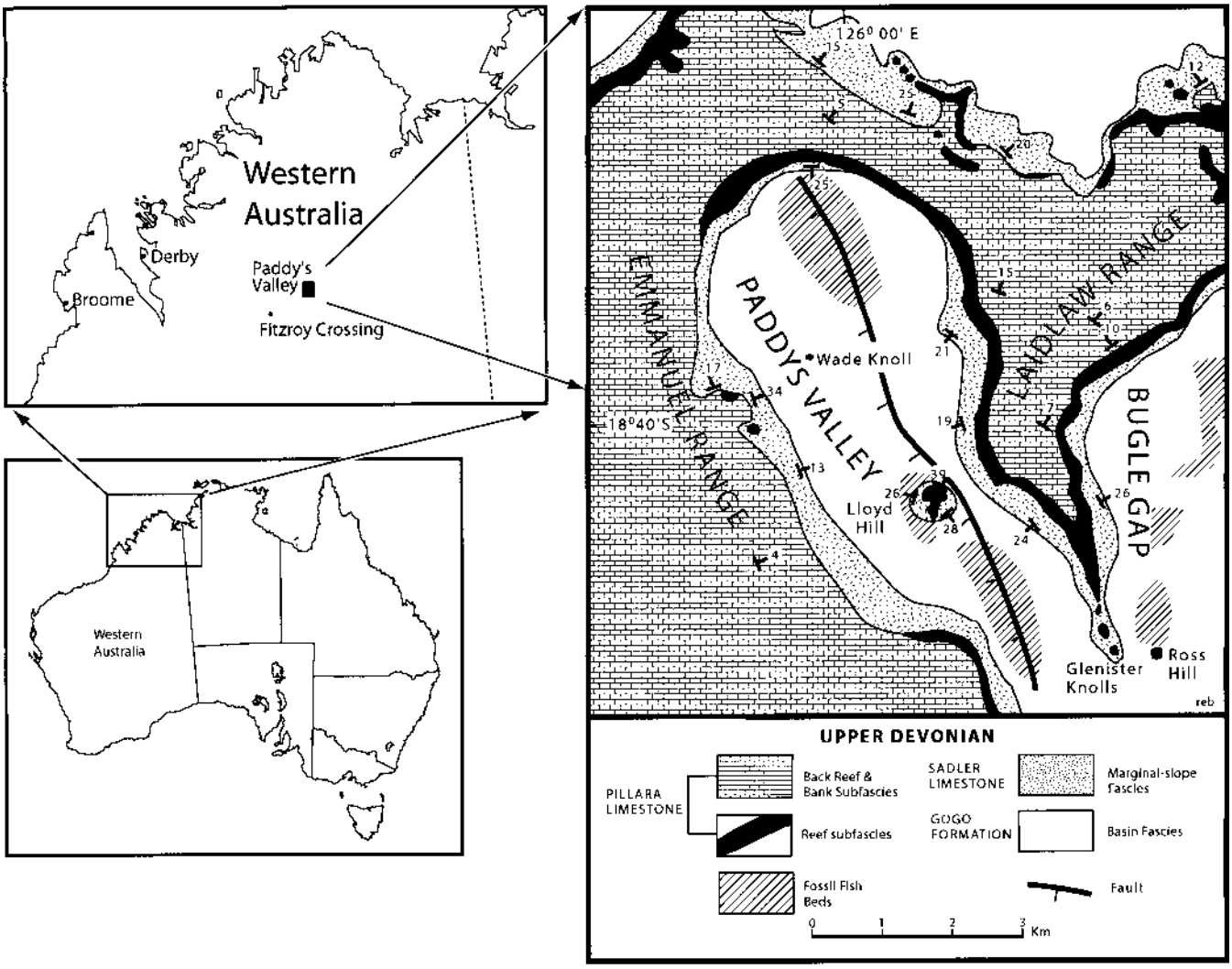

Figure 1 Map of the area in the Devonian reefs of the Kimberley region, Western Australia, where the *Onychodus* specimens have been found.

https://doi.org/10.1017/S0263593300001309 Published online by Cambridge University Press

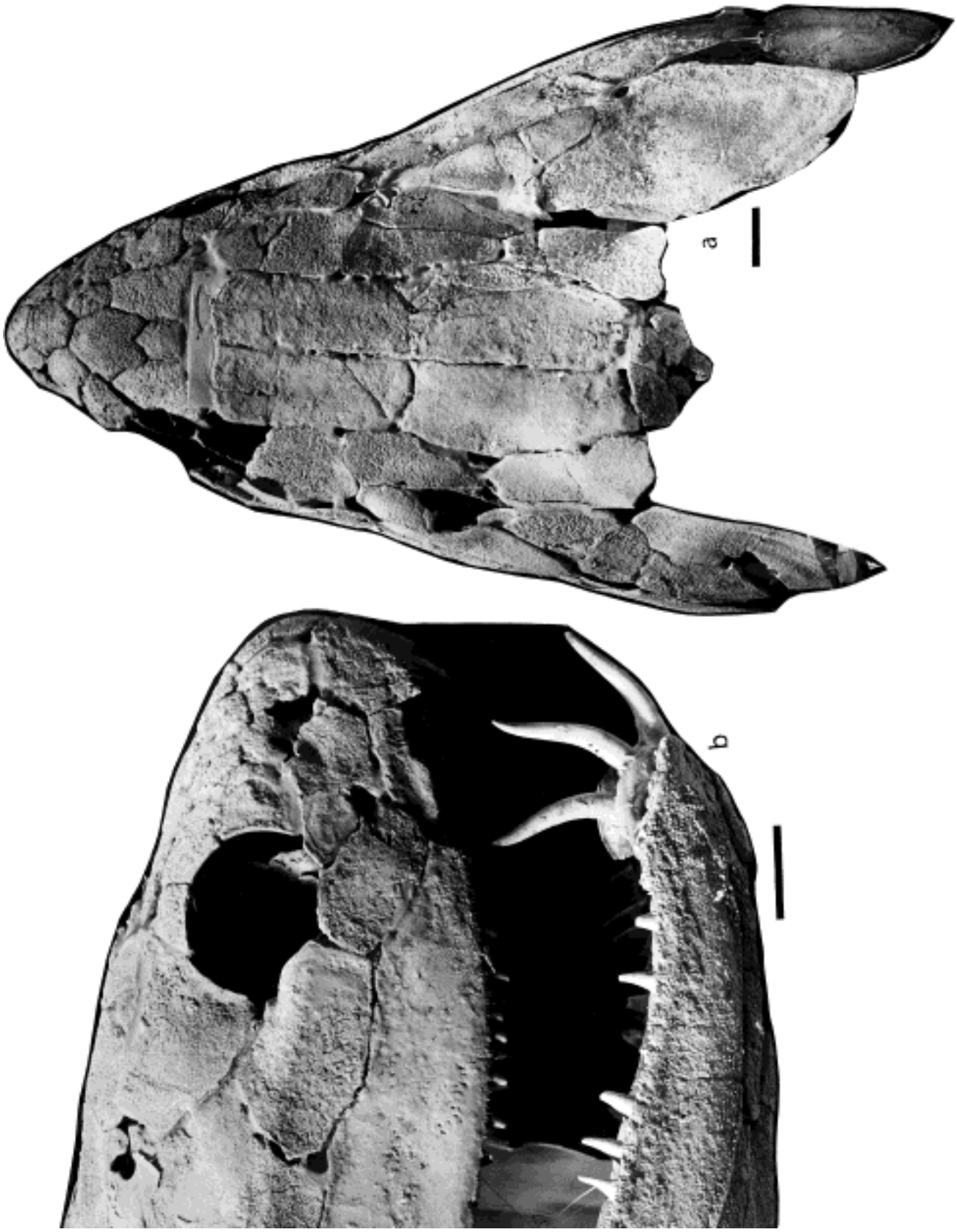

Figure 2 (a) Dorsal and (b) anterolateral views of the holotype. Note the fine lateral lines on the jugal and the maxilla in (b). Premaxilla broken. Scale bars = 10 mm.

https://doi.org/10.1017/S0263593300001309 Published online by Cambridge University Press

Figure 3 (a) Lateral view of the head of the holotype. (b) Internal view of same with the skull removed, but with the mandible, the endopterygoid, the dermopalatine series and the infradentaries in position. Note the position of the teeth on the dermopalatine series and how they lie in relation to the prearticular. (c) External view of same. In (b) & (c) the parasymphysial tusk whorl is placed too highly. Specimens photographed by Dr Andrews; not whitened with ammonium chloride. Scale bars = 10 mm.

https://doi.org/10.1017/S0263593300001309 Published online by Cambridge University Press

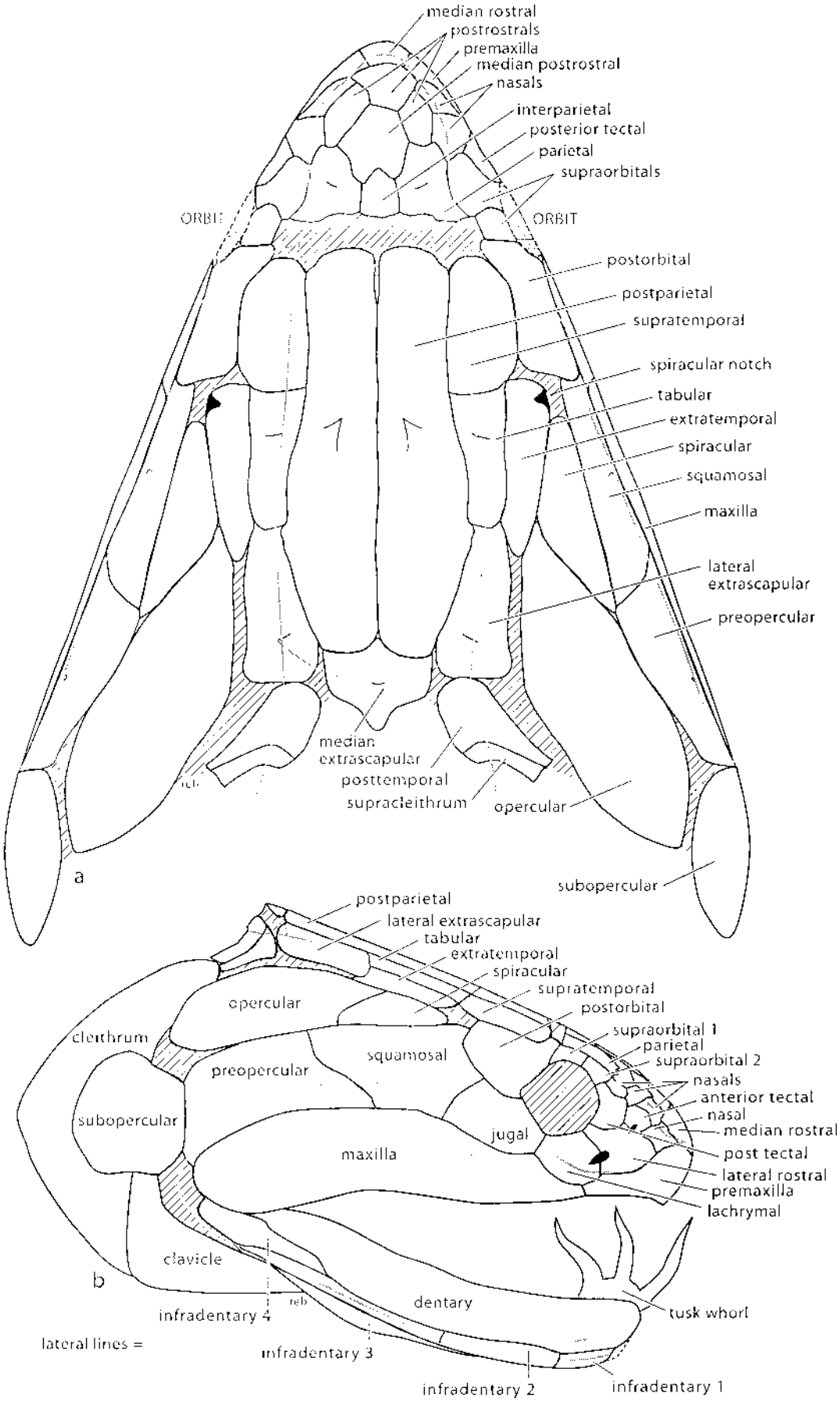

Figure 4 (a) Reconstruction of the skull roof based on the holotype. One half of the specimen has been restored and then transferred to the other side. (b) Reconstruction of the lateral view of the head developed from a number of specimens including the holotype.

https://doi.org/10.1017/S0263593300001309 Published online by Cambridge University Press

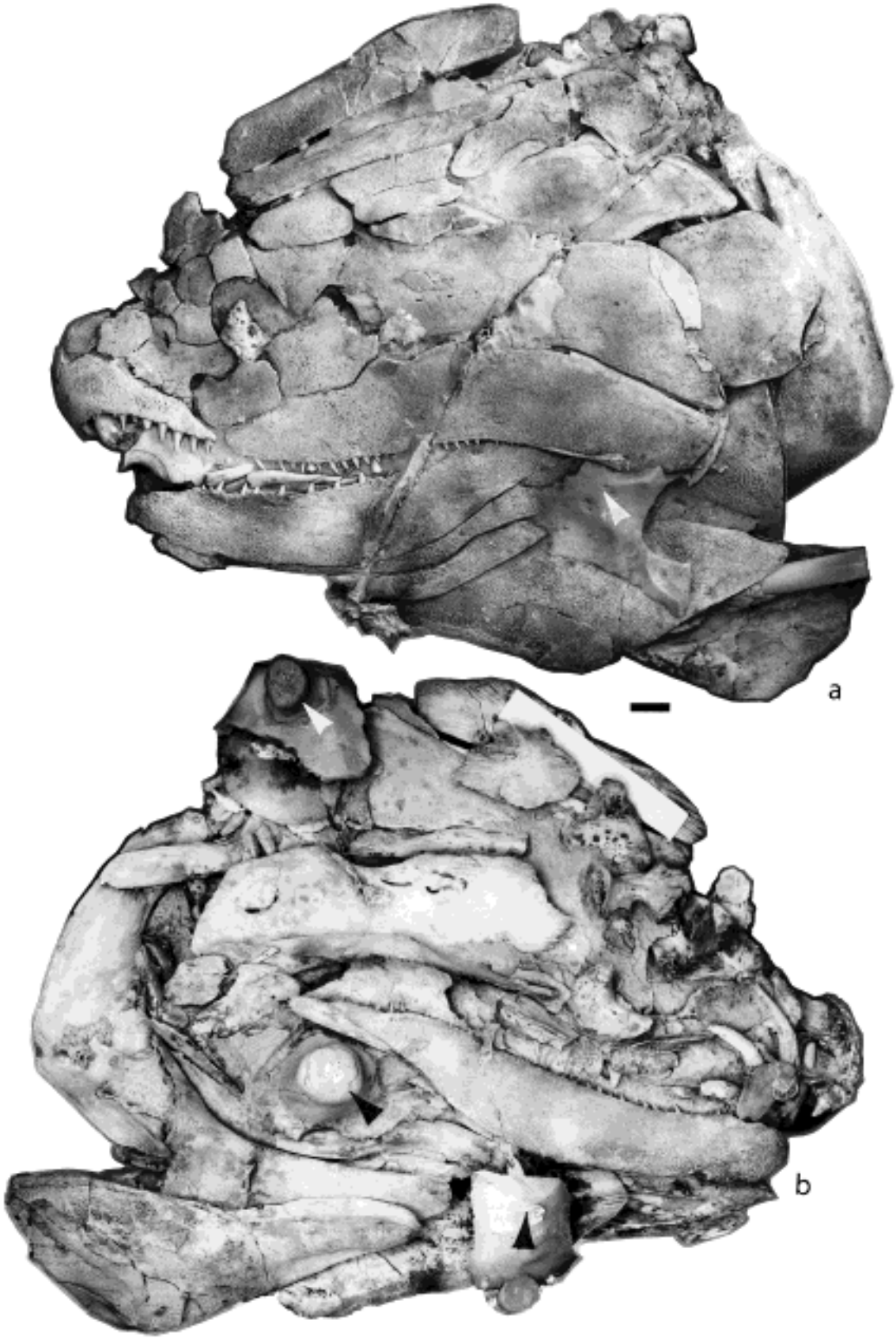

Figure 5 (a, b) Two views of a specimen that has not been completely etched. Sediment is shown by arrows. In (a), the following points are noted: the overlapped space at the dorsal end of the cleithrum; the position of the opercular and subopercular; the infradentaries with the gap left anteriorly for another plate; the loose tusks between the maxilla and the dentary, which had not yet been inserted in the parasymphysial whorl; the submandibular; the small plate posterior to the maxilla; and the posterior triangular shape of the gular. White arrow indicates overlap of maxilla. In (b): the posterior end of the dentary; the tusk whorl; the overlapped surfaces at the end on the gular; and the position of the anocleithrum. ANU 36844. White paper on the inside of the postparietal. Black arrow is a supporting strut added in preparation. Scale bar = 10 mm.

https://doi.org/10.1017/S0263593300001309 Published online by Cambridge University Press

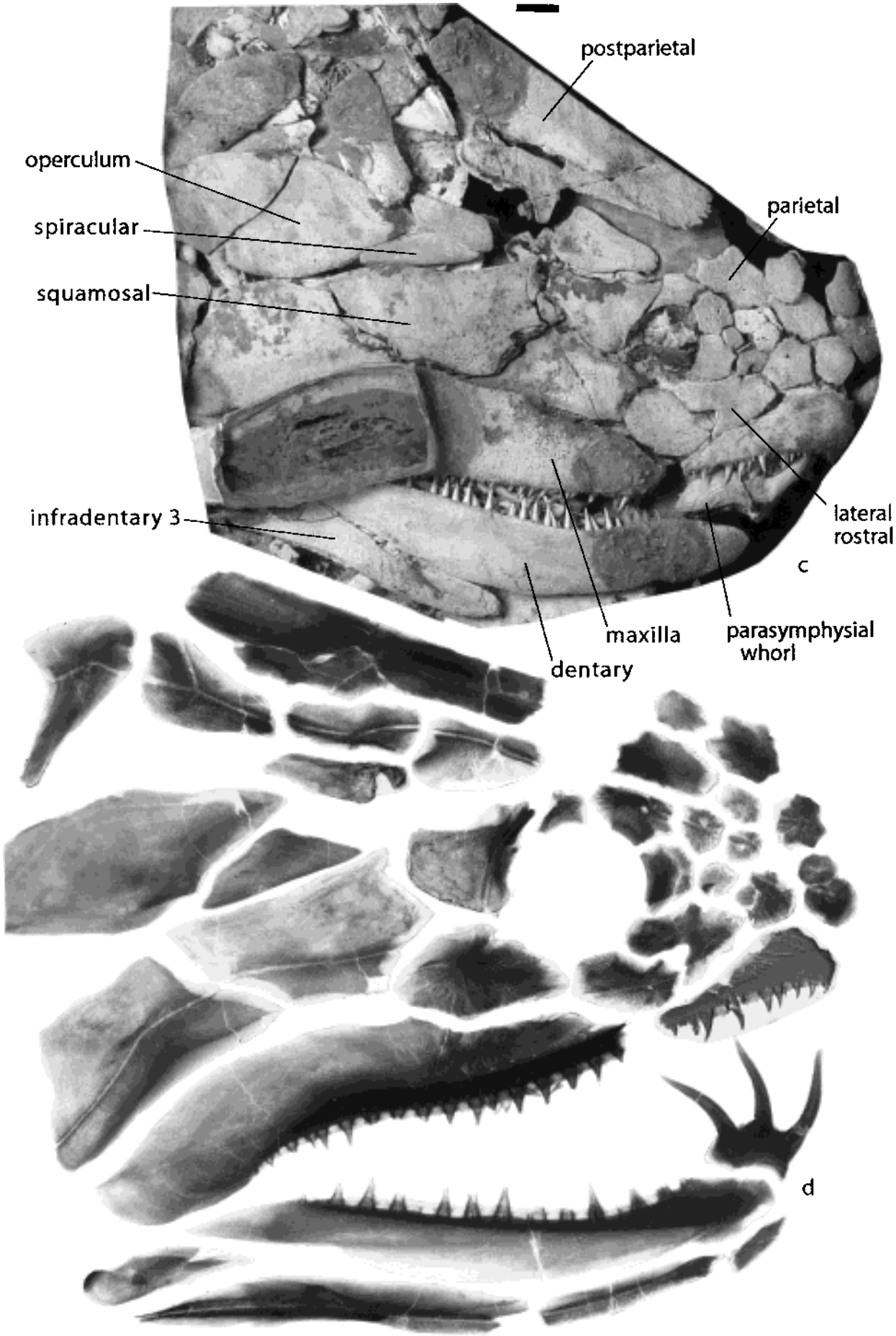

Figure 5 (c) Lateral view of specimen BMNH P63576 showing the plates in the anterior region of the head, the parasymphysial whorl and a tusk that was about to be shed. (d) X-rays of a head partly prepared by Dr Andrews. The bones have been displaced and reassembled. Part of the opercular has been added and the gulars have been removed. Scale bar = 10 mm.

https://doi.org/10.1017/S0263593300001309 Published online by Cambridge University Press

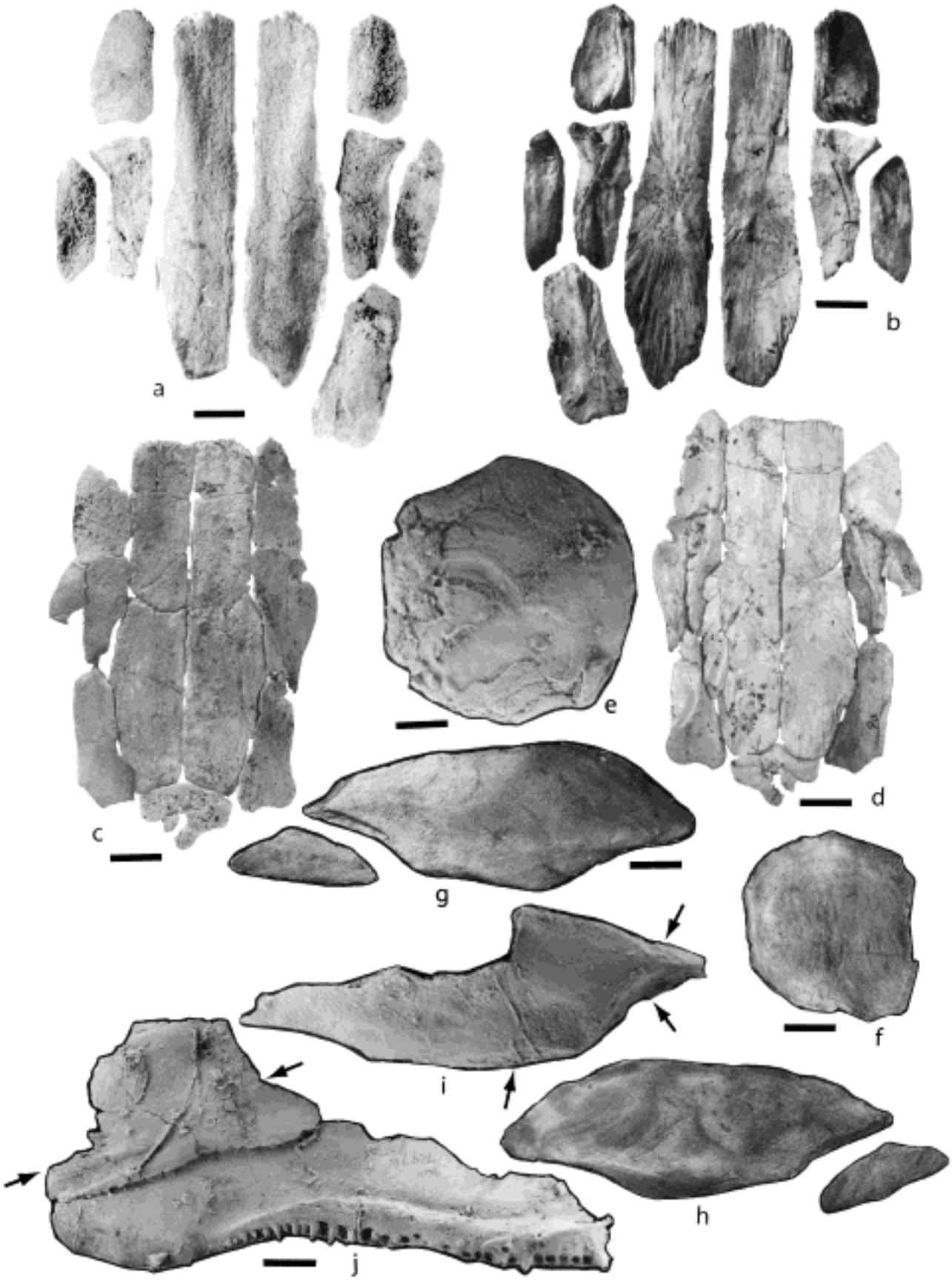

Figure 6 (a, b) External and internal views of the posterior of a skull roof. BMNH P63570. The lateral line in the extrascapular, tabular and supratemporal is clearly seen in (b). Pit lines on the postparietal and the tabular are shown in (a). Centres of radiation visible. Photographs by Dr Andrews of an unwhitened specimen. (c, d) External and internal views of another skull roof. In (d), note how the postparietal expands laterally beneath the tabular and the lateral extrascapular. Photograph by Dr Andrews of an unwhitened specimen in the BMNH Collection. (e) Internal view of an isolated subopercular showing the centre of ossification. ANU 72976. (f) An isolated subopercular showing a slightly different outline. (g, h) External and internal views of part of an isolated opercular, with the spiracular anterior to it. (i) A broken isolated opercular. Overlapped surfaces indicated by arrows. ANU 72976. (j) Internal view of a maxilla and a preopercular. Preopercular overlapped by the maxilla. Ridge along the internal side of the maxilla carrying the teeth which become smaller posteriorly. Arrows indicate the lateral line position. ANU 72976. Scale bars = 10 mm.

https://doi.org/10.1017/S0263593300001309 Published online by Cambridge University Press

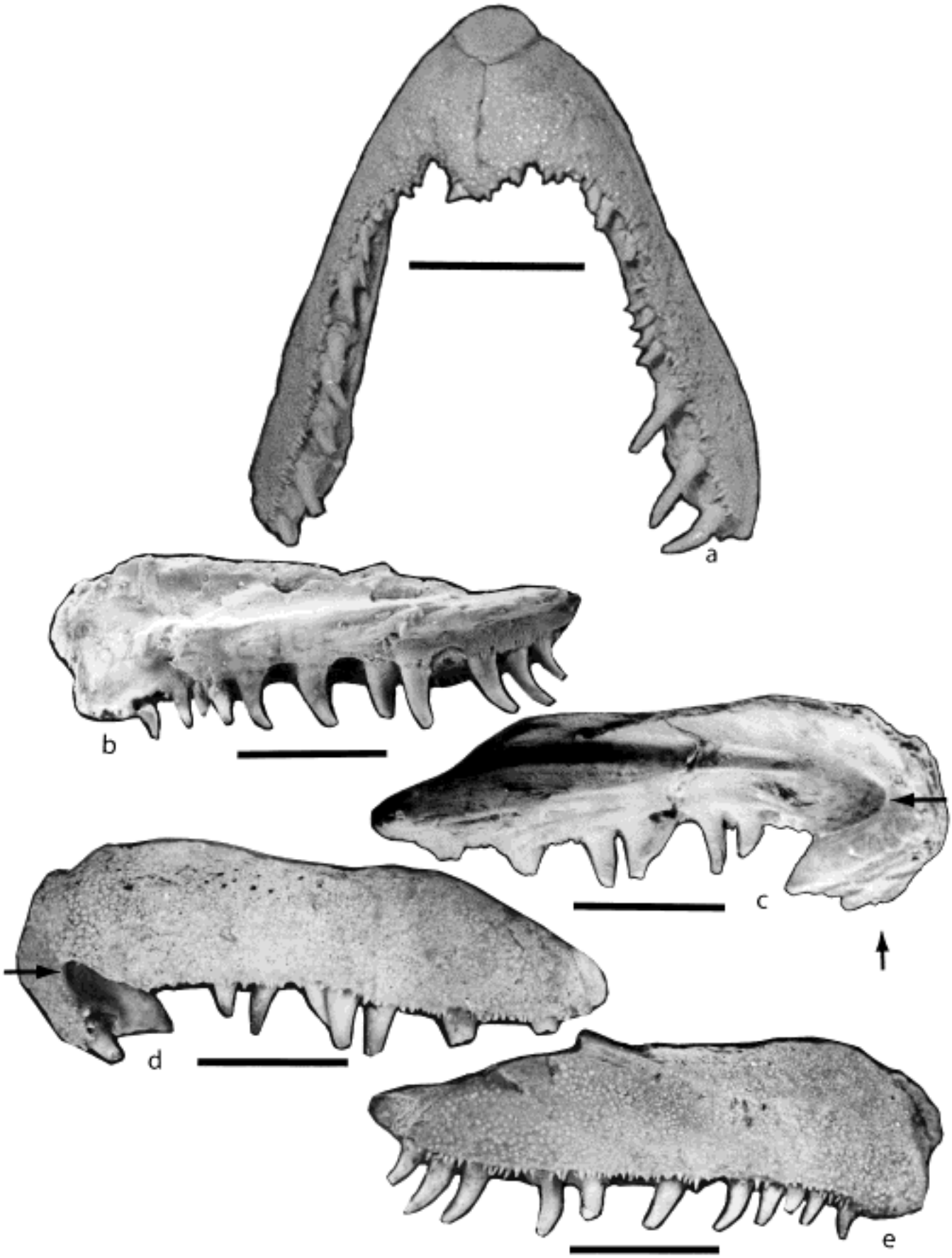

Figure 7 (a) Ventral view of two premaxillae and the median rostral plate. Note the distribution of the teeth and the denticles along the margin. BMNH P64125. (b, c) Internal view of the premaxilla and the adjacent maxilla; anterior to the right. ANU 72978. In (c), the flange showing the linear marks (arrowed) of the symphysis and arrows mark the position for the parasymphysial whorls on closure. (d, e) External views of the same specimens; anterior to the left. (d) The gap for the parasymphysial whorl (arrowed), the pores of the lateral line on the dorsal side of the bone and the fine denticles around the lateral edge of the bone. (e) Maxilla shows the overlap with the premaxilla, the teeth and the fine denticles. Scale bars = 10 mm.

https://doi.org/10.1017/S0263593300001309 Published online by Cambridge University Press

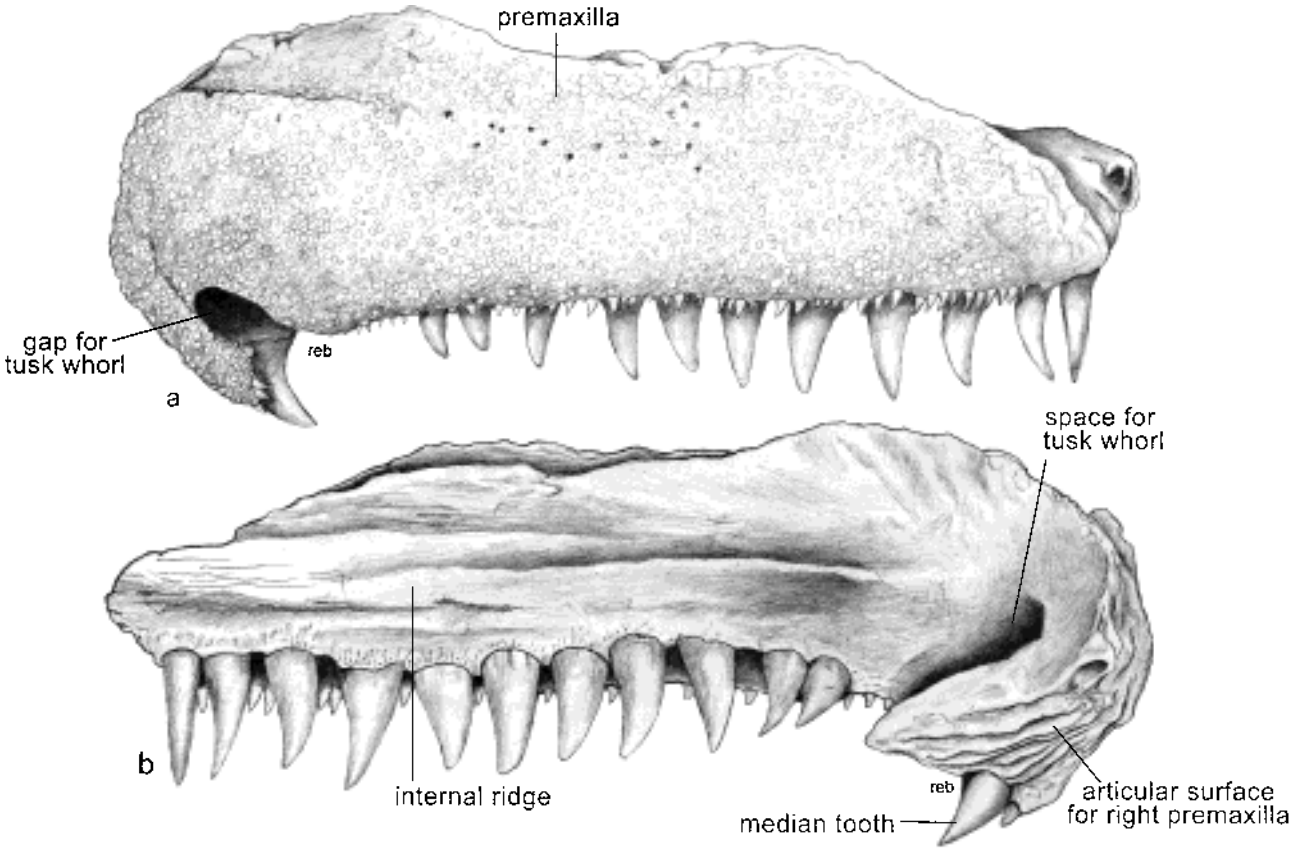

Figure 8 Reconstruction of the premaxilla shown in Figure 7c, d. Teeth which have been lost have been replaced in diagram, and the articulation between the premaxilla and the maxilla is well shown. Scale as shown in Figure 7c, d.

https://doi.org/10.1017/S0263593300001309 Published online by Cambridge University Press

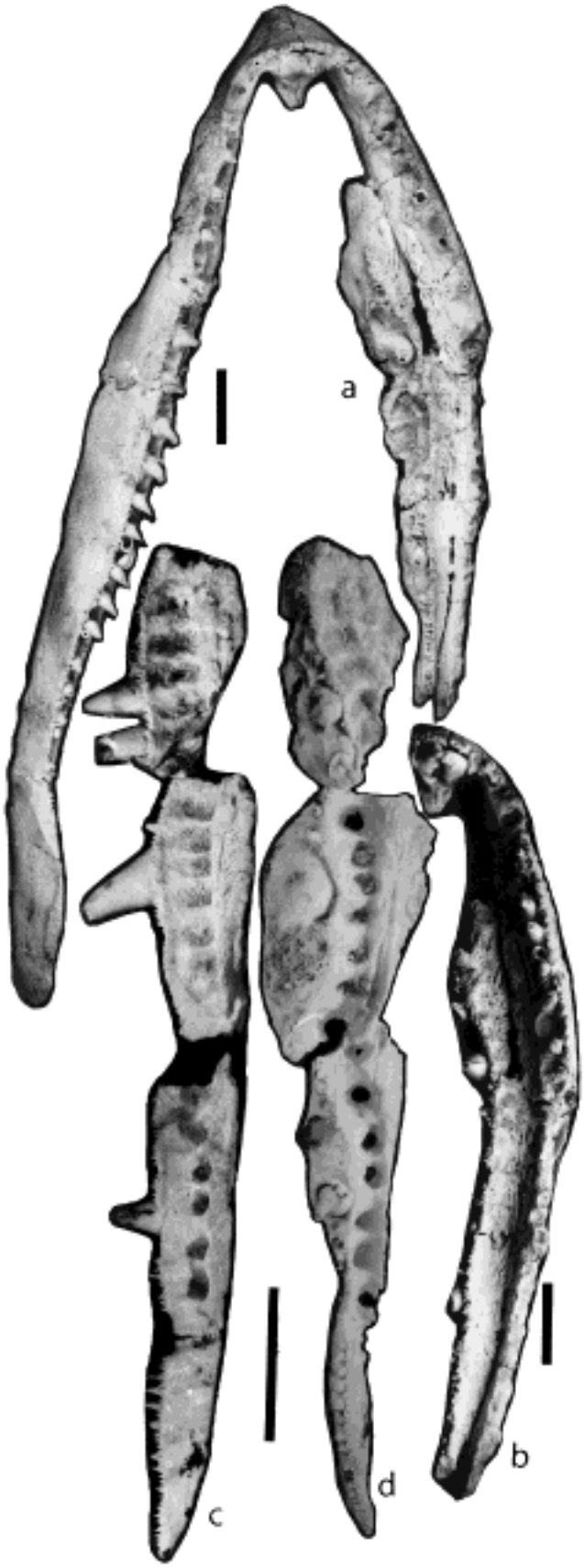

Figure 10 (a) Ventral view of a right maxilla and premaxilla, and part of the left side of same with the dermopalatine series in position. ANU 72975. (b) Left side of same specimen in a more tilted position than (a), and more obliquely lit, showing the three bones of the dermopalatine series and the furrow between them and the maxilla for the dentary teeth on jaw closure. (c) An enlargement of the tilted dermopalatine series showing the lingual face with furrows into which the dentary teeth fit on jaw closure. WAM 92.8.2. (d) The same individual viewed ventrally and showing the pits into which the dentary teeth fit. Scale bars=10 mm.

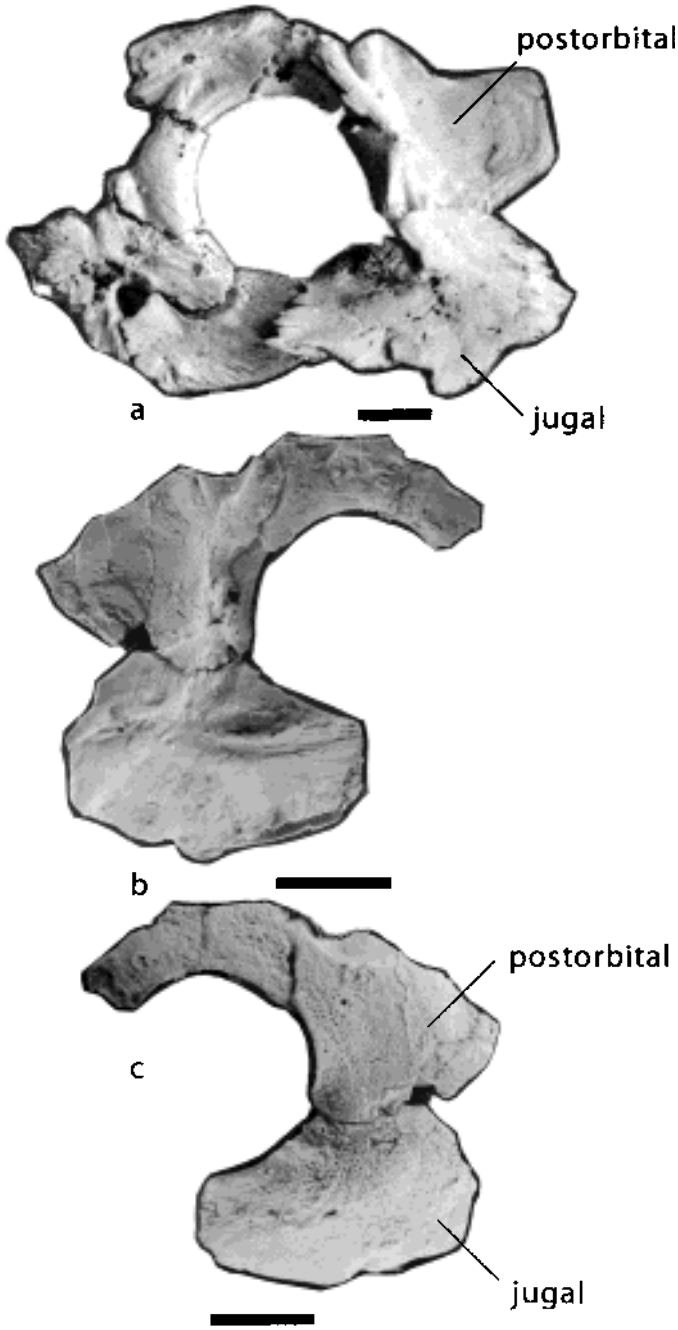

Figure 12 (a) Internal view of the right circumorbital bones of a BMNH specimen; anterior to the left. (b, c) Interior and exterior of the incomplete left circumorbital bones. ANU 72977. Note the gap and ornament between the postorbital and the jugal. Scale bars: (a) 10 mm; (b) 16 mm; (c) 15 mm.

https://doi.org/10.1017/S0263593300001309 Published online by Cambridge University Press

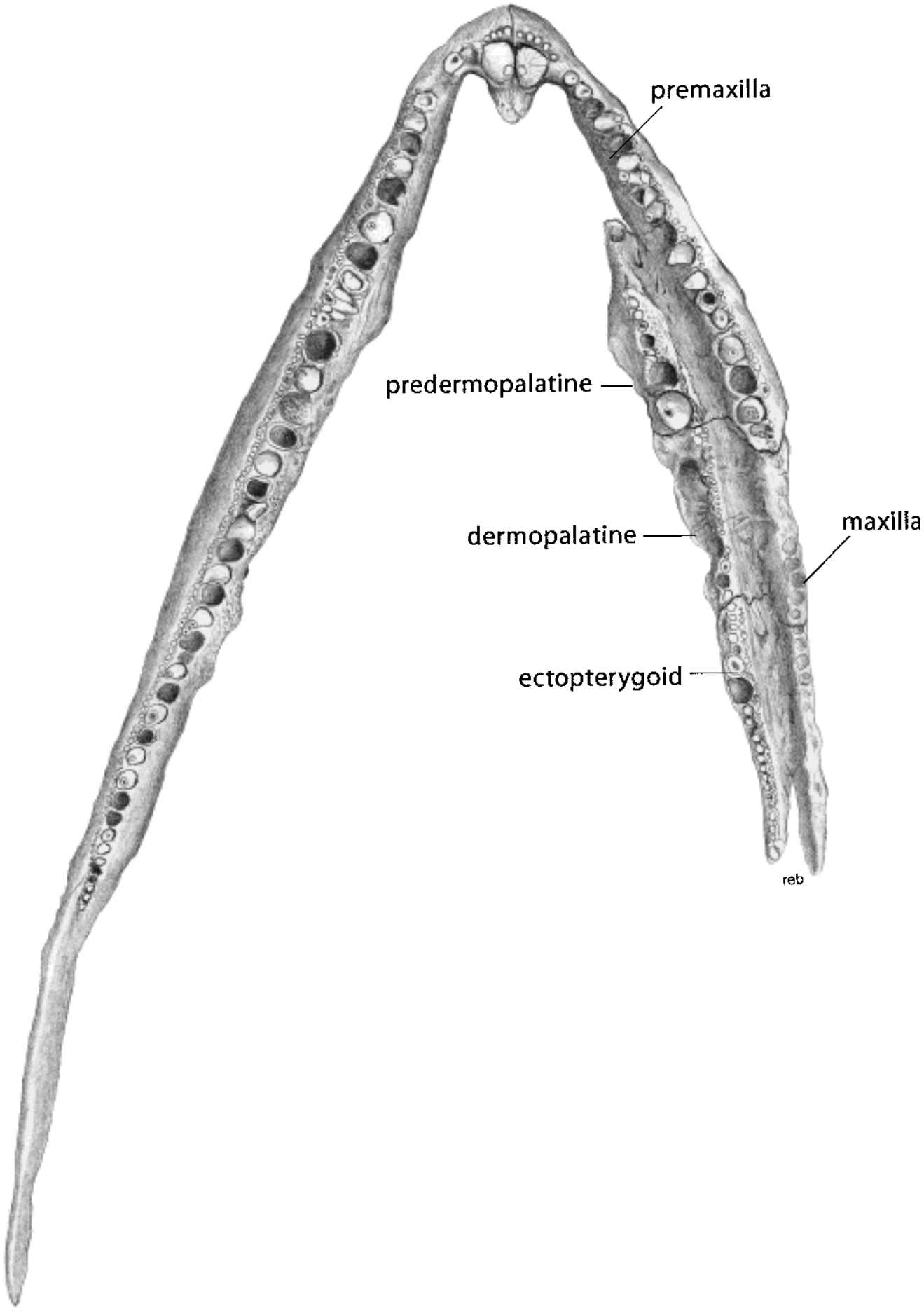

Figure 11 Reconstruction of the specimen in Figure 10a showing details of bones.

https://doi.org/10.1017/S0263593300001309 Published online by Cambridge University Press

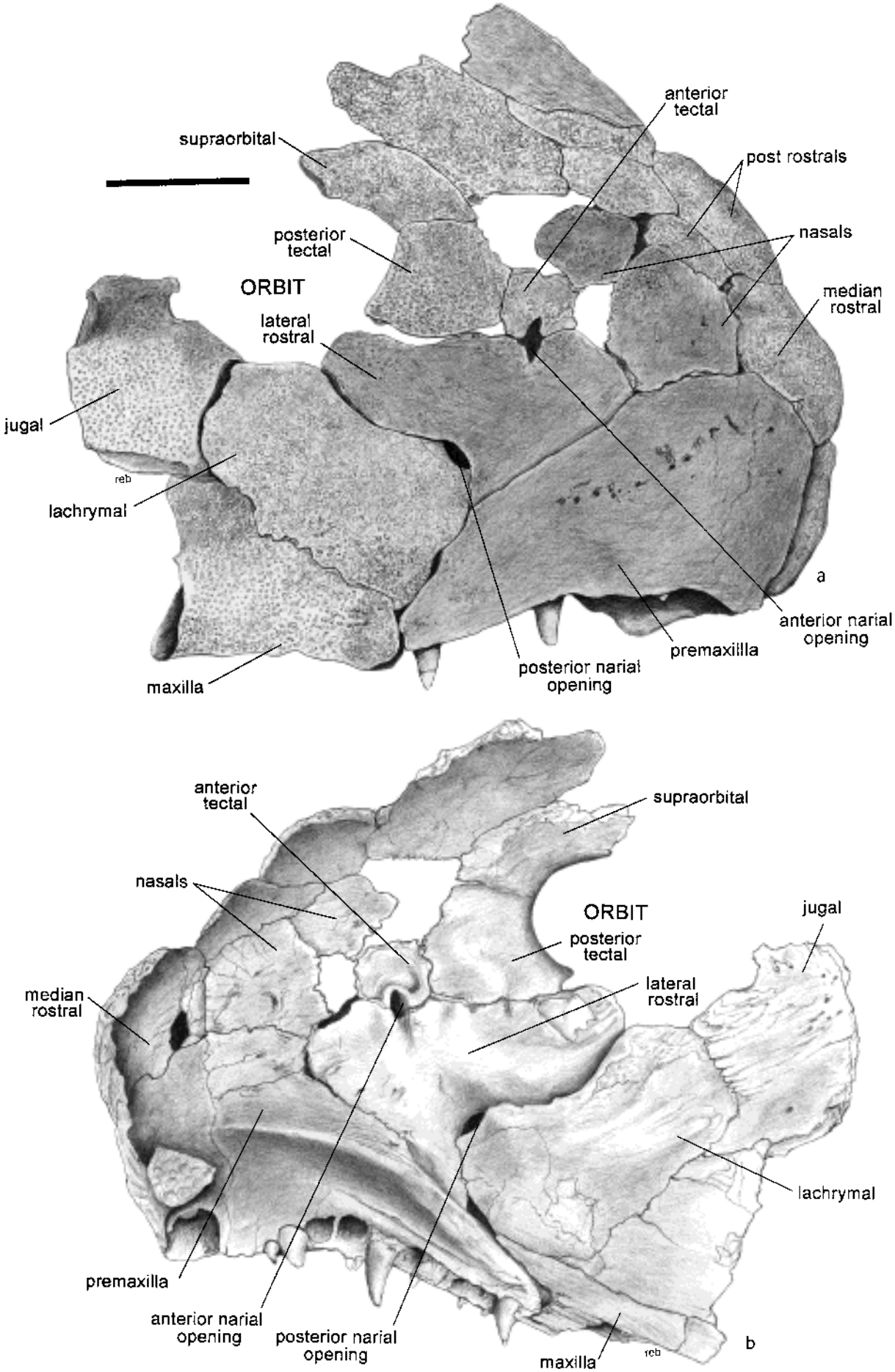

Figure 9 (a) Lateral view of ANU 72978, showing details of bones. Note the narial openings and the deep depression on the jugal. (b) Internal view of the same. Note the maxilla–premaxilla articulation, and the shape of the rim around the anterior narial openings. Scale bar = 10 mm.

https://doi.org/10.1017/S0263593300001309 Published online by Cambridge University Press

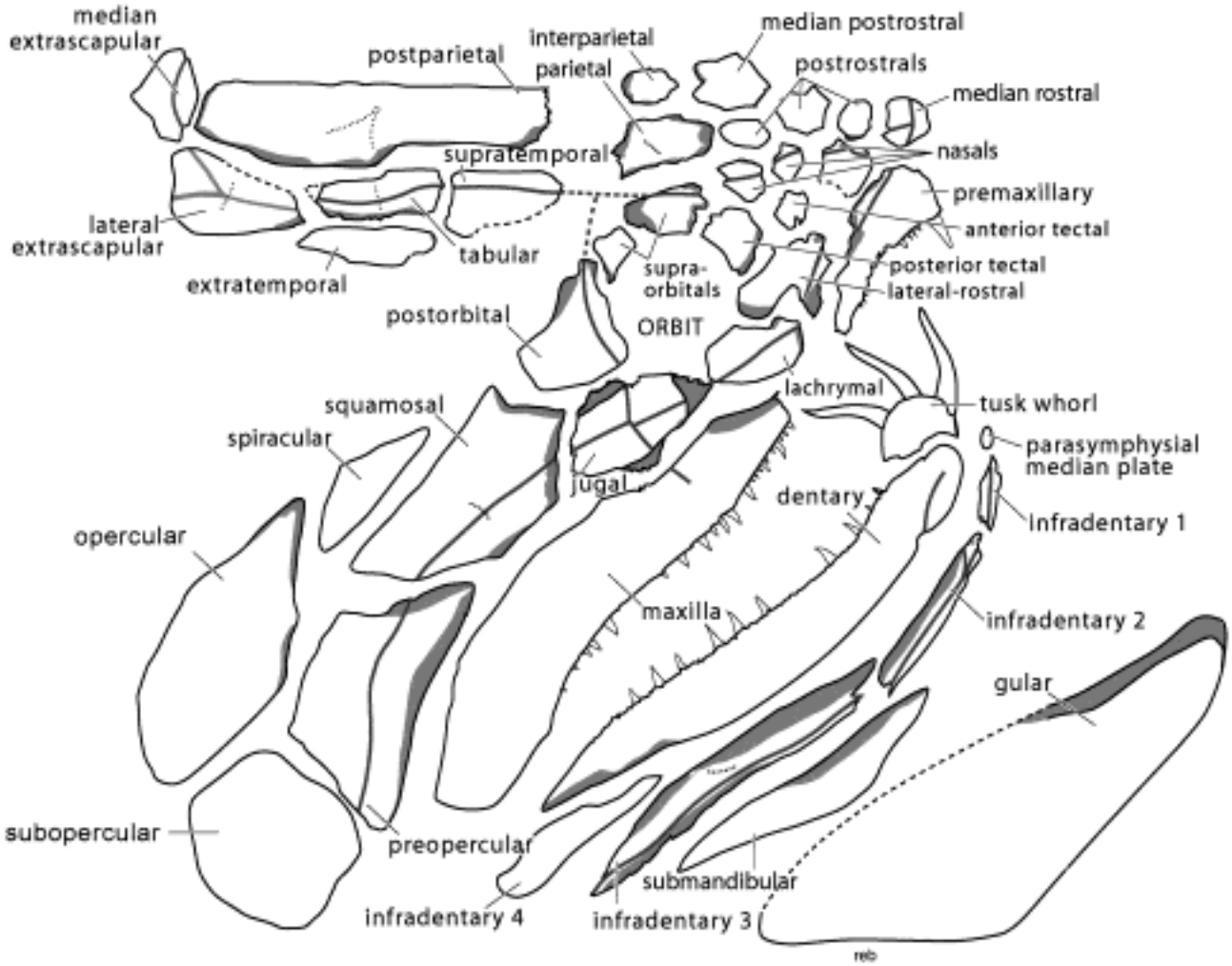

Figure 13 Dissociated plates of the half skull, mandible and the gulars, showing the overlaps between plates and the positions of the lateral lines. Overlapped areas are shaded. Based on a drawing by Dr Andrews from an X-ray.

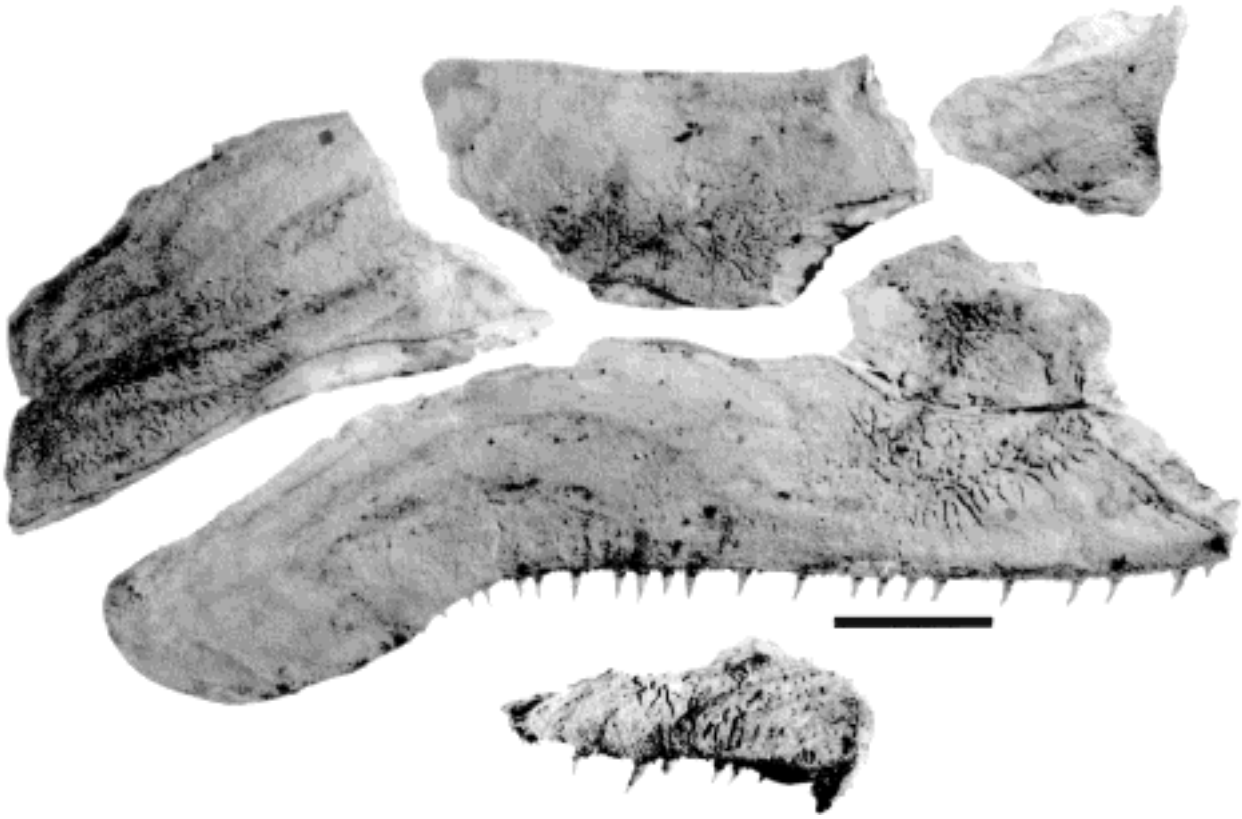

Figure 14 Lateral view of the cheek plates, jugal and postorbital, with the surface layers of the bone stripped away by washing with an organic solvent. The fine lines of the superficial grooves in the surface layers of these bones is well shown. The premaxilla from the same specimen is placed in a ventral position. BMNH P63570. Scale bar = 10 mm.

https://doi.org/10.1017/S0263593300001309 Published online by Cambridge University Press

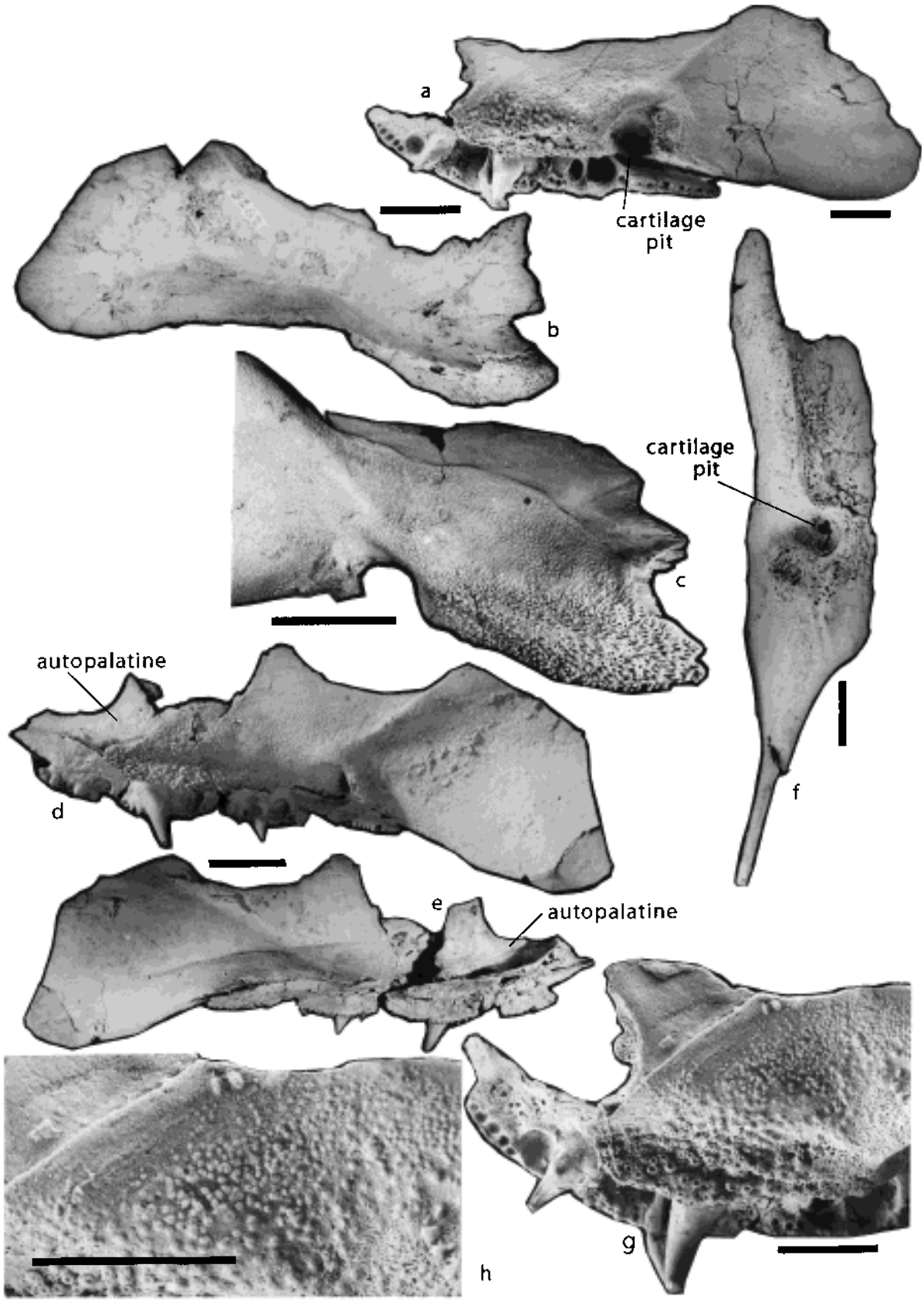

Figure 15 Lingual view of the endopterygoid with the dermopalatine series attached. ANU 72976. (b) Internal view of the endopterygoid with the large flange anterodorsally and the internal facing ridge ventrally. ANU 72975. (c) Lingual view of the anterior part to show the denticulate surface surmounted by the smooth surface for overlap. The ridge separating the coarse ventral from the dorsal part with finer denticles is not so sharp as in (a, g, h). WAM 90.11.1. (d, e) Lingual and lateral views of an endopterygoid with the dermopalatine series present. The autopalatine is present at the anterior end. WAM 92.8.2 (holotype). (f) Ventral view of the left endopterygoid showing the flange that supports the dermopalatine series, the anterior end of which is thin and slightly broken. The pit for the cartilage, which extends ventrally to control the closure of the mandible, is clear. ANU 729765. (g) Anterior surface of the specimen in (a). Note the clear boundary between the dorsal process, and the ventral surface with denticles between which the smooth surface layers show an arcuate linear arrangement anteriorly. More ventrally is the concave surface with open-ended denticles showing the pulp cavity. This division is not always present, as is shown in (c). The lingual face of (b) does not even show a sharp edge between the smooth processes dorsally and the denticulate surface. (h) Enlargement of the anterior part of the denticulate section of (g). Scale bars = 10 mm.

https://doi.org/10.1017/S0263593300001309 Published online by Cambridge University Press

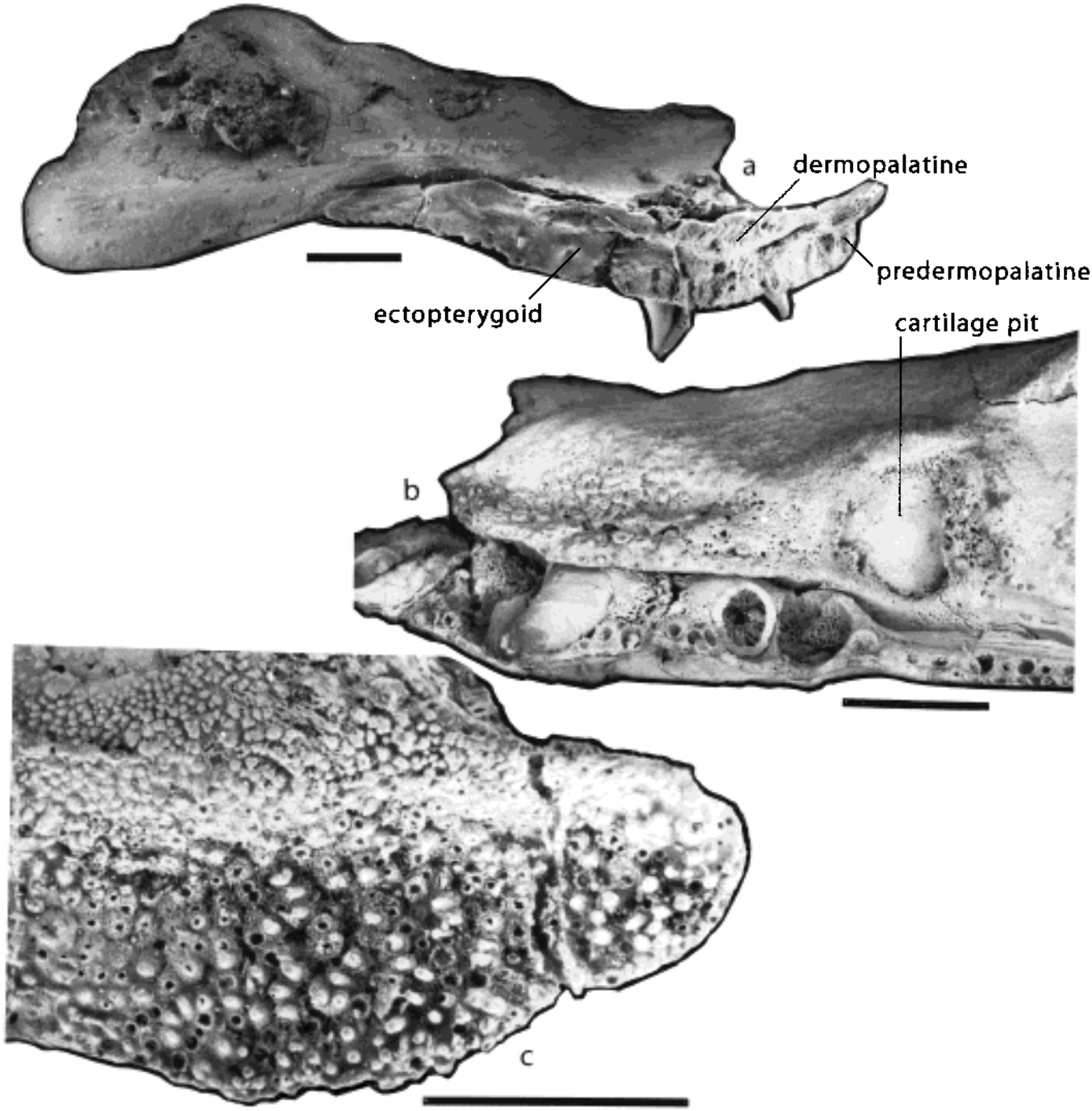

Figure 16 (a) An endopterygoid viewed laterally. The lateral side of Figure 15a. Ectopterygoid, dermopalatine and predermopalatine attached, and all showing the attachment surfaces to the maxilla. Note the projection of the dermopalatine behind the predermopalatine. (b) Ventral view of part of the same specimen enlarged to show the cartilage pit with the bone structure and the crest with smooth periosteal bone, the two teeth on the anterior of the ectopterygoid with one completely removed and the other with its radial base still present, and one large tooth on the dermopalatine with a broken tooth in front of it. (c) Anteroventral part of the endopterygoid of ANU 72975 showing the large denticles on the ventral part of the plate, passing up over a ridge onto the dorsal part with much finer denticles. Scale bars = 10 mm.

https://doi.org/10.1017/S0263593300001309 Published online by Cambridge University Press

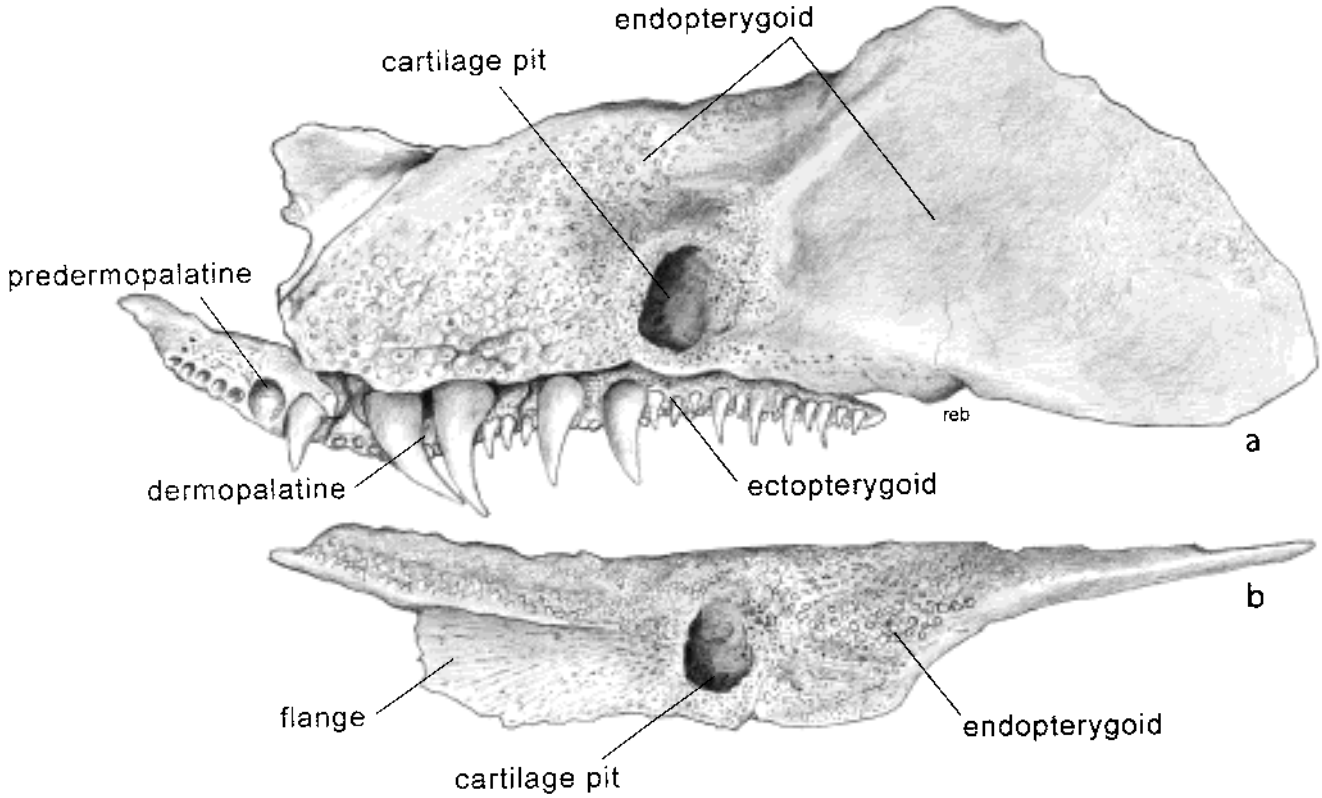

Figure 17 (a) Reconstruction of the endopterygoid. ANU 72976. Teeth have been restored and the difference between the tissue on the anterodorsal parts of the endopterygoid is emphasised. (b) Ventral view of the other endopterygoid from the same specimen. Anterior end of flange slightly broken.

https://doi.org/10.1017/S0263593300001309 Published online by Cambridge University Press

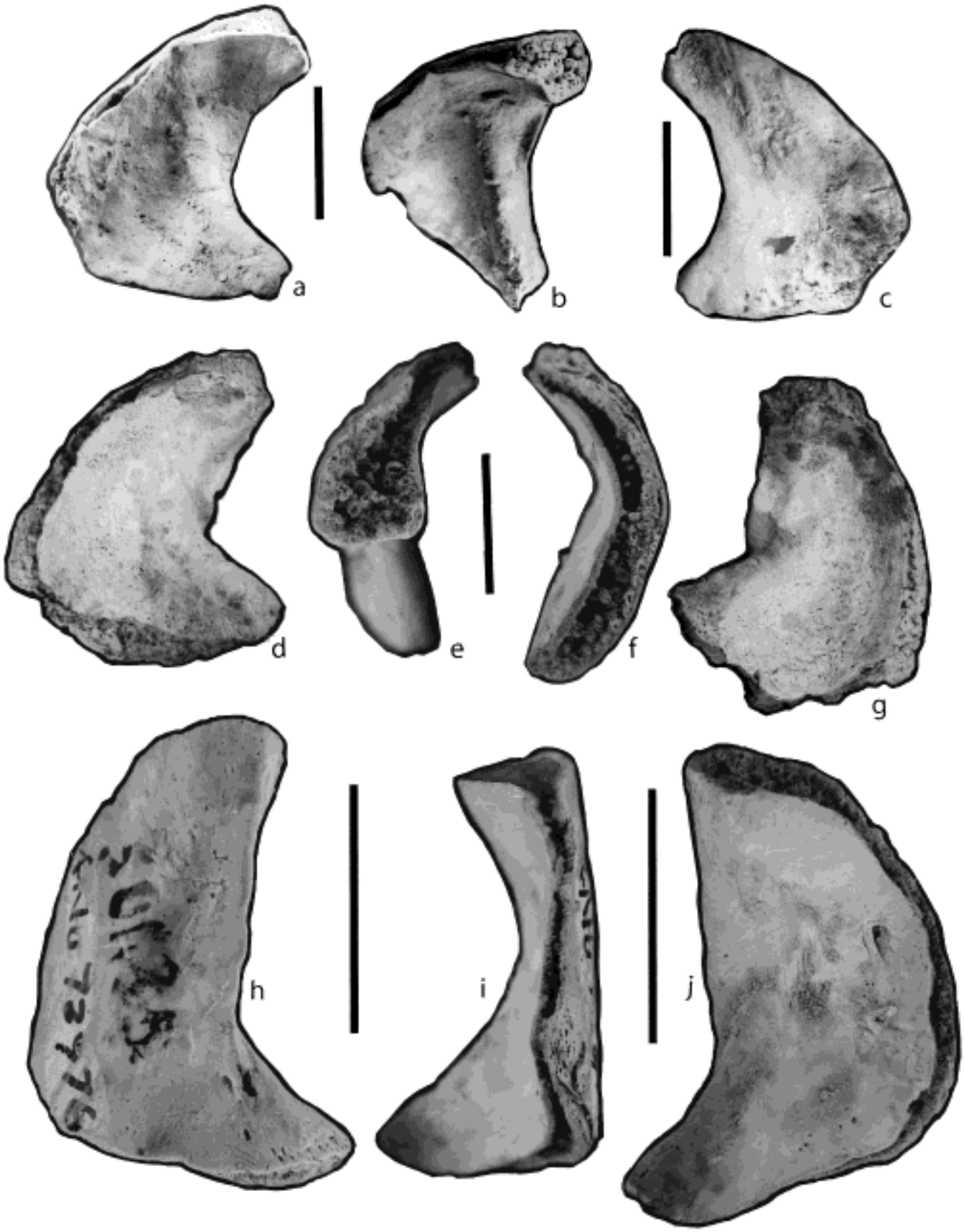

Figure 18 Autopalatines. (a–c) Three views of ANU 72978. (b) The attachment surface to the braincase. (d–g) Four views of a WAM specimen. (e, f) The two attachment surfaces. (h–j) Three views of ANU 72976. Attachment surface to the braincase is at the top side of the figure. Scale bars = 10 mm.

https://doi.org/10.1017/S0263593300001309 Published online by Cambridge University Press

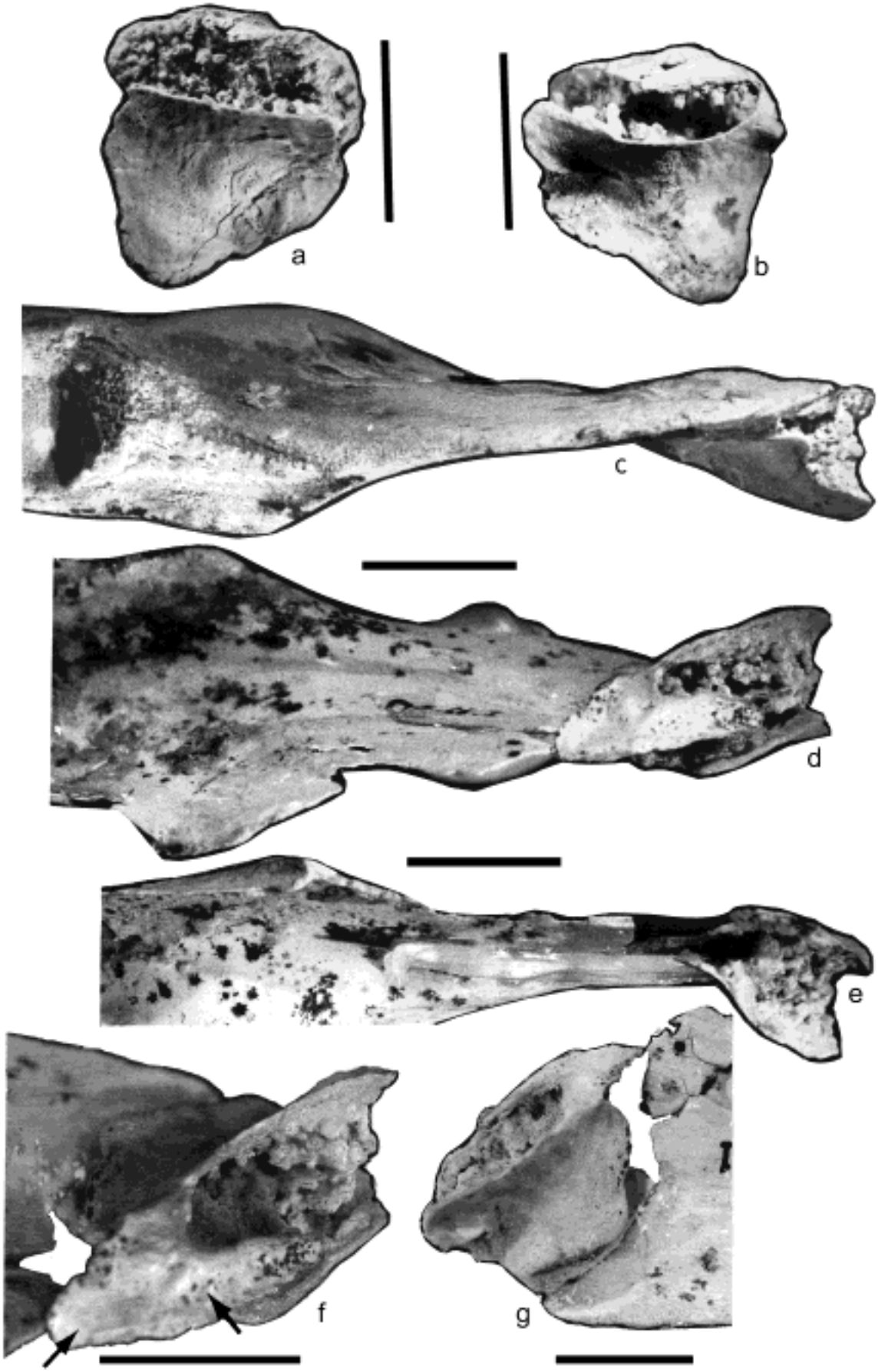

Figure 19 (a, b) Views of two isolated quadrates viewed from the strongly concave inner face. WAM 90.11.1. (c) Ventral views of an endopterygoid showing the quadrate in position and the cartilage pit anteriorly. (d, e) Dorsal views of two endopterygoids with the quadrate in position showing the much larger articulation of the cartilage pad on the dorsal surface and the smooth area of bone on (d). (e) Similar area on an opposite endopterygoid, but the anterior edge of the quadrate has been broken away. Specimens not whitened with ammonium chloride. (f) Another view of the quadrate shown in (d) rotated to show the arrowed attachment surrounding the anterior edge of the cartilage attachment. (g) An internal view of the quadrate in position on the posterior end of the pterygoid of WAM 90.11.1; note that the quadrate lies dorsal to the base of the endopterygoid and that the junction between the ventral and the dorsal edges of the quadrate makes a high angle. Scale bars = 10 mm.

https://doi.org/10.1017/S0263593300001309 Published online by Cambridge University Press

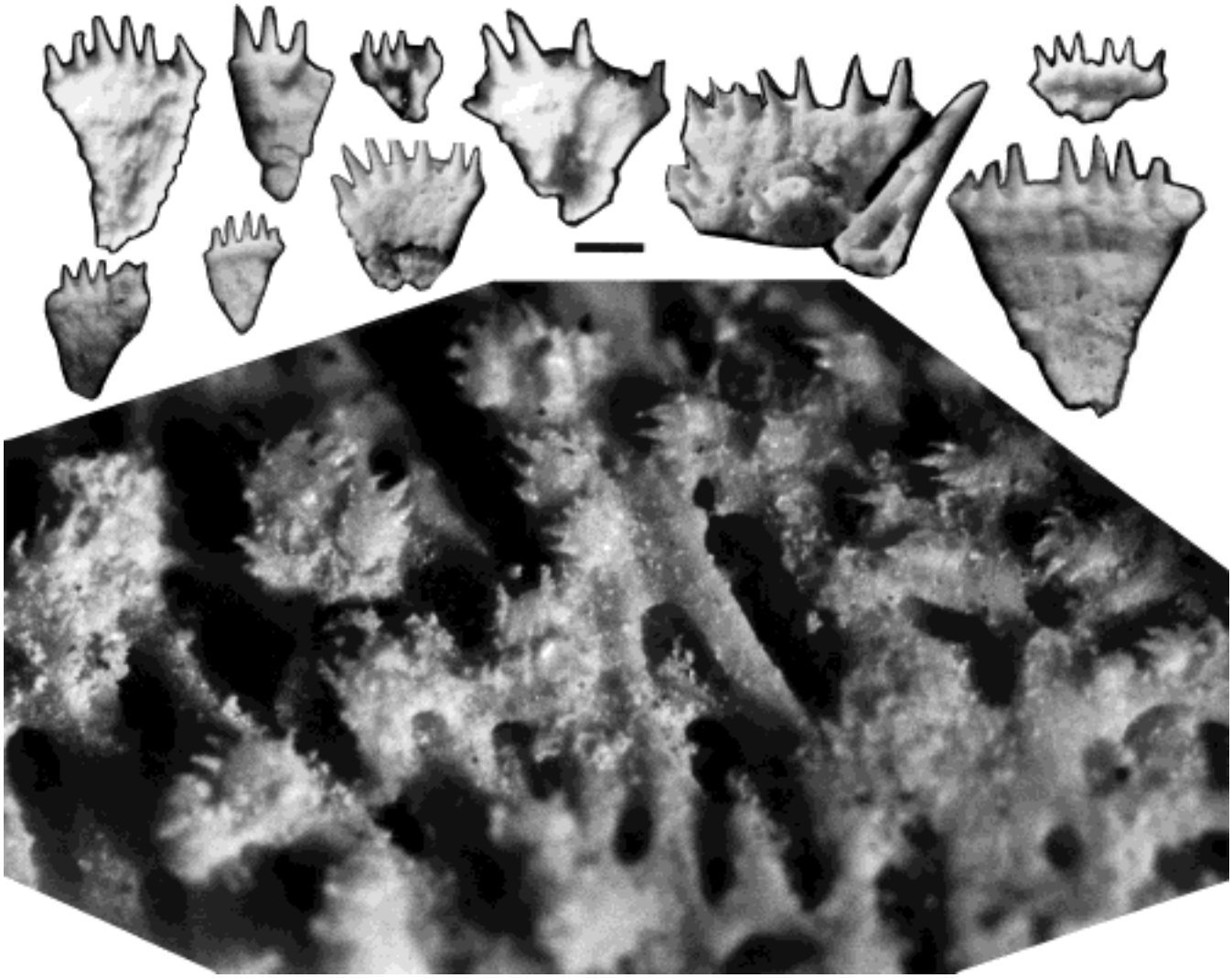

Figure 20 Part of the posterior of the palate. Clusters of denticles supported on a matrix of bone. Other photographs give a representative group of denticles which appear in etches. Presumably they have fallen free from the matrix during preparation. BMNH P63571. Photograph by Dr Andrews. Scale bar = 1 mm.

https://doi.org/10.1017/S0263593300001309 Published online by Cambridge University Press

Figure 22 (a, b, e) Median, lateral and dorsal views of a symplectic. ANU 72976. (c, d, f) Three views of another broken symplectic. ANU 72975. Note the elongate shape which matches the end of the hyomandibula (see j). (g–j) Four views of the hyomandibula. ANU 72975. Note the large scar (arrowed) on the bottom right of (g), the striations on (h), and the dorsal and ventral openings on (i) and (j) respectively. (k–m) Three views of the hyomandibula of the holotype. (k) Especially good view of the opercular flange which on (g) is just a narrow ridge standing towards the viewer. (n, o) An unwhitened specimen photographed by Dr Andrews of a small individual labelled BMNH P63571. Scale bars = 10 mm.

https://doi.org/10.1017/S0263593300001309 Published online by Cambridge University Press

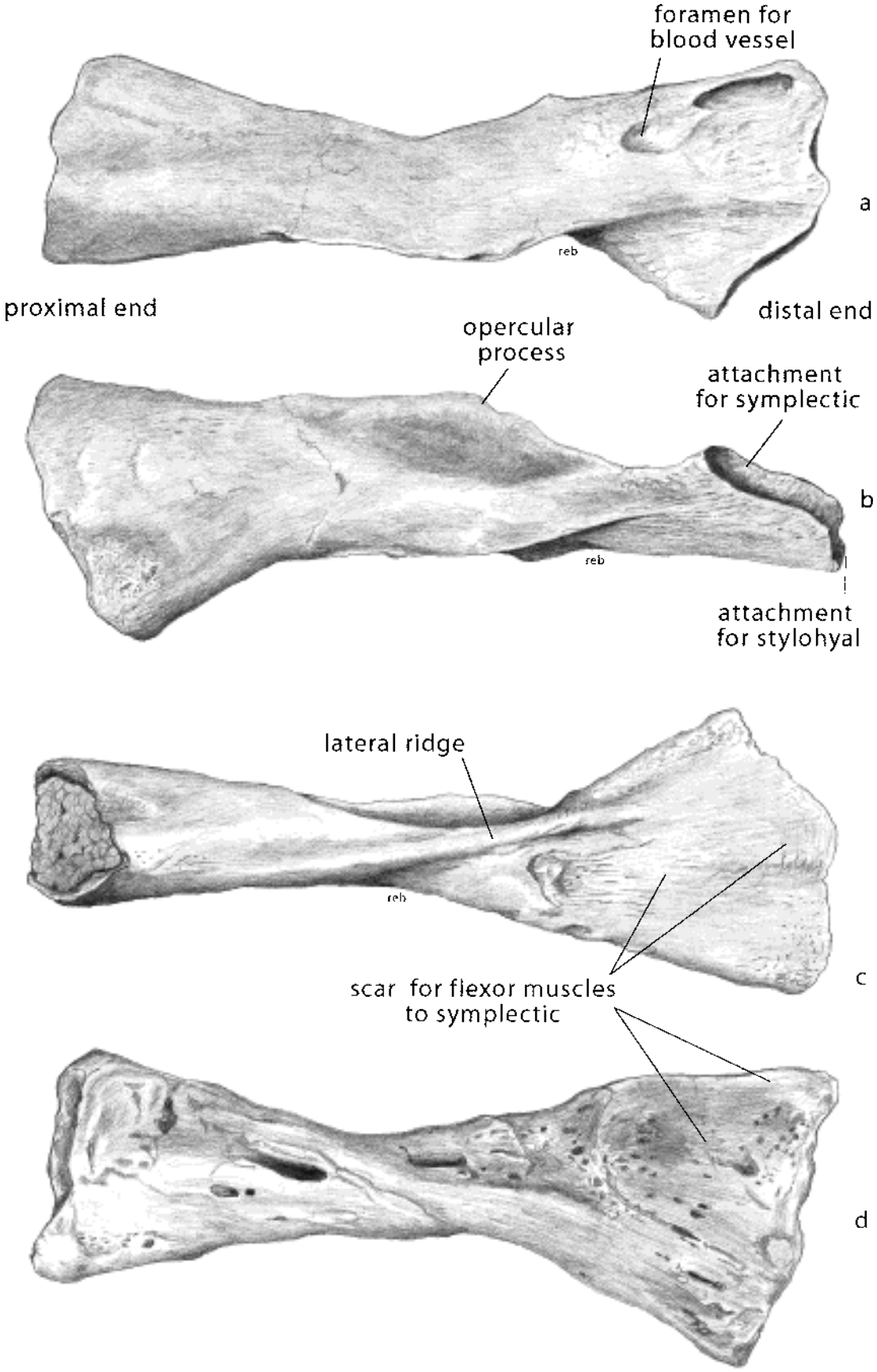

Figure 23 Reconstruction of the hyomandibula of the holotype showing the main features: (a–c) drawn from the specimen on Figure 22k–m; and (d) drawn from Figure 22g.

https://doi.org/10.1017/S0263593300001309 Published online by Cambridge University Press

Figure 21 (a, b) External and internal views of the supracleithrum and posttemporal of the holotype. Arrows mark the position of the lateral line. The upper surface of (a) is covered with fine nodules, but the ventral part is smooth where the bone fits under the soft tissue from the suboperculum. (c, d) Two views of the anocleithrum, from the holotype. (e) Enlargements of isolated anocleithra showing modification of the dorsal end. (h, i) Two views of a larger specimen with a different dorsal terminus. ANU 72976. (f, g) An even larger specimen, ANU 72975, with an anchor-like dorsal terminus and indications of ligament or muscle attachment on (i). Scale bars = 10 mm.

https://doi.org/10.1017/S0263593300001309 Published online by Cambridge University Press

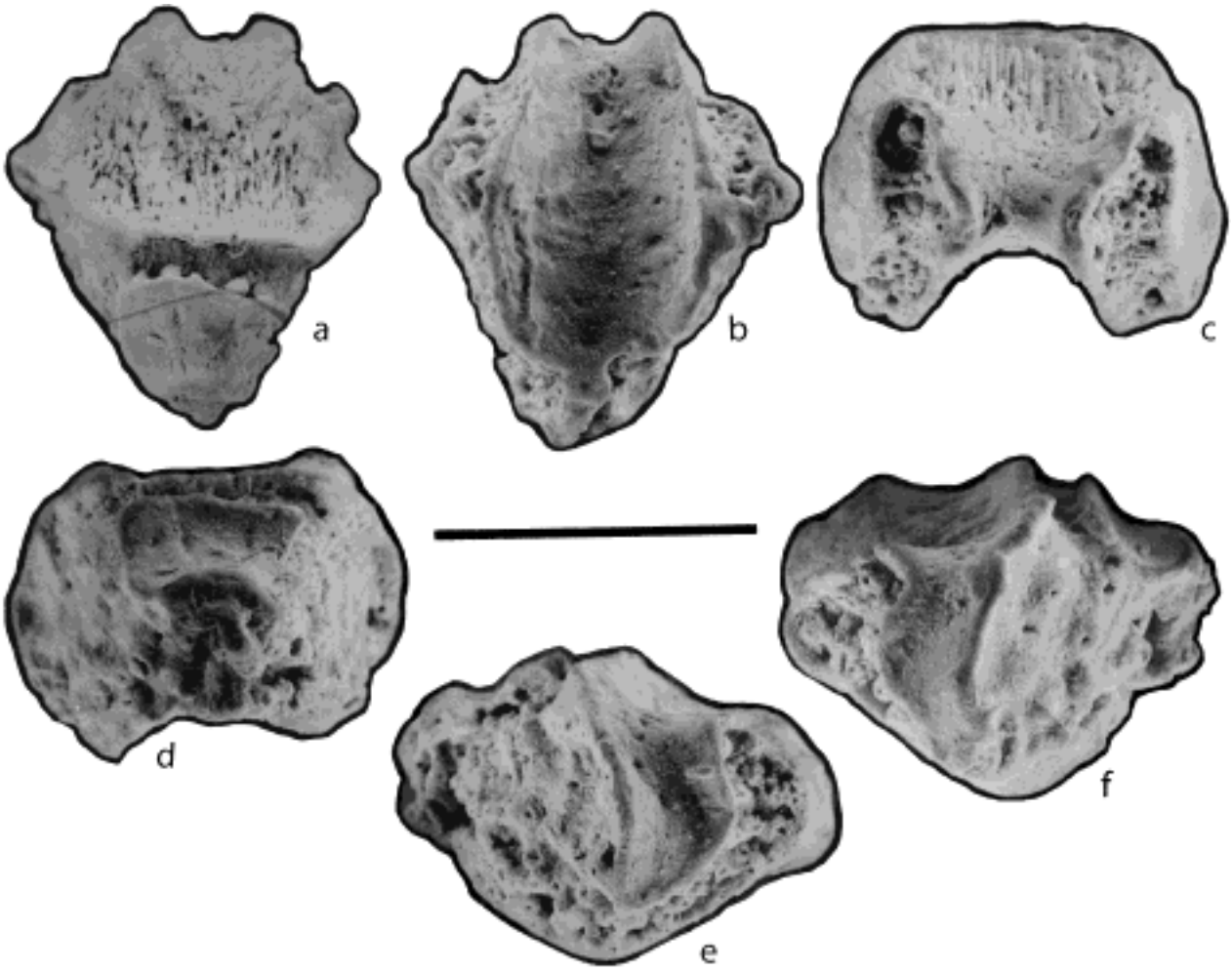

Figure 24 Six views of the basibranchial ANU 72978. (a) Dorsal view showing the attachment for the junction between the large anterior basibranchial 1 and the partly broken basibranchial 2. (b) Ventral view with the deep furrow. (c) Anterior view showing the attachment for the hypohyal dorsally and the basibranchial 1 ventrally. (d) Posterior view. (e, f) Right and left lateral views showing the deep smooth surface extending from the basibranchial 1, and separating the hypohyal and basibranchial scars from the large scars for the hyobranchial 2 and 3, occupying the posterolateral parts of the structure. Structures named on Figure 25. Scale bars=10 mm.

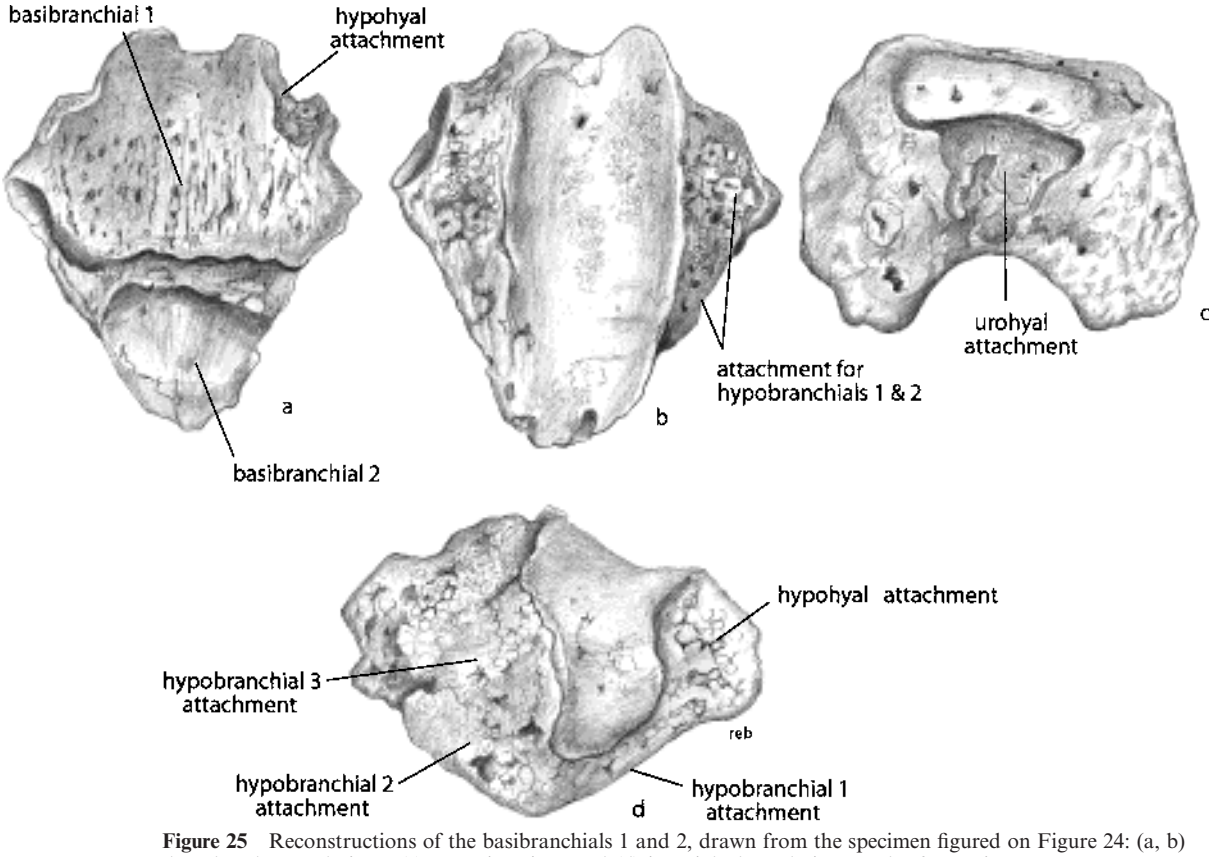

Figure 25 Reconstructions of the basibranchials 1 and 2, drawn from the specimen figured on Figure 24: (a, b) dorsal and ventral views; (c) posterior view; and (d) is a right lateral view. Scales from Figure 24.

https://doi.org/10.1017/S0263593300001309 Published online by Cambridge University Press

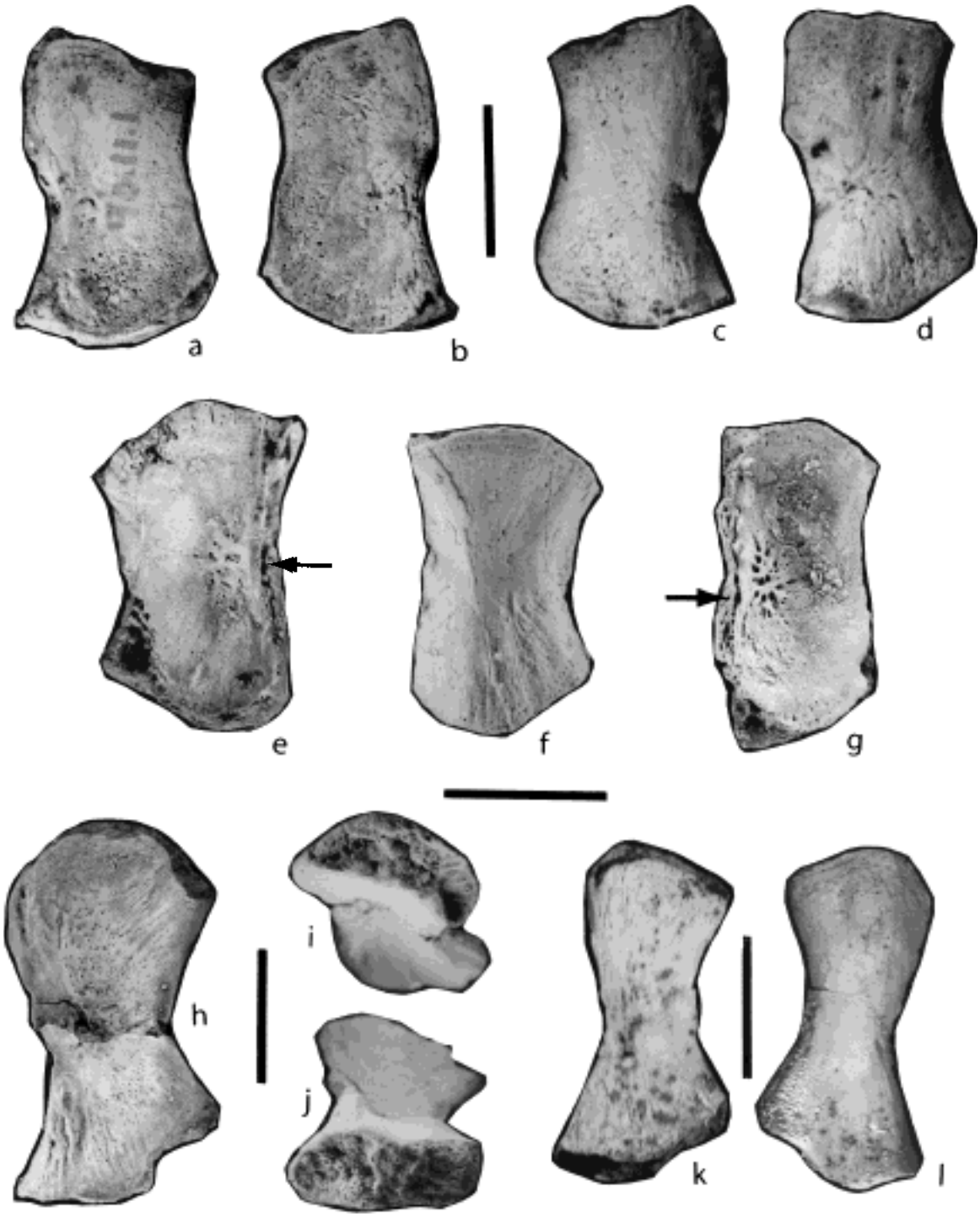

Figure 26 (a, b) Dorsal and ventral sides of ceratohyal. WAM 90.11.1. The dorsal (internal) face is convex, and the ventral face is slightly concave and has fine markings indicating attachment of soft tissues. Note the open-ended face at each terminus. (c, d) Similar views of another specimen. WAM 86.9.693. The surface markings are better organised around the centre of ossification. (e, f) Ventral and dorsal views of ANU 72975. Note the long furrow on (e). (g) The attachment structures and the furrow along the edge are well displayed. (h–j) Medial view of a specimen. ANU 72978. (i) The proximal and (j) the distal end with two surfaces for attachment. (k, l) Medial and lateral views of an elongate specimen. WAM 86.9.693. Scale bars = 10 mm.

https://doi.org/10.1017/S0263593300001309 Published online by Cambridge University Press

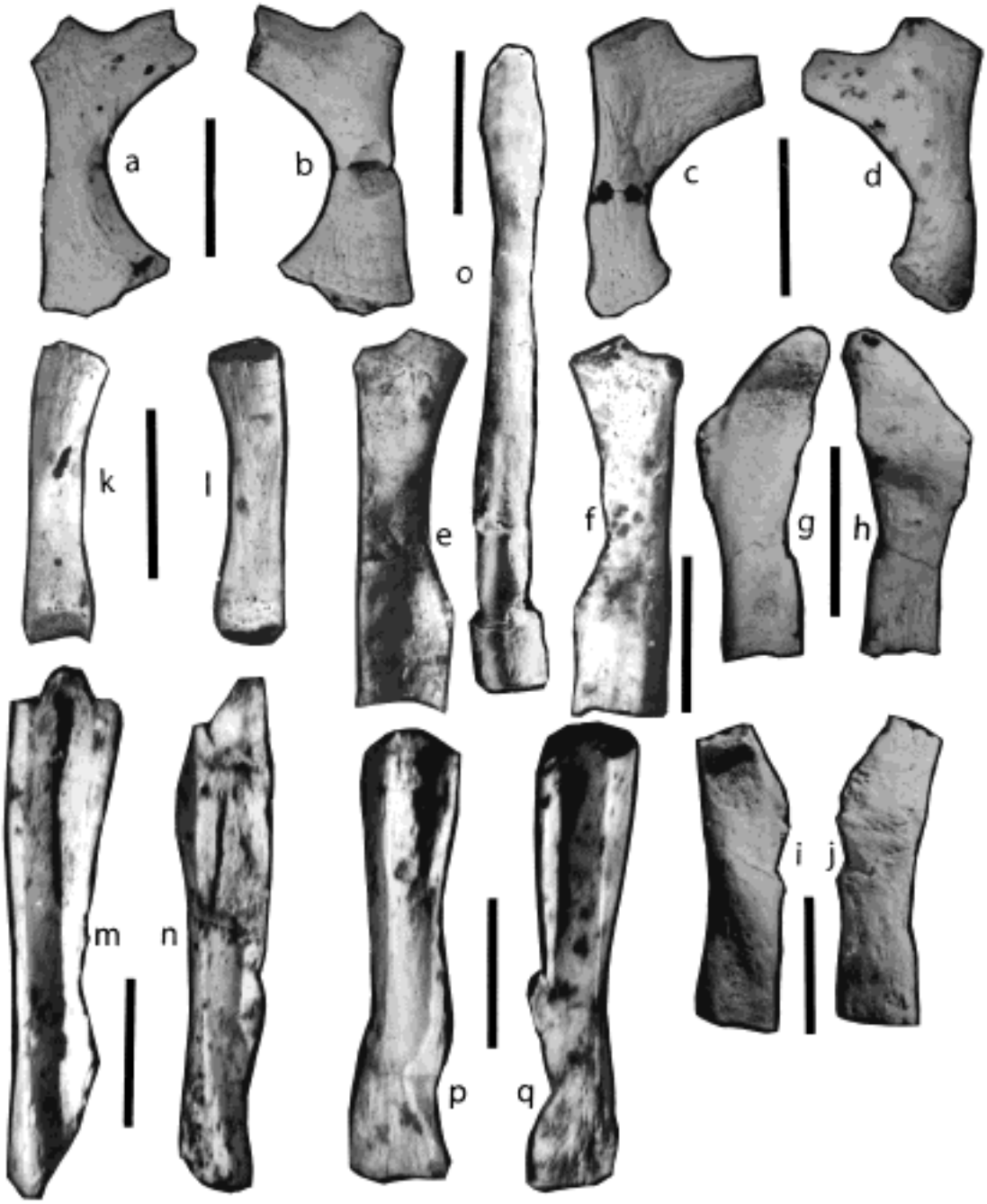

Figure 27 All specimens are from the holotype WAM 92.8.2 unless otherwise stated. (a, b) Two views of the ?first epibranchial. The branching ends are interpreted as for the infrapharyngobranchial and the supraharyngobranchial attachments. (c, d) Similar views of a ?second epibranchial. (e, f) Two views of a hypobranchial. (g, h) & (i, j) Two other segments interpreted as hypobranchials. Each element shows two small scars towards the one end, and a much larger scar at the other that was for the attachment to the ceratobranchials. On (e & f), where the two small scars are close together, the larger one is for attachment to the basibranchial and the smaller one for attachment to the adjacent hypobranchial. On (g, h and i, j), the second scar is removed from the basibranchial scar. This is what would be expected since they show attachment to the next basibranchial and the pattern changes along the series (Jarvik 1972, fig. 29). (k, l) An isolated arch which probably is a small ceratobranchial, but with no deep furrows for the vascular channels. This is probably one of the most posterior ceratobranchials. (m, n) Ceratohyals showing the long groove for the vascular supply. (o) Sublingual rod. ANU 72978. (p, q) Two more ceratobranchials in which the furrows terminate towards one end. Scale bars = 10 mm.

https://doi.org/10.1017/S0263593300001309 Published online by Cambridge University Press

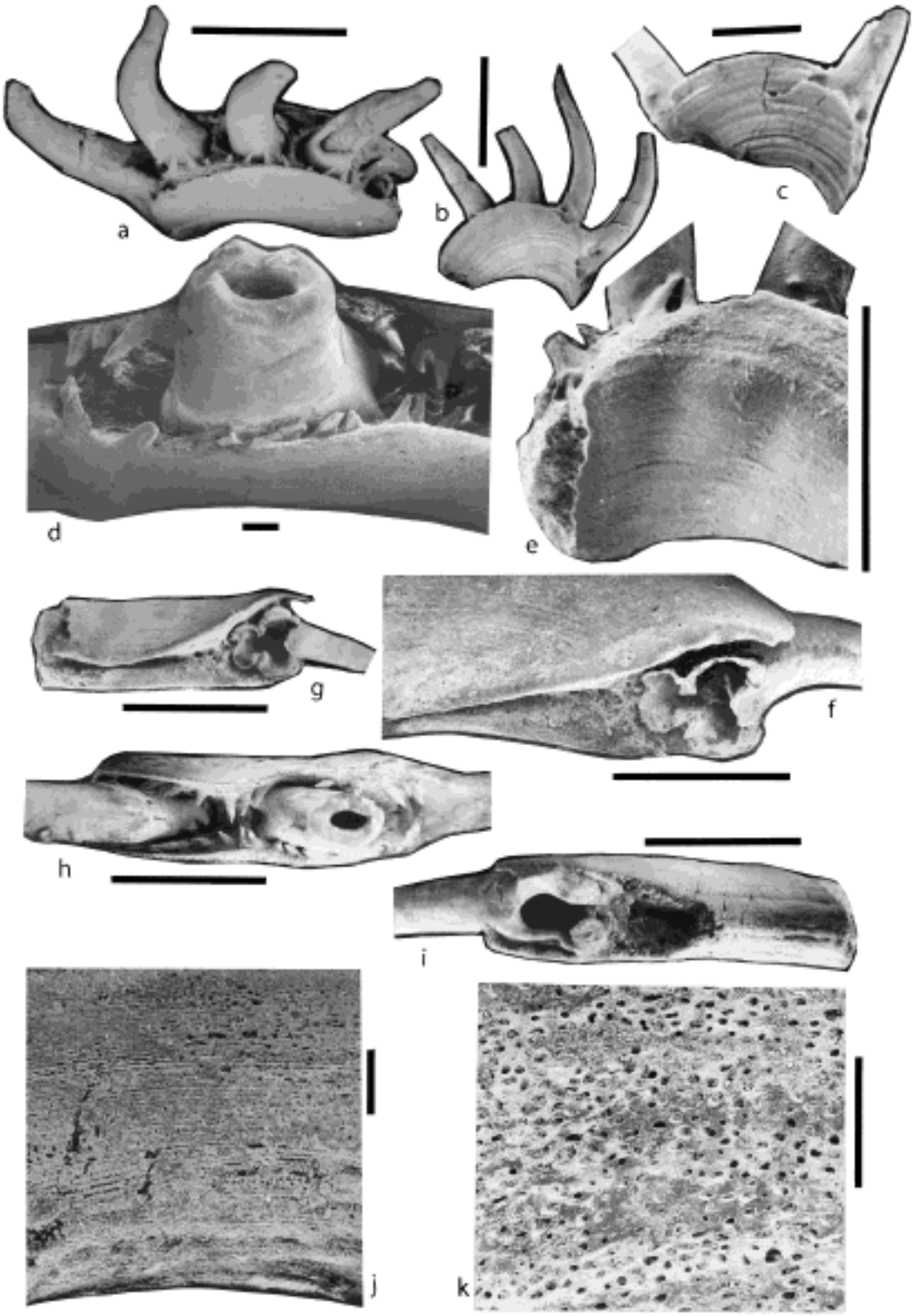

Figure 29 Parasymphysial whorls. (a) Dorsolateral view of a young specimen, ANU 72978, showing four tusks and the fifth one broken at its base. Note the denticles standing upright against the tusks, and a small number occupying the spaces between the tusks. (b) The other tusk from the same individual, with four tusks in position and a fifth one broken off posteriorly. Note the resorption at the anterior end of the whorl exposing the lateral side of the most anterior tusk, which was about to be shed. The fine lines mark additions to the whorl, which are complete anteriorly but running into the ventral edge more posteriorly. (c) Lateral view of a large specimen, ANU 72975, with only three tusks present, the medial tusk having been largely removed. Note the growth lines more numerous at the anterior (right) end. Part of posterior end eroded. (d) Dorsolateral view of the other whorl of the same individual with three tusks. The photograph is of the middle tusk. Note the extensive space between adjacent tusks, the denticles against the tusk lying at a low angle and those between the tusks projecting inwards to cover the space. (e) A small individual that was shedding the anterior tusk; the resorption of the whorl is clearly shown and the two denticles adjacent to the tusk stand at a high angle. ANU 72678. (f, g) Posterior ventral ends of two juveniles showing the newly inserted tusks and the two walls of the whorl not meeting ventrally. The edges of the tusks are without tissue binding the tusk into any basal structure. (h) Dorsal view of the individual in (d). Denticles arising from the sides of the whorls and not from their tops. (i) Ventral view of the individual in (c) showing the eroded base of the posterior tusk and the junction of the walls along the ventral edge. (j) SEM enlargement of the ventral edge of specimen in (c) showing fine lineations. (k) SEM of the same surface with pores clearly outlined. Scale bars = 10 mm; but d, j, k = 1 mm.

https://doi.org/10.1017/S0263593300001309 Published online by Cambridge University Press

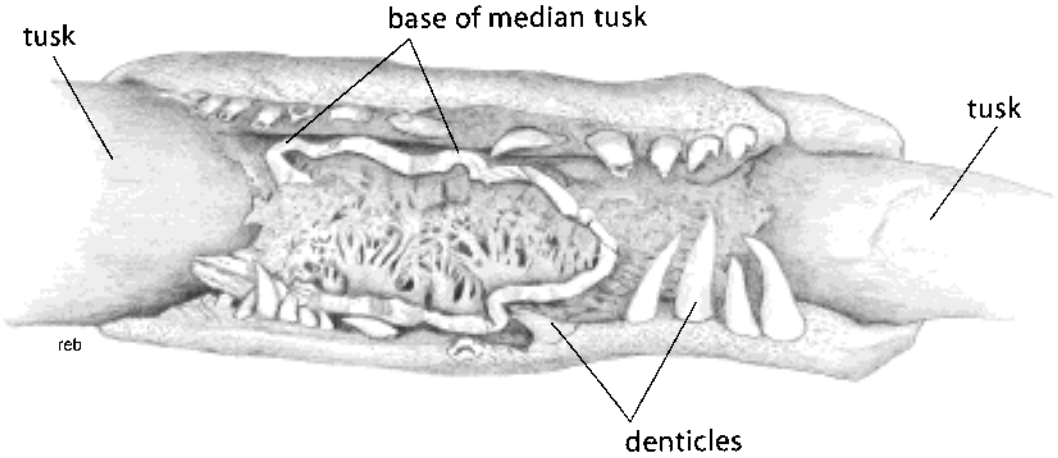

Figure 30 Dorsal view of median tusk base in an adult. ANU 72375. Note the position of the tusks and the tubes at the base of the tusk. The left side shows a newly inserted tusk that lies closer to the missing median tusk than the older tusk to the right. The whorl tissue has not grown around it. The base of the missing tusk shows the branching intergrown material running off the base of the tusk, and forming the attachment of the tusk into the whorl. Scale=2·8 times Fig. 29c.

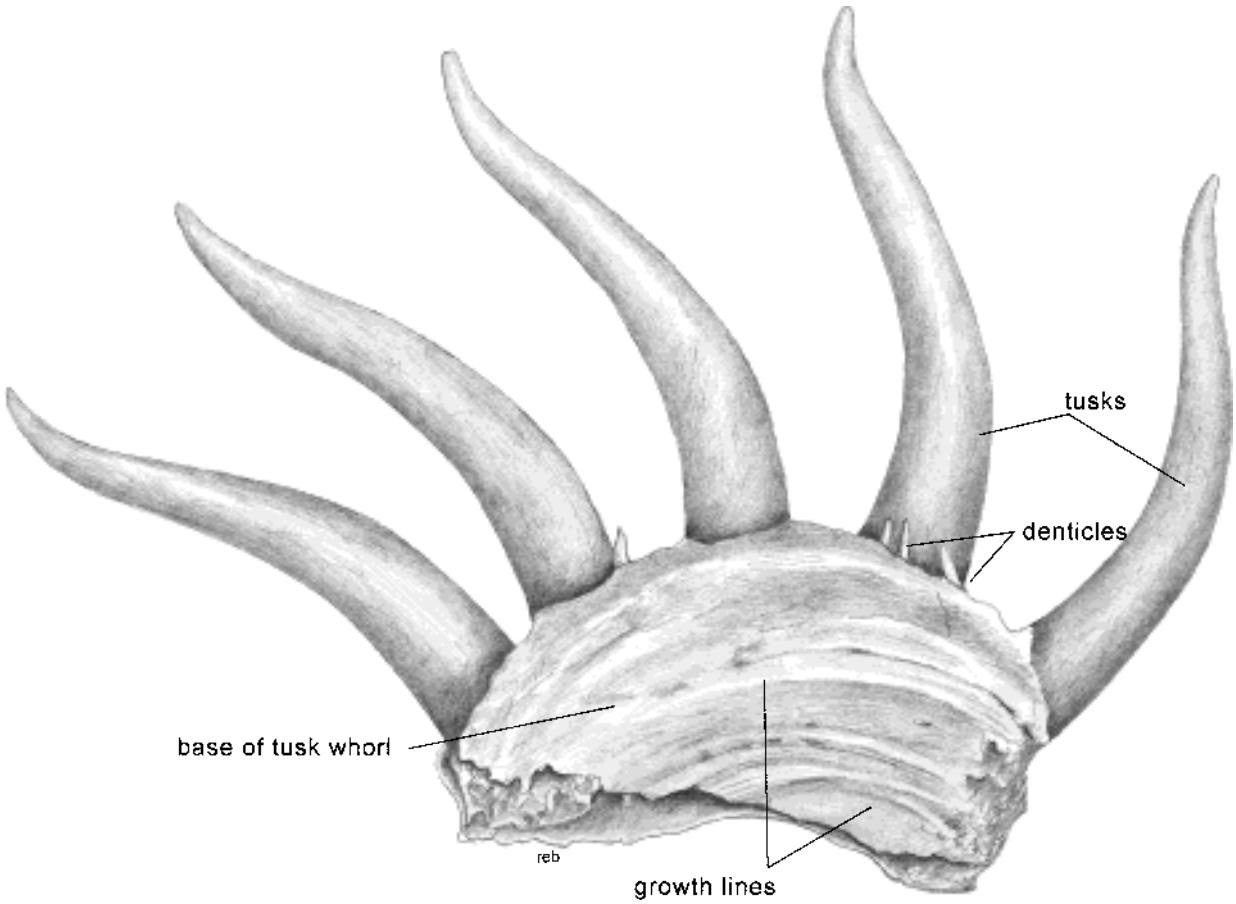

Figure 31 Reconstructed lateral view of a juvenile specimen (anterior to the right) showing the main features and also the open space posteriorly with a new tusk inserted, and an eroded anterior edge where a tusk was soon to be shed. Note the marginal denticles standing upright against the tusk, as is normal for the juvenile specimens. Growth lines are incomplete posteriorly where they lie against the opening for the insertion of new tusks. Compare with Figure 29b.

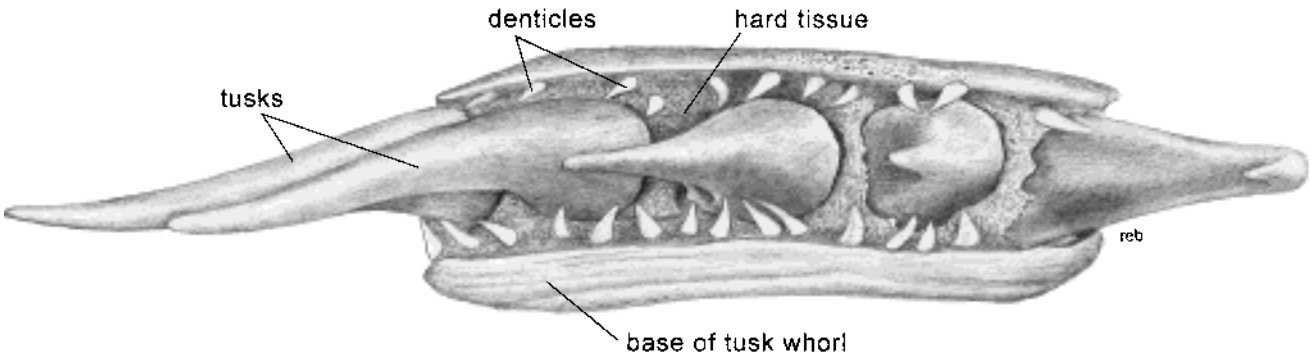

Figure 32 Reconstruction of a dorsal view of a juvenile parasymphysial whorl showing the small spaces between the tusks, the upright denticles, the depression in the posterior face of the tusks, and the derivation of the denticles from the hard layers between the walls. Anterior to the right. Specimen based on Figure 29b.

https://doi.org/10.1017/S0263593300001309 Published online by Cambridge University Press

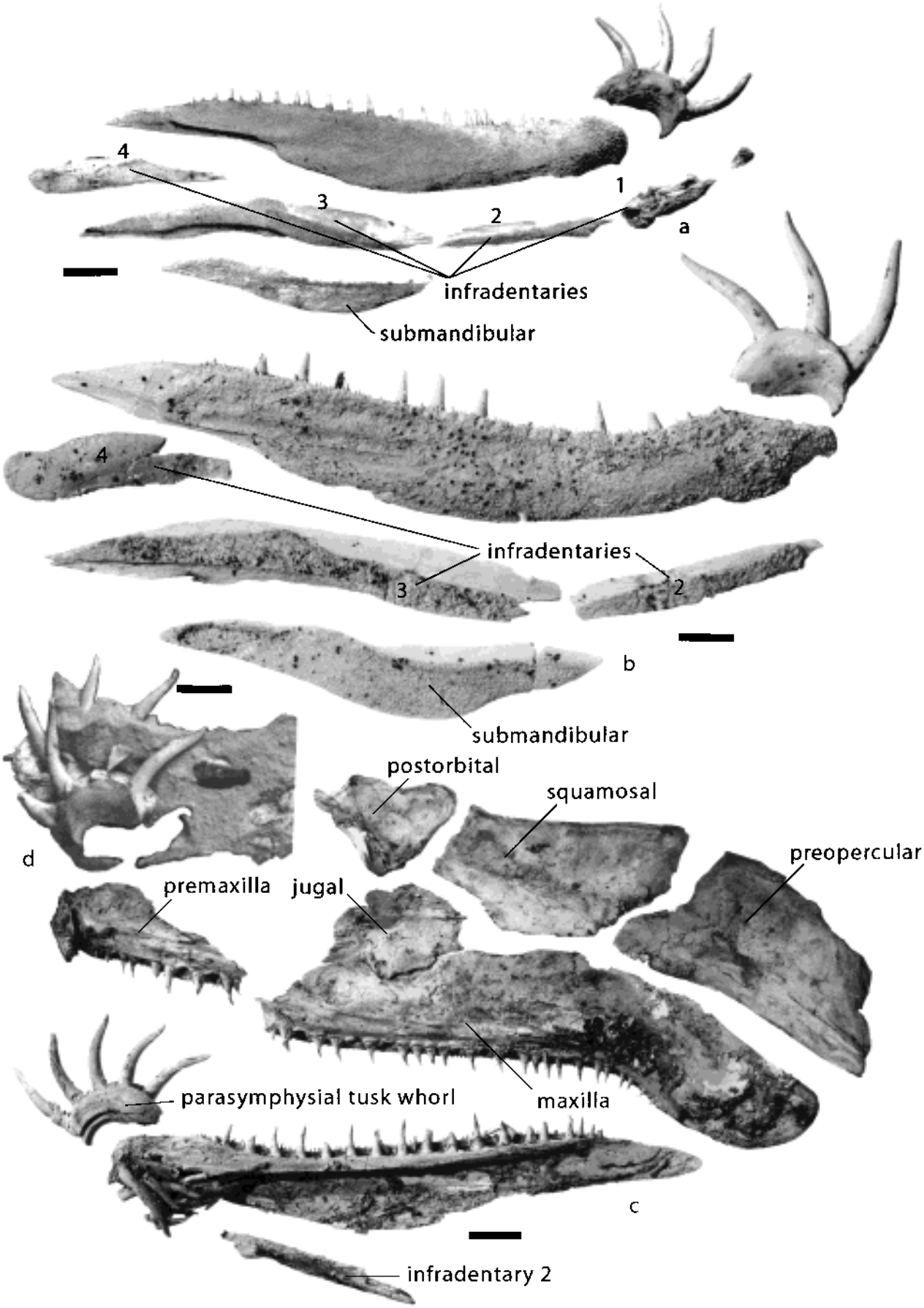

Figure 28 (a) Dissociated young specimen. Note four exposed tusks in the whorl, the anterior one about to be shed and space for a new tusk to be inserted posteriorly. Four infradentaries present, labelled 4–1, and a small parasymphysial plate anteriorly. Infradentary 4 shows clearly the overlap with the dentary. BMNH P64125. (b) A larger individual with only three tusks in the whorl. Infradentaries 2–4 and submandibula all showing overlaps. (c) A young BMNH specimen with five tusks in the whorl. Tusks lying loose in the anterior of the mandible prior to their insertion into the whorl. Almost all dentary teeth present, and fine denticles present along the outer edge of the dentary. The maxilla, premaxilla and cheek plates are all present. The teeth on the maxilla are almost all present, and those on the premaxilla show the gradation in size from front to back. (d) Unlabelled fragment of a partly etched specimen with the two parasymphysial tusk whorls, with four tusks, some broken, in position. All photographs prepared by Dr Andrews. Specimens without ammonium chloride. Scale bars = 10 mm.

https://doi.org/10.1017/S0263593300001309 Published online by Cambridge University Press

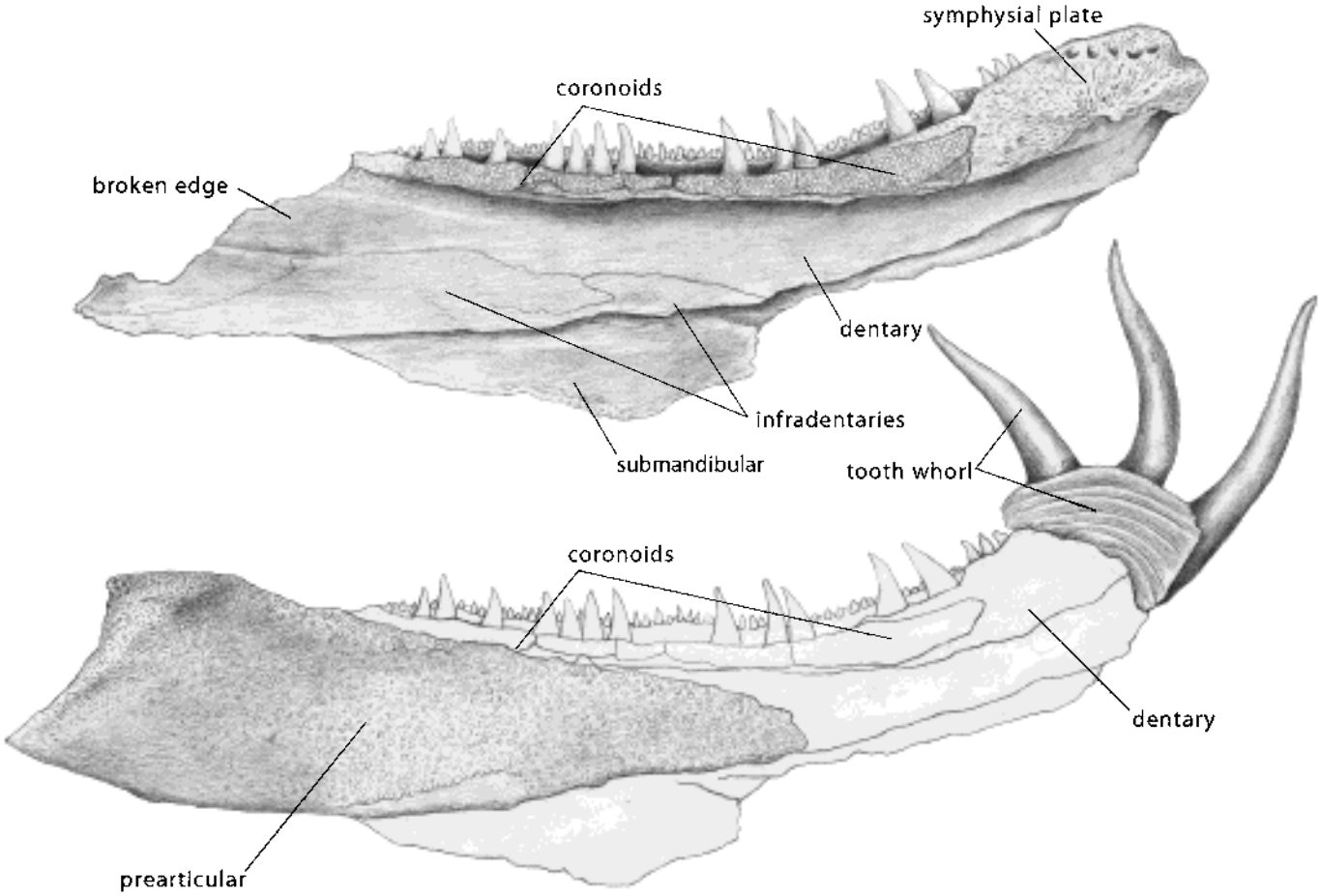

Figure 33 (a) Reconstruction of the interior of the left mandible based on ANU 72975, but with the drawing reversed (see Fig. 42h). Coronoids added from another specimen. Note the position of the symphysial plate at the anterior end of the dentary with the centre of the radial lines and the perforations for nerve and blood supply. (b) The same specimen with the prearticular and the tusk whorl replaced from the same specimen.

https://doi.org/10.1017/S0263593300001309 Published online by Cambridge University Press

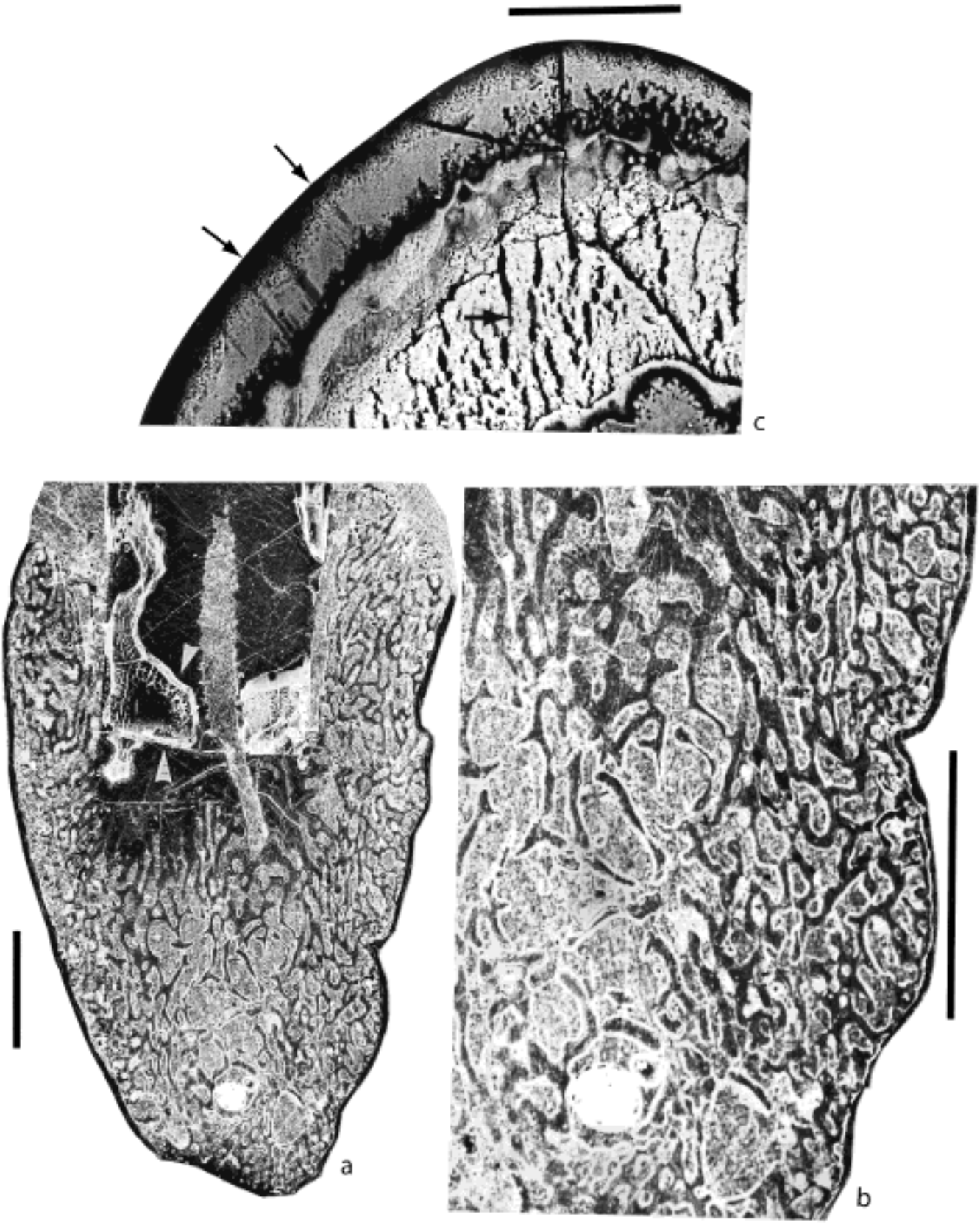

Figure 34 (a) SEM back scatter of the whorl with a tusk lying in its socket, a sediment infill of the pulp cavity and a column of other sediment filling the core. In the whorl, the dark material is calcified cartilage, and the large open spaces in the midline are for the passage of nerves and vessels. The white arrows mark material infolded into the base of the tooth. (b) Enlargement of the right side of (a). The dark material is hard tissue. Within this tissue are open spaces which represent the remains of the cartilage which had not been calcified. Around each hard layer is a light band of tissue that probably represents partly ossified cartilage. (Compare with Fig. 35b.) (c) The crest of the infolded whorl tissue arrowed in Figure 35a. The broken material labelled with an arrow is calcite of the infill. The outer layer is the infolded base of the tooth. Note that the outer and inner faces were still partly forming. The arrowed perforations through the layer are real and are not scratches. Scale bars: (a, b) 1 mm; (c) 100 μm.

https://doi.org/10.1017/S0263593300001309 Published online by Cambridge University Press

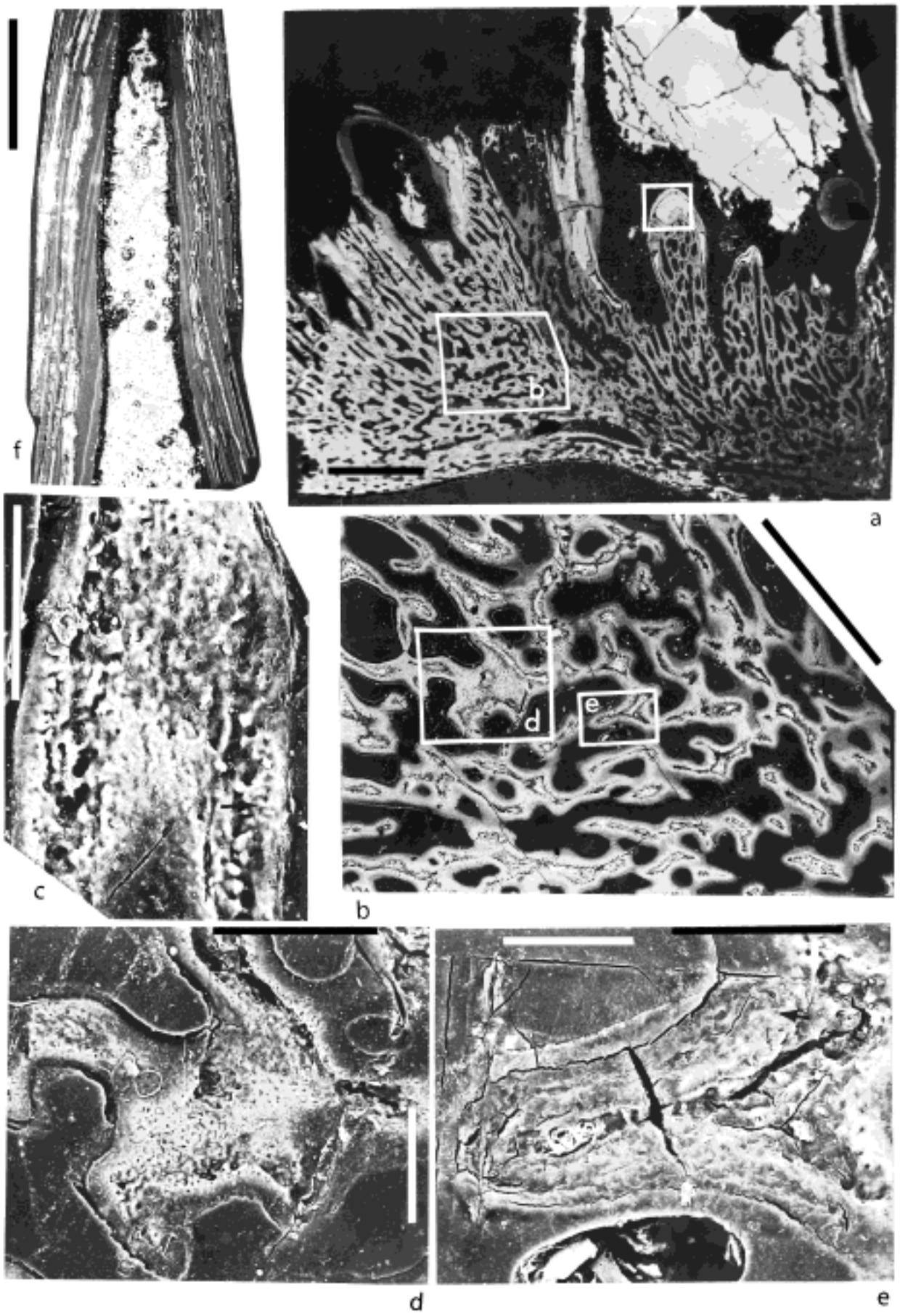

Figure 35 (a) A SEM back scatter of the base of tusks in the parasymphysial whorl. The right side shows the base of a tusk and the left side the broken off base of a second tusk. The columns are vesicular material of whorl tissue folded into the base of tusk as shown in Figure 30. (b) A SEM back scatter enlargement of the whorl tissue at the area marked in (a). Calcification of the cartilage has taken place around the edge of the hard tissue and uncalcified spaces are left in the cores. (c–e) Parts of (b) showing the details of the calcified cartilage. The lumpy structures arrowed (c & e) are the sections of the globular tissue shown in Figure 36. (d) A distinctive pattern of calcification, where a number of cartilage layers join. (f) SEM section of a tusk in which the successive layers have been added as invaginating cones. Scale bars: (a) 1 mm; (b) 500 μm; (c) 20 μm; (d) 100 μm; (e) 50 μm; (f) 1 mm.

https://doi.org/10.1017/S0263593300001309 Published online by Cambridge University Press

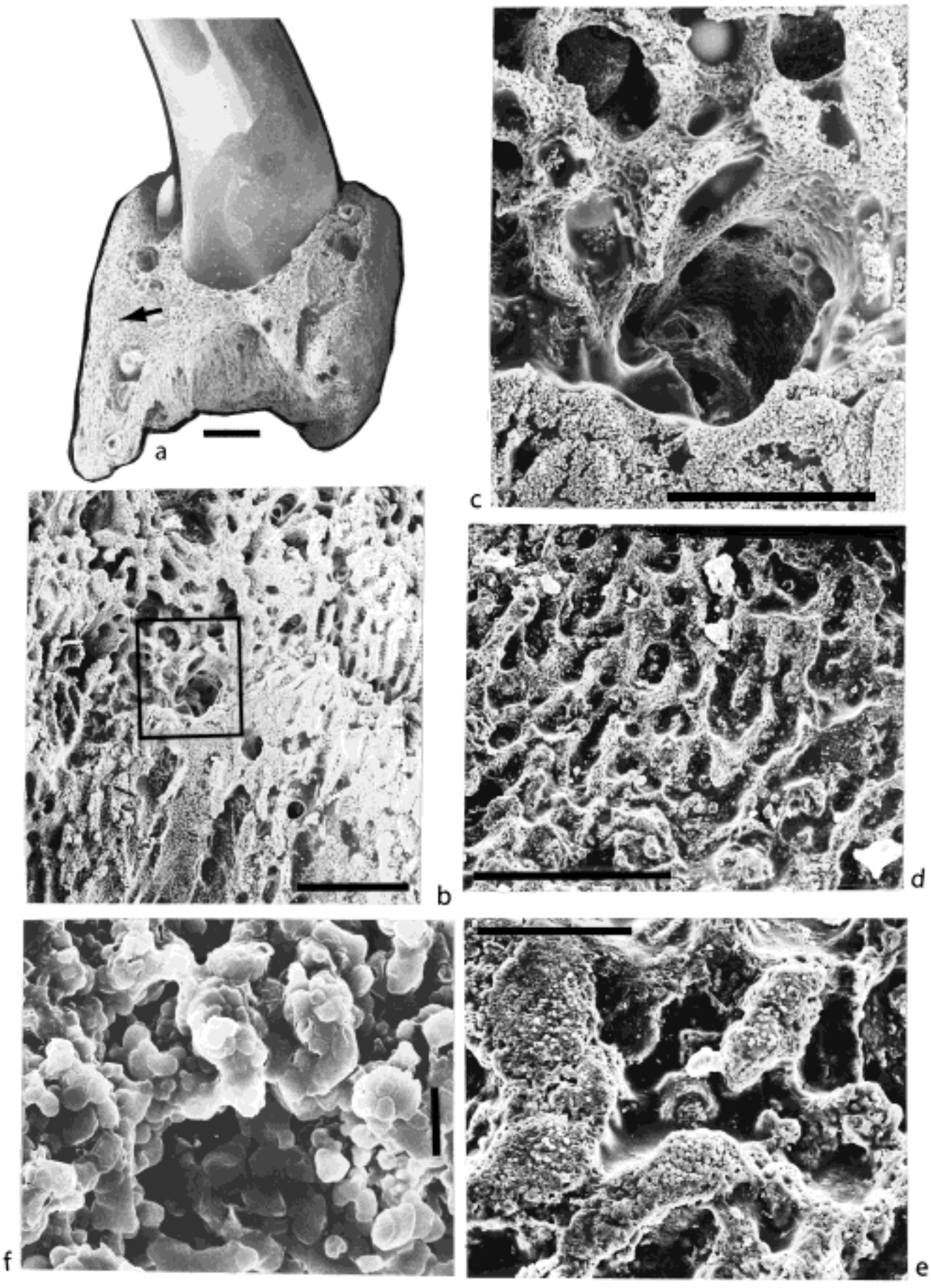

Figure 36 (a) An isolated tooth embedded in the parasymphysial whorls. Small tentacles partly in position, but others eroded. Space for the net tooth facing viewer, and showing the pores for the nerve and vascular bundles. Arrow showing the growth lines. (b) Surface of the cavity in (a) enlarged. (c) Enlarged part of the bracketed area in (b) showing the coarse granular whorl tissue. (d–f) Successively enlarged images of the whorl tissue showing the granules that form the structure. Scale bars: (a) 1 cm; (b) 0·5 mm; (c) 260 μm; (d) 500 μm; (e) 100 μm; (f) 15 μm.

https://doi.org/10.1017/S0263593300001309 Published online by Cambridge University Press

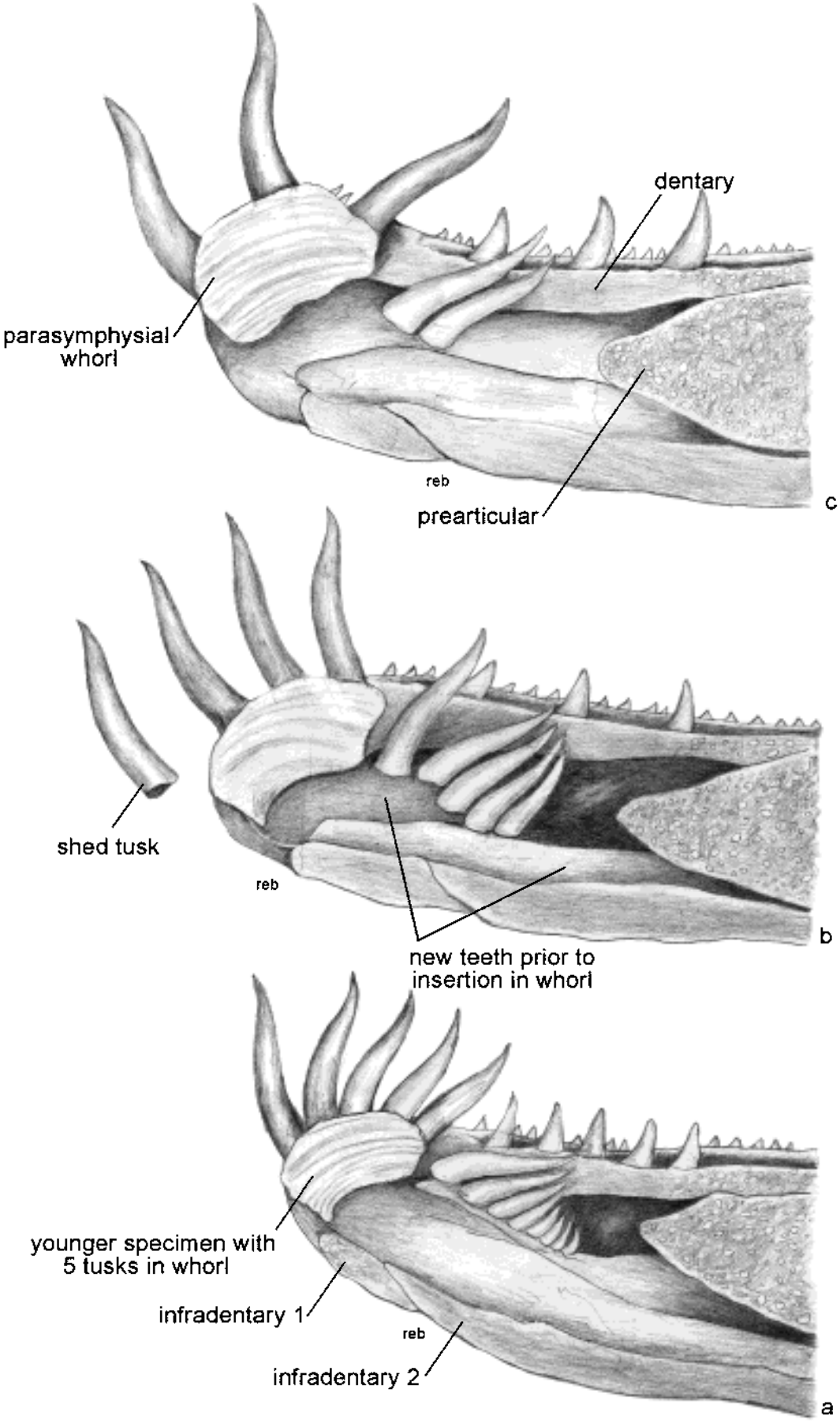

Figure 37 Diagrammatic reconstruction of the method of insertion of new tusks into the parasymphysial whorl. (a) A juvenile specimen with five tusks. A new series of tusks decreasing in size posteriorly are placed behind the whorl and anterior to the prearticular. (b) An older individual with a tusk shed anteriorly and a new tusk ready to be inserted in the whorl. The uninserted tusks are here larger in size, and the next tusk to be inserted is comparable in size to the posterior one in the whorl. (c) The oldest individual in which most of the tusks have been inserted. The anterior tusk is being shed. The uninserted tusks are limited in number because they are the last in the series.

https://doi.org/10.1017/S0263593300001309 Published online by Cambridge University Press

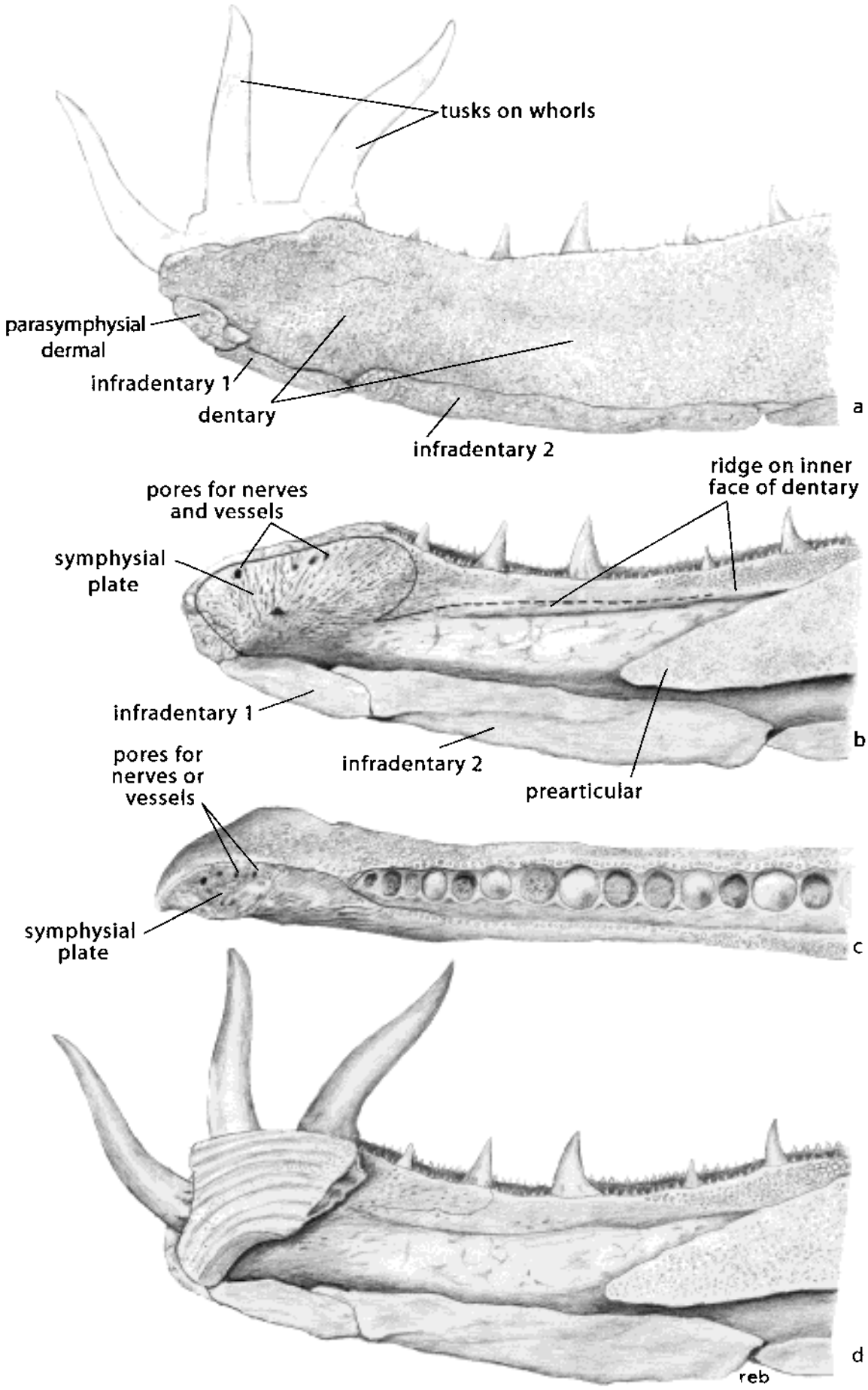

Figure 38 (a) A reconstruction of the anterior part of a mandible showing the position of the tusk whorls and the infradentaries. (b) A rotated internal view of the same. Note the position of the symphysial plate with radial growth lines, and pores for nerve and vascular bundles. The outline of Meckel's Cartilage is shown by a broken line beneath the overhanging edge of the dentary and as a continuous line against the symphysial plate. (c) Dorsal view of the same showing the outline of the symphysial plate. (d) Rotated internal view of (a) with the tusk whorl in position. Note the folding on the base of the tusk that was being shed.

https://doi.org/10.1017/S0263593300001309 Published online by Cambridge University Press

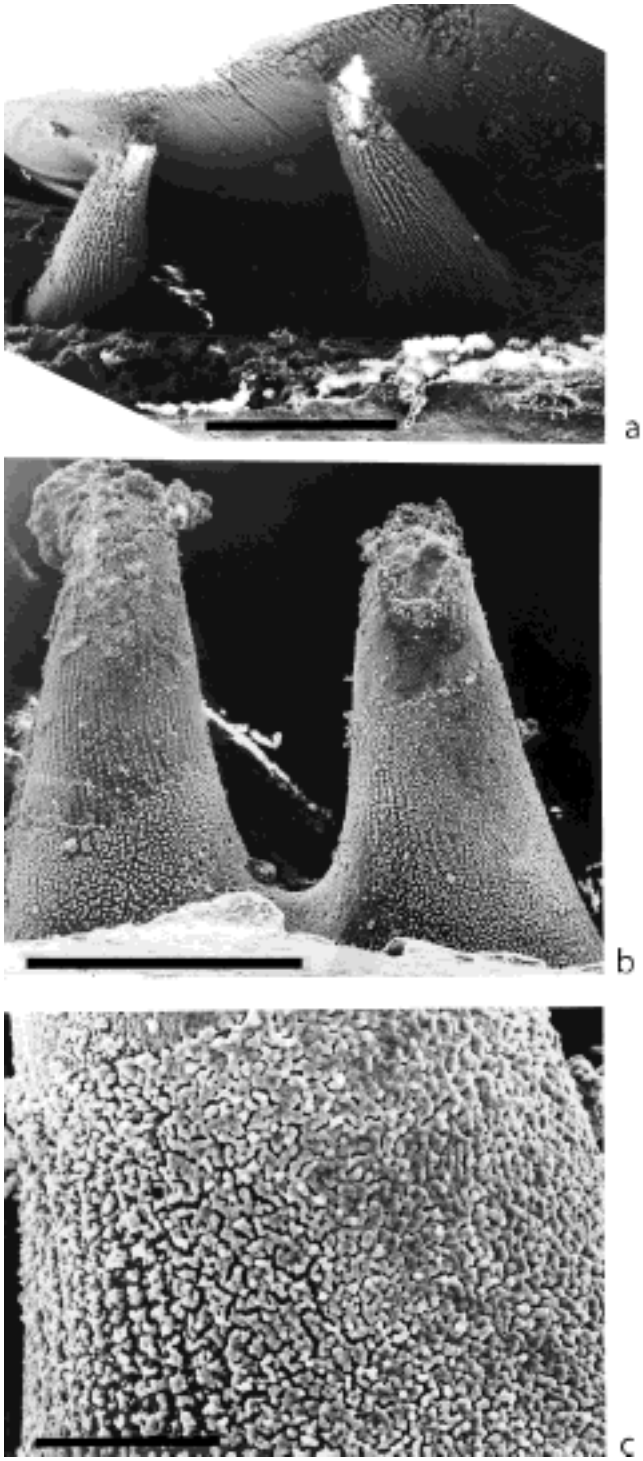

Figure 39 (a, b) Views of lateral denticles adjacent to the tusks in a juvenile specimen. Tusks in the background. At the base of the denticle, the granules are randomly arranged, but more dorsally, they are arranged in linear series. (c) Part of the right denticle in (b). ANU 72978. Scale bars: (a) 1 mm; (b) 500 μm; (c) 100 μm.

https://doi.org/10.1017/S0263593300001309 Published online by Cambridge University Press

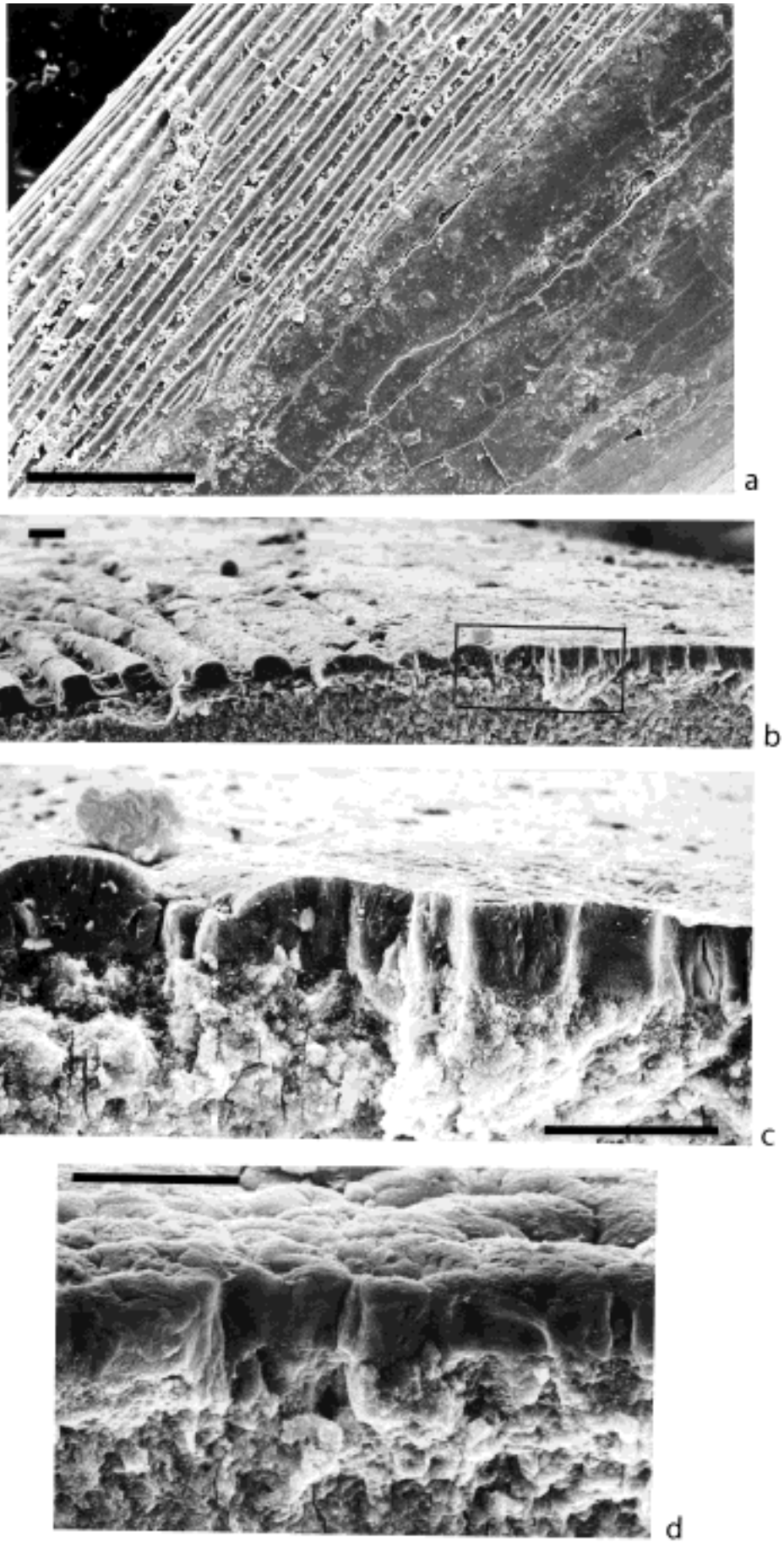

Figure 40 (a) A SEM of part of a tusk surface showing longitudinal ridges passing laterally into an almost smooth surface. (b) Cross-section of the junction between the ridged and the smooth surfaces. The dark layer is enamel, and note that it retains its thickness in the smooth areas. (c) Part of the above surface [outlined in (b)] showing the gradual transition from the ridged to the smoother surface. (d) Slightly tilted section through the so-called smooth surface showing the dimpled pattern on the enamel. WAM 86.9.693. Scale bars: (a) 250 μm; (b–d) 20 μm.

https://doi.org/10.1017/S0263593300001309 Published online by Cambridge University Press

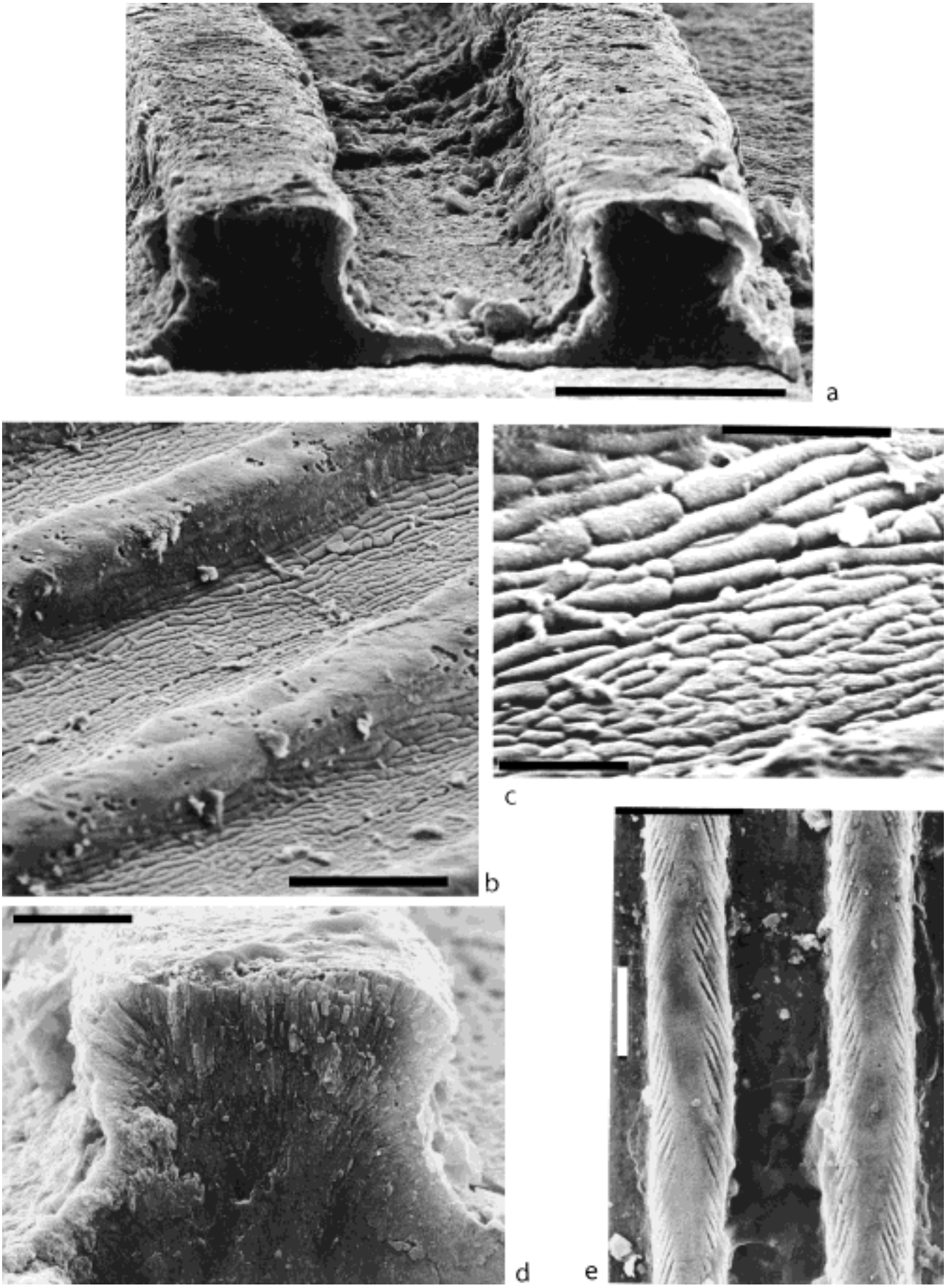

Figure 41 (a) Sections through the ridges which have no radial markings, but only transverse (growth) lines. (b) Oblique ridges without radial markings, and the valleys between them filled with discontinuous radial ridges. The smooth surface is not the result of erosion, but is the result of a layer of tissue laid down on the surface. (c) Enlargement of the structures in the valleys. Small excrescences on the flanks of the long ridges. (d) Cross-section of the ridge on the left side of (a) showing the radial array of crystals. (e) A pair of ridges with fine surface ornament but no ornament in the valleys. WAM 86.9.693. Scale bars: (a–c) 20 μm; (d) 5 μm; (e) 20 μm.

https://doi.org/10.1017/S0263593300001309 Published online by Cambridge University Press

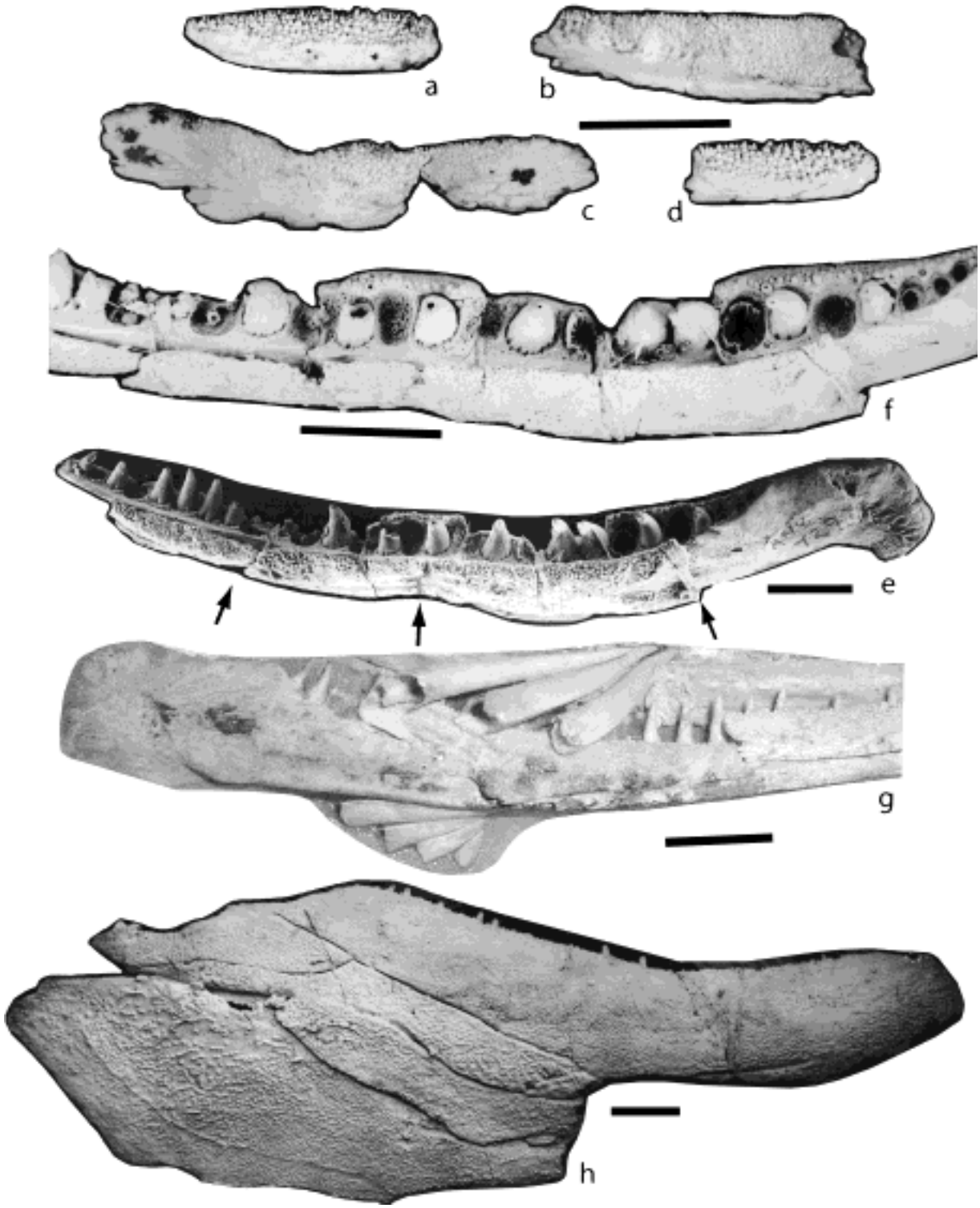

Figure 42 (a–d) Four coronoids isolated from the prearticulars. (a–c) These are similar to the posterior three coronoids, which are well shown in (e). (b) This shows the rather smooth triangles against which the teeth on the dermopalatine fitted. Note their shape, which is open to the base because the surface of the coronoid is bent with the top surface inclined away. (e) Lingual view of a broken mandible, ANU 72975, showing three of the four coronoids. Boundaries between the coronoids are indicated by arrows. Other breaks are cracks. (f) The same specimen viewed from a more dorsal direction. Note the crenellated base of the tusks, and the internal folding of some of the broken teeth, the reduction in their size anteriorly and the shape of the bone where a tooth has been completely removed. (g) Part of a broken mandible, anterior to the left, showing groups of tusks which have not yet been inserted into the parasymphysial whorl. The uppermost set of three tusks show the narrow ends where the dentine has not reached its full thickness before being inserted in the whorl, whereas the lower set of four consists of smaller tusks which are gradually reduced in size. BMNH P63572. (h) A mandible with the posterior end of the dentary broken, three infradentaries present but with the third one lacking the middle part, the submandibular with its broken posterior end having its outline defined by the surrounding bones, and the gular with its anterior end incomplete. The line on the surface of the gular is the edge of plastic laid down during preparation, and a hair is present across the infradentary 4 and the submandibular. Bones labelled on Figure 43. ANU 72975. Scale bars = 10 mm.

https://doi.org/10.1017/S0263593300001309 Published online by Cambridge University Press

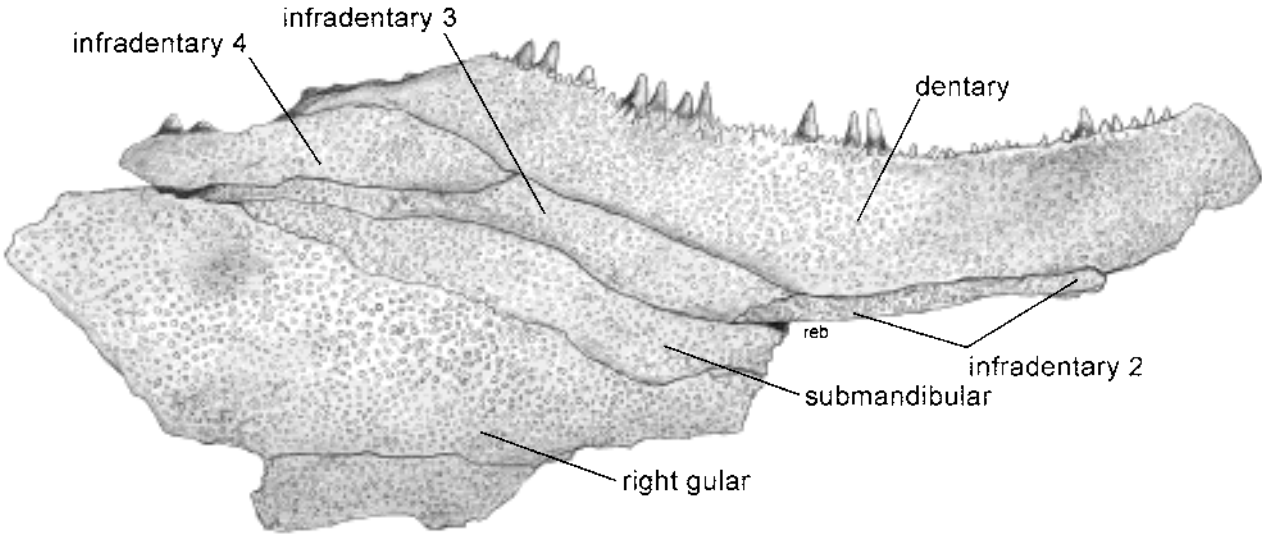

Figure 43 Reconstruction of Figure 42h.

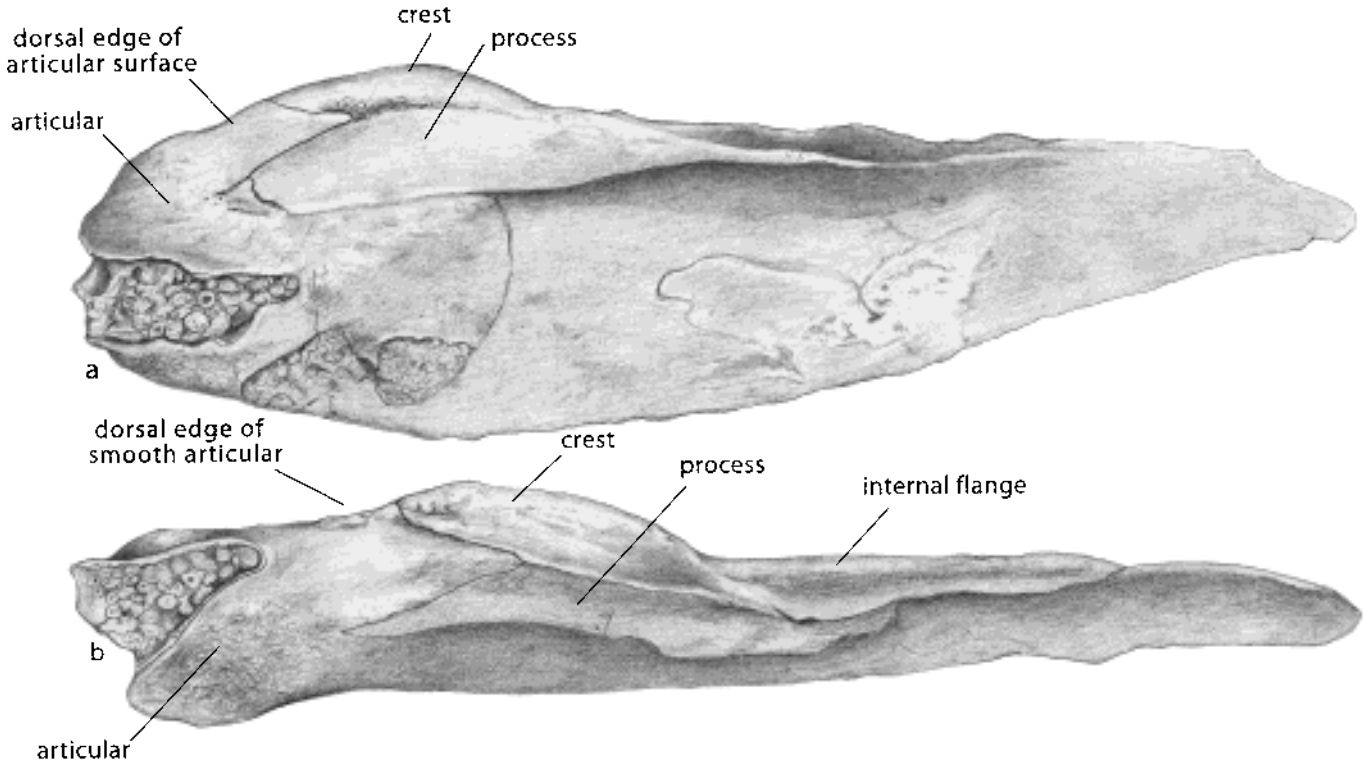

Figure 45 (a) Reconstructions of a prearticular in median view exposing the ventral side of the articular. (b) The same in the dorsal view: adductor attachment and extension of ridge anterior to it. Based on the specimen in Figure 44e.

https://doi.org/10.1017/S0263593300001309 Published online by Cambridge University Press

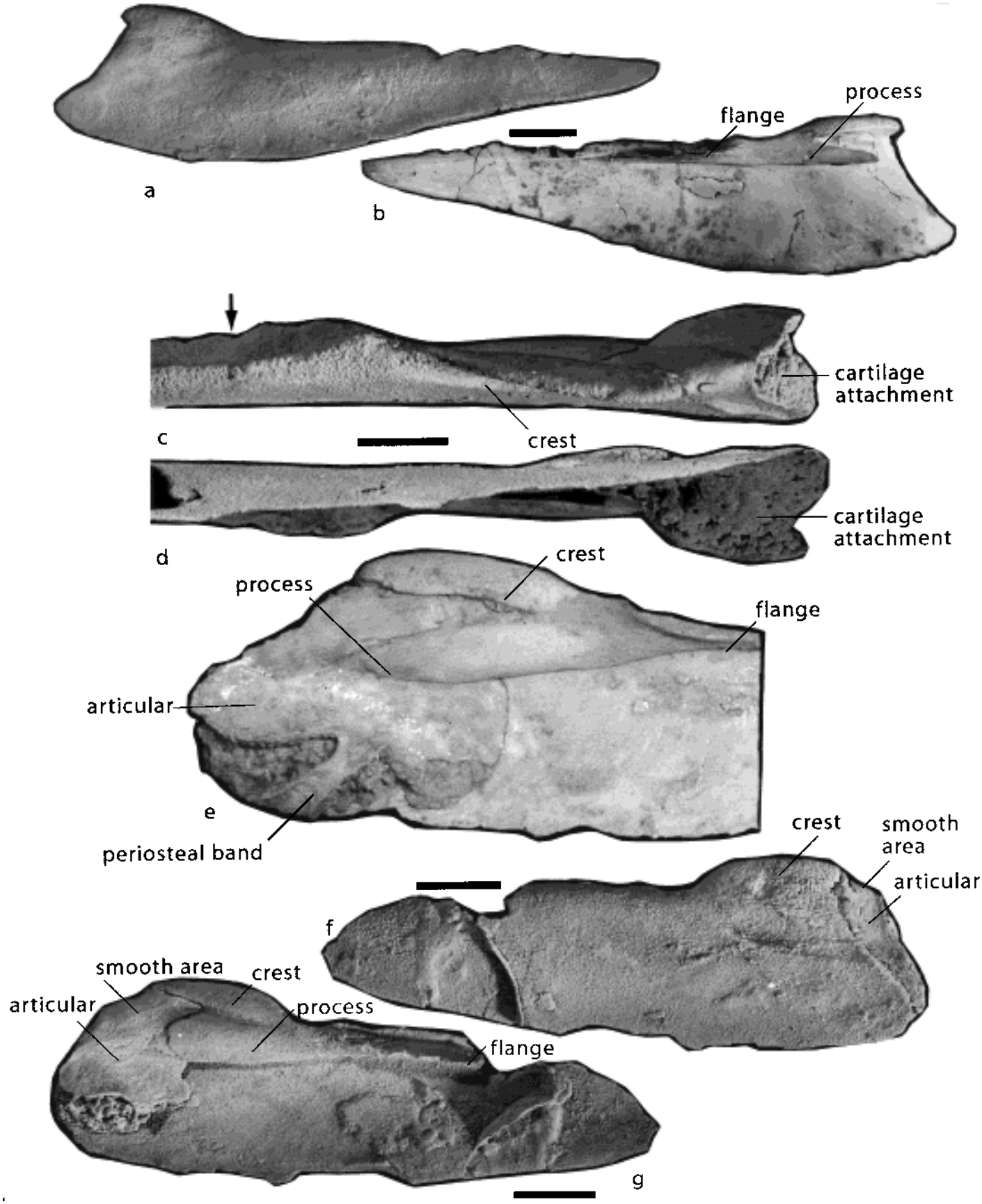

Figure 44 (a, b) External and internal surfaces of an isolated prearticular. The articular has been removed, but the process which lay along it is present, and this leads to the internal flange. WAM 92.8.2. (c, d) Dorsal and ventral views of a prearticular with the articular in position. The smooth area of articular lies posterior to the top of the adductor surface. The dorsal part of the cartilage attachment on the articular is much smaller than the ventral. Note the dorsal edge of the adductor pit and the flange which extends anterior to the pit (arrowed). WAM 90.11.1. (e) An enlarged lingual view of the posterior of a mandible showing the articular in position. The process and the flange anterior to it are well preserved. Projection of the periosteal bone across the ventral face of the articular. BMNH P64125. (Photograph enhanced electronically.) (f, g) External and internal faces of a prearticular and the articular of WAM 90.11.1. In (f), the articular shows up posteriorly, and the smooth surface is clear. In (g), the articular is broken off anteriorly, and the posterior projection on the prearticular is also broken. Scale bars = 10 mm.

https://doi.org/10.1017/S0263593300001309 Published online by Cambridge University Press

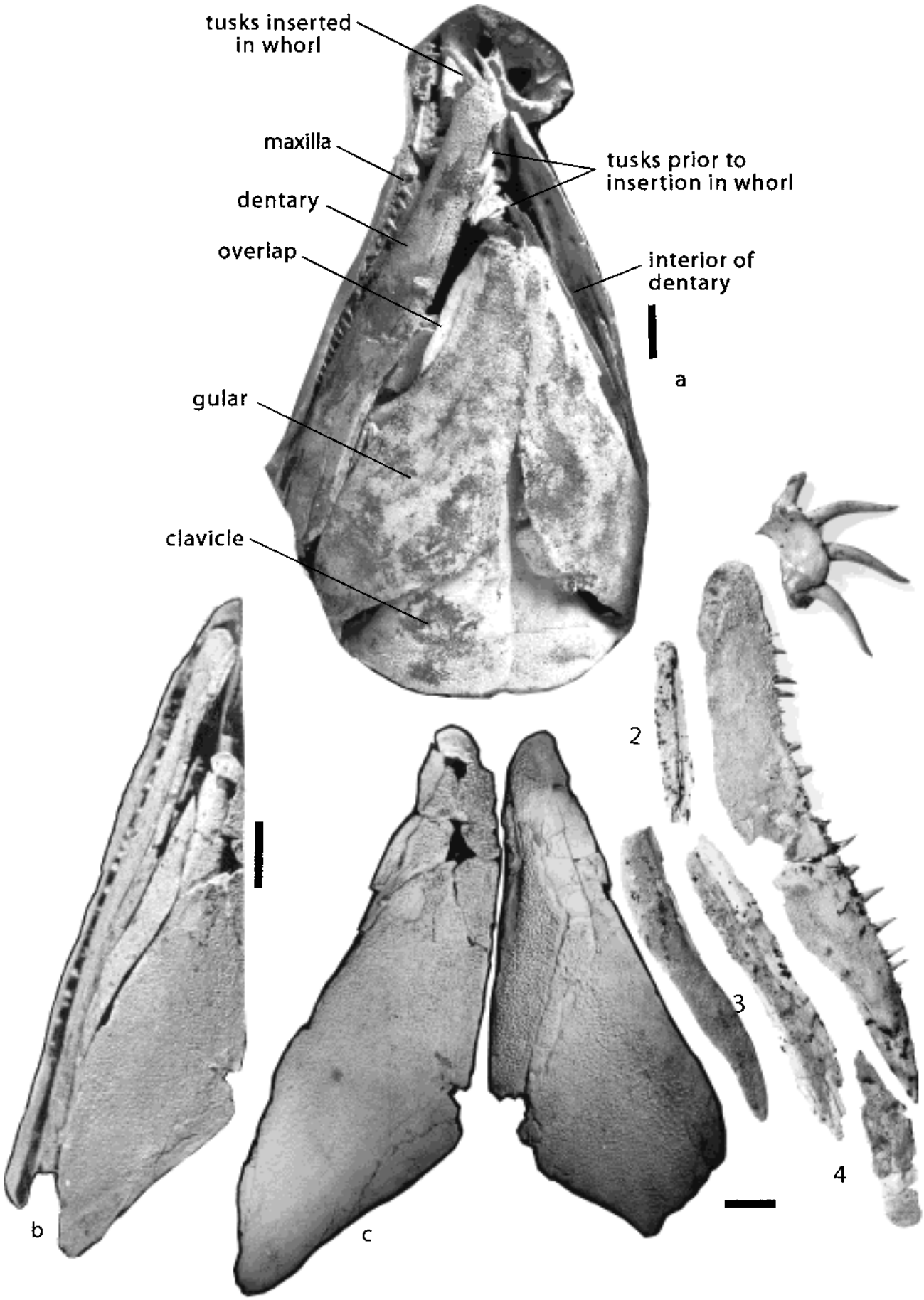

Figure 46 (a) Specimen BMNH P63566 with gular, clavicle, and the mandible and part of the maxilla. The clavicle edge lies under the gular. Uninserted tusks lie at the anterior end of the mandible. (b) Ventral view of half the head of the holotype, showing the infradentaries, submandibular and the gular approximately in position. (c) The holotype with the gulars and the dentary and infradentary plates isolated. Infradentaries labelled 4, 3 and 2, and the submandibular plate exposed. Tusks on the whorls indicate that the animal was not fully grown. Photograph by Dr Andrews. Specimen unwhitened. Compare with Figure 28a, b. Scale bars = 10 mm.

https://doi.org/10.1017/S0263593300001309 Published online by Cambridge University Press

Figure 47 (a, b) Isolated cleithrum BMNH P63570 in external and internal views; note the large overlap surface on the anterodorsal edge in (a) (arrowed), and the radial surface where the clavicular process joins the bone in (b) (arrowed). (c, d) Lateral and median views of the girdle of the holotype. The dorsal end shows the posttemporal, supracleithrum and anocleithrum placed in position by Dr Andrews. Much of the clavicle removed from (d). Scapulocoracoid largely destroyed. (e) Internal view of cleithrum; dorsal end with a raised section underlying the overlapped external surface. Scapulocoracoid in position with its anterior face outlined by shadow as the lighting was from the left. WAM 92.8.2. (f) Similar to (e), but outline of the scapulocoracoid emphasised and the central part broken away. Holotype. (g) Internal view of the pectoral girdle of ANU 72976 showing the overlap of the edge of the cleithrum by the clavicle, and the inner face of the clavicular process stands towards the viewer. Scale bars = 10 mm.

https://doi.org/10.1017/S0263593300001309 Published online by Cambridge University Press

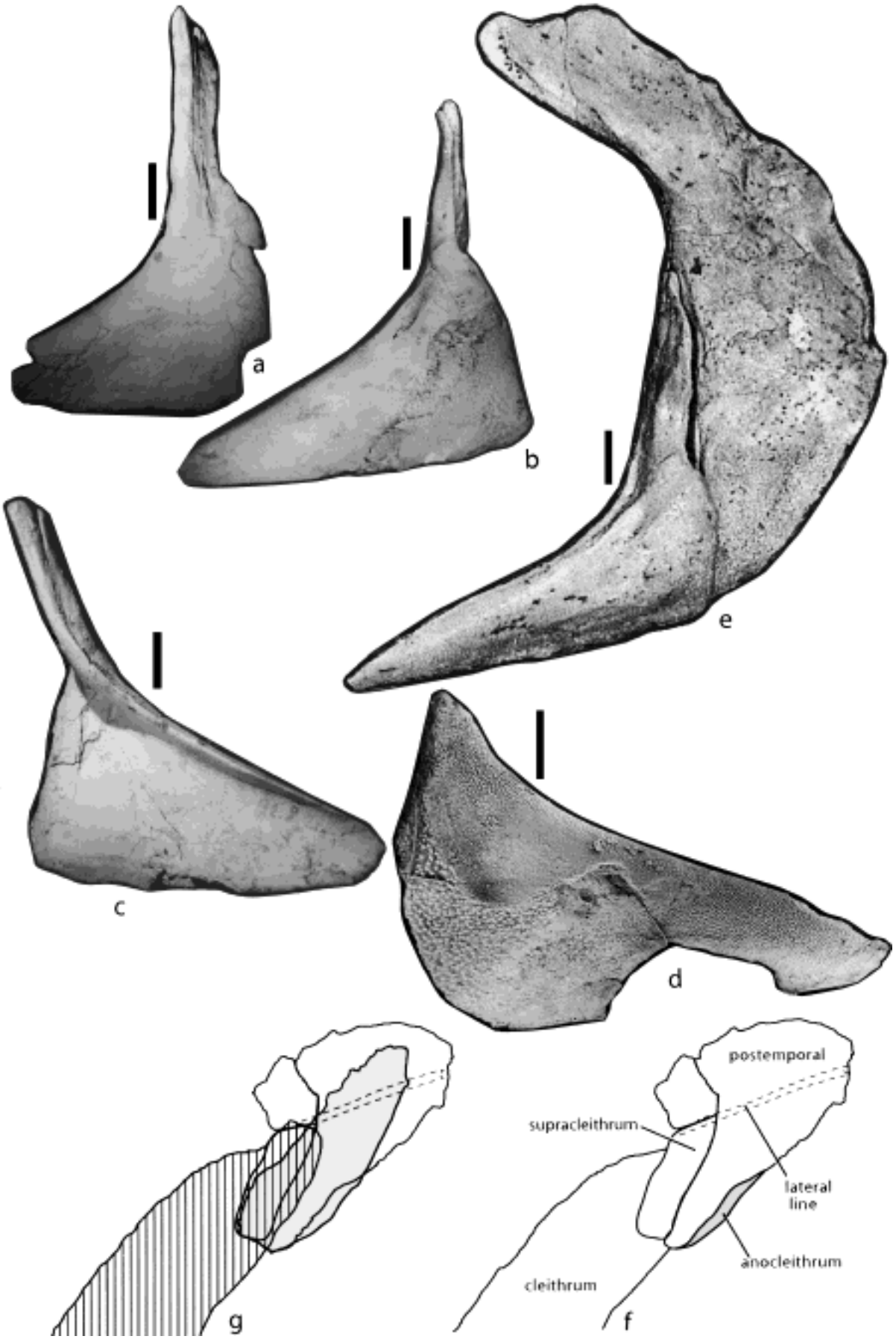

Figure 48 (a) Clavicle twisted slightly to the left so that grooving of the articulation posterior face of the dorsal process is clear. WAM 92.8.2. (b) Ventrolateral view. ANU 72976. (c) Internal view of the clavicle with the dorsal process in normal position and a deep furrow on the anterior face. Ridge running down the anterodorsal face throwing a shadow. (d) Specimen with the broken dorsal process to the top and the broken ventral edge to the bottom. Coarsely granular area marks exposed surface. The smooth surface with some fine granulation indicates the large surface covered by soft tissue, possibly from the subopercular, which also covered part of the cleithrum. The finely ornamented anteroventral surface was covered by the gular. ANU 72978. (e) Reassembled pectoral girdle showing close relationship between cleithrum and clavicle. (f, g) Reconstruction from the surface showing the posttemporal, supracleithrum and the anocleithrum in relation to the cleithrum. (f) An external view. (g) The supracleithrum and the posttemporal shown as transparent, demonstrating the overlapped cleithrum and the anocleithrum. Drawn from the holotype. Scale bars = 10 mm.

https://doi.org/10.1017/S0263593300001309 Published online by Cambridge University Press

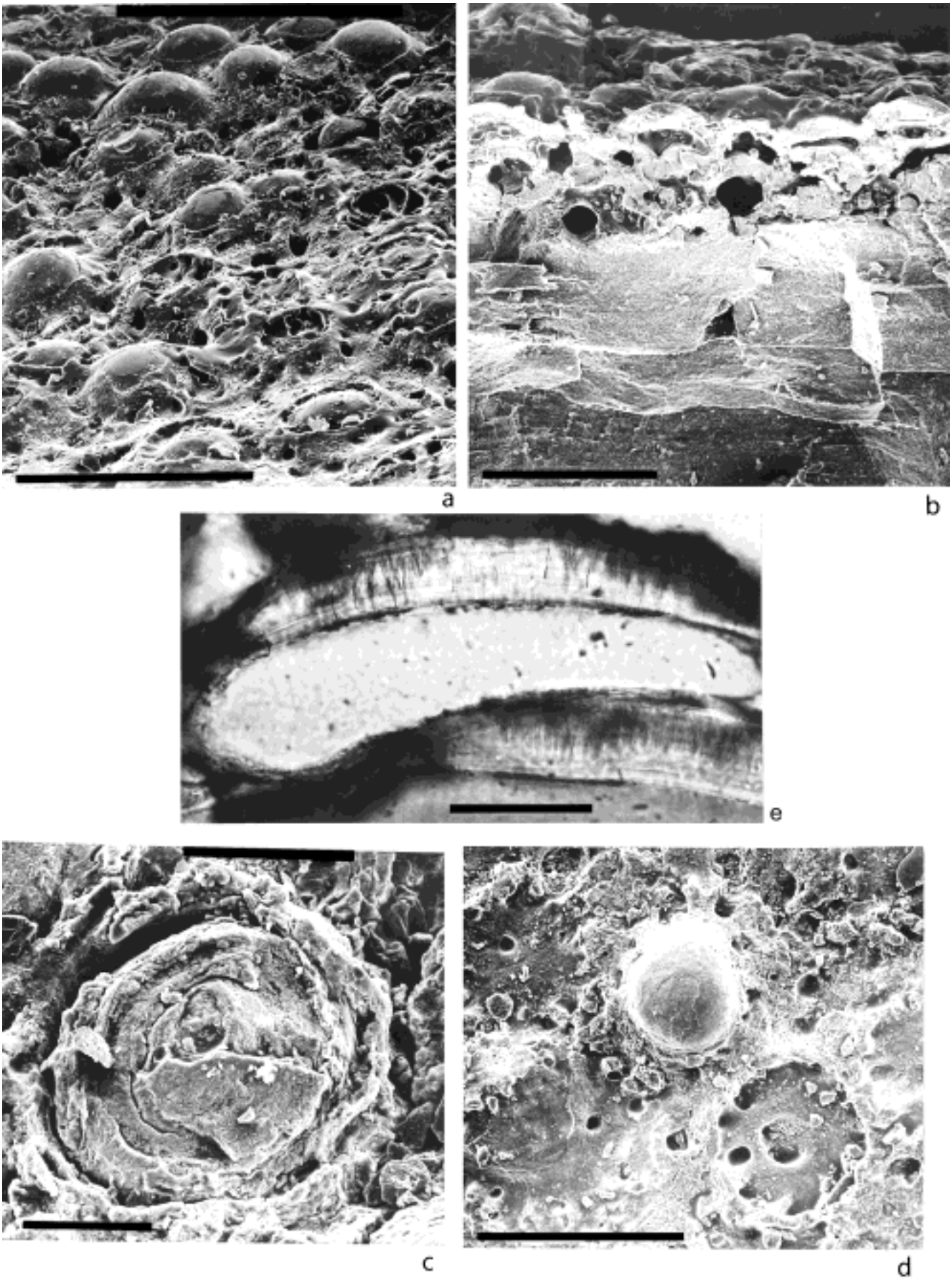

Figure 49 (a) A SEM oblique view of a surface showing tubercles at the top of the figure, parts in the middle with the tubercles removed, and in the front, the replacement tubercles with the new structures growing through the surrounds left around the old tubercles. ANU 49321. (b) A SEM of a broken face with mounds at the top lying on a much reduced lamina layer and then on a globular layer. The very thick deep layer makes up most of the thickness. ANU 49321. (c) A SEM of a surficial view of a broken tubercle showing growth lines. Note the concentric layering of the tubercle indicating that it was growing around a central core. Compare with (d). (d) A SEM showing a completed tubercle bounded to the bottom right by an open space from which a tubercle has been lost. (e) Two tubercles enlarged from the rectangle marked in Figure 50a. Both tubercles carry tubules and show one tubercle completely superimposed on another. Space between the tubercles filled with sediment. Scale bars: (a) 1·0 mm; (b) 500 μm; (c) 100 μm; (d) 500 μm; (e) 100 μm.

https://doi.org/10.1017/S0263593300001309 Published online by Cambridge University Press

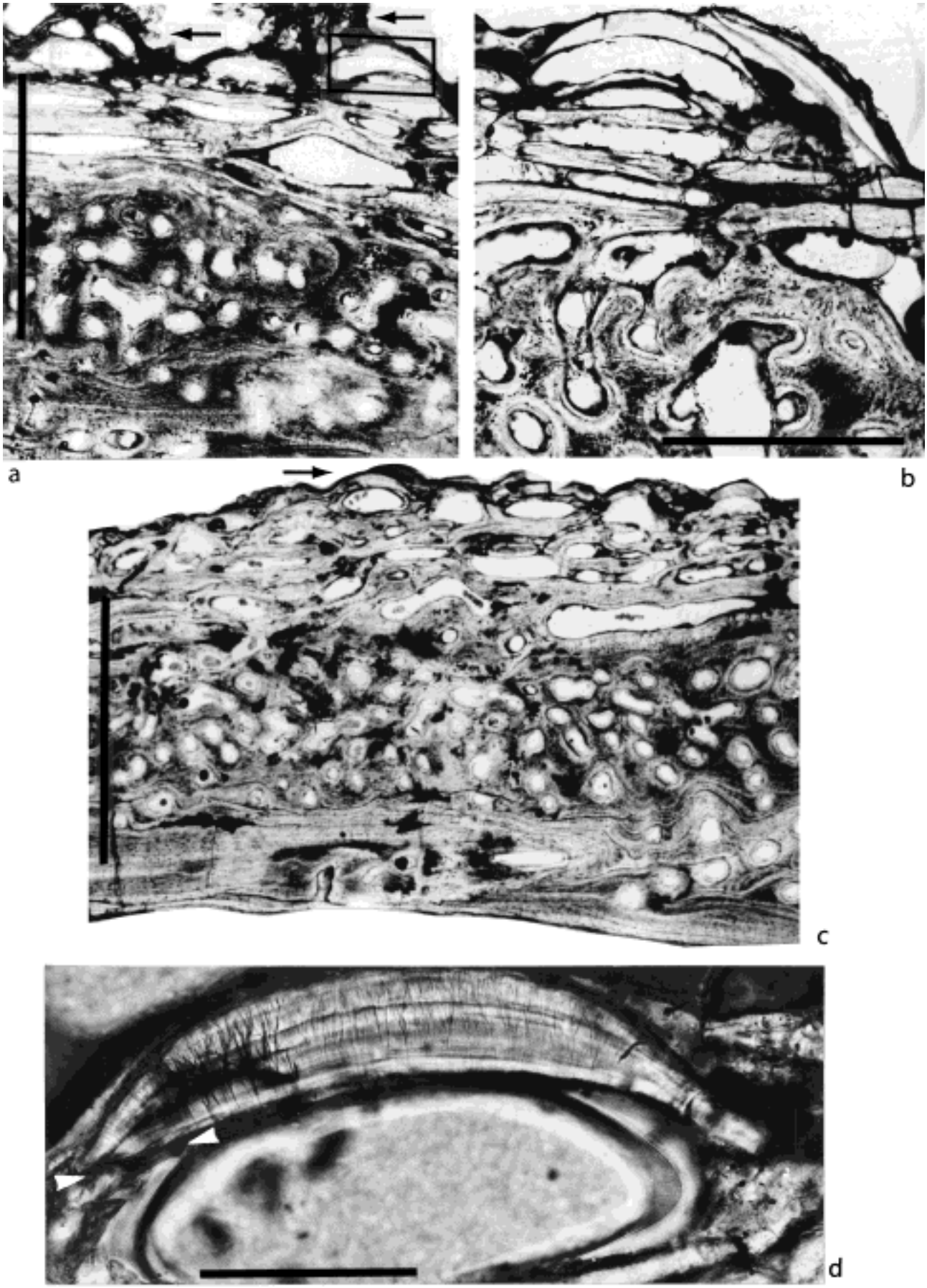

Figure 50 (a, b) Two views of thin sections through superficial tubercles. (a) From a section with bone of another individual, marked with arrows, superimposing its surface. (This specimen has been misplaced.) Two tubercles are superimposed, as is shown by the fine radial lines. (See also Fig. 49e.) (b) One tubercle lying on top of another. Both sections show the laminar layer of bone beneath the tubercles and the lower coarse meshwork of bone with osteocyte spaces. (c) A typical cross-section showing tubercles lying on laminated bone, a third layer of rounded vesicular bone and a basal layer of laminated bone. (d) An enlargement of the tubercle indicated by the arrow in (c). The left end has a fracture (arrowed) through the lower layers. The laminate structure of the tubercles with fine tubules filled with dark material is obvious. Note the arrangement of laminae, with those at the base being more widespread than those at the top. Area at base subsequently filled with inorganic deposit after tubercle has completed growth. ANU 49325. Scale bars: (a) 1 mm; (b) 400 μm; (c) 1 mm; (d) 100 μm.

https://doi.org/10.1017/S0263593300001309 Published online by Cambridge University Press

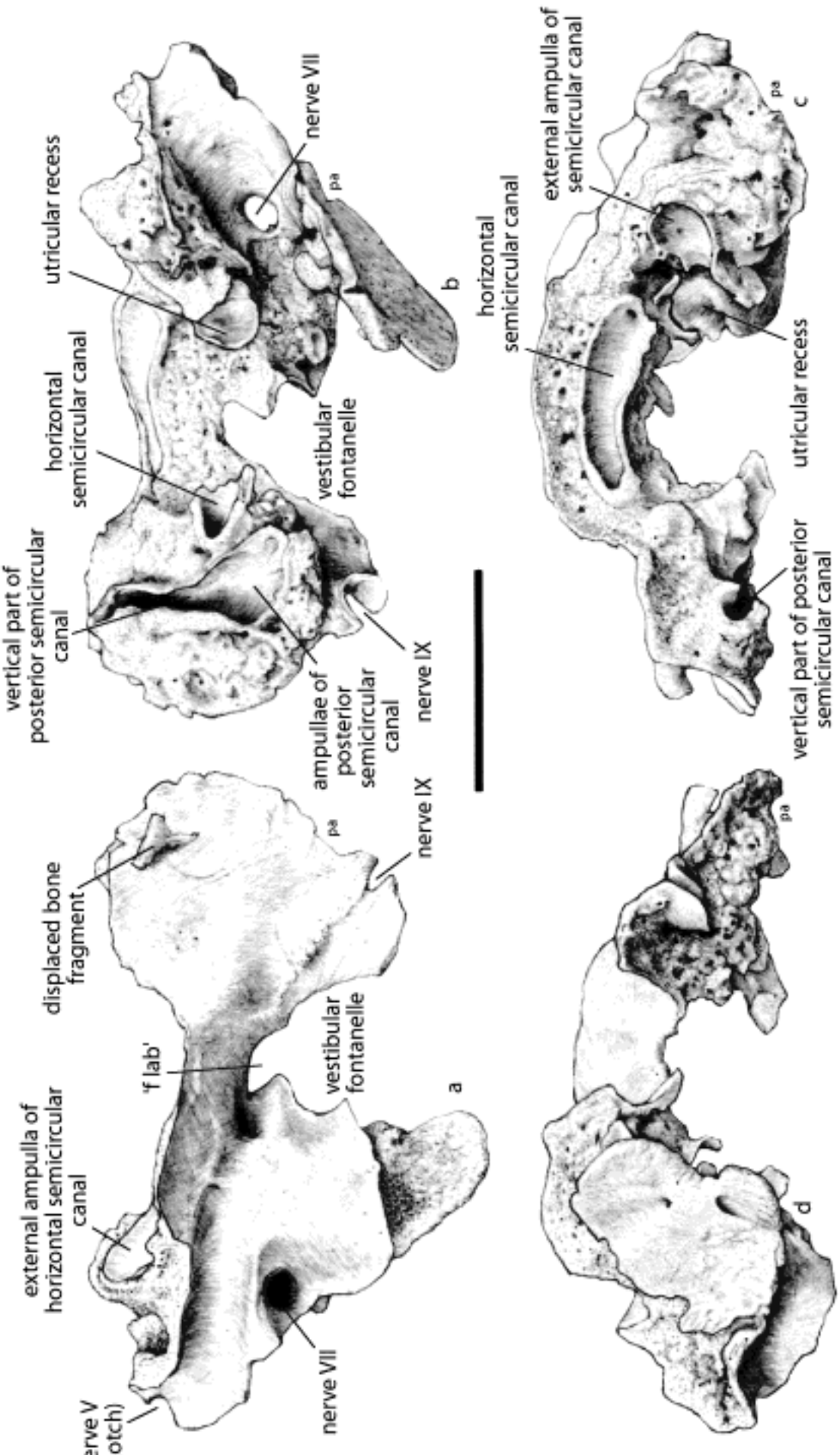

Figure 51 Four views of part of the left otic capsule: (a) lateral view; (b) mesial view; (c) dorsal view; and (d) ventral view. All drawn from a fragment of BMNH P64125.

https://doi.org/10.1017/S0263593300001309 Published online by Cambridge University Press

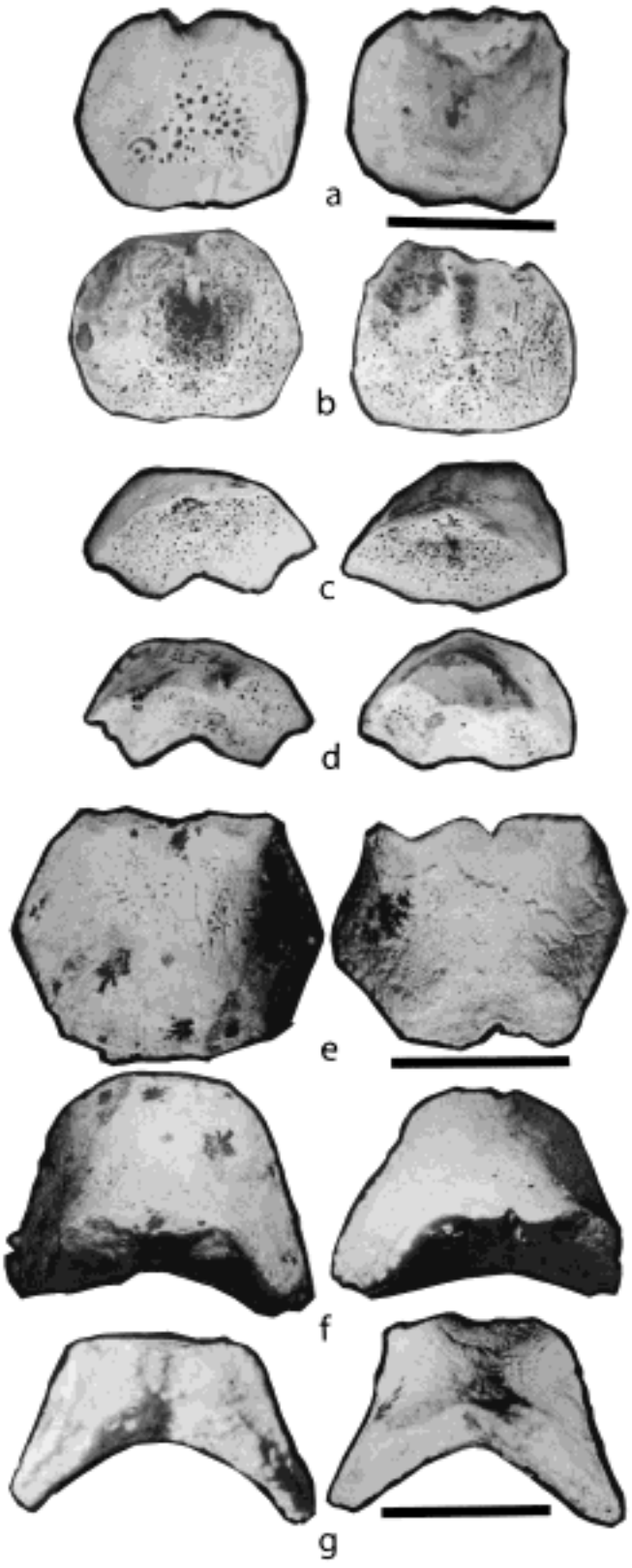

Figure 52 (a–d) Dorsal, ventral, anterior and posterior views of two specimens of anazygals. ANU 72976. (e–g) Two specimens of catazygals in ventral, anterior and posterior views. WAM 90.11.1. Scale bars = 10 mm.

https://doi.org/10.1017/S0263593300001309 Published online by Cambridge University Press

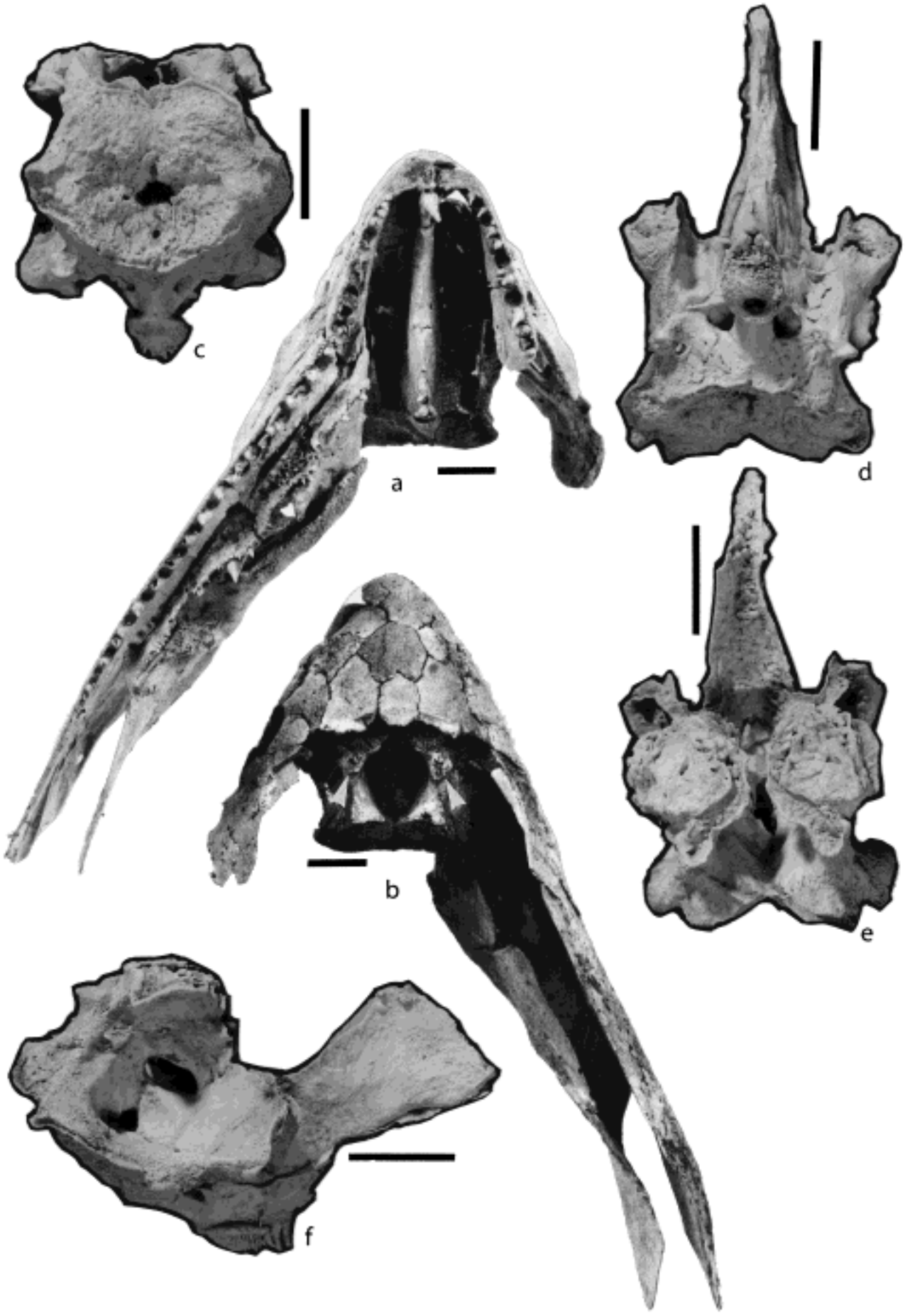

Figure 53 (a, b) Ventral and dorsal views of an incomplete skull, BMNH P63571, showing the ethmosphenoid roof and the right maxilla, the dermopalatine series, and the endopterygoid. The gap for the parasymphysial tusk whorls is clearly shown in (a). (b) This shows the posterior of the ethmosphenoid braincase and the cartilage surfaces (arrowed) which provided the dorsal processes posterior to the dorsal cushions, and they provide a loose attachment for the dermal bones of the roof. Photographs prepared by Dr Andrews, and are here given an electronic reproduction. (c–f) Posterior, ventral, dorsal and lateral views of the ethmosphenoid braincase, which has fallen free of the surrounding bones. WAM 90.11.1. Scale bars = 10 mm.

https://doi.org/10.1017/S0263593300001309 Published online by Cambridge University Press

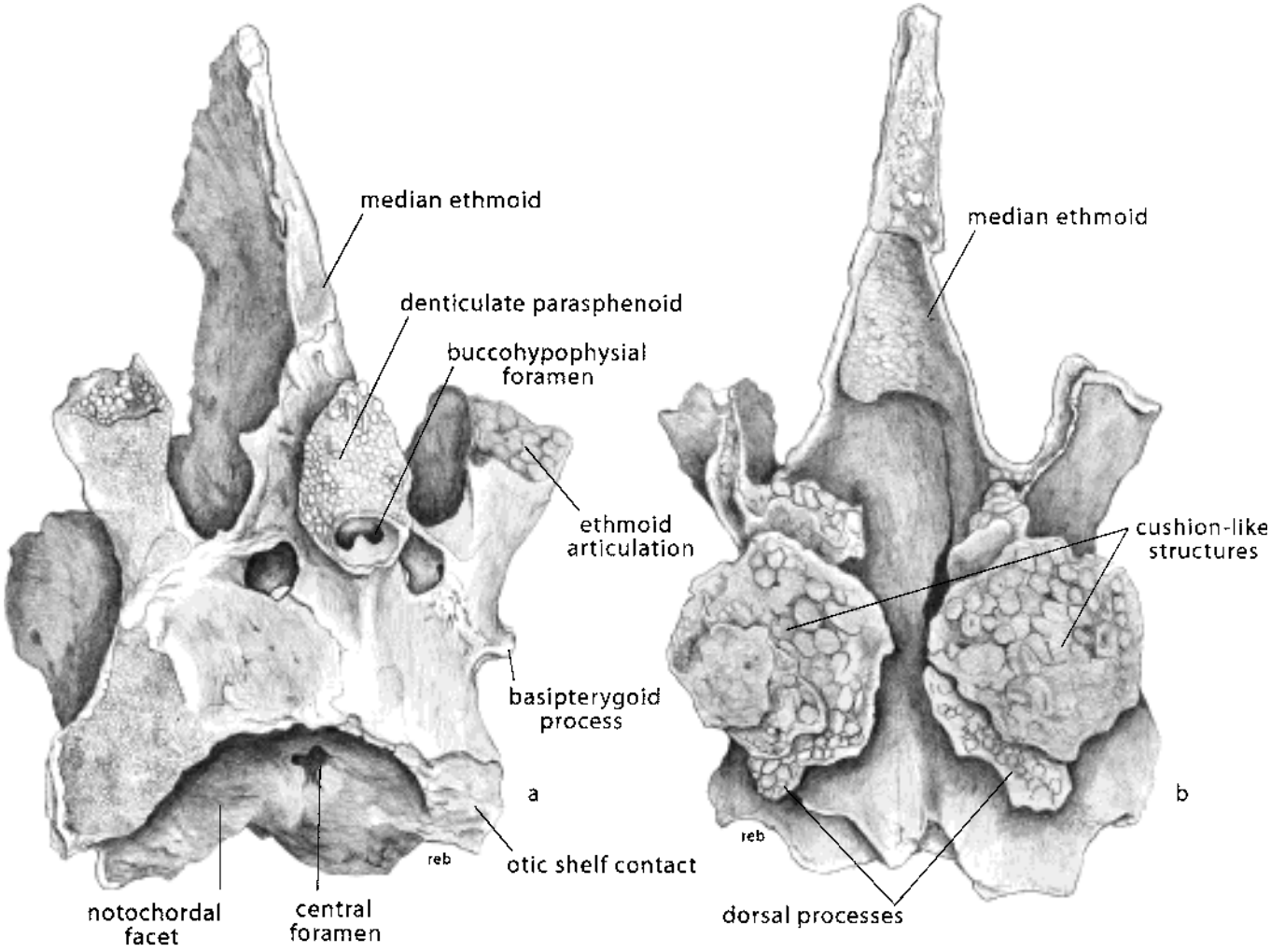

Figure 54 (a, b) Ventrolateral and dorsal view of the same specimen, WAM 90.11.1, naming the various elements. The ventrolateral view is given because it gives a better perspective to the detail given in Figure 53d.

https://doi.org/10.1017/S0263593300001309 Published online by Cambridge University Press

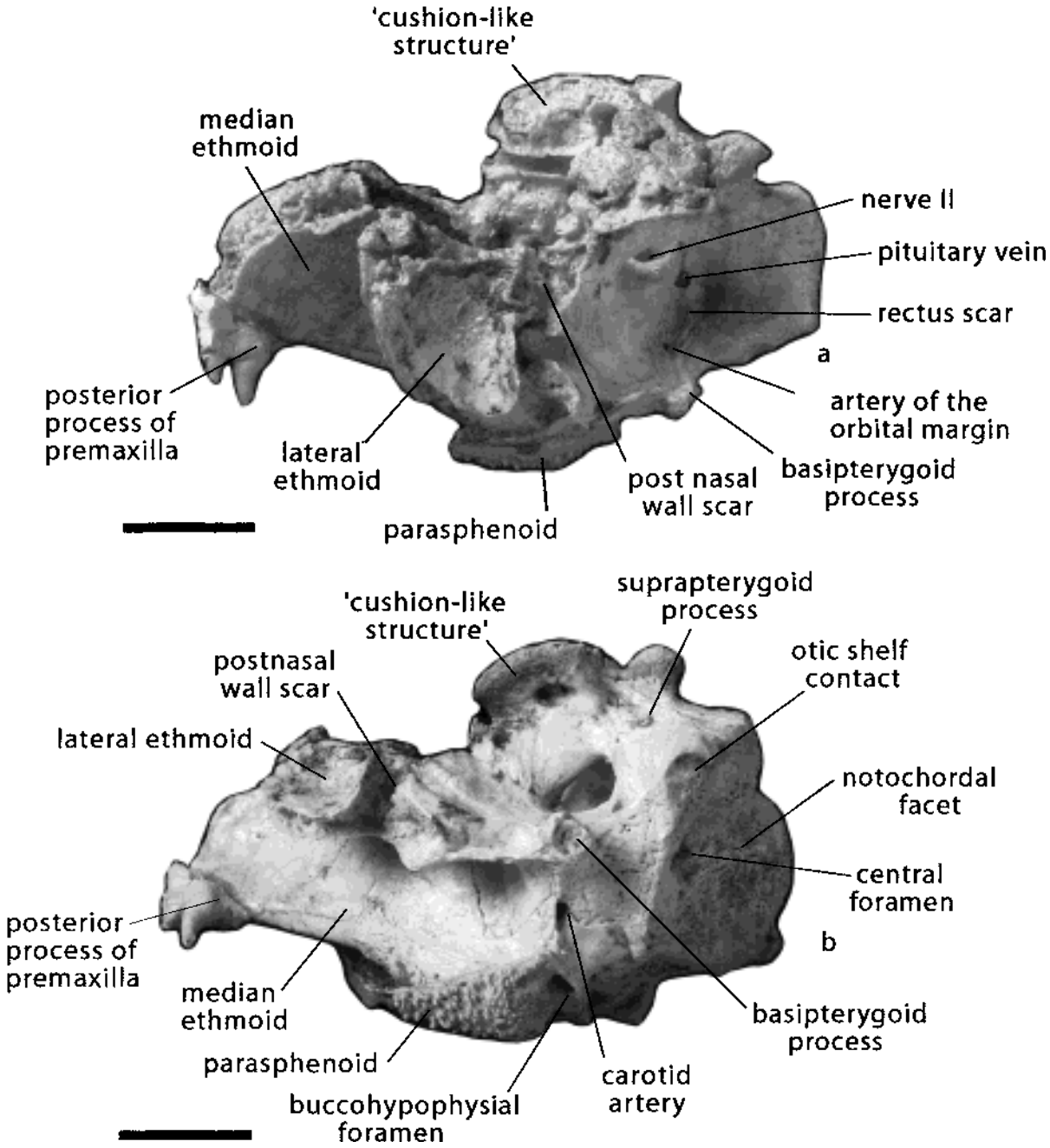

Figure 55 (a, b) Lateral and ventrolateral views of BMNH P64125. Structures of (a) also named in Figure 56a. Scale bars = 10 mm.

https://doi.org/10.1017/S0263593300001309 Published online by Cambridge University Press

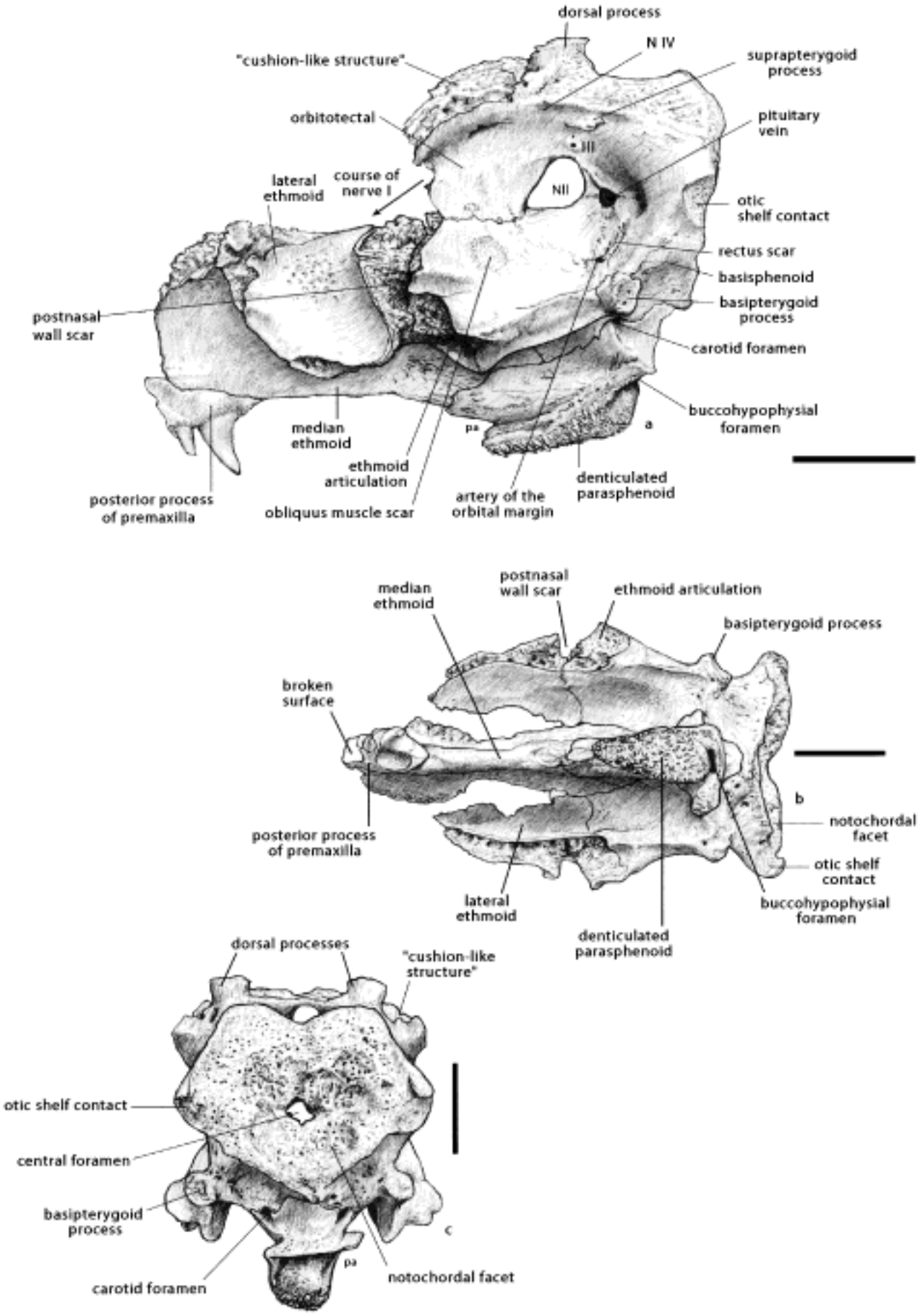

Figure 56 (a) Lateral view of an ethmosphenoid braincase at approximately the same angle as shown in Figure 55a. (b) Ventral view of the same specimen with details of the individual bones and scars shown. (c) A notochordal surface of the same ethmosphenoid braincase, which gives an illustration of the posterior of the parasphenoid. Scale bars = 10 mm.

https://doi.org/10.1017/S0263593300001309 Published online by Cambridge University Press

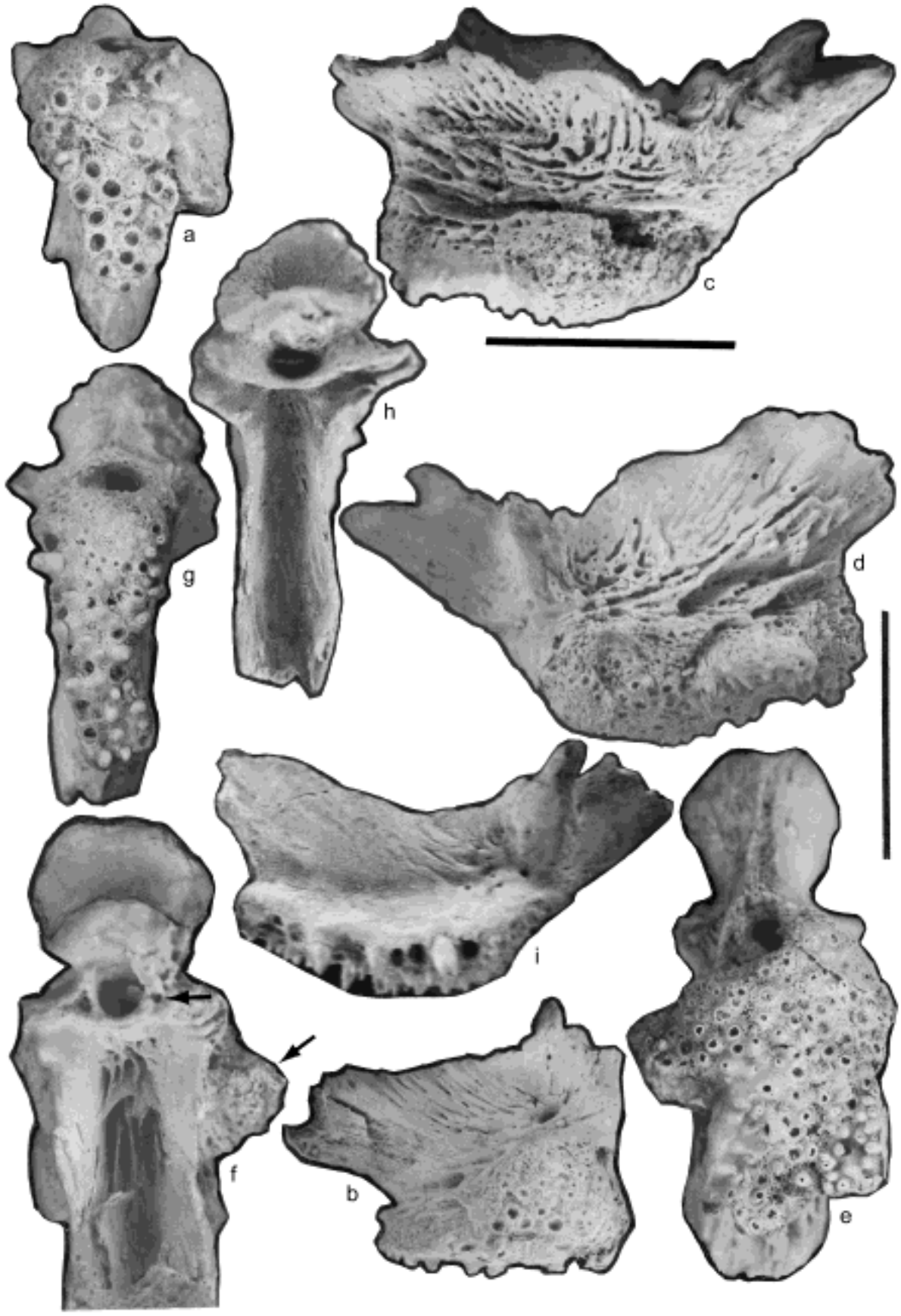

Figure 57 (a, b) Ventral and right lateral view of the denticulate area of the parasphenoid of ANU 72978. Note the large asymmetry of the denticulation on (b), and the small posterior process. (c–f) Left lateral, right lateral, ventral and dorsal views of the parasphenoid of ANU 72975. (c) This shows a gap between the denticulate surface and its support, but this is not present on (d). (e) Ventral view showing the gross asymmetry of the denticulate area. A small patch has been removed from the one side of the buccohyophysial stalk. Large posterior sutural surface shown on all images. (f) This shows the fine layers of bone in the dorsal cavity not seen on other specimens. Lateral process (arrowed) developed on one side but not the other. Carotid foramina (arrowed) well shown. (g–i) Ventral and dorsal views of an isolated denticulate parasphenoid. Asymmetry of the anterior end obvious. The posterior sutural area is much larger than that on (b) and more similar to (c). Lateral process strong on the left, but reduced on the right. (i) Shows no sutural boundary between the denticulate plate and its support, as shown on Figure 58. Scale bars=10 mm.

https://doi.org/10.1017/S0263593300001309 Published online by Cambridge University Press

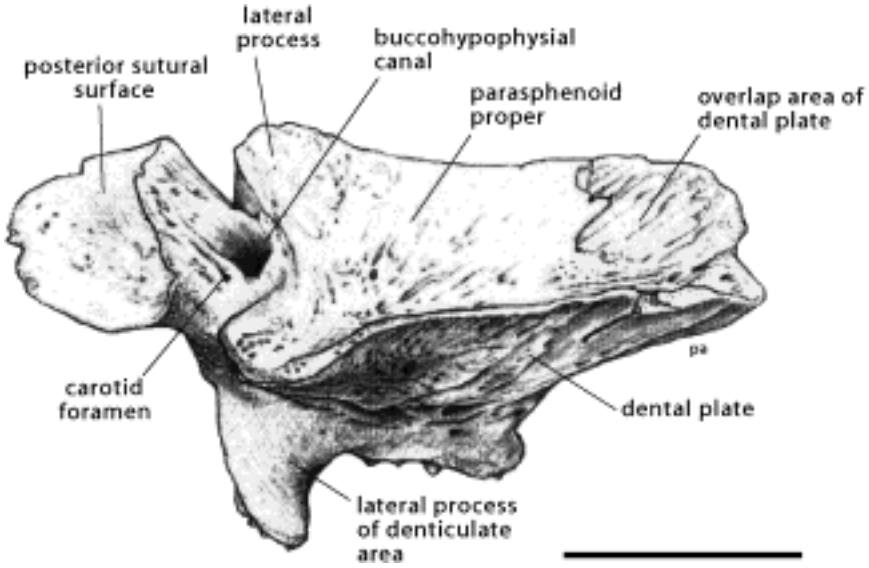

Figure 58 Dorsolateral view of the parasphenoid of BMNH P63571. This specimen shows the support plate for the denticulate plate curving around the front of he parasphenoid proper to join the anterior sutural surface. Scale bar = 10 mm.

https://doi.org/10.1017/S0263593300001309 Published online by Cambridge University Press

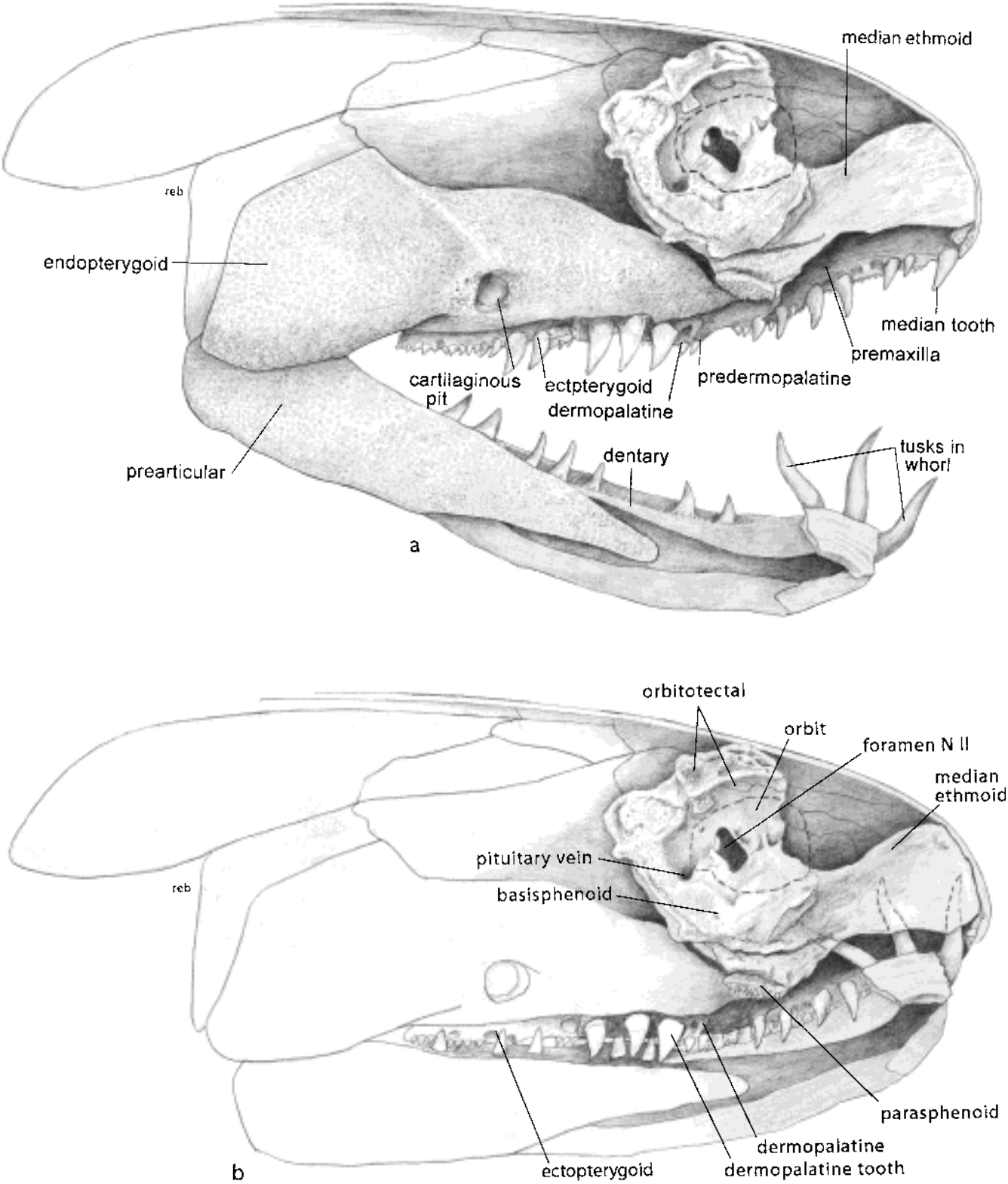

Figure 59 (a) Reconstruction of the skull structure showing the position of the ethmosphenoid braincase in relation to the endopterygoid and the other palatine plates and (b) with the mouth closed showing the details of how the teeth, tusks, orbit and nerves fit together.

https://doi.org/10.1017/S0263593300001309 Published online by Cambridge University Press

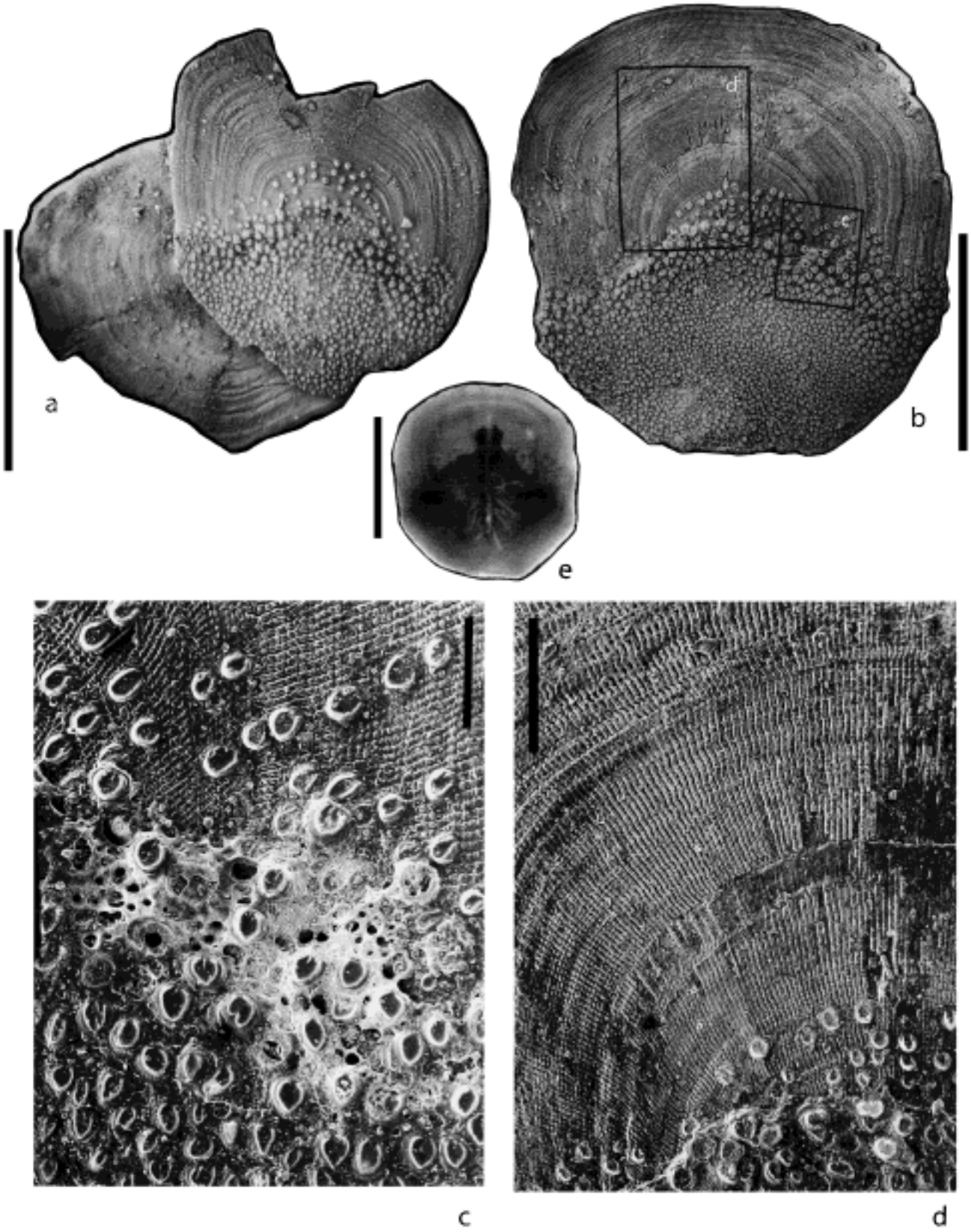

Figure 60 (a) Two scales from a small specimen, the one on the left viewed internally. Photograph printed in reverse. ANU 49106. (b) Large scale. ANU 49320. (c, d) Enlargement of the same scale from the areas outlined on (b). Note the open tubercles roughly arranged along radial lines, and in (c), note the open-worked bone on the surface between the tubercles. Open tubercles are present only on the margins of the tuberculate areas. (a–d) SEM illustrations. (e) An X-ray of a lateral line scale showing the position of the canal through the scale and the branches of the canal under the exposed part of the scale. Scale bars: (a, b) 10 mm; (c) 1 mm; (d) 2 mm; (e) 10 mm.

https://doi.org/10.1017/S0263593300001309 Published online by Cambridge University Press

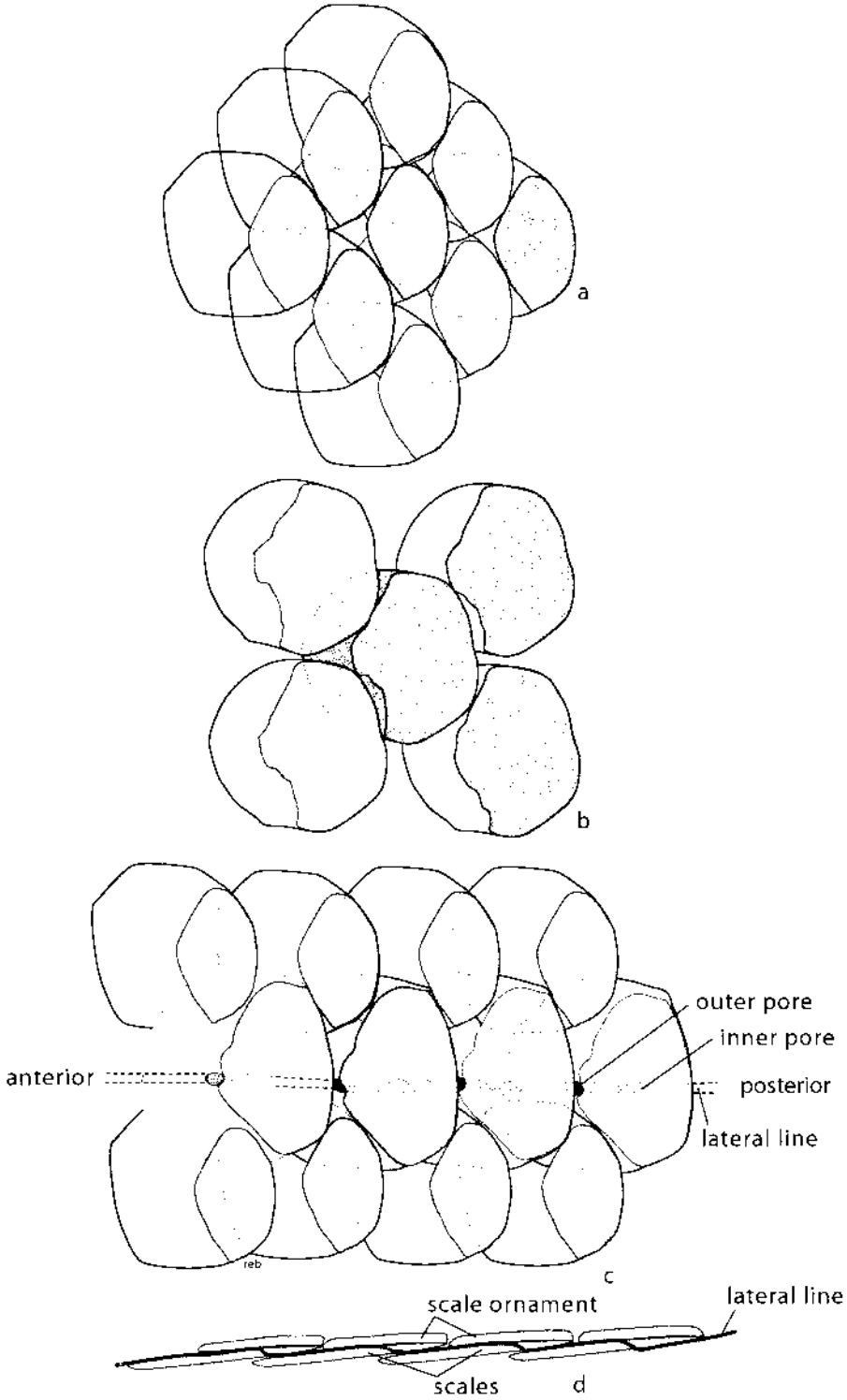

Figure 61 (a–c) Three scale patches showing the degree of overlap. The dark scale is a key unit. The lightly stippled area is the exposed part of the scale. (c) This shows the position of the lateral line through the main length of the body. Note that it enters the scale at an outer pore near the anterior end of the ornamented portion, and it exits the scale at an inner pore near the anterior end of the underlying scale. (d) This is a longitudinal section of four scales. The stippled area is the exposed part of the scale.

https://doi.org/10.1017/S0263593300001309 Published online by Cambridge University Press

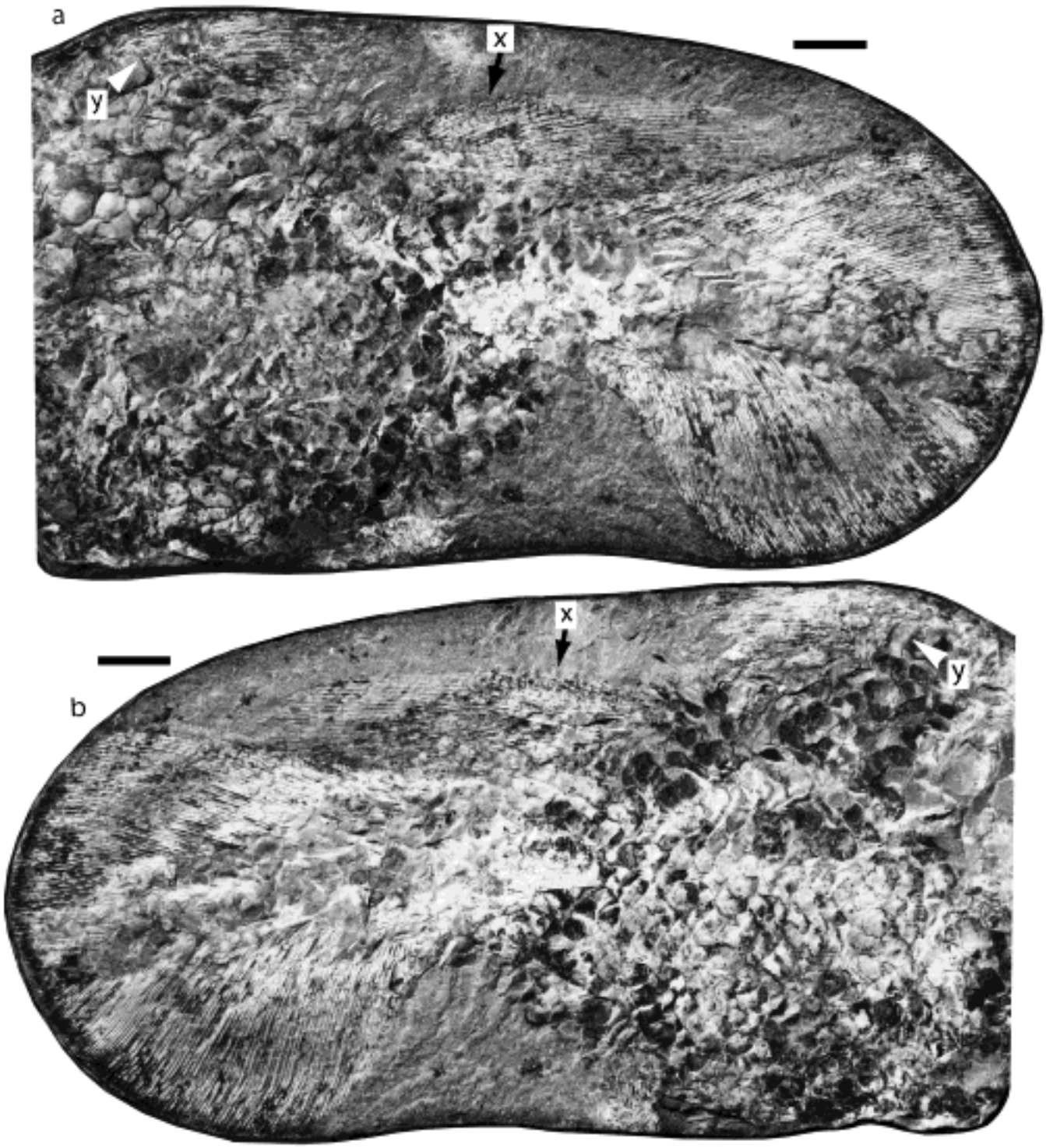

Figure 62 Part and counterpart of the posterior part of the body showing the caudal fin, the well-preserved second dorsal fin (labelled X) and a fragment of the first dorsal fin (labelled Y). The ventral surface has a fragment of the anal fin. The orientation of this specimen is difficult because the caudal fin, as we have interpreted it, bends ventrally. Presumably this is the result of distortion. The matter would be solved if the lateral line canal could be seen, but we have not been able to do this. In the text, the illustrated orientation has been used to identify the fins. Photograph by Dr Andrews of an unwhitened specimen. BMNH P63569. Scale bars=10 mm.

https://doi.org/10.1017/S0263593300001309 Published online by Cambridge University Press

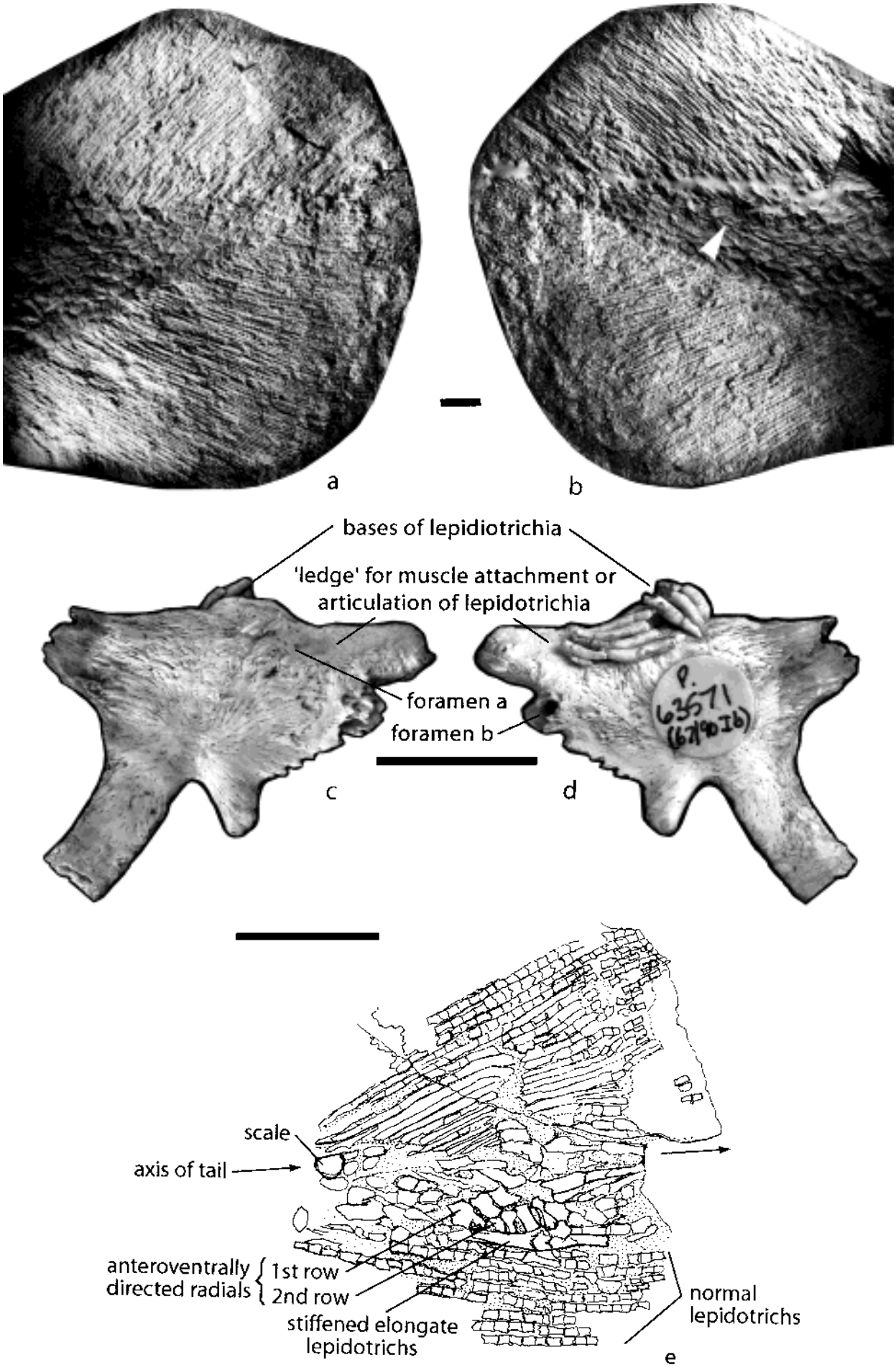

Figure 63 (a, b) Part and counterpart of a caudal fin showing the distribution of the scales, the indistinctness of the scales at the posterior end, the position of the lateral line canal (arrowed) and the division of the distal lepidotrichs. WAM 01.11.4. (c, d) Two views of the support plate of a first dorsal fin. No radials are present and the lepidotrichs were attached directly to a ridge near the dorsal surface. BMNH P63571. (e) Fragment of the caudal region of WAM 01.11.04 with the internal skeleton preserved. At least five series of inclined radials in two rows (labelled) stiffen the tail and join elongate lepidotrichia. Scale bars = 10 mm.

https://doi.org/10.1017/S0263593300001309 Published online by Cambridge University Press

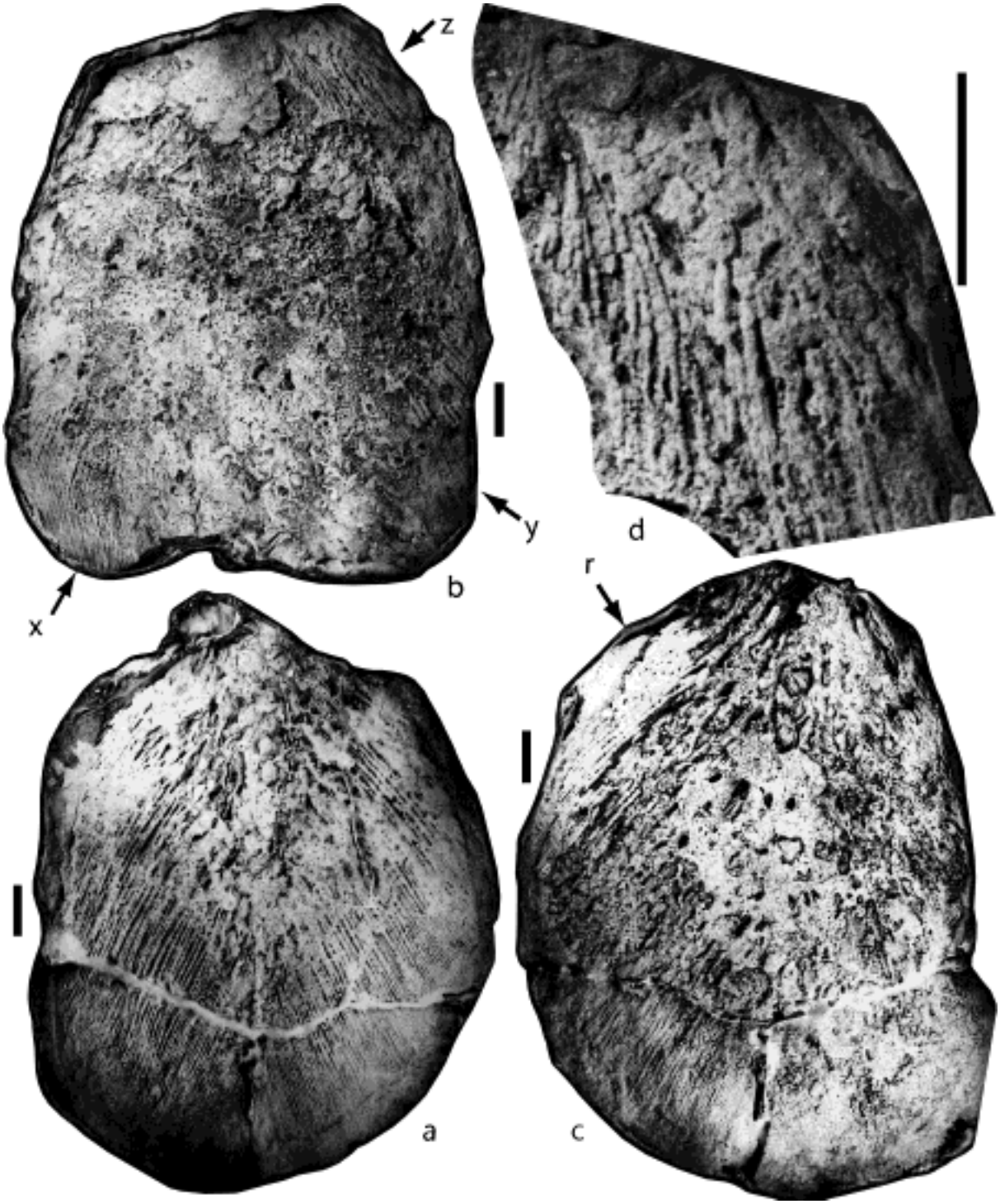

Figure 64 The head of this specimen was located in a dissociated fragment and it cannot be used to orient the specimen. The difference between the sizes of the dorsal and ventral caudal lepidotrichs and the difference in the sizes of the lepidotrichs between the second dorsal and the anal fins have been used to orient the specimen. (a) The caudal fin of WAM 86.9.694. (b) The segment anterior to (a) from the same specimen. The ventral side to the left. The anal fin is partly preserved on the left side (labelled 'X'), and the second dorsal fin (labelled 'Y') and the first dorsal fin (labelled 'Z') are partly preserved on the right side. Fragments of scales are preserved scattered over the surface. (c) Counterpart of (a). Note the radials supporting the dorsal end of the caudal fin (labelled 'r'). (d) The first dorsal fin, labelled 'Z' in (b), enlarged to show the grouped lepidotrichia as they pass under the scales, and their splitting more distally. Scale bars = 10 mm.

https://doi.org/10.1017/S0263593300001309 Published online by Cambridge University Press

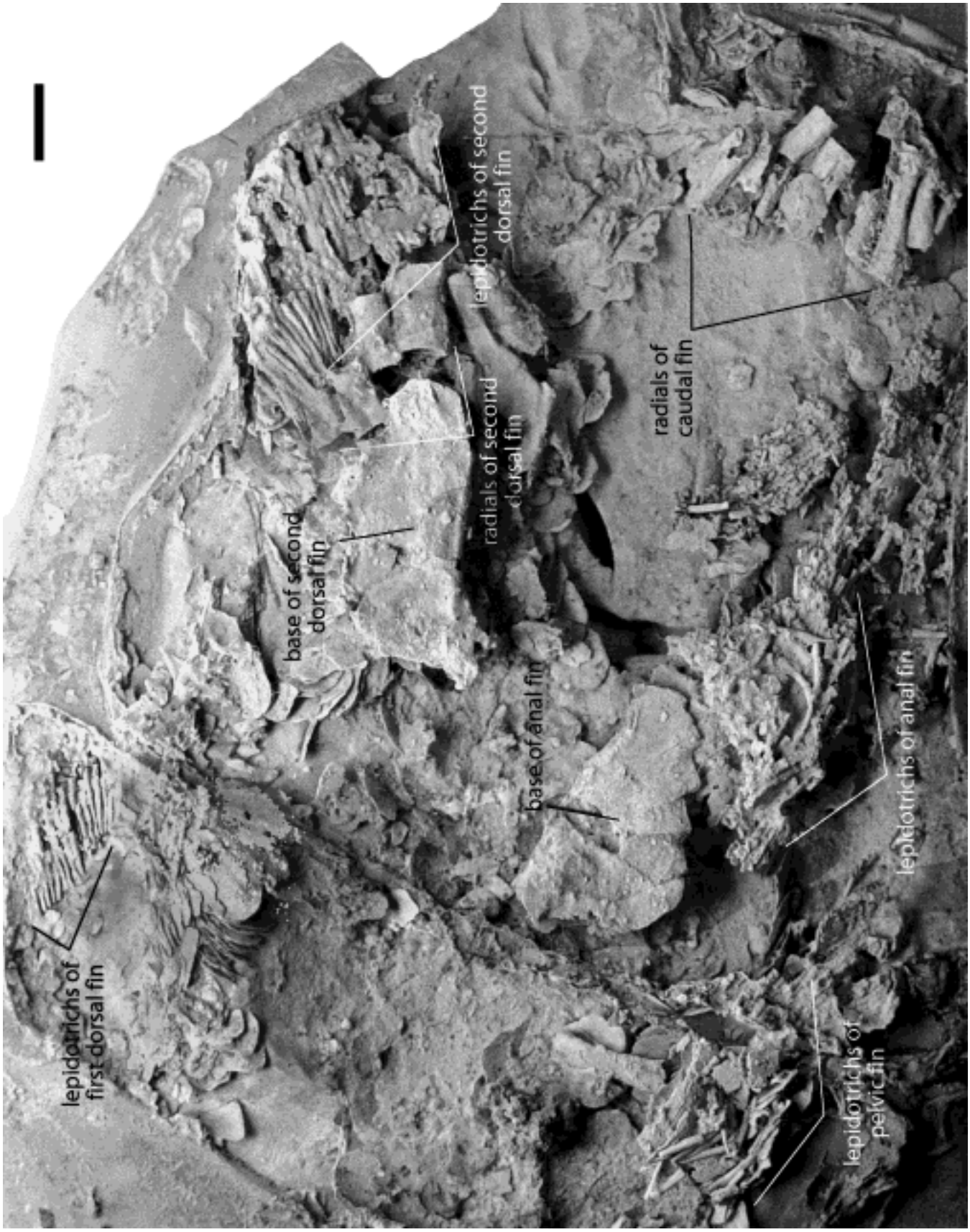

Figure 65A The posterior part of a body which gives the orientation of the fins. Part of the anterior part of the caudal fin is preserved, but the posterior part is missing. Some of the neural arches were preserved ventral to the second dorsal fin. The well-preserved elements have been removed and illustrated elsewhere, but they are also shown on Figure 65Ba. ANU 49504. Scale bar=10 mm.

https://doi.org/10.1017/S0263593300001309 Published online by Cambridge University Press

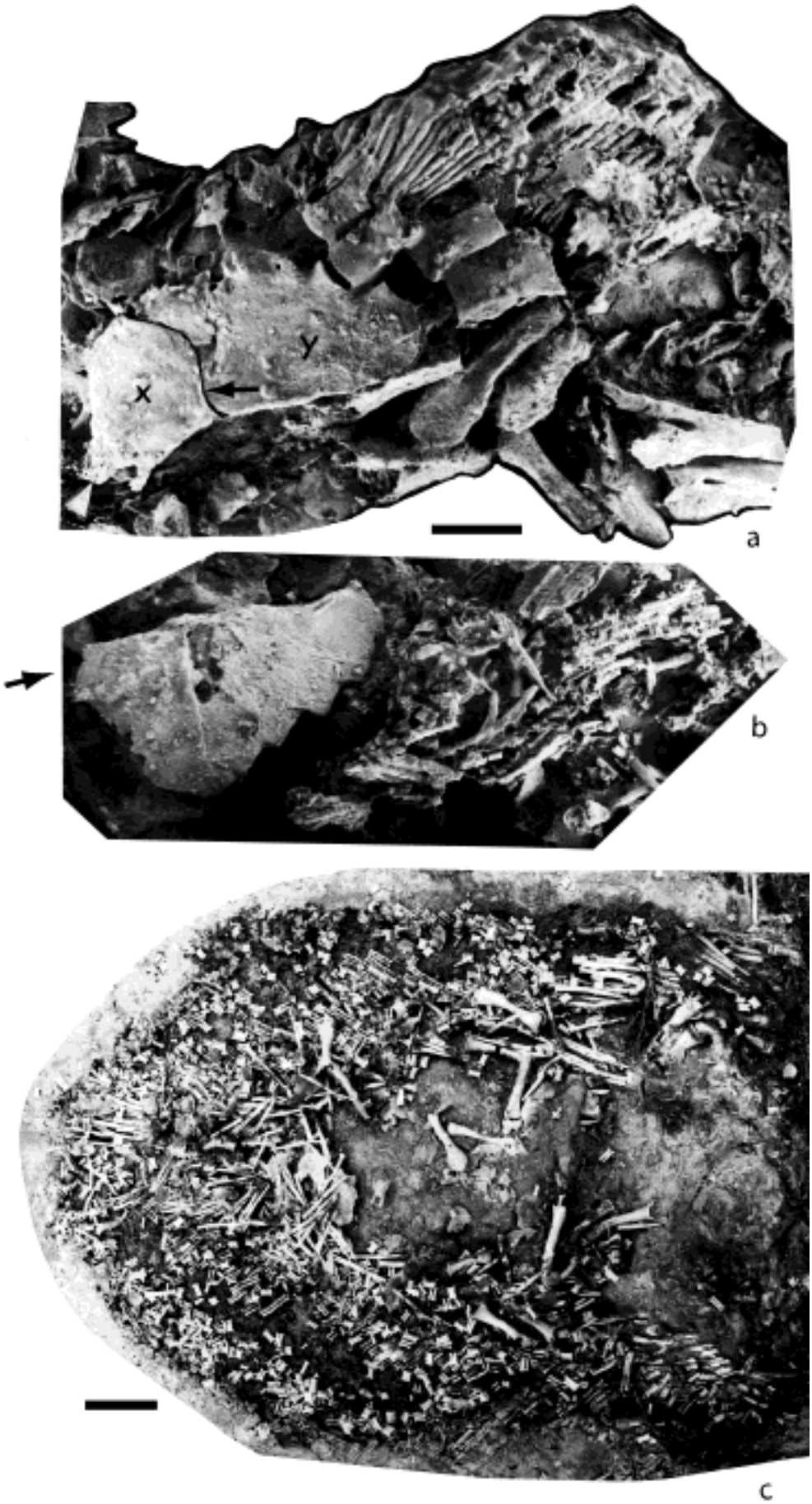

Figure 65B (a) Lateral views of the second dorsal fin with the large basal structure. ANU 49504. The division between the two units making up the support is shown by an inked line. Broken attachment surface with a white arrow. Four radials, some of the proximal lepidotrichia at the top, and some secondary lepidotrichia medially are shown. Several broken neural arches are present posteroventrally on the photograph. One of these is illustrated on Figure 71a, b. (b) Anal fin support, with the attachment to the left (arrowed), and five spaces for the radials, none of which is preserved. Some primary and some secondary lepidotrichia in the tangled material to the right. The more distal lepidotrichs are shown on Figure 65A. (c) An isolated caudal fin, showing no evidence of an axial structure, isolated scattered radials usually expanded at one end, single primary lepidotrichia, and many secondary and tertiary lepidotrichia. ANU 49505. Scale bars = 10 mm.

https://doi.org/10.1017/S0263593300001309 Published online by Cambridge University Press

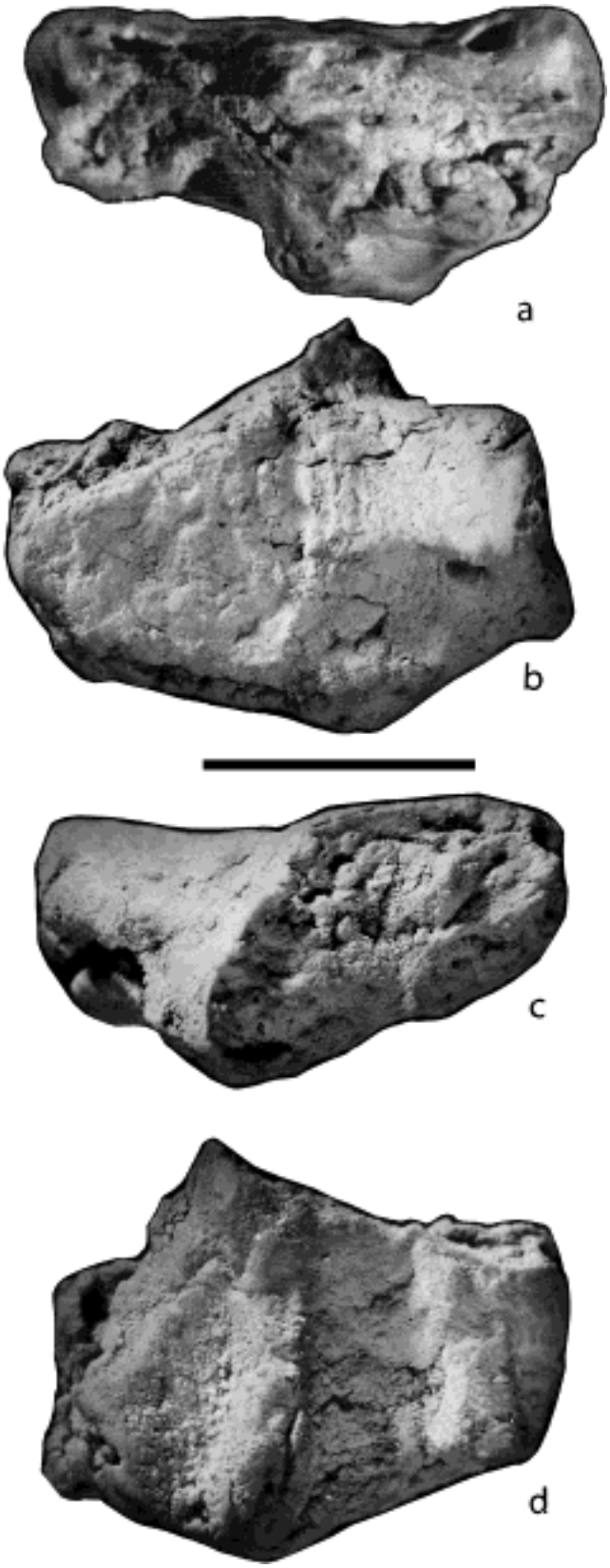

Figure 66 (a) Distal surface of the humerus WAM 92.2.8 showing the attachment for the ulna and radius. (b) Dorsal view showing the ectepicondylar foramen. (c) Proximal view showing the attachment to the scapulocoracoid. (d) Ventral view with the strong longitudinal ridges. Scale bar = 10 mm.

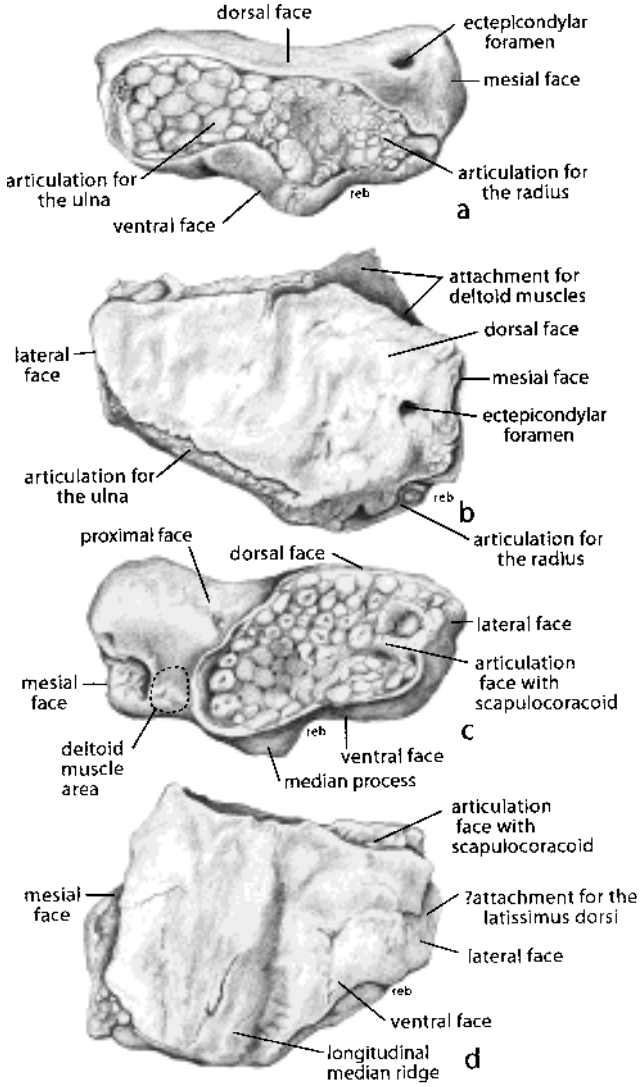

Figure 67 Reconstructions of the humerus of WAM 92.2.8, following from the previous figure. (a) Distal view showing the two articulation surfaces for the radius and the ulna. (b) Dorsal view with the radius and ulna attachments at the base of the figure. (c) Proximal view with articulation with the scapulocoracoid. (d) Ventral face with the longitudinal ridges well developed.

https://doi.org/10.1017/S0263593300001309 Published online by Cambridge University Press

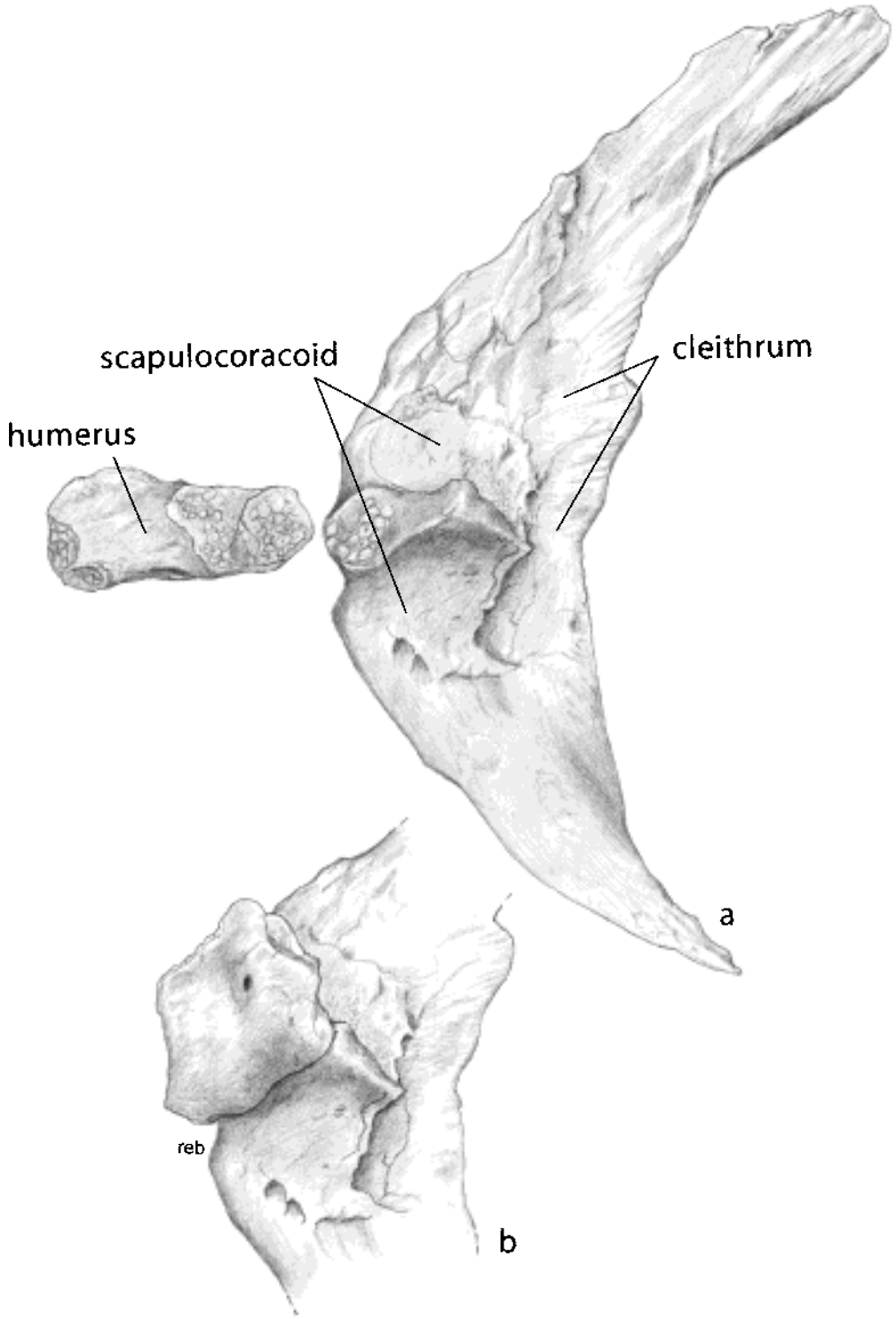

Figure 68 (a) Cleithrum, scapulocoracoid and humerus showing their relative positions. Note the double attachment to the distal end of the humerus. What appear to be two foramina at the ventral end of the scapulocoracoid are wear surfaces. (b) The humerus restored to life position. WAM 92.2.8.

https://doi.org/10.1017/S0263593300001309 Published online by Cambridge University Press

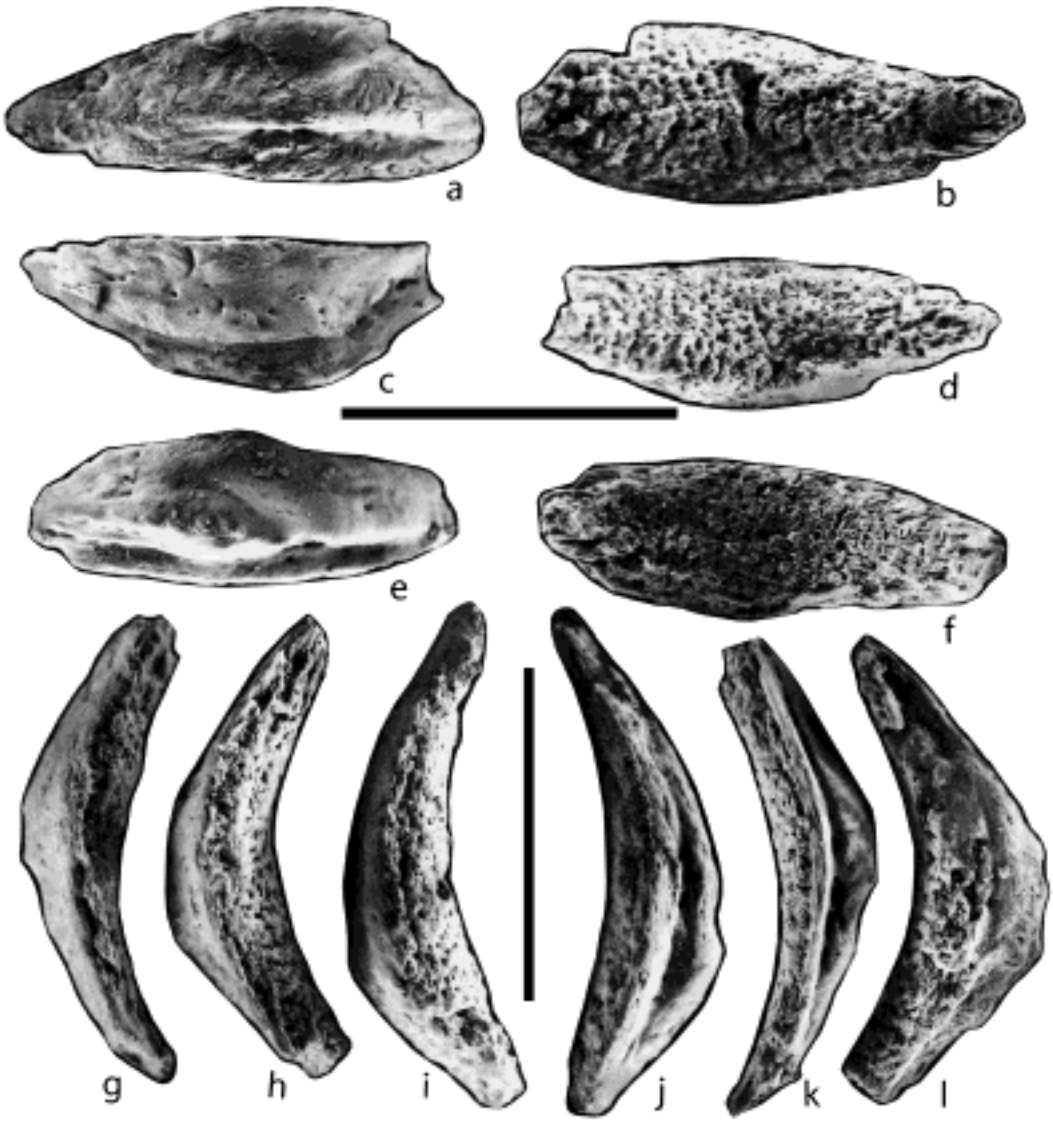

Figure 69 Intercentra. (a–f) Intercentra in external (smooth) and internal (globular) positions. Anterior to the bottom of the figure. Note the flange along the anterior edge in (a, c, e). (g–i) Posterior view of the same specimens showing the external surface covering a thick layer of globular bone. (j–l) Anterior view of same showing the sharp edge bounding a smooth surface and the globular internal bone. ANU 72975. Scale bars = 10 mm.

https://doi.org/10.1017/S0263593300001309 Published online by Cambridge University Press

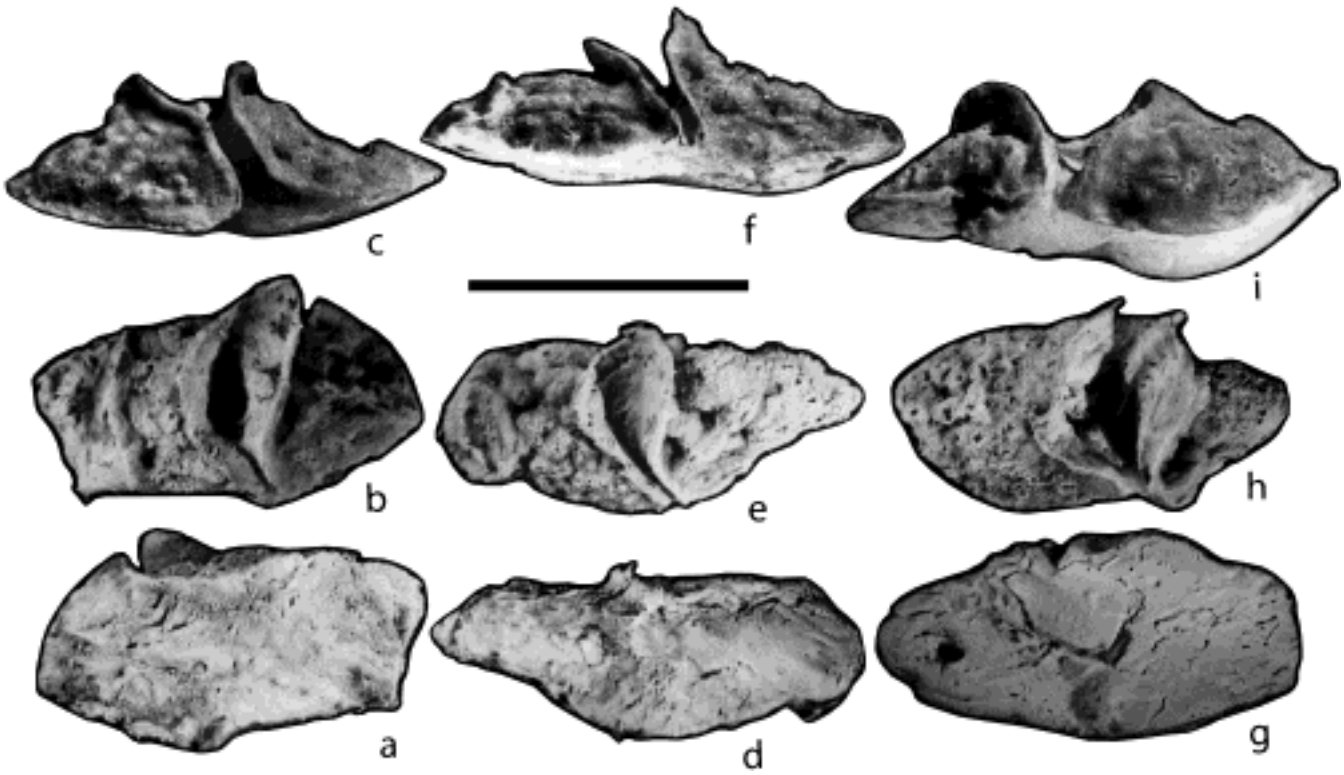

Figure 70 (a–c) External, medial, posterior views of a pleurocentrum. (d–i) Similar views of two pleurocentra. WAM 92.8.2. Scale bar = 10 mm.

https://doi.org/10.1017/S0263593300001309 Published online by Cambridge University Press

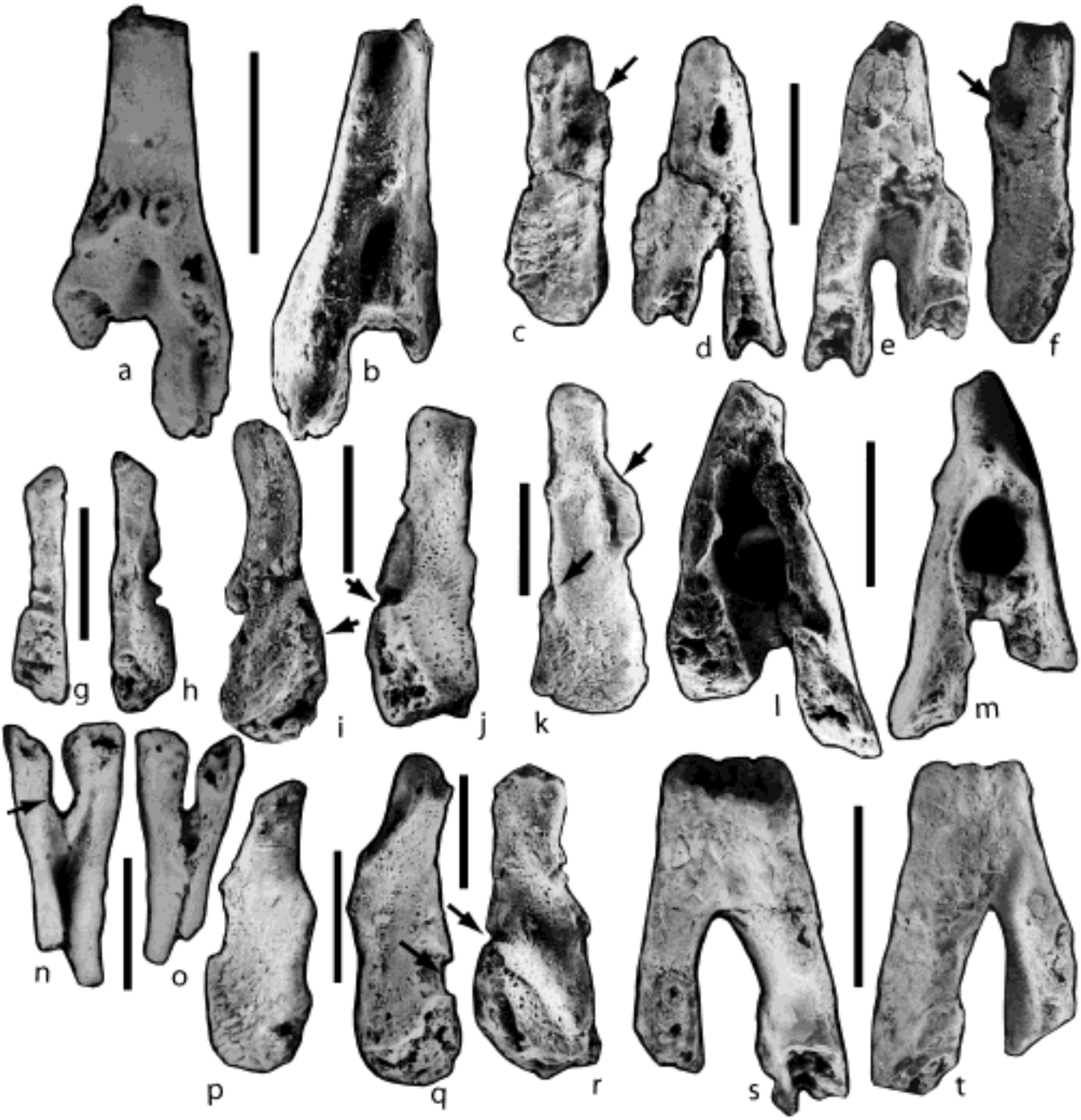

Figure 71 Neural and haemal arches. (a, b) Posterior and anterior of a neural arch from ventral to the second dorsal fin on ANU 49504. See Figure 72a. (c–f) Left lateral, anterior, posterior and right lateral views from an element near the second dorsal fin attachment. The scar on the anterior is not a foramen, but was probably an attachment scar. ANU 49504. (c, f) These show where the foramina leave the structure (arrowed), an unusual occurrence. (See Fig. 72b.) (g, h) Small specimen where the arches are not joined, in posteromedial and lateral views. The double opening is unusual. ANU 49211. (i, j) Internal faces of two sides of an arch separated. Note the asymmetry. Arrows indicate the ventral nerve root. ANU 49211. (k–m) Arch in right lateral, posterior and anterior views; nerve canal and the notochord separated by a bony layer; dorsal foramen shown in (m), but its internal opening covered in shadow in (l); lateral opening in (k) also unusual, and ventral nerve root clear (both arrowed); fine lineations low on (k) common on other specimens. ANU 49211. (See Fig. 73a, b.) (n, o) Haemal arch in anterior and posterior views. ANU 49504. (p) External view of an isolated arch, part of the dorsal edge removed by weathering. Fine ornament on the ventral surface a characteristic feature of all arches. ANU 49211. (q, r) Two arches from a single unit, both viewed internally; part of the top left of (q) destroyed during preservation; (q) has arrowed the gap for the ventral nerve root. (r) There is a deep groove across the surface for the nerve canal; a much weaker canal occurs on (q). ANU 49211. (s, t) Arch from the position of the second dorsal fin. ANU 40504. (s) Posterior and (t) anterior with a large protrusion on the right. This is well shown in Figure 72c. Scale bars = 10 mm.

https://doi.org/10.1017/S0263593300001309 Published online by Cambridge University Press

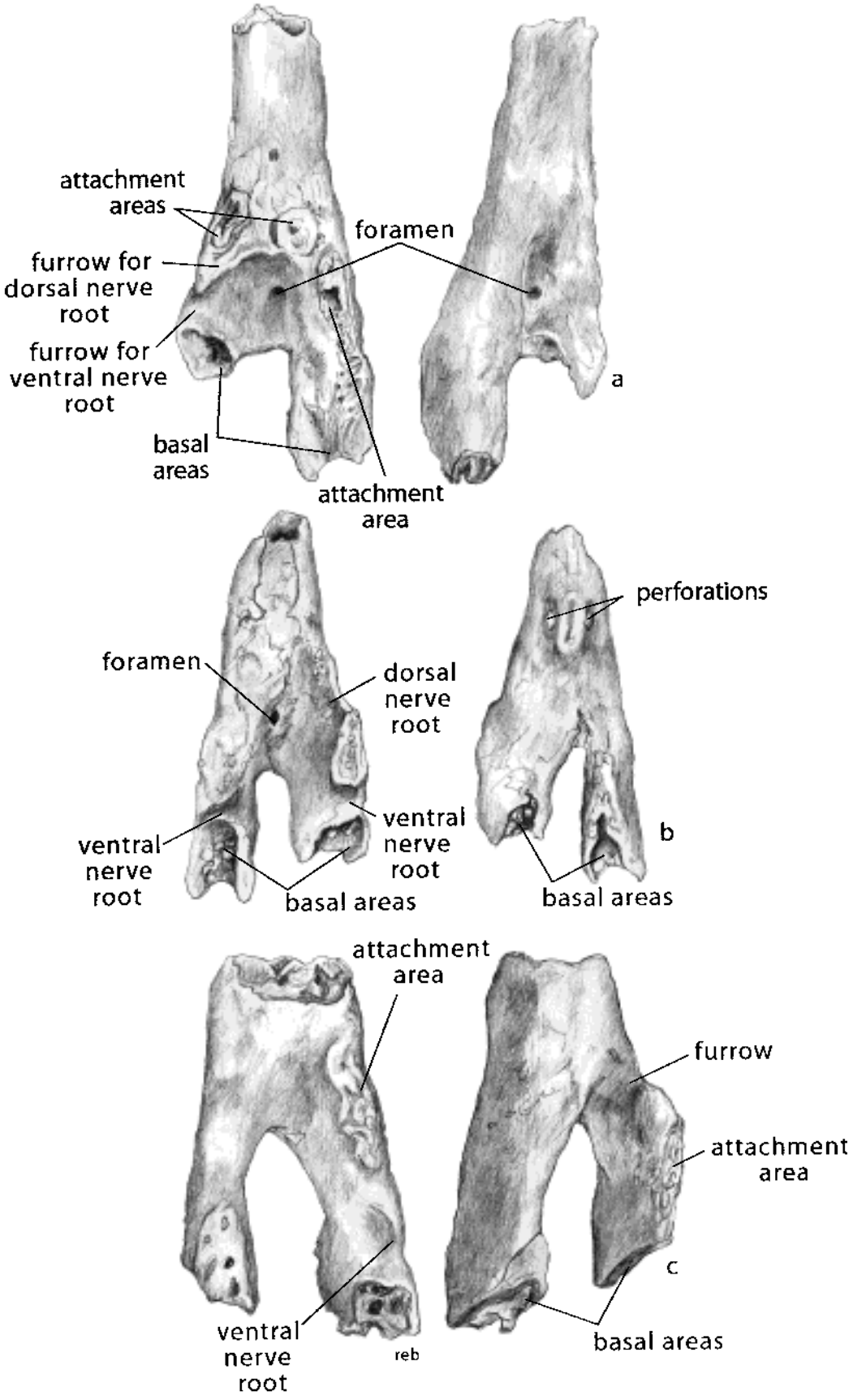

Figure 72 Drawings of the specimens shown in Figures 71a, b, d, e, s, t.

https://doi.org/10.1017/S0263593300001309 Published online by Cambridge University Press

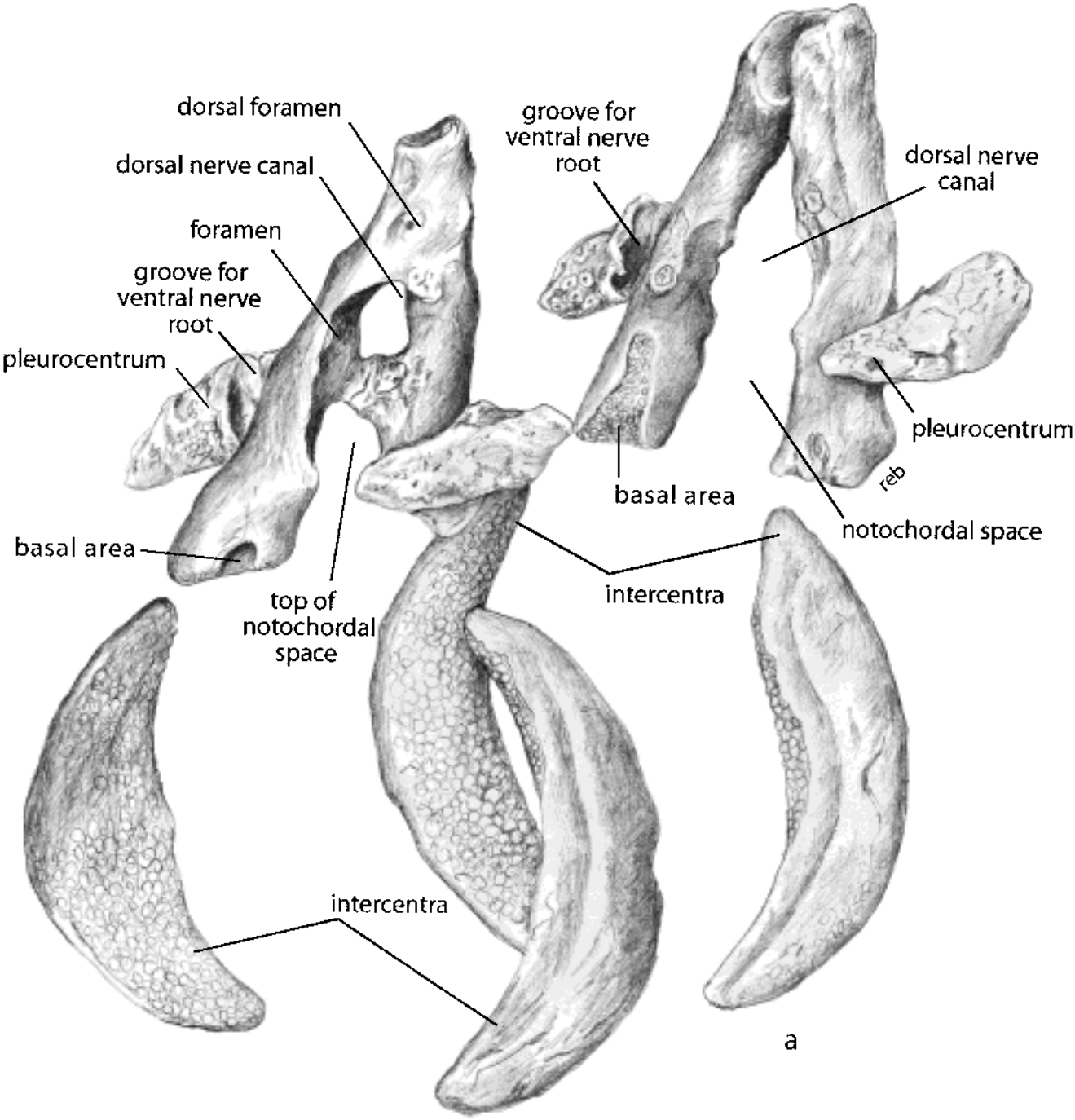

Figure 73A (a) Rearrangements of neural arches, intercentra and pleurocentra in anterior positions, drawn as exploded views to show the main features of the arches. One neural arch has the apex fused together, as shown in Figure 71k–m, and the other is of the two arches separate dorsally. The attachment of the arches to the cartilage around the notochord are labelled as 'basal areas'. The pleurocentra are shown in external views on the right side and as internal views on the left side of the interpretation.

https://doi.org/10.1017/S0263593300001309 Published online by Cambridge University Press

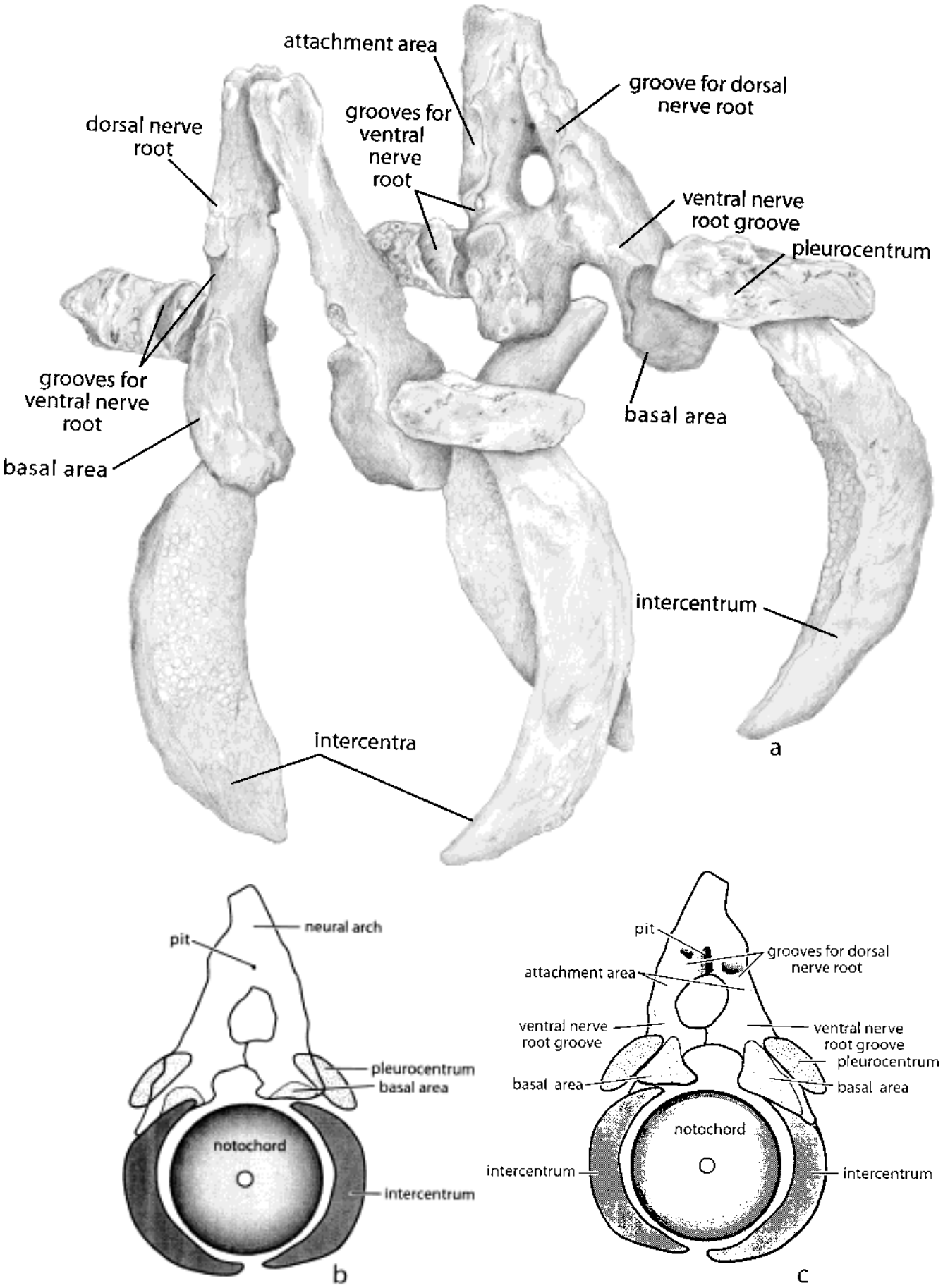

Figure 73B (a) Posterior views of the specimens shown in Figure 73A. Symbols the same as used in that figure. (b, c) Reconstructed anterior and posterior views of the individual with the bone beneath the dorsal nerve canal, and with the elements labelled.

https://doi.org/10.1017/S0263593300001309 Published online by Cambridge University Press

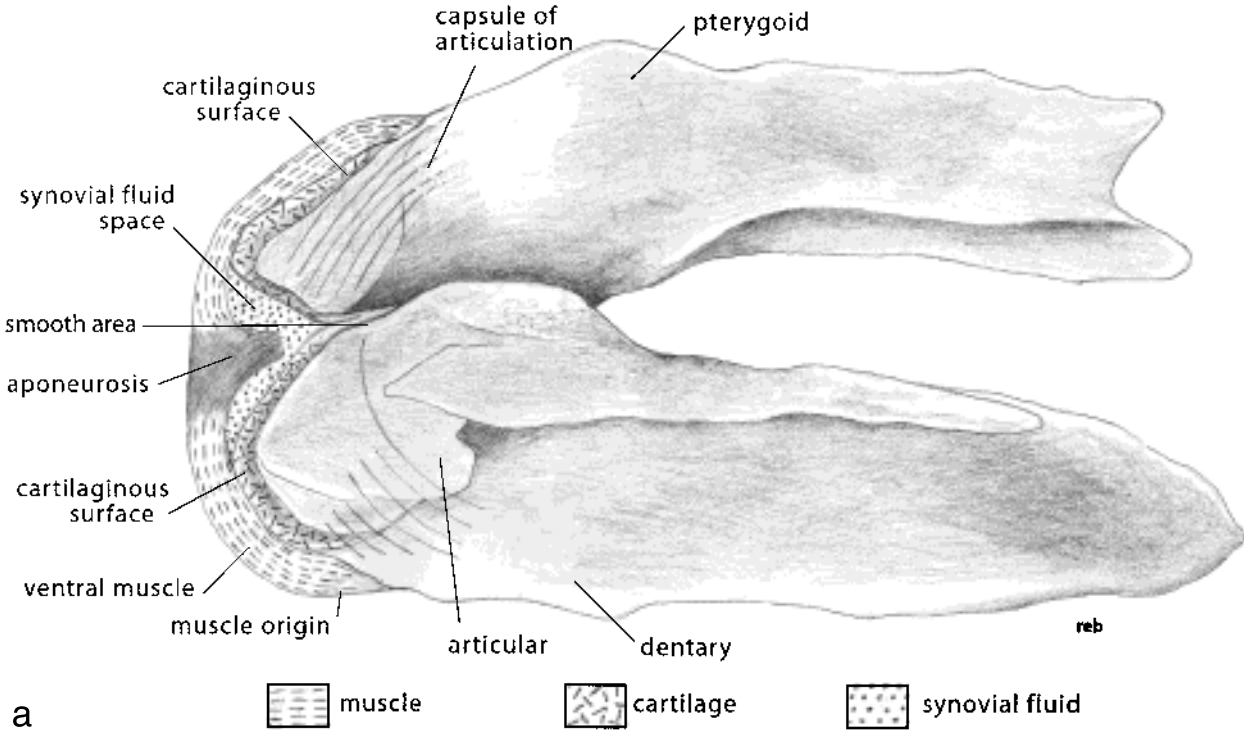

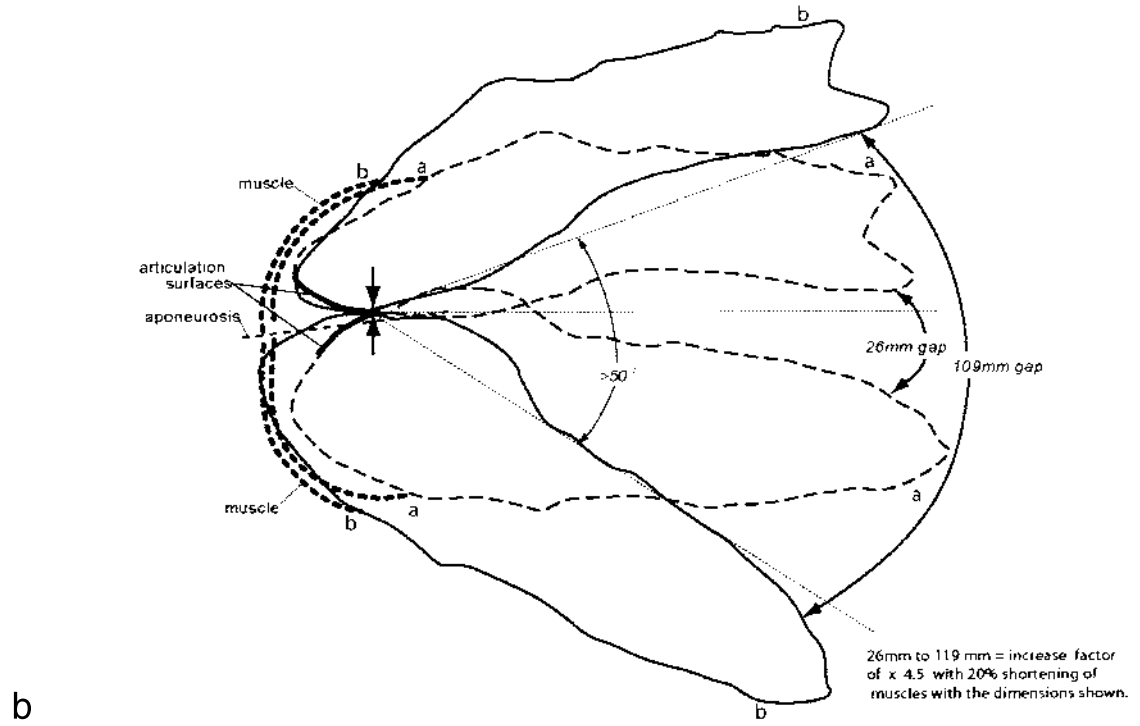

Figure 74 (a) An interpretation of the mandibular articulation. The articular is in cartilage, the attachment of which to the bone is clearly defined. The angular junctions between the dorsal and the ventral bone attachments of the quadrate and the articular mark the junction between the articular parts of the cartilage and the cartilage that surrounds the posterior edge of the junction. The dorsal edge of the quadrate was shown in Figure 19 and the ventral edge of the articulate in Figures 44 & 45. These were interpreted as the surface to which the cartilage was attached. Cartilage muscles passed around this. The smooth area on the dorsal surface of the articular could allow the slippage of the mandibular at full opening. The whole articulation was enclosed in a capsule that would have allowed lateral at well as vertical movement. (b) The specimen shown in (a). The initial positions of the jaw elements are shown by the dotted outlines of (a) and the open positions by the continuous outline (b). The initial hinging point of the articulation is marked by the vertical arrows. With 20% contraction of the muscles, a gape exceeding 50° can be effected.

https://doi.org/10.1017/S0263593300001309 Published online by Cambridge University Press

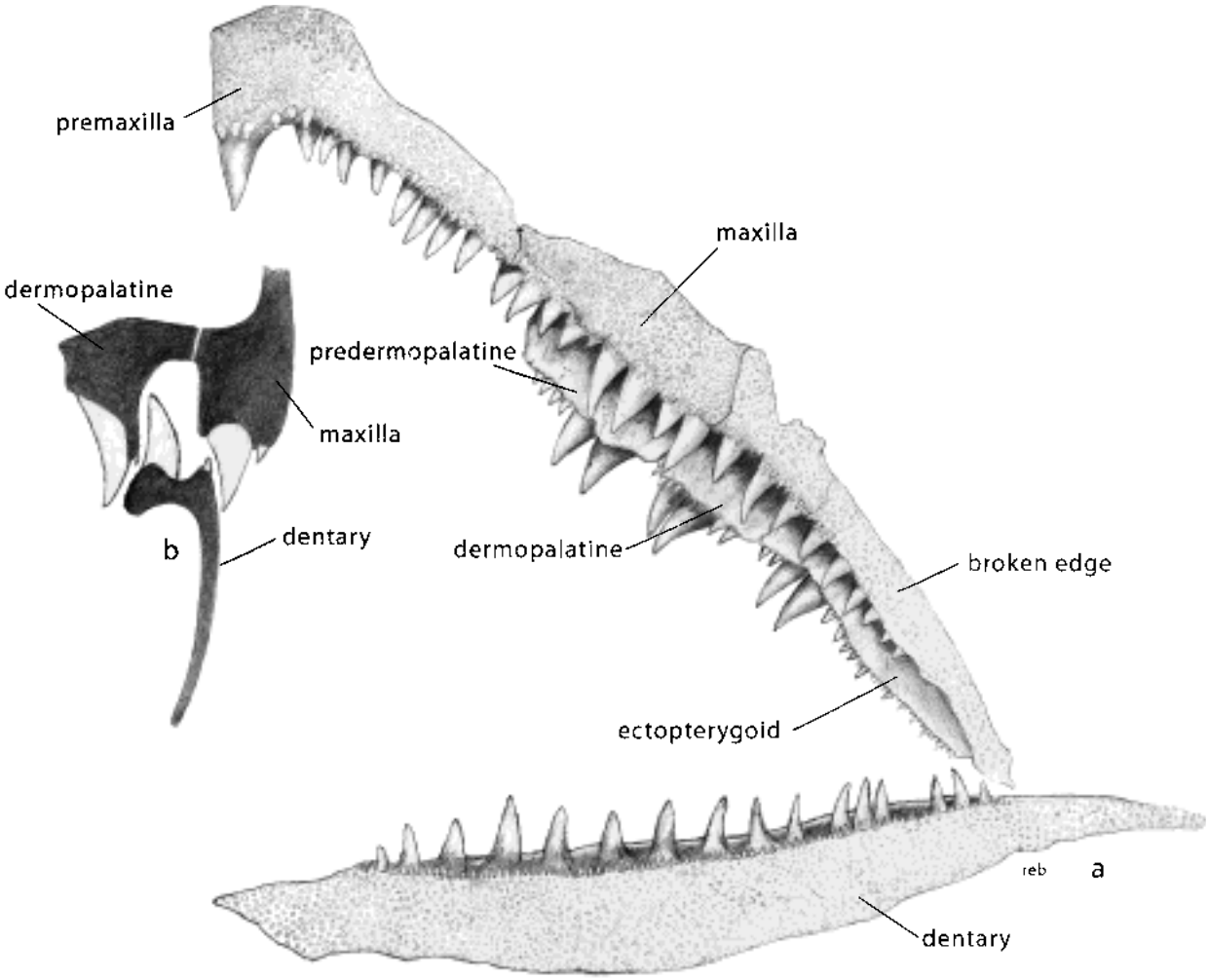

Figure 75 Reconstruction of the relationship between the palatal and the mandibular teeth during the bite. The overlap shown in (b) makes it possible for the tusks on the parasymphysial whorls to retract into the space between the median ethmoid and the lateral bones on jaw closure. The impression of the mandibular teeth on the innerface of the dermopalatine series is shown in Figure 10.

https://doi.org/10.1017/S0263593300001309 Published online by Cambridge University Press